

UNIVERSIDAD DE CÓRDOBA

Programa de doctorado:

Química fina

Título de la tesis:

Valorización de residuos y de biomasa mediante técnicas respetuosas con el medio ambiente

Environmentally friendly paths for wastes and biomass valorization

Directores

Rafael Luque Álvarez de Sotomayor

Antonio Pineda Pineda

Autor de la tesis

Camilla Maria Cova

Fecha de depósito tesis en el Idep:

14/11/2019

TITULO: *Environmentally friendly paths for wastes and biomass valorization*

AUTOR: *Camilla María Cova*

---

© Edita: UCOPress. 2020  
Campus de Rabanales  
Ctra. Nacional IV, Km. 396 A  
14071 Córdoba

[https://www.uco.es/ucopress/index.php/es/  
ucopress@uco.es](https://www.uco.es/ucopress/index.php/es/ucopress@uco.es)

---



## **TÍTULO DE LA TESIS:**

**ENVIRONMENTALLY FRIENDLY PATHS FOR WASTES AND BIOMASS VALORIZATION**

## **DOCTORANDO/A:**

**CAMILLA MARIA COVA**

## **INFORME RAZONADO DE LOS DIRECTORES DE LA TESIS**

(se hará mención a la evolución y desarrollo de la tesis, así como a trabajos y publicaciones derivados de la misma).

En esta Tesis Doctoral, se han llevado a cabo investigaciones relacionadas con el desarrollo de nuevos materiales para la transformación catalítica de la biomasa y residuos a compuestos de alto valor añadido. Estas metodologías se diseñaron en base a procedimientos no convencionales y respetuosos con el medio ambiente combinados con tecnologías que ofrecen características ecológicas y de bajo impacto energético. En particular, el potencial que presentan los procesos de microondas, mecanoquímica y química de flujo quedó patente en el desarrollo y aplicación de nuevos materiales derivados de biomasa y desechos.

En primer lugar, se sintetizó con éxito una serie de heteroestructuras de carbón Ag/Ag<sub>2</sub>S mediante un procedimiento asistido por microondas. Su preparación se llevó a cabo empleando pelos de cerdo como fuente de carbono y azufre. La síntesis asistida por microondas ha demostrado ser una metodología simple, innovadora y eficiente, permitiendo la explotación de desechos como fuente no tóxica de carbono y azufre en lugar de sustancias tóxicas y peligrosas (por ejemplo, tioles y H<sub>2</sub>S). La presencia de plata metálica y sulfuro de plata se determinaron mediante la técnica de difracción de Rayos-X (DRX). La utilización de este material en procesos electrocatalíticos ha sido prometedora, en particular, para la reacción de producción de hidrogeno (HER).

Seguidamente, se ha presentado una metodología para la preparación de ZnS utilizando asimismo pelos de cerdo, un desecho económico y ampliamente disponible. La metodología incluyó un procedimiento de reflujado fácil y de bajo costo. La estructura cristalina de ZnS se demostró mediante las técnicas de difracción de rayos-X (DRX) y espectroscopía fotoelectrónica de rayos-X (XPS). Los nanocatalizadores sintetizados mostraron una actividad catalítica elevada, así como estabilidad química en las reacciones de oxidación selectiva del tolueno y del alcohol bencílico a benzaldehído (compuesto ampliamente utilizado en las industrias de fragancias y perfumería).

Finalmente, se prepararon materiales basados en nano-rutenio empleando como materiales de soporte los núcleos cerámicos usados en los catalizadores de desecho de los coches. Los materiales fueron sintetizados mediante molienda mecanoquímica seguida de una reducción química. Los catalizadores sintetizados fueron utilizados en la hidrogenación selectiva del cinamaldehído en flujo continuo. Se optimizaron distintos parámetros que incluyeron la presión de H<sub>2</sub>, la temperatura, el flujo y el contenido en rutenio. La actividad catalítica de los materiales Ru/CATs fue comparada con otros

catalizadores de rutenio soportados en distintos materiales, SiO<sub>2</sub>, Al<sub>2</sub>O<sub>3</sub> y Al<sub>2</sub>O<sub>3</sub> activado, sintetizados mediante la misma metodología mecanoquímica.

Como resultado de las investigaciones realizadas y demostrando la calidad de éstas, Camilla Maria Cova ha participado como primera autora en 3 publicaciones científicas en revistas dentro del primer cuartil (Q1) del "Journal Citation Reports".

- Título:** Microwave-assisted preparation of Ag/Ag<sub>2</sub>S carbon hybrid structures from pig bristles as efficient HER catalysts.  
**Autores:** Camilla Maria Cova, Alessio Zuliani, Alain R. Puente-Santiago, Alvaro Caballero, Mario J. Muñoz-Batista y Rafael Luque  
**Revista:** Journal of Materials Chemistry A  
**Indicios de calidad (2018):**  
Categoría: Chemistry, Physical / Energy & Fuels / Materials science, Multidisciplinary.  
Índice de impacto: 10.733  
Posición dentro de la categoría: 14/148 (Q1) / 6/103 (Q1) / 21/293 (Q1)  
Volumen: 6; Páginas: 21516-21523; Año: 2018.
- Título:** A sustainable approach for the synthesis of catalytically active peroxidase-mimic ZnS catalyst.  
**Autores:** Alessio Zuliani, Mario J. Muñoz-Batista y Rafael Luque  
**Revista:** ACS Sustainable Chemistry & Engineering  
**Indicios de calidad (2018):**  
Categoría: Multidisciplinary / Engineering, Chemical / Green & Sustainable Science & Technology.  
Índice de impacto: 6.970  
Posición dentro de la categoría: 26/172 (Q1) / 9/138 (Q1) / 5/35 (Q1)  
Volumen: 7(1); Páginas: 1300-1307; Año: 2019.
- Título:** Efficient Ru-based scrap waste automotive converter catalysts for the continuous-flow selective hydrogenation of cinnamaldehyde.  
**Autores:** Camilla Maria Cova, Alessio Zuliani, Mario J. Muñoz-Batista y Rafael Luque  
**Revista:** Green Chemistry  
**Indicios de calidad (2018):**  
Categoría: Chemistry, multidisciplinary / Green & Sustainable Science & Technology.  
Índice de impacto: 9.405  
Posición dentro de la categoría: 20/172 (Q1) / 2/35 (Q1)  
Volumen: 21; Páginas: 4712-4722; Año: 2019.

Por todo ello, se autoriza la presentación de la tesis doctoral.

Córdoba, 12 de Noviembre de 2019

Firma de los directores

  
Fdo.: Rafael Luque Álvarez de Sotomayor

  
Fdo.: Antonio Pineda Pineda







*A Córdoba, che è diventata casa e famiglia,  
e a tutto quello che ha fatto nascere*

*“E senti allora, se pure ti ripetono che puoi,  
fermarti a mezza via o in alto mare,  
che non c'è sosta per noi, ma strada, ancora strada,  
e che il cammino è sempre da ricominciare”*

*Eugenio Montale*







Departamento de Química Orgánica  
Facultad de Ciencias  
Universidad de Córdoba  
Grupo FQM-383



## Doctoral Thesis

# ENVIRONMENTALLY FRIENDLY PATHS FOR WASTES AND BIOMASS VALORIZATION



### Supervisors

Prof. Rafael Luque Álvarez de Sotomayor  
Dr. Antonio Pineda Pineda

### PhD Candidate

Camilla Maria Cova



# Content

<b>Introduction</b> .....	<b>7</b>
Foreword .....	9
Sustainable and environmentally friendly techniques .....	15
“Balling the jack!”: Mechanochemistry .....	16
“Ride the wave!”: Microwave radiation .....	42
“Roll with the flow!”: Continuous flow chemistry .....	53
Biomass and waste valorization: case studies .....	63
“Everything but the oink!”: pig bristles .....	64
“Pedal to the metal!”: scrap automotive catalytic converters .....	67
References .....	72
<b>Hypothesis &amp; Objectives</b> .....	<b>89</b>
Hypothesis I .....	91
Objective I .....	91
Hypothesis II .....	92
Objective II .....	93
Hypothesis III .....	93
Objective III .....	95
References .....	96
<b>Results &amp; Discussion</b> .....	<b>101</b>
Microwave-assisted preparation of Ag/Ag <sub>2</sub> S carbon hybrid structures from pig bristles as efficient HER catalysts .....	103
A sustainable approach for the synthesis of catalytically active peroxidase-mimic ZnS catalysts .....	128

Efficient Ru-based scrap waste automotive converter catalysts for the continuous-flow selective hydrogenation of cinnamaldehyde .....	151
<b>Conclusions .....</b>	<b>185</b>
<b>Summary .....</b>	<b>191</b>
<b>Index of quality .....</b>	<b>201</b>
<b>Achievements.....</b>	<b>207</b>
<b>Acknowledgments.....</b>	<b>213</b>
<b>Materials &amp; Methods .....</b>	<b>219</b>
Materials .....	222
Methods.....	223
References .....	242
<b>Articles permissions .....</b>	<b>245</b>





# Introduction





## Foreword

The global production of biological and industrial wastes is constantly intensifying. By 2050, the world is expected to generate 3.40 billion tons of waste yearly, increasing dramatically from current production of 2.01 billion tons [1,2]. Remarkably, in the last two decades, the total World population has increased more than 20%, and the level of industrialization, especially in emerging countries, has rapidly grown.

If on the one hand this means better life conditions, on the other hand the rampant consumerism (following the linear economy) is destroying our planet. Unfortunately, images of paradisiac landscapes devastated by uncontrolled release of wastes are a daily occurrence. With no doubts, some countries have started recycling programs and improvements of industrial efficiency with encouraging results [3]. For example, Sweden waste treatment policy has driven the country to a so efficient recycling system that they can import household waste from other countries [4]. However, the effort in that direction is still not enough to compensate the dramatic global waste growth.

Research efforts have been directed to advanced technologies and processes for the valorization of different wastes for large scale applications. Apart from the well-known biogas production (organic waste fractions), other processes include for example the production of biodiesel from bio-waste (*e.g.*, waste cooking oils) or the utilization of renewable biomass for fuels, chemicals and materials in bio-refineries or its utilization as energy source (*e.g.*, for bioethanol) [5].

However, the research on the upgrading of waste and biomass to fine chemicals or high added-value compounds, such as catalysts, is still under development and limited to laboratory scale. The main limit in this type of

research rises from the difficulty to compete with petroleum derivatives, where the starting materials are slightly contaminated and easy-to-handle.

Indeed, the current limits of waste and biomass valorization are excessive energy consumption (due to the purification of the starting materials), variable product quality (due to the variability in the different batches), low efficiency (due to the generation of high volumes of by products) and limited scalability. As a result, the development of alternative and competitive approaches capable of overpass these limits is a priority.

Numerous research groups are involved in the use of biomass and waste for the synthesis of new materials, motivated by the multiple advantages that these wastes show as compared to petroleum products or other conventional sources. For instance, by-products from the agricultural industry have been used in order to obtain high added-value products according to the principles of green chemistry [6], or end-of-life vehicle waste has been used to produce photocatalysts [7].

In this context, the current Doctoral Thesis explored the development of sustainable approaches for the valorization of biomass and wastes through innovative and environmentally friendly methodologies. These included microwave-assisted techniques, mechanochemical approaches and continuous flow processes. These innovative technologies perfectly match with the Green Chemistry concept towards sustainability [8-10].

Over the last ten years, the use of microwave has been identified as a technology with the potential to intensify chemical processes in terms of energy efficiency. Indeed, microwave irradiation allows to perform chemical reactions in a very short time, minimizing or suppressing side-reactions, reducing solvents waste and energy consumption, using low volumes of solvents [8,11-14].

Mechanochemistry has emerged as a valid sustainable methodology, allowing the accomplishment of reactions under solvent-free conditions, avoiding conventional heating and any addition of toxic reagents. Moreover, mechanochemical-assisted protocols are less expensive and comparably faster to traditional ones [9,15-17].

Lastly, flow-chemistry is ideally suited to meeting the principles of Green Chemistry. Indeed, flow processes are inherently safer with small reaction volumes and lower amounts of solvents and reagents needed. There is low risk of environmental exposure to reagents, and processes can be scaled up without the need for re-optimization [10,18-20].

This Doctoral Thesis aims at the design and the application of new materials derived from industrial wastes or biomass (such as pig bristles or scrap waste automotive converter catalysts) through microwave heating, mechanochemistry and flow chemistry processes. In particular, new waste/biomass-based materials have been synthesized together with transition metals. In all cases, various synthetic and reaction parameters were analyzed, with greater attention to times and performances, and with a special focus on the production of no toxic waste.

Main results obtained from the study carried out in this Doctoral Thesis have led to three research articles published in different scientific journals, which constitute the Chapter “Results & Discussion”.

In the first paper, a microwave-assisted synthesis of a waste-based Ag/Ag<sub>2</sub>S heterocomposite is proposed. Pig bristles were used as sulfur and carbon precursor and the synthesized materials were used as electrocatalysts for the hydrogen evolution reaction. In the second scientific article, pig bristles were used in order to prepare zinc sulfide, carrying on a very simple and quick boiling procedure. The catalysts were tested in the oxidation of toluene and benzyl alcohol to benzaldehyde *via* microwave trials. Lastly, the third

publication presents the mechanochemical-assisted synthesis of Ru-based catalysts supported on ceramic cores of scrap automotive catalytic converters. The waste-based materials were used as catalysts in the selective continuous-flow hydrogenation of cinnamaldehyde to cinnamyl alcohol.

To well frame the context and the state-of-art, the introduction is subdivided into two sections. In the first one, environmentally friendly techniques are discussed, showing, in particular, the last studies for biomass and waste valorization. In the second section, the industrial and biological waste used in the research are briefly described in terms of the annual production, worldwide market, environmental impact as well as the state-of-art relative to their reuse.

## References

1. Hoornweg, D.; Bhada-Tata, P. What a Waste: A Global Review of Solid Waste Management. *The World Bank Group, Washington, DC, USA*. **2012**. pp. 1–98.
2. Kaza, S.; Yao, L. C.; Bhada-Tata, P.; Van Woerden, F. What a Waste 2.0: A Global Snapshot of Solid Waste Management to 2050. *Urban Development; Washington, DC: World Bank*. **2018**.
3. Woon, K. S.; Lo, I. M. C. A proposed framework of food waste collection and recycling for renewable biogas fuel production in Hong Kong. *Waste Manage.* **2016**, *47*, 3-10.
4. Andersson, C.; Stage, J. Direct and indirect effects of waste management policies on household waste behaviour: The case of Sweden. *Waste Manage.* **2018**, *76*, 19-27.
5. Arancon, R. A. D.; Lin, C. S. K.; Chan, K. M.; Kwan, T. H.; Luque, R. Advances on waste valorization: new horizons for a more sustainable society. *Energy Sci. Eng.* **2013**, *1*(2), 53-71.
6. Chiew, Y. L.; Cheong K. Y. A review on the synthesis of SiC from plant-based biomasses. *Mater Sci. Eng. B-Adv.* **2011**, *176*, 951-964.
7. Gombac, V.; Montini, T.; Falqui, A.; Loche, D.; Prato, M.; Genovese, A.; Mercuri, M. L.; Serpe, A.; Fornasiero, P.; Deplano, P. From trash to resource: recovered-Pd from spent three-way catalysts as a precursor of an effective photo-catalyst for H<sub>2</sub> production. *Green Chem.* **2016**, *18*, 2745-2752.
8. Balu, A. M.; Dallinger, D.; Obermayer, D.; Campelo, J. M.; Romero, A. A.; Carmona, D.; Balas, F.; Yoshida, K.; Gai, P. L.; Vargas, C.; Kappe, C. O.; Luque, R. Insights into the microwave-assisted preparation of supported iron oxide nanoparticles on silica-type mesoporous materials *Green Chem.* **2012**, *14*, 393-402.
9. Xu, C.; De, S.; Balu, A. M.; Ojeda, M.; Luque, R. Mechanochemical synthesis of advanced nanomaterials for catalytic applications. *Chem. Commun.* **2015**, *51*, 6698-6713.
10. Vaccaro, L.; Lanari, D.; Marrocchi, A.; Strappaveccia, G. Flow approaches towards sustainability. *Green Chem.* **2014**, *16*, 3680-3704.
11. Caddick, S. Microwave-assisted organic-reactions. *Tetrahedron.* **1995**, *51*(38), 10403-10432.
12. Lidstrom, P.; Tierney, J.; Wathey, B.; Westman, J. Microwave assisted organic synthesis - a review. *Tetrahedron.* **2001**, *57*(45), 9225-9283.
13. Kappe, C. O. Controlled microwave heating in modern organic synthesis. *Angew. Chem. Int. Edit.* **2004**, *43*(46), 6250-6284.

## Introduction

14. Kokel, A.; Schafer, C.; Torok, B. Application of microwave-assisted heterogeneous catalysis in sustainable synthesis design. *Green Chem.* **2017**, *19*(16), 3729-3751.
15. Balaz, P.; Balaz, M.; Bujnakova, Z. Mechanochemistry in Technology: From Minerals to Nanomaterials and Drugs. *Chem. Eng. Technol.* **2014**, *37*(5), 747-756.
16. Xu, C. P.; De, S.; Balu, A. M.; Ojeda, M.; Luque, R. Mechanochemistry: Toward Sustainable Design of Advanced Nanomaterials for Electrochemical Energy Storage and Catalytic Applications. *Acs Sustain. Chem. Eng.* **2015**, *51*(31), 6698-6713.
17. Munoz-Batista, M. J.; Rodriguez-Padron, D.; Puente-Santiago, A. R.; Luque, R. Mechanochemical synthesis of advanced nanomaterials for catalytic applications. *Chem. Commun.* **2018**, *6*(8), 9530-9544.
18. Watts, P.; Wiles, C. Micro reactors, flow reactors and continuous flow synthesis. *J. Chem. Res.* **2012**, *4*, 181-193.
19. Pastre, J. C.; Browne, D. L.; Ley, S. V. Flow chemistry syntheses of natural products. *Chem. Soc. Res.* **2013**, *42*(23), 8849-8869.
20. Gerardy, R.; Emmanuel, N.; Toupay, T.; Kassin, V. E.; Tshibalonza, N. N.; Schmitz, M.; Monbaliu, J. C. M. Continuous Flow Organic Chemistry: Successes and Pitfalls at the Interface with Current Societal Challenges. *Eur. J. Org. Chem.* **2018**, *20-21*, 2301-2351.

## **Sustainable and environmentally friendly techniques**

The following section aims at presenting and briefly explaining the techniques that have been used in the preparations and applications of the novel biomass/waste derived-materials. Specifically, three environmentally friendly and energetically efficient techniques are presented, *i.e.* mechanochemistry, microwave chemistry and continuous flow chemistry. The advantages and merits of these technologies are brought to light, underlining the benefits of these methods compared to traditional counterparts. The most recent and innovative progresses in the area are also described with emphasis on the description of the last studies for biomass and waste valorization. The first part related to mechanochemistry is constituted of a recent review article.



## “Balling the jack!”: Mechanochemistry

### Advances in mechanochemical processes for biomass valorization

Camilla Maria Cova<sup>1</sup> and Rafael Luque<sup>1,2\*</sup>

\* Correspondence: [q62alsor@uco.es](mailto:q62alsor@uco.es)

<sup>1</sup> Departamento de Química Orgánica, Universidad de Córdoba, Edificio Marie-Curie (C-3), Ctra Nnal IV-A, Km 396, Córdoba, Spain

<sup>2</sup> Peoples Friendship University of Russia (RUDN University), 6 Miklukho Maklaya str, 117198 Moscow, Russia

DOI: 10.1186/s42480-019-0015-7

Reproduced by permission of Springer Nature, link to publication:  
<https://bmcchemeng.biomedcentral.com/articles/10.1186/s42480-019-0015-7>

### **Abstract**

Compared to standard time and solvent consuming procedures, mechanically-assisted processes offer numerous environmentally-friendly advantages for nano-catalytically active materials design. Mechanochemistry displays high reproducibility, simplicity, cleanliness and versatility, avoiding, in most cases, the use of any solvent. Moreover, mechanically-assisted procedures are normally faster and cheaper as compared to conventional processes. Due to these outstanding characteristics, mechanochemistry has evolved as an exceptional technique for the synthesis of novel and advanced catalysts designed for a large range of applications. The literature reports numerous works showing that mechanosynthetic procedures offer more promising paths than traditional solvent-based techniques. This review aims to disclose the latest advances in the mechanochemical assisted synthesis of catalytically active materials, focusing on nanocatalysts designed for biomass conversion and on bio-based catalysts.

**Keywords:** Mechanochemistry, Catalysis, Bio-based catalysts, Biomass conversion.

### **Introduction**

**Mechanochemistry timeline.** As formalized by IUPAC, a mechanical-assisted reaction is "a reaction caused by the mechanical energy" [1]. In fact, mechanical actions, such as compression, stress, or friction, usually provides the energy to activate a process. According to Takacs, the most ancient document concerning a mechanical-assisted process is described in a book in 315 B.C.. The document, titled "On Stones", was written by Theophrastus, one of Aristotle's students.

The philosopher-scientist described the reduction of cinnabar ( $\text{HgS}$ ) to mercury ( $\text{Hg}^0$ ) using a copper vessel and a copper pestle filled with some vinegar (containing acetic acid) [2, 3]. After that first experiment reported by Theophrastus, no mechanical-based protocols were reported for the following 2000 years. Only in 1820 mechanochemistry appeared again, when Faraday carried out mechanical-assisted trials, reducing  $\text{AgCl}$  to elemental  $\text{Ag}$  using zinc, copper, tin or iron in a pestle. Faraday noticed that mechanical-assisted reaction could give different products compared to the ones obtained by normal thermal heating. Specifically, he proved that the mechanical-assisted processes favoured the decomposition of  $\text{Ag}$  and  $\text{Hg}$  halides to their elements by chemical reaction, rather than by melting or sublimation [4]. A few years later, Wilhelm Ostwald (1853–1932) defined “mechano-chemistry” as one of four chemistry disciplines (together with photo-, electro- and thermo-chemistry). In 1894, Gerard Heinicke formalized mechanochemistry as “the discipline relative to physical-chemical modifications of the solid produced by the action of mechanical factors” [5]. Figure 1 gives a summary of the milestones of mechanochemistry evolution.

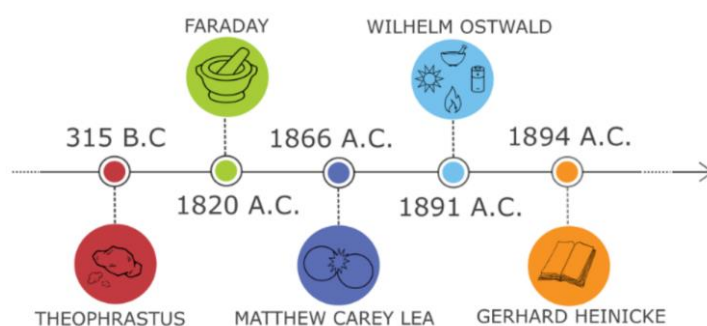


**Fig. 1** Milestones of mechanochemistry.

**Mechanochemistry theory.** The principal feature of mechanical-assisted process is the achievement of chemical changes by the only action of grinding (or milling), without needing to dissolve reagents (therefore without using any

solvent). Grinding is a broad term that describes the effect of mechanical forces on a compound that allow a solid breaking into small parts. By grinding, the improved potential energy together with friction and shear contributions, generate surface and shape defects in the reactants. These defects can considerably change the reactivity of chemicals, giving the final product, as described in Fig. 2.

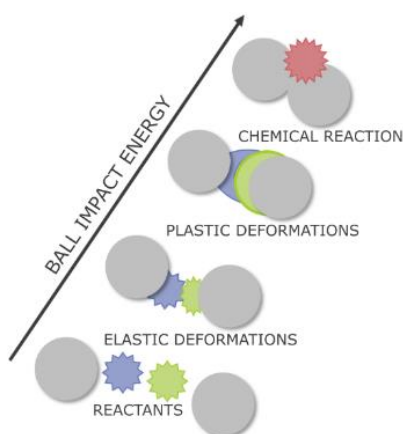


**Fig. 2** Mechanochemical reactions: from reactants to products.

**Mechanochemistry equipment.** Mechanical-assisted processes could be carried out using different equipment based on manual methods (mortar and pestle) or non-manual methods, such as mixer mills [6]. Mortars and pestles were largely studied in the past especially because they are the cheapest tools for conducting mechanical-assisted protocols. Unfortunately, many environmental factors can influence the aforementioned instruments. In addition, these manual methods do not allow properly controlling the protocol parameters such as frequency or grinding force. Consequently, nowadays the use of this type of equipment can be considered obsolete. Recently, more advanced non-manual instrumentations have been developed in order to achieve highly reproducibility of the mechanochemical synthesis. These tools include, among the others, mixer and planetary mills, and offer the possibility to accomplish

solvent-free processes through well-defined reaction parameters, such as milling force and grinding speed.

**Mechanochemical-related literature.** The study of mechanical-assisted processes has increased considerably, especially in the last 5 years [7], as showed in Fig. 3.

Historically, most of the publication has focused on the mechanical-assisted synthesis of different intrinsically insoluble inorganic material. In the last years, an increasing number of publications were related to the application of mechanical-assisted protocols in organic chemistry. Finally, the newest works re-designed the concept of mechanochemistry, exploiting mechanochemical-assisted techniques for the preparation of novel nanocatalytic materials [8].

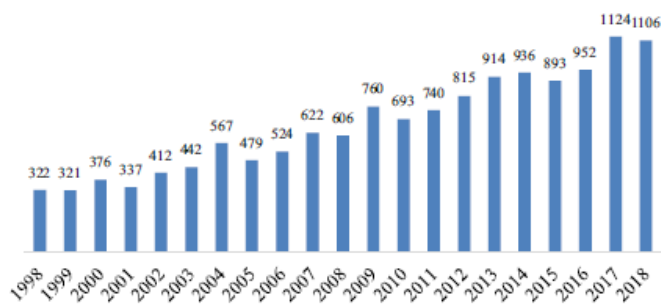


**Fig. 3** Total publications (yearly) in the mechanochemistry field. Data taken from SciFinder Web.

**Scope of the review.** Notably, most studied methods for the synthesis of nanocatalysts include sol-gel methods, impregnation, precipitation, hydrothermal procedures and microwave-assisted techniques [9-11]. These protocols have successfully led to the synthesis of advanced catalysts, but they also show numerous drawbacks. In details, these methods are normally time and solvent-consuming, expensive and need aggressive reaction conditions. In this context, mechanical-assisted processes have been proposed as alternative paths

for the industrially applicable synthesis of nanocatalysts. In fact, thanks to easiness, versatility and solvent-free conditions, mechanochemistry can compete with standard synthetic methods, avoiding multi-step routes, traditional heating and any addition of toxic reagents. A wide range of nanocatalysts have been synthesized using mechanical-assisted methods. Most studied applications of mechanical-synthesized catalysts include energy and environmental uses or applications in organic synthesis [12-17]. Among all these applications, an interesting sub-class is represented by mechanochemical-synthesized nanocatalyst used for biomass valorization. This review aims to illustrate key examples of these types of novel materials. In particular, a first section is dedicated to the mechanochemically assisted synthesis of nanocatalysts used for biomass conversion reactions. The subsequent part discloses mechanochemical-assisted protocols for the preparation of bio-based catalytically active materials. Figure 4 schematizes the scope of the review.

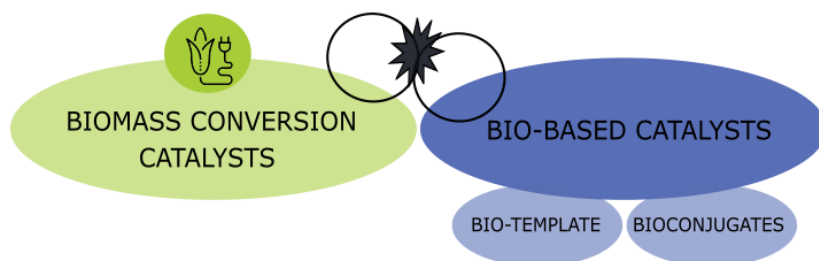


**Fig. 4** Scheme of the different fields of applications of mechanochemically-synthesized nanocatalysts described in the review.

## **Mechanochemically-assisted protocols for nanocatalysts preparation**

**Mechanochemically prepared nanocatalysts for biomass conversion.** The design of nanocatalysts for biomass conversion has become a very hot topic since the

society have started the ambitious transition to a bio-based circular economy [18]. In fact, especially in the last decades, biomass has emerged as an alternative and renewable feedstock which can be converted into valuable materials and chemicals using different protocols that include greener and environmentally friendly paths respect to traditional routes [19, 20]. A key factor for the valorization of biomass through the different processes, is the utilization of an efficient catalyst. The most important characteristic that a catalyst used for biomass valorization must have is the stability under the conditions in which the biomass is normally treated. These include highly stability to moderate-high pressure/temperature and to the presence of water. These characteristics can be effectively found in nanocatalysts prepared with a suitable mechanochemical synthesis.

For examples, highly active nanocatalysts prepared by mechanosynthesis have been employed to produce vanillin. Vanillin is a broadly used aromatic compound in the food industry and in cosmetic formulations and consequently its synthesis is of considerable economic interest. However, the traditional synthetic procedures of this compound require petro-derivatives and non-environmentally friendly protocols. Therefore, more green and alternative methodologies have been studied. Specifically, isoeugenol and vanillyl alcohol can be employed as bio-based starting chemical. In fact, both isoeugenol and vanillyl alcohol are produced from lignin, one of the most abundant biowaste.

In a recent publication, an effective process to obtain vanillin from raw materials derived from lignin (isoeugenol) has been studied [21]. Fast kinetics and high selectivity were achieved using transition metal-based catalysts. The metals were supported on reduced graphene using simple, clean and fast mechanical-assisted protocols. In details, the supporting material of reduced graphene oxide was mixed with the iron salt ( $\text{FeCl}_2 \cdot 4\text{H}_2\text{O}$ ) in order to support

1% weight of metal and subsequently subjected to grinding under mild conditions (350 rpm, 10 min) in a ball mill. The preparation of the 1% wt. cobalt catalyst was carried out *via* the same mechanical-assisted protocol, using  $\text{Co}(\text{NO}_3)_2 \cdot 6\text{H}_2\text{O}$  as metal precursor. The iron or cobalt-based nanocatalysts were tested in the reaction of isoeugenol oxidation, achieving good conversion and remarkable selectivity using hydrogen peroxide as oxidant. The mechanical-assisted procedure was proved to be a valid alternative synthesis for Fe and Co catalysts, showing outstanding activity for biomass conversion, as schematized in Figure 5.

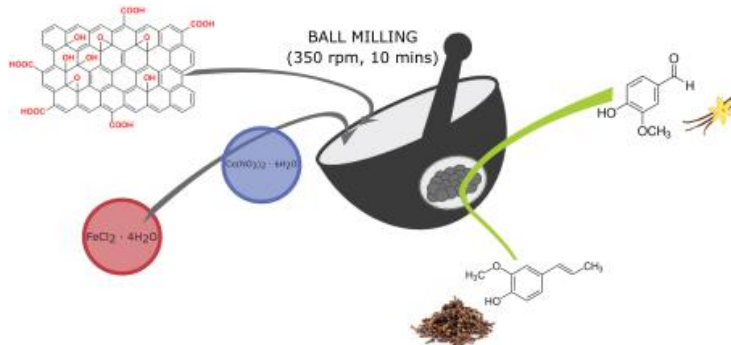


**Fig. 5** Overview of the preparation and application of the 1% wt. Fe (or Co) /graphene oxide catalysts.

A mechanochemical-assisted protocol was also designed to obtain a magnetic material  $\text{Fe}_2\text{O}_3$ -based using mesoporous silica (Al-SBA-15) as supporting material [22]. The mechanical-assisted preparation of  $\text{Fe}_2\text{O}_3$  particles on Al-SBA-15 was achieved by milling together propionic acid,  $\text{Fe}(\text{NO}_3)_3 \cdot 9\text{H}_2\text{O}$  and Al-SBA-15 at 350 rpm for 10 min. The following step of the protocol was a calcination one at 300 °C for half an hour. The synthesized materials were tested in the synthesis of vanillin through the oxidation of vanillyl alcohol, showing great selectivity and conversion, as displayed in Fig. 6. Interesting, the material was demonstrated to possess a great stability in the aforementioned oxidation, since the activity did not decrease also after 10 cycles of reuse.



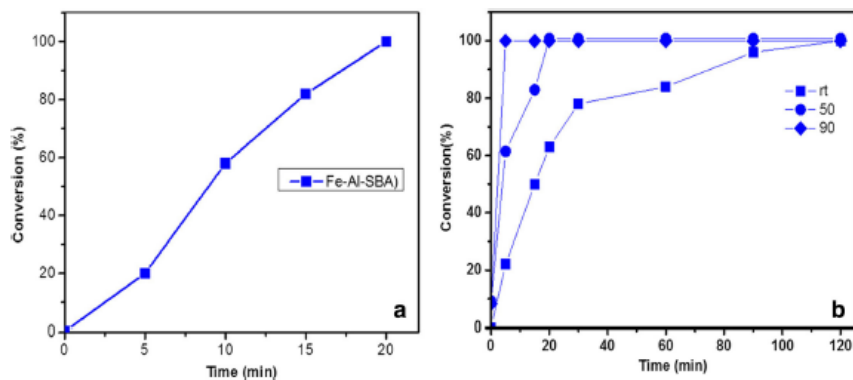


**Fig. 6 a** Kinetic analysis of the oxidation of vanillyl alcohol for 20 min at 50 °C and **b** catalytic behavior at different temperature for 120 min. Reprinted with permission from Ref. [22] Copyright (2019) Elsevier B.V.

Another captivating biomass-derived chemical is benzyl alcohol, which can be oxidized to benzyl aldehyde. This last compound is a highly demanded product as it is extensively employed as ingredient in the food or in the pharmaceutical industry or as a fragrance for cosmetic formulations, or even as an intermediate in many chemicals synthesis.

Recently, graphitic carbon nitride ( $g\text{-C}_3\text{N}_4$ ) doped with zinc oxide or iron oxide were prepared using a one-step mechanical-assisted protocol [23]. The oxide incorporation on graphitic carbon nitride was obtained by a simple mechanical-assisted step in a planetary ball mill for 10 min at 350 rpm. Zinc oxide and  $\text{Fe}_2\text{NO}_3$  were used as precursors. Lastly, the material was calcined at 300 °C for 3 h. The prepared materials were used as catalysts for the selective benzyl alcohol photo-oxidation to benzaldehyde. Both prepared composite materials showed an improvement of selectivity (70%) and conversion (20%) with respect to pure  $g\text{-C}_3\text{N}_4$  used as reference, as displayed in Fig. 7. The selective oxidation of benzyl alcohol could be also achieved using cobalt oxide nanoparticles supported on mesoporous silica (SBA-15). The catalyst was prepared through a mechanochemical-assisted protocol. Briefly, the appropriated amount of cobalt precursor was milled with 2 g of SBA-15

metallo-silicate at 350 rpm for 10 min. This first step was followed by a calcination at 400 °C for 4 h. The so-prepared material was tested in the selective oxidation of benzyl alcohol, allowing conversions up to 40%. Moreover, the efficiency of the cobalt-based catalysts was proved in the alkylation of toluene with benzyl chloride, achieving complete conversion to alkylated derivatives in a very short time [24].

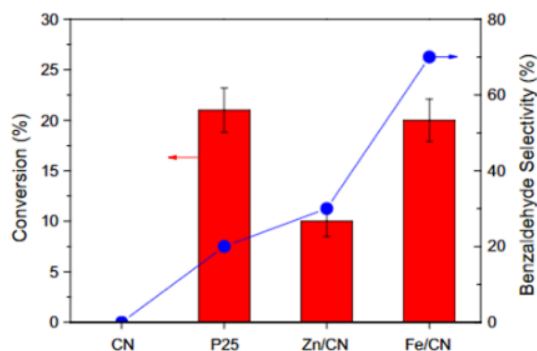


**Fig. 7** Activity and selectivity in the photo-oxidation of benzyl alcohol for the graphitic carbon nitride enriched with zinc or iron. Reprinted with permission from Ref. [23] Copyright (2019) Elsevier B.V.

Similarly, novel copper-containing aluminosilicate materials were synthesized using a mechanical-assisted protocol. Two types of aluminosilicate catalyst with and without zinc were tested. A typical preparation includes the milling of 1 g of Al-SBA-15 or AlZn-SBA-15 and the correct quantity of a copper precursor ( $\text{CuCl}_2 \cdot 2 \text{H}_2\text{O}$ ) in order to reach 2 wt%. The reactants were milled together in a ball mill (Retsch 100) at 350 rpm for 10 min [25]. Lastly, the materials were calcined in air at 400 °C for 4 h, as showed in Fig. 8. The catalysts were tested in the microwave-assisted valorization of glucose to the added-value product 5-methylfurfuryl alcohol (5-MFA). Firstly, glucose was dehydrated with formic acid and subsequently hydrogenated to 5-MFA. This unprecedented mechanical-assisted protocol could pave the way for upcoming studies for the preparation of a wide range of products with high added-value from sugars.



**Fig. 8** Pictorial representation of the synthetic procedure of CuAl-SBA and CuAlZn-SBA.

Table 1 briefly summarizes the works described above for biomass conversion using mechanochemically synthesized materials.

**Table 1.** Summary of mechanochemically prepared catalysts for biomass conversion.

Catalyst	Preparation method	Equipment	Application	Ref.
1%wt Fe(Co)/graphene oxide	Ball milling graphene and $\text{FeCl}_2 \cdot 4\text{H}_2\text{O}$ (or $\text{Co}(\text{NO}_3)_2 \cdot 6\text{H}_2\text{O}$ ) in a planetary ball mill for 10 min at 350 rpm.	Retsch-PM-100 planetary ball mill	Production of vanillin from isoeugenol, a lignin-derived feedstock.	[21]
$\text{Fe}_2\text{O}_3$ supported on Al-SBA-15	Al-SBA-15, $\text{Fe}(\text{NO}_3)_3 \cdot 9\text{H}_2\text{O}$ and propionic acid were used as chemicals and were milled in a planetary ball mill at 350 rpm for 10 minutes. Finally, the material was calcined at 300 °C for 30 min.	Retsch-PM-100 planetary ball mill	Production of vanillin from vanillyl alcohol, a lignin-derived material.	[22]
Graphitic carbon nitride enriched with ZnO or $\text{Fe}_2\text{O}_3$	$\text{ZnO}$ (or $\text{Fe}_2\text{NO}_3$ ) were supported on graphitic carbon nitride using a mechanical-assisted step in a planetary ball mill for 10 minutes at 350 rpm. Lastly, the materials were calcined at 300 °C for 3 h.	Retsch-PM-100 planetary ball mill	Selective photo-oxidation of benzyl alcohol to benzaldehyde.	[23]
Co oxide nanoparticles supported on mesoporous material	$\text{CoCl}_2 \cdot 6\text{H}_2\text{O}$ together with 2 g of support were milled at 350 rpm for 10 min in a planetary ball mill; then the materials obtained were calcined at 400 °C for 4 h.	Retsch-PM-100 planetary ball mill	Oxidation of benzyl alcohol and alkylation of toluene.	[24]
CuAlZn-SBA and CuAl-SBA	Ball milling solid support and $\text{CuCl}_2 \cdot 2\text{H}_2\text{O}$ in a planetary ball mill for 10 min at 350 rpm, followed by calcination at 400 °C for 4 h.	Retsch-PM-100 planetary ball mill	Microwave-assisted conversion of glucose to products with high added value.	[25]

**Mechanochemically prepared bio-based materials for energy conversion/storage and photodegradation.** A recent innovative approach in mechanochemistry is the utilization of biological/natural compounds as sacrificial templates or as bio-conjugates in the synthesis of nanocatalysts. In the last years, the interest in the use of diverse biomass sources as sacrificial template has been growing. In fact, the use of natural template sources is extremely attractive for the preparation of nanocatalysts in ecological friendly ways, avoiding the utilization of toxic or expensive classical templates [26]. These bio-templates materials include starch [27-30], cellulose [31], chitosan [32-35], lignin [36, 37] and alginate [38, 39]. Compared to classical templates, these materials are also often employed in milder reaction conditions [40].

For example, the synthesis of porous zinc oxide nano-materials was carried on employing zinc nitrate with various polysaccharides including a biomass-derived agar extracted from *Gracilia gracilis*, as sacrificial template [41]. An easy mechanical-assisted step was efficiently carried out. The milling step was followed by calcination at 600 °C in order to remove the template. The prepared materials were tested for phenol degradation displaying an encouraging photocatalytic activity. Due to its simplicity, large applicability and reproducibility, the proposed mechanical-assisted process has a remarkable potential and could be employed to obtain alternative nanocatalysts from different metal oxides.

Schneidermann et al. have prepared nitrogen-doped carbon using a mixture of lignin with a mechanical-assisted one-pot process [36]. The synthesis was carried out using a sustainable, available, cheap and largely diffuse precursor. The nitrogen-doped carbons were synthesized milling together, in a zirconia vessel for 30 min, the product of the carbonization of a mixture of lignin (wasted from pulp industry) as carbon precursors, urea as nitrogen source and potassium carbonate as activation agent. The obtained materials were

sequentially carbonized at 800 °C. Remarkably, carbons showed excellent performance as supercapacitor. The mechanical-assisted protocol was demonstrated to be an environmentally friendly alternative route to obtain nitrogen-doped materials from sustainable precursor. The protocol is schematized in Fig. 9.



**Fig. 9** Pictorial representation of the synthetic procedure of N-doped porous carbon. Reprinted with permission from Ref. [36] Copyright (2017) Wiley-VCH.

More recently, the aforementioned researchers have carried out a mechanical-assisted synthesis of N-doped carbons using renewable biomass waste. In particular, they used sawdust, an agricultural by-product, as sacrificial template [37]. Sawdust was used as carbon precursor, melamine and/or urea as a nitrogen precursor, and  $K_2CO_3$  as an activation agent. In a typical mechanochemical procedures, the three precursors were milled for 30 min. The mechanical-assisted step was followed by a carbonization of the obtained polymer at 800 °C. The nitrogen-doped carbon materials showed a good performance as cathode for lithium–sulfur batteries. The adopted approach is schematically presented in Fig. 10.

Usually, the preparations of nitrogen-doped carbons involve multiple process steps, which are time-, energy- and solvent-consuming and they often employ expensive chemicals. Furthermore, many traditional routes produce large amounts of wastes, especially solvents, which are potentially harmful to

the environment or even toxic to humans [42, 43]. The two syntheses of nitrogen-doped carbon materials described above are based on economic and non-toxic feedstock and follow environmentally friendly synthetic paths.



**Fig. 10** Mechanical step and carbonization of a mixture of sawdust, urea and/or melamine and  $K_2CO_3$  to prepare N-doped carbons as electrode for lithium-sulfur batteries. Reprinted with permission from Ref. [37] Copyright (2019) Wiley-VCH.

Synthetic methods and applications of mechanically obtained nanocatalysts using biomass-template materials are summarized in Table 2.

**Table 2.** Summary of mechanochemically prepared biomass-template catalysts.

Catalyst	Biomass template	Preparation method	Equipment	Application	Ref.
Porous ZnO nano materials	Poly saccharides	Ball milling of zinc nitrate and polysaccharide at 350 rpm for 10 min, followed by calcination in air at 400 °C for 4 h.	Retsch-PM-100 planetary ball mill	Photocatalytic phenol degradation	[41]
N-doped carbon	Lignin	Milling the carbonization of lignin, urea and potassium carbonate for 30 min; then carbonization at 800 °C.	Fritsch Pulverisette 7 premium line planetary ball mill	Cathode for lithium-sulfur batteries	[36]
N-doped carbon	Sawdust	Sawdust melamine and/or urea and $K_2CO_3$ were milled for 30 min in a zirconia vessel. Then the obtained polymers were carbonized at 800 °C.	Fritsch Pulverisette 7 premium line planetary ball mill	Supercapacitors	[37]

Besides the aforementioned application of biomass as carbon precursors, our group has extended the mechanochemistry field to synthesize bioconjugates-based materials. In the literature, different paths have been explored to functionalize biological molecules on magnetic nanoparticle surfaces. However, almost all reported protocols need the use of solvents. In order to obtain bio-modified magnetically recoverable nanocatalyst in an easier and less toxic way, mechanical-assisted synthesis was employed reducing reaction time and avoiding solvent consumption [44]. For example, a bio-modified nanomaterial was prepared using horse hemoglobin (Hb) and cobalt oxide magnetic nanoparticles ( $\text{Co}_3\text{O}_4$  MNPs) through a solvent-free mechanical-assisted step [45]. Firstly, dopamine (DA) hydrochloride was solubilized in water and added to pre-synthesized  $\text{Co}_3\text{O}_4$  magnetic nanoparticles. The mixture was milled in a planetary mill (200 rpm, 10 min) obtaining DA- $\text{Co}_3\text{O}_4$ . This first step was followed by another ball milling-assisted step: using the same milling parameters, a dispersion of horse hemoglobin (Hb) in  $\text{NaH}_2\text{PO}_4$  buffer was milled together with DA- $\text{Co}_3\text{O}_4$ , obtaining Hb-DA- $\text{Co}_3\text{O}_4$ . This novel nanocomposite was used as catalyst in durable supercapacitor. The dry mechanical-assisted preparation of the bio-modified catalytic material was demonstrated to be an easy, green and effective unconventional route.

Basing on the mechanical-assisted approach described above, another bioconjugate was synthesized using a redox-active protein and  $\text{Fe}_2\text{O}_3$  nanoparticles. For the synthesis, dopamine (DA) previously coated with  $\text{Fe}_2\text{O}_3$  particles (DA- $\text{Fe}_2\text{O}_3$ ) was functionalized with hemoglobin, using two successive mechanical-assisted steps [46]. The so-prepared materials were employed as catalysts to polymerize ortho-, meta- and para-substituted phenylenediamines. The products achieved through the polymerization showed outstanding fluorescence behavior and could be used in optoelectronic devices.

The mechanically functionalization of  $\text{Fe}_2\text{O}_3$  nanoparticles with laccase has been also recently reported [47]. The procedure involved two mechanical-assisted steps and allowed the exploitation of a biomass, orange peel waste as sacrificial template and also of an enzyme for the synthesis of a bioconjugates. Firstly,  $\text{Fe}_2\text{O}_3$  nanoparticles supported over carbon were prepared using iron nitrate and orange peel waste as carbon source using a mechanochemical-based approach. Sequentially, a mechanical-assisted step was performed milling iron oxide magnetic nanoparticles, dopamine hydrochloride (DA-HCl) and commercial laccase from *Trametes Versicolor* (LAC) for 10 min at 200 rpm. Finally, the materials were dried in the oven at 100 °C for 24 hours, and consecutively heated up to 300 °C for 30 min. The bioconjugate catalysts were used in the direct electrochemically reduction of oxygen, showing good performances. Figure 11 represents an overview of the mechanical-assisted synthesis of bioconjugate-based materials and their application in the electroreduction of oxygen.

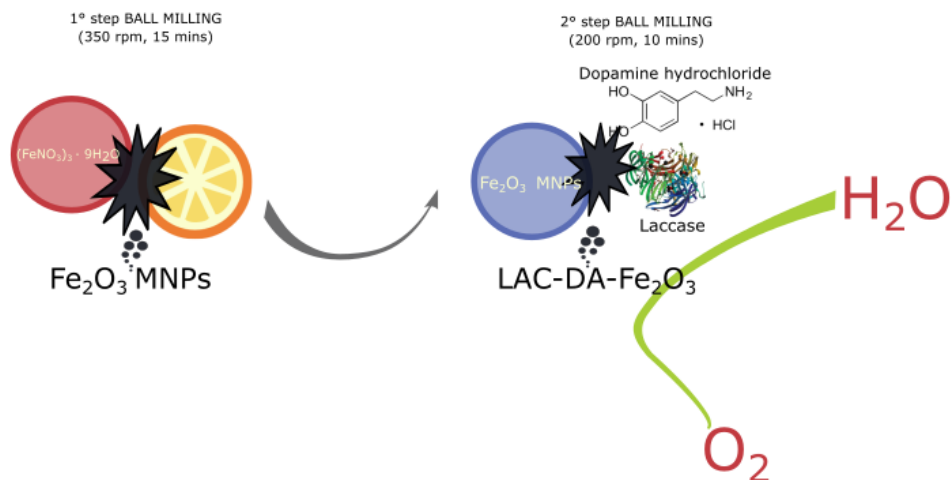


**Fig. 11** Overview of the preparation and application of LAC-DA- $\text{Fe}_2\text{O}_3$ .

The synthetic methods and applications of the mechanochemically obtained bioconjugates materials are summarized in Table 3.

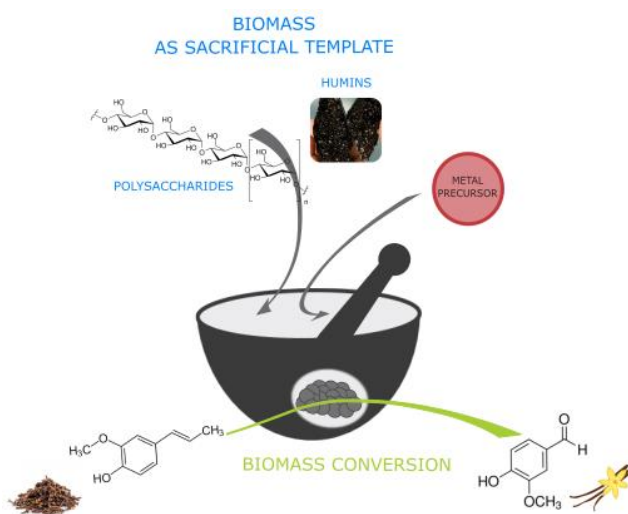


**Table 3.** Summary of mechanochemically prepared bioconjugates catalysts.

Catalyst	Preparation method	Equipment	Application	Ref.
Hb-DA-Co <sub>3</sub> O <sub>4</sub>	Ball milling of DA-HCl and Co <sub>3</sub> O <sub>4</sub> in a planetary ball for 10 min at 200 rpm. Ball milling of Hb and DA-HCl-Co <sub>3</sub> O <sub>4</sub> for 10 min at 200 rpm. Dried at 30 °C for 24 h.	Retsch-PM-100 planetary ball mill	Energy storage devices	[45]
Hb-DA-Fe <sub>2</sub> O <sub>3</sub>	Ball milling of DA-HCl and Fe <sub>2</sub> O <sub>3</sub> for 10 min at 350 rpm. Ball milling of Hb and DA-HCl-Fe <sub>2</sub> O <sub>3</sub> for 10 min at 350 rpm. Dried at 30 °C for 24 h.	Retsch-PM-100 planetary ball mill	Optoelectronic devices	[46]
LAC-DA-Fe <sub>2</sub> O <sub>3</sub>	Ball milling of iron precursor and orange peel waste for 15 min at 350 rpm. Ball milling of laccase, DA-HCl and Fe <sub>2</sub> O <sub>3</sub> for 10 min at 350 rpm. Dried at 100 °C for 24 h and heated up at 300 °C.	Retsch-PM-100 planetary ball mill	Electrocatalytic reduction of oxygen	[47]

### Mechanochemically prepared bio-based catalysts for biomass conversion.

Other novel and captivating examples of mechanical-synthetic protocols describe the preparation of bio-template nanocatalysts used for the biomass conversion, as schematized in Fig. 12.

**Fig. 12** Mechanochemically synthesized bio-based catalysts for biomass conversion.

This paragraph combines the two aspects previously presented: the mechanochemical-assisted synthesis of nanocatalysts for biomass conversion and the mechanical preparation of bio-based materials. Recently, a humins valorization through a mechanical-assisted preparation of humin-based iron oxide nanocatalysts was reported [48]. Humins are a class of biowaste organic compounds derived from the catalytic conversion of biomass in acid conditions. However, they are generally an undesirable feedstock for chemical purposes. In the mechanical-assisted process  $\text{FeNO}_3 \cdot 9\text{H}_2\text{O}$  and  $\text{FeCl}_2 \cdot 4\text{H}_2\text{O}$  were used as iron precursors and these chemicals were milled with 4 g of humins in a planetary ball mill for 45 min at 350 rpm. Materials were subsequently dried at 100 °C for 12 h in the oven and finally subjected to a calcination for 4 h at 400 °C.

The so-prepared catalysts were tested in a reaction for biomass valorization. The catalysts displayed a significant activity in the production of vanillin from isoeugenol, obtaining conversion >87%. For the first time, humins were employed as sacrificial template for the mechanochemical preparation of catalysts for biomass conversion to obtain high added-value products like vanillin.

In a more recent work, mechano-chemically prepared polysaccharides-based niobium nanomaterials were tested in the same isoeugenol oxidation reaction [49]. The mechanical-assisted preparation of the novel nanocatalysts was performed milling, at 350 rpm for 30 min, a niobium precursor and polysaccharides, derived from natural source and employed as sacrificial templates. Sequentially, the materials were oven-dried at 100 °C for 24 h and calcined at 600 °C for 3 h. In this study, niobium-based biotemplate composites were prepared using a green and facile mechanical-assisted process, milling a niobium precursor and different polysugars. The so-prepared

materials allowed isoeugenol conversion up to 60% with selectivity to vanillin up to 60%, as Fig. 13 schematically showed.

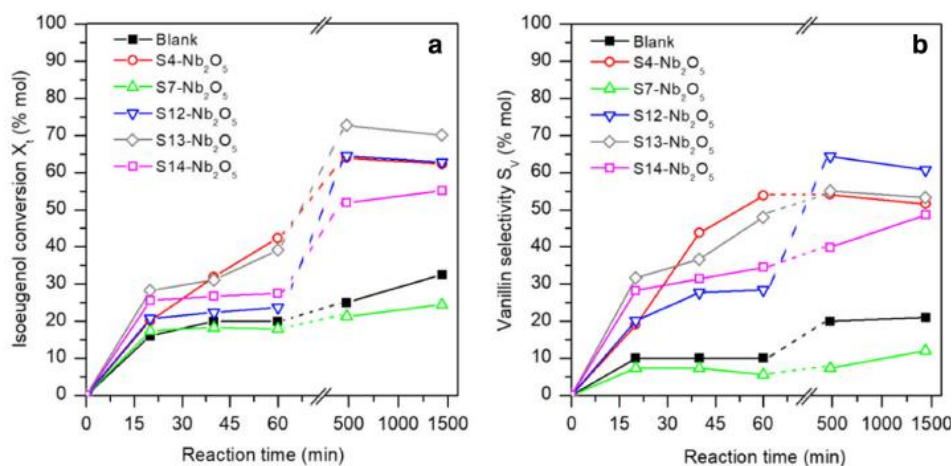


**Fig. 13 a** Isoeugenol conversion (%) and **b** vanillin selectivity (%) of mechanochemically prepared polysaccharide-based Nb catalysts. Reproduced from Ref. [49].

The synthetic methods and applications in the conversion of biomass of the mechanochemically obtained bio-based materials are summarized in Table 4.

**Table 4.** Summary of mechanochemically prepared bio-based catalysts for biomass conversion.

Catalyst	Biomass template	Preparation method	Equipment	Application	Ref.
Humin-based iron oxide catalysts	Humins	Ball milling of $\text{FeNO}_3 \cdot 9\text{H}_2\text{O}$ or $\text{FeCl}_2 \cdot 4\text{H}_2\text{O}$ with 4 g of humins for 45 min at 350 rpm. Materials were dried at 100 °C for 12 h and finally subjected to a calcination for 4 h at 400 °C.	Retsch-PM-100 planetary ball mill	Oxidation of isoeugenol to vanillin	[48]
Polysaccharide-based niobium composites	Polysaccharide	Ball milling of ammonium niobate (V) oxalate hydrate and polysaccharide in a planetary ball for 30 min at 350 rpm; then oven-dried at 100 °C for 24 h and calcination at 600 °C for 3 h.	Retsch-PM-100 planetary ball mill	Oxidation of isoeugenol to vanillin	[49]

## Conclusions and perspectives

Selected literature examples have been used to highlight the potential and broad perspectives of the mechanical-assisted preparation of advanced catalytically active nanomaterials. Particular emphasis was given to stability and activity enhancement in view of their utilization in biomass conversion and to the mechanical-assisted synthesis of bio-based nanocatalyst. In many cases, mechanically prepared nanocatalysts exhibited comparable or improved catalytic activities respect to the activities observed in nanocatalysts synthesized by traditional methods. The described examples clearly highlighted the extraordinary characteristics of mechanochemistry. These features include greater efficiency in terms of time, costs, sustainability and reproducibility as well as the possibility to discovery new products unreproducible with traditional techniques. In addition, the solventless quality of mechanochemistry implies greener reaction conditions, low E-factor and high atom efficiency.

The chemical industry has already started the transition to sustainable technologies, including some application of mechanochemistry. Remarkably, also various patents have been successfully published [50]. One extraordinary step will be the application of biomass into mechanochemistry for the massive production of bio-based materials, in order to full fill the concept of a green economy free of petroleum-based chemicals.

## Abbreviations

g-C<sub>3</sub>N<sub>4</sub>: Graphitic carbon nitride; 5-MFA: 5-methylfurfuryl alcohol; Hb: Horse hemoglobin; Co<sub>3</sub>O<sub>4</sub> MNPs: cobalt oxide magnetic nanoparticles; DA: dopamine; DA-HCl: dopamine hydrochloride; LAC: laccase.

## **Acknowledgments**

The authors gratefully acknowledge MINECO for funding under project CTQ2016-78289-P, co-financed with FEDER Funds including a contract for Camilla Cova in the framework of such project. The publication has been prepared with support from RUDN University Program 5-100.

## **Funding**

This work was conducted in the framework of MINECO project CTQ2016-78289-P. The funding body (MINECO, Spain) provided support for the design of the study, analysis and interpretation of data and in writing the manuscript.

## **Availability of data and materials**

This is a review paper and does not contain original data, which can be put in an open repository database.

## **Authors' contributions**

RL conceived of the study and participated in its design and coordination as well as revised/finalized the manuscript for submission. CC made the most substantial contributions to the draft writing of the manuscript. Both authors read and approved the final manuscript.

## **Ethics approval and consent to participate**

Not applicable.

## **Consent for publication**

Not applicable.

## **Competing interests**

The authors declare that they have no competing interests.

## References

1. Fernandez-Bertran JF. Mechanochemistry: an overview. *Pure Appl Chem.* 1999;71(11):581-6.
2. Takacs L. Quicksilver from Cinnabar: The first documented mechanochemical reaction? *J. Minerals Metals & Mater. Soc.* 2000;52(1):12-3.
3. Takacs L. The mechanochemical reduction of AgCl with metals. *J. Thermal Anal. Calor.* 2007;90:81-4.
4. Takacs L. M. Carey Lea, the first mechanochemist. *J. Mater. Sci.* 2004;39(16-17):4987-93.
5. Petruschke M. Tribochemistry. von G. Heinicke. *Acta Polym.* 1985;36(7):400-1.
6. James SL, Adams CJ, Bolm C, Braga D, Collier P, Friscic T, Grepioni F, Harris KDM, Hyett G, Jones W, Krebs A, Mack J, Maini L, Orpen AG, Parkin IP, Shearouse WC, Steed JW, Waddell DC. Mechanochemistry: opportunities for new and cleaner synthesis. *Chem. Soc. Rev.* 2012;41(1):413-47.
7. Xu CP, De S, Balu AM, Ojeda M, Luque R. Mechanochemical synthesis of advanced nanomaterials for catalytic applications. *Chem. Commun.* 2015;51(31):6698-713.
8. Balaz P, Achimovicova M, Balaz M, Billik P, Cherkezova-Zheleva Z, Criado JM, Delogu F, Dutkova E, Gaffet E, Gotor FJ, Kumar R, Mitov I, Rojac T, Senna M, Streletskii A, Wieczorek-Ciurova K. Hallmarks of mechanochemistry: from nanoparticles to technology. *Chem. Soc. Rev.* 2013;42(18):7571-637.
9. Haas-Santo K, Fichtner M, Schubert K. Preparation of Microstructure Compatible Porous Supports by Sol-gel Synthesis for Catalyst Coatings. *Appl. Catal., A.* 2001;220(1-2):79-92.
10. Colmenares JC, Aramendía MA, Marinas A, Marinas JM, Urbano FJ. Synthesis, Characterization and Photocatalytic Activity of Different Metal-Doped Titania Systems. *Appl. Catal., A.* 2006;306:120-27.
11. Zuliani A, Balu AM, Luque R. Efficient and Environmentally Friendly Microwave-Assisted Synthesis of Catalytically Active Magnetic Metallic Ni Nanoparticles. *ACS Sustainable Chem. Eng.* 2017;5(12):11584-87.
12. Zuliani A, Ranjan P, Luque R, Van der Eycken V. Heterogeneously Catalyzed Synthesis of Imidazolones via Cycloisomerizations of Propargylic Ureas Using Ag and Au/Al SBA-15 Systems *ACS Sustainable Chem. Eng.* 2019;doi: 10.1021/acssuschemeng.9b00198.

## Introduction

13. Jodlowski AD, Yopez A, Luque R, Camacho L, de Miguel G. Benign-by-Design Solventless Mechanochemical Synthesis of Three-, Two-, and One-Dimensional Hybrid Perovskites. *Angew. Chem. Int.* 2016;55(48):14972-7.
14. Kamolphop U, Taylor SFR, Breen JP, Burch R, Delgado JJ, Chansai S, Hardacre C, Hengrasmee S, James SL. Low-Temperature Selective Catalytic Reduction (SCR) of NO<sub>x</sub> with n-Octane Using Solvent-Free Mechanochemically Prepared Ag/Al<sub>2</sub>O<sub>3</sub> Catalysts. *ACS Catal.* 2011;1:1257-62.
15. Pardeshi SK, Patil AB. Effect of morphology and crystallite size on solar photocatalytic activity of zinc oxide synthesized by solution free mechanochemical method. *J. Mol. Catal. A.* 2009;308(1-2):32-40.
16. Ralphs K, Hardacre C, James SL. Application of heterogeneous catalysts prepared by mechanochemical synthesis. *Chem. Soc. Rev.* 2013;42(18):7701-18.
17. Dodd A, McKinley A, Saunders M, Tsuzuki T. Mechanochemical synthesis of nanocrystalline SnO<sub>2</sub>-ZnO photocatalysts. *Nanotechnol.* 2006;17(3):692-8.
18. Luque R. Benign-by-design catalysts and processes for biomass conversion. *Current Op. Green Sust. Chem.* 2016;2:6-9.
19. Corma A, Iborra S, Velty A. Chemical routes for the transformation of biomass into chemicals. *Chem. Rev.* 2007;107:2411-502.
20. Ragauskas AJ, Williams CK, Davison BH, Britovsek G, Cairney J, Eckert CA, Frederick WJ, Hallett JP, Leak DJ, Liotta CL, Mielenz JR, Murphy R, Templer R, Tschaplinski T. The path forward for biofuels and biomaterials. *Science.* 2006;311:484-9.
21. Franco A, De S, Balu AM, Garcia A, Luque R. Mechanochemical synthesis of graphene oxide-supported transition metal catalysts for the oxidation of isoeugenol to vanillin. *Beilstein J. Org. Chem.* 2017;13:1439-45.
22. Saberi F, Rodriguez-Padron D, Doustkhah E, Ostovar S, Franco A, Shaterian H, R Luque R. Mechanochemically modified aluminosilicates for efficient oxidation of vanillyl alcohol. *Catal. Commun.* 2019;118:65-69.
23. Cerdan K, Ouyang WY, Colmenares JC, Munoz-Batista MJ, Luque R, Balu AM. Facile mechanochemical modification of g-C<sub>3</sub>N<sub>4</sub> for selective photo-oxidation of benzyl alcohol. *Chem. Eng. Sci.* 2019;194:78-84.
24. Yopez A, Pineda A, Garcia A, Romero AA, Luque, R. Chemical transformations of glucose to value added products using Cu-based catalytic systems. *Phys. Chem. Chem. Phys.* 2013;15:12165-72.

25. Pineda A, Balu AM, Campelo JM, Romero AA, Carmona D, Balas F, Santamaria J, Luque R. A Dry Milling Approach for the Synthesis of Highly Active Nanoparticles Supported on Porous Materials. *Chemsuschem*. 2011;4(11):1561-5.
26. Kimling, M. C.; Caruso, R. A., Sol-gel synthesis of hierarchically porous TiO<sub>2</sub> beads using calcium alginate beads as sacrificial templates. *J. Mater. Chem*. 2012;22:4073-82.
27. Raveendran P, Fu J, Wallen SL. A simple and "green" method for the synthesis of Au, Ag, and Au-Ag alloy nanoparticles. *Green Chem*. 2006;8:34-8.
28. Chairam S, Poolperm C, Somsook E. Starch vermicelli template-assisted synthesis of size/shape-controlled nanoparticles. *Carbohydrate Polym*. 2009;75:694-704.
29. Vigneshwaran N, Nachane RP, Balasubramanya RH, Varadarajan PV. A novel one-pot 'green' synthesis of stable silver nanoparticles using soluble starch. *Carbohydrate Res*. 2006;341:2012-18.
30. Bozanic DK, Djokovic V, Blanusa J, Nair PS, Georges MK, Radhakrishnan T. Preparation and properties of nano-sized Ag and Ag<sub>2</sub>S particles in biopolymer matrix. *Eur. Phys. J. E*. 2007;22:51-9.
31. Cai J, Liu SL, Feng J, Kimura S, Wada M, Kuga S, Zhang LN. Cellulose-Silica Nanocomposite Aerogels by In Situ Formation of Silica in Cellulose Gel. *Angew. Chem.-Int. Ed*. 2012;51:2076-9.
32. El Kadib A, Molvinger K, Cacciaguerra T, Bousmina M, Brunel D. Chitosan templated synthesis of porous metal oxide microspheres with filamentary nanostructures. *Micropor. Mesopor. Mater*. 2011;142:301-7.
33. Sipos P, Berkesi O, Tombacz E, St Pierre TG, Webb J. Formation of spherical iron(III) oxyhydroxide nanoparticles sterically stabilized by chitosan in aqueous solutions. *Inorg. Biochem*. 2003;95:55-63.
34. Wang BL, Tian CG, Wang L, Wang RH, Fu HG. Chitosan: a green carbon source for the synthesis of graphitic nanocarbon, tungsten carbide and graphitic nanocarbon/tungsten carbide composites. *Nanotechnol*. 2010;21(2).
35. Laudenslager MJ, Schiffman JD, Schauer CL Carboxymethyl Chitosan as a Matrix Material for Platinum, Gold, and Silver Nanoparticles. *Biomacromolecules*. 2008,9:2682-5.
36. Schneidermann C, Jackel N, Oswald S, Giebeler L, Presser V, Borchardt L. Solvent-Free Mechanochemical Synthesis of Nitrogen-Doped Nanoporous Carbon for Electrochemical Energy Storage. *Chemsuschem*. 2017;10(11):2416-24.



## Introduction

37. Schneidermann C, Kensity C, Otto P, Oswald S, Giebeler L, Leistenschneider D, Gratz S, Dorfler S, Kaskel S, Borchardt L. Nitrogen-Doped Biomass-Derived Carbon Formed by Mechanochemical Synthesis for Lithium-Sulfur Batteries. *Chemsuschem*. 2019;12(1):310-9.
38. Schnepf Z, Hall SR, Hollamby MJ, Mann S. A flexible one-pot route to metal/metal oxide nanocomposites. *Green Chem*. 2011;13:272-5.
39. Schnepf, Z.; Wimbush, S. C.; Mann, S.; Hall, S. R., Alginate-mediated routes to the selective synthesis of complex metal oxide nanostructures. *Crystengcomm*. 2010;12(5):1410-5.
40. Liu YD, Goebel J, Yin YD. Templated synthesis of nanostructured materials. *Chem. Soc. Rev*. 2013;42:2610-53.
41. Francavilla M, Pineda A, Romero AA, Colmenares JC, Vargas C, Monteleone M, Luque R. Efficient and simple reactive milling preparation of photocatalytically active porous ZnO nanostructures using biomass derived polysaccharides. *Green Chem*. 2014;16:2876-85.
42. Sheldon RA. Green solvents for sustainable organic synthesis: state of the art. *Green Chem*. 2005;7:267-78.
43. Sheldon RA. Green and sustainable manufacture of chemicals from biomass: state of the art. *Green Chem*. 2014;16:950-63.
44. Tsuzuki T, McCormick PG. Mechanochemical synthesis of nanoparticles. *J. Mater. Sci*. 2004;39:5143-6.
45. Rodriguez-Padron D, Puente-Santiago AR, Caballero A, Benitez A, Balu AM, Romero AA, Luque R. Mechanochemical design of hemoglobin-functionalised magnetic nanomaterials for energy storage devices. *J. Mater. Chem. A*. 2017;5:16404-11.
46. Rodriguez-Padron D, Jodlowski AD, de Miguel G, Puente-Santiago AR, Balu AM, Luque, R. Synthesis of carbon-based fluorescent polymers driven by catalytically active magnetic bioconjugates. *Green Chem*. 2018;20:225-9.
47. Rodriguez-Padron D, Puente-Santiago AR, Caballero A, Balu AM, Romero AA, Luque R. Highly efficient direct oxygen electro-reduction by partially unfolded laccases immobilized on waste-derived magnetically separable nanoparticles. *Nanoscale*. 2018;10:3961-8.
48. Filiciotto L, Balu AM, Romero AA, Rodriguez-Castellon E, van der Waal JC, Luque R. Benign-by-design preparation of humin-based iron oxide catalytic nanocomposites. *Green Chem*. 2017;19(18):4423-34.

49. Rincon E, Garcia A, Romero AA, Serrano L, Luque R, Balu AM. Mechanochemical Preparation of Novel Polysaccharide-Supported Nb<sub>2</sub>O<sub>5</sub> Catalysts. *Catalysts*. 2019;9:38.
50. Barge A, Baricco F, Cravotto G, Fretta R, Lattuada L, Ravizza C, Bracco Imaging SPA. Mechanochemical synthesis of radiographic agents intermediates. WO2018104228

## “Ride the wave!”: Microwave radiation

In the perspective of Green Chemistry, among the non-traditional techniques for organic synthesis, microwave radiation takes pride of place, so that this technique has been defined as the *technology of tomorrow* [1]. Specifically, this non-conventional heating method uses the capability of various materials (solids or liquids) to convert electromagnetic energy into heat [2].

**Microwave milestones.** The discovery of microwave heating has serendipitously occurred in 1945, while the World War II was raging, thanks to some studies related to radars' design. Percy Lebaron Spencer, a self-educated engineer, was involved in the study of magnetrons for radars when he observed the melting of a chocolate tablet placed in the pocket of his jacket. The engineer supposed that the radars had melted the tablet thanks to microwaves. Another anecdote tells that some popcorns in Spencer's pocket began to pop while the man was in the proximity of a microwave source. Successively, the first microwave oven was proposed by Tappan in collaboration with Raytheon, by the middle of the twentieth century. It was necessary to wait until the early 70s to find the first microwave-irradiation application in an inorganic chemistry research. This study concerned the decomposition of organic molecules applying a gas phase discharge. During the same period, microwave ovens became very helpful for domestic use. In 1978, the first commercial oven was introduced by CEM Corporation. As far as organic chemistry is concerned, studies about microwave applications appeared in the 80s, when two patents were published: one related to the derivatization of starch and the other related to polymerization [3,4]. Figure 1 gives a summary of the milestones of microwave evolution.

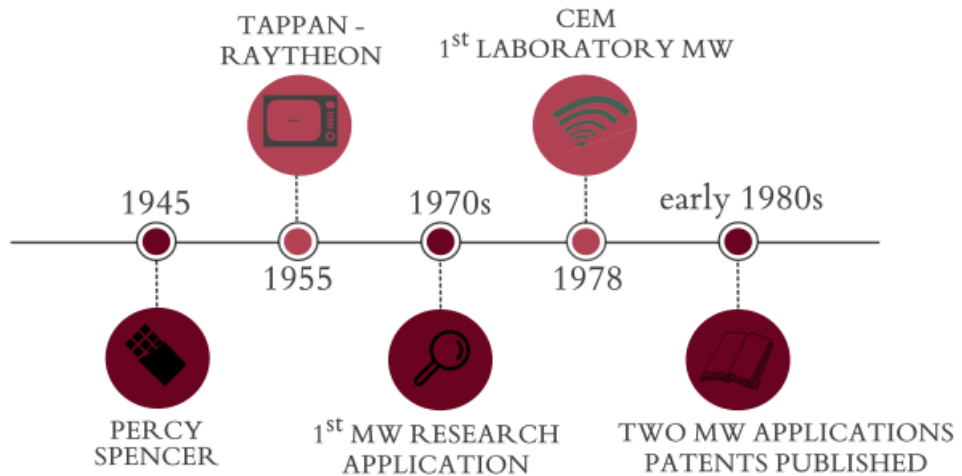


**Fig. 1** Milestones of the evolution of microwave along with the frequencies values.

**Principles and microwave theory.** In the electromagnetic spectrum, the microwave region lies between infrared and the radiofrequencies. Therefore, microwave frequencies are between 0.3 GHz and 300 GHz and microwaves wavelengths range between 1 cm and 1 m [5-7], as showed in Figure 2.

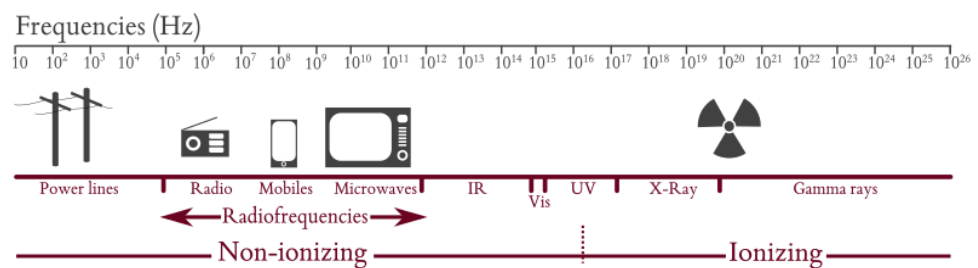


**Fig. 2** Illustration of the electromagnetic spectrum.

As all the electromagnetic radiations, microwave radiation can also be subdivided into two components, one related to the electric field and the other one to the magnetic field. The electric component of an electromagnetic wave generates heat through two principal mechanisms: dipolar polarization and ionic conduction [3,8].

The first one is defined as the interaction between the matter and the electric field. In general, a molecule can produce heat when is exposed to

microwave irradiation only if it is characterized by a dipole moment. When a sample is irradiated with microwave radiations, it realigns its dipoles according to the electric field. As the field oscillates, the dipoles effort to readjust themselves in accordance with the oscillating field and the energy is lost as heat through dielectric losses and molecular frictions. Therefore, the ability of a material to generate heat is correlated to its aptitude to align its dipoles with the electric field.

The second heating process is the ionic conduction mechanism and this effect is more important than the former effect. As it is concerned with this second mechanism, the ions in a matrix oscillate and they collide with molecules or atoms, causing motion or agitation, therefore generating heat.

**Dielectric properties.** The interaction of microwaves with matter is characterized by three different processes: absorption, reflection and transmission [9-11]. Depending on the interaction of the microwaves with the matter, materials can be distinguished according to the following three groups:

1. Microwave-transparent materials: materials with low dielectric loss or insulators (*e.g.*, glass, teflon or quartz,) that allow the wave to pass through the matter with only a little attenuation.
2. Absorbers materials: dielectric materials able to absorb the electromagnetic wave and transform it into heat (*e.g.*, water, methanol).
3. Microwave-reflective materials: electrical conductors with free electrons (*e.g.*, metals) which reflect radiation and do not allow the electromagnetic wave to penetrate the material.

**Microwave vs conventional heating.** Microwave heating takes place at the molecular level, coupling with the molecules of the mixture thus leading to very fast reactions. When microwave irradiation is applied, energy interacts with molecules at such high speed that molecules do not have time to relax.

Therefore, the generated heat can be much higher than the recorded temperature of the reaction of the mixture at some moments, *i.e.* there could be a localized superheating [12].

In contrast, traditional heating is a slow and inefficient route for the heat transmission to the sample as it is determined by thermal conductivity of the reaction mixture and by convection currents. Furthermore, the reactor walls can absorb some of the heat making the heating more inefficient. Consequently, conventional reactions usually take longer reaction times than the ones accomplished by microwave heating [13].

The main differences between microwave and traditional heating are illustrated in Table 1.

**Table 1** Differences between microwave and traditional heating.

Microwave heating	Conventional heating
Energetic coupling	Convection/conduction
Coupling at the molecular level	Superficial heating
Fast	Slow
Volumetric	Superficial
Specific and selective	Nonspecific
	Less dependent on materials
Dependent on the properties of the molecules	Dependent on reactor size/type and thermal conductivity of reaction mixture

**Effects of microwave heating.** Microwave effects cannot normally be observed with conventional heating. Basically, two different types of effects could be recognized in the microwave phenomena [14,15]:

1. Thermal effects
2. Specific microwave effects

The thermal/kinetic effects derive from the high temperatures that could be achieved when a substance is heated with microwave radiation. When

irradiating in a microwave field, a solvent can be quickly superheated reaching much higher temperatures than its boiling point; such situation is not reproducible with conventional heating. Therefore, kinetic/thermal effects can explain reported rate enhancement, due to the extremely high temperatures observable and due to the rapid heating.

The second type of effects, called specific microwave effects, are ascribable to the dielectric heating mechanism. These effects are definite as chemical transformations than cannot be reproduced with traditional heating and could be summarized as follows:

1. Superheating effect of solvents at atmospheric pressure
2. Differential heating of liquid/liquid biphasic mixtures
3. Mass heating/volumetric heating
4. Selective heating
5. Wall effects

**Microwaves advantages.** Microwave-assisted processes have numerous advantages over conventional heating [16,17], counting reduction in reaction times and minimization of solvents waste, reduction of energy consumption, utilization of low solvent volumes and improvement of yields and selectivity coupled with easy work-up. Moreover, microwave heating fits with sustainable procedures and most of the merits of microwave-assisted processes reflects the 12 principles of Green Chemistry [18,19], as listed below.

1. **Fast reaction.**
2. **Accurate process control**
3. **Space-saving**
4. **Energy-saving**
5. **Rapid startup and shutdown**
6. **Upgraded working conditions**

**Microwave equipment.** Two different types of microwave reactors are normally employed for academic research [20-22].

1. Multimode microwave reactors: in this apparatus more than one batch could be processed. However, the emitted radiation is not uniform inside the matrix. Therefore, the distribution of the electric and magnetic field can be obtained rotating the samples or employing a stirrer.
2. Single-mode microwave reactors: in this apparatus the processing of only one sample is permitted. This tool allows to achieve a homogeneous distribution of the electric field in the matrix. The sample is located where the electric and magnetic components have the highest intensities. This kind of instruments emits less power but has a high return of energy. Hence the mono-mode reactor is more efficient in terms of energy and leads to the best yields.

**Microwaves for biomass and waste valorization.** Waste and biomass can be transformed into a large number of value-added chemicals, platforms and materials [12,23-27]. However, traditional thermal procedures suffer a lot of disadvantages and drawbacks. One of the disadvantages of conventional heating is due to heat transfer processes which limit the efficiency of the processes [28]. The main benefit of the use of microwave heating with respect to the conventional counterpart is the energy transfer through radiation rather than convection or heat transfer. This advantage guarantees that the energy penetrates the materials and the consequent energy release is very fast, hence the matter is instantaneously heated. Consequently, microwave radiation can generate significantly higher temperatures at the center of the materials than in the neighboring matters, while the outer parts and the walls of the container are normally hotter under traditional thermal heating [29]. As a result, the microwave procedures decrease the time of reaction, increasing yields and



selectivities, reducing reagents and energy consumption and improving products quality [12,30].

Three principal mechanisms are implicated in the interaction between the microwave field and biomass [28]:

1. Dielectric polarization. This first effect is the principal mechanism and is due to the presence of oxygenated species and water into biomass and waste.
2. Currents of free charges. This second mechanism is typical of catalyst that are characterized by significant conductivity. These currents contribute to the heating of the materials because of Ohmic losses.
3. Loss of vortex currents. These currents are excited by magnetic fields.

The use of microwave heating is a rapidly growing research field thanks to which it is possible to reach high reaction rates and remarkable selectivities along with noteworthy reductions in energy consumption and processes times.

Furthermore, it is possible to obtain more reproducible procedures thanks to the use of a new generation of microwave equipment including "mono-mode" and "multi-mode" equipment that allow very precise control of the reaction conditions. In addition, these modern instruments allow the exploitation of valorization of biomass to a pilot/industrial scale. As a result, in the last years, numerous microwave-assisted protocols have been proposed for waste/biomass conversion to highly valuable chemicals, counting transformations of biomass-derived platform molecules, such as levulinic acid, furfural, xylose, benzyl alcohol or isoeugenol [31-60]. An overview of the microwave-assisted processes for the conversion of biomass into some of the chemical platforms is provided.

Among various biomass-derived products, 5-hydroxymethylfurfural (5-HMF), which can be synthesized by the dehydration of glucose, fructose, sucrose, inulin, starch or cellulose, emerged as one of the most attractive and

promising platform compounds [61,62]. Indeed, 5-HMF can be converted into various high-quality fuels, such as 2,5-dimethylfuran (DMF) or ethyl levulinate, and can be transformed into a large number of high value-added chemicals such as levulinic acid or 2,5-furandicarboxylic acid [63].

Among the others, the production of 5-HMF from inulin and fructose was carried out in an aqueous medium with a low loading of the catalyst (zirconium or niobium phosphate) by applying microwave irradiation [46]. The dehydrations were conducted in a mono-mode microwave reactor CEM Discover S-class System. Starting from fructose, the highest HMF yield (39.3 mol%) was obtained after 8.8 min, operating at 190 °C, using zirconium phosphate (ZrPO) as a catalyst. The dehydration of inulin carried out in the same reaction conditions for 10 min led to 42.1 mol% of HMF yield.

Biomass-derived 5-HMF was also obtained from the conversion of cellulose and xylan in a biphasic reaction system under microwave heating, using an acidified (HCl) phase and methyl isobutyl ketone (MIBK) as the organic phase [57]. A maximum 5-HMF yield of 43.3 mol% was achieved at 177 °C, concentration of HCl of 0.1285 M by performing the reaction for 60 min.

Another interesting value-added product is levulinic acid (LA). LA is considered one of the top building block chemicals as it is widely used in agricultural, food, medicine and fuels applications, and it can be converted into numerous valuable chemicals (such as gamma-valerolactone (GVL) or 2-methyltetrahydrofuran) [64].

Recently, a microwave-assisted conversion of LA to GVL has been conducted using iron oxide nanoparticles supported on porous silicates [42]. The tests were conducted on a pressure-controlled CEM Discover microwave reactor for 30 min at 150 °C under continuous stirring, employing formic acid as a hydrogen donating agent for the hydrogenation of LA. Fe-based catalysts

provided comparable LA conversions and GVL selectivities as compared to Pd-based hydrogenation reference catalysts under identical conditions. A maximum of 20-30 mol% of conversion and 64-78 mol% of selectivity were obtained.

An attractive biomass-derived chemical that can be used to replace petrochemicals is furfural (furan-2-carbaldehyde). This compound is generally synthesized in one or two steps based on the acid hydrolysis and dehydration of xylose [65].

Mazza *et al.* have studied the acid-catalyzed conversion of xylose and xylan to furfural by microwave-assisted reactions [35]. The production of furfural was carried out in an ETHOS EX Microwave Extraction System (Milestone, Italy) equipped with a 16 closed-vessel position carousel. The best results in terms of furfural yields (48.4%, 45.7%, and 72.1%) were achieved using a temperature of 180 °C, a solid:liquid ratio of 1:200, a residence time of 20 min, and a pH of 1.1 as parameters.

Labidi *et al.* have investigated the microwave-assisted conversion of hemicellulosic monomers into furfural using different acid catalysts [66]. Furfural yield of 37% was obtained performing the reaction at 180 °C, for 5 min and using 2% (v/v) as HCl concentration.

Another captivating biomass-derived molecule is benzyl alcohol, which can be converted to benzyl aldehyde. Indeed, benzaldehyde is a highly demanded product as it is widely used as ingredient in the food and pharmaceutical industry or as a fragrance for cosmetic formulations, or even as an intermediate in many chemicals synthesis.

Bio-nanocomposites synthesized from polysaccharides and iron precursors were tested in the oxidation of benzyl alcohol to benzaldehyde [49]. The microwave-assisted experiments were carried out in a CEM Discover microwave reactor at 300 W, using 25 mg of catalyst, 0.2 mL of benzyl alcohol,

0.3 mL of hydrogen peroxide in 2 mL of acetonitrile, performing the reaction for 5 and 10 min. After 10 min, the most active catalyst, Fe<sub>2</sub>O<sub>3</sub>-PS4, achieved conversion up to 45% with a remarkable selectivity to benzyl aldehyde up to 97.7%.

Most recently, Fe-catalysts supported on porous poly furfuryl alcohol (PFA) resins were tested in the selective conversion of benzyl alcohol to benzyl aldehyde using H<sub>2</sub>O<sub>2</sub> as the oxidant under microwave irradiation [54]. The experiments were carried out in a CEM Discover microwave reactor. The reactions were irradiated at 300 W, achieving temperatures in the 90-132 °C range and pressures from 5 to 17 bar. After 5 min of microwave irradiation, 22% of conversion with 78% of selectivity to benzaldehyde was observed.

Lastly, isoeugenol, a lignin-derived feedstock, could be converted to vanillin. Indeed, vanillin is a widely employed aromatic compound in cosmetic formulations and in the food industry. Recently, iron oxide nanocatalysts supported on mesoporous Al-SBA-15 were tested as catalysts in the conversion of isoeugenol to vanillin, using hydrogen peroxide [55]. The microwave-assisted reactions were carried out in a CEM Discover focused, using 1.25 mmol of isoeugenol and 2.9 mmol of hydrogen peroxide in 2 mL of CH<sub>3</sub>CN, with 25 mg catalyst at 90 °C at 300 W. After 5 min, high activities (60-80% conversion) and good selectivities to vanillin (54-65%) were achieved.

Vanillin could also be synthesized starting from vanillyl alcohol, a model lignin compound. Lin *et al.* have conducted a microwave assisted oxidation of vanillyl alcohol using metal organic frameworks (MOFs) as transition metal-containing heterogeneous catalysts [53]. A mixture of 0.15 g of vanillyl alcohol, 0.1 g of catalyst and H<sub>2</sub>O<sub>2</sub> solution (30%) was processed in a microwave reactor (Milestone Ethos UP, Italy) at 120 °C. The best results were obtained using MOF-801, reaching conversion >80% and selectivity to vanillin >30%. The catalyst showed also a good stability.

Table 2 summarizes all the reported examples of microwave-assisted protocols for biomass and waste valorization.

**Table 2** Summary of microwave-assisted reactions for biomass and waste valorization.

Catalyst	Application	Reaction conditions	Equipment	Conversion ( <i>C</i> ) Selectivity ( <i>S</i> ) Yield ( <i>Y</i> )	Ref.
ZrPO	Dehydration of inulin and fructose to 5-HMF	formic acid continuous stirring 150 °C 30 min	CEM Discover S-class System	<i>C</i> = 98.5% <i>S</i> > 99%	[46]
HCl	Conversion of cellulose and xylan to 5-HMF	25 mg of cellulose or xylan 250 µL acidified water 4.75 mL MIBK 800 rpm stirring rate 177 °C 800 W	Monowave 300, Anton Paar	<i>Y</i> = 43.3%	[57]
FeZrCF	Conversion of LA to GVL	0.1 mL levulinic acid 0.3 mL formic acid 200 °C 300 W 30 min	CEM Discover microwave reactor	<i>C</i> = 30% <i>S</i> = 78%	[42]
HCl 37% HNO <sub>3</sub> 70%	Conversion of xylose and xylan to furfural	solid:liquid ratio 1:200 pH 1.1. 180 °C 20 min	ETHOS EX Microwave Extraction System	<i>Y</i> = 72.1%	[35]
HCl	Furfural production from corn cobs autohydrolysis liquors	2% (v/v) HCl 180 °C 5 min	CEM Discover microwave reactor	<i>Y</i> = 37.06%	[66]
Bio-nanocomposite based on polysaccharide and iron oxide	Oxidation of benzyl alcohol to benzaldehyde	25 mg of catalyst 0.2 mL benzyl alcohol 0.3 mL H <sub>2</sub> O <sub>2</sub> 2 mL CH <sub>3</sub> CN 300 W 10 min	CEM Discover microwave reactor	<i>C</i> = 45% <i>S</i> = 97.7%	[49]
Iron catalyst supported on P500 resin	Oxidation of benzyl alcohol to benzaldehyde	benzyl alcohol (1.92 mmol) 2 mL CH <sub>3</sub> CN 0.3 mL 33 or 50 w/v% H <sub>2</sub> O <sub>2</sub> 300 W 5 min	CEM Discover microwave reactor	<i>C</i> = 22% <i>S</i> = 78%	[54]
Iron oxide supported on Al-SBA-15	Oxidation of isoeugenol to vanillin	1.25 mmol isoeugenol 2.9 mmol H <sub>2</sub> O <sub>2</sub> 2 mL CH <sub>3</sub> CN 25 mg catalyst 90 °C 300 W 5 min	CEM Discover microwave reactor	<i>C</i> = 80% <i>S</i> = 65%	[55]
MOFs	Oxidation of vanillyl alcohol to vanillin	0.15 g vanillyl alcohol 0.1 g of catalyst H <sub>2</sub> O <sub>2</sub> solution (30%) 120 °C	Milestone Ethos UP	<i>C</i> > 80% <i>S</i> > 30%	[53]

## “Roll with the flow!”: Continuous flow chemistry

Continuous-flow processes are defined as protocols carried out in continuous-flowing streams.

Recently, flow chemistry has been included among one of the tools to achieve some of the United Nations Sustainable Development Goals (Fig. 3), whose target is to reach a more sustainable and better future by 2030 [67]. In particular, continuous-flow chemistry, where the experiments are accomplished in continuous flow reactors rather than in batch conditions, is particularly crucial to accomplish SDG12: responsible production and consumption [68].



**Fig. 3** Schematic representation of the United Nations Sustainable Development Goals. Data source: <https://www.un.org/sustainabledevelopment/sustainable-development-goals/> [67].

Furthermore, IUPAC has recently outlined the “top ten chemical innovations that will change our world” which could have *the potential to*

*make our planet sustainable*. Among these revolutionary technologies, IUPAC has also named flow chemistry [68]. Indeed, continuous-flow reactors can offer numerous advantages including the consumption reduction by using small volumes of solvents and small amounts of chemical reagents [69]. Moreover, flow chemistry processes can drastically reduce the risk of handling hazardous substances and can enhance reaction yields and selectivities, limiting the environmental impact.

As stated by Vaccaro *et al.*, flow chemistry can be a perfect match to green chemistry in order to achieve sustainability, delivering new routes to make processes more sustainable [70]. This novel technology can build a bridge between the academic and the industrial world. Indeed, in terms of production, continuous flow procedures are more effective than batch ones and offer much higher reaction throughput per unit of time and volume, providing safer, more scalable, efficient and reproducible performances [71-74].

Continuous flow reactors have already been used in chemical industries for over a hundred years. During this past century, the progress in flow chemistry has been remarkable and has led to significant upgrades in terms of safety, reduction of energy consumption and access to a broader variety of reaction conditions.

**Principles, advantages and challenges of flow-chemistry.** Essentially, in a continuous flow process, the chemicals are constantly introduced into the flow reactor and reactions take place at the point of contact with the catalytic material at a well-defined temperature, flow rate and pressure. Then, the products of the reaction leave the reactor in a continuous manner, as represented in Figure 4.

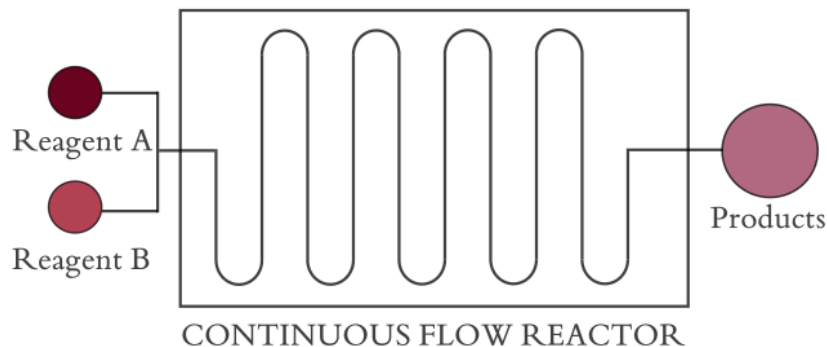


**Fig. 4** Schematic representation of a continuous flow reactor.

It has been widely verified that flow-chemistry offers numerous merits in chemical synthesis that perfectly fit with various green metrics [71,75-79]. The advantages are enumerated and explained below:

1. **Waste minimization.** In general, the largest contribution in the generation of waste in a chemical process is given using solvents for carrying out the reaction as well as for the purification and isolation of the products [80]. Continuous flow reactors are effective tools for the minimization of wastes, reaching a high environmental and chemical efficiency. In fact, in these protocols, the starting materials can be added in equimolar quantities and solvents can be used in the minimum amount. Additionally, the exploitation of a heterogeneous catalyst helps to reduce waste since it may be easily recoverable and reusable.
2. **Reduction of reaction times.** Continuous flow processes tend to shorten reaction times as compared to traditional batch processes [81]. This technology allows multistep synthesis which is very efficient in avoiding the consumption of time needed to separate and isolate the reaction intermediates.
3. **Optimization for time screening and automation.** Using flow chemistry, it is possible to reduce the quantity of reactants used and the time required



for the reaction in a very flexible way compared to standard batch processes. In particular, this methodology reduces the use of expensive starting materials thanks to the small volumetric capacity of the reactor. Furthermore, flow technology minimizes the screening time to obtain the best reaction conditions by exploiting automation; this allows to test hundreds of reaction parameters and conditions per hour [82]. Therefore, the easily optimization of several crucial process parameters (pressure, temperature, flow rate, reaction time, catalyst quantity and reagents concentration) with high-throughput technologies leads to quickly obtain the best yields, conversions and selectivity.

4. **Enhanced process safety.** The application of flow procedures is useful to improve chemical safety because it is advantageous in the exploitation of unstable intermediates, in the handling of dangerous chemicals or of highly toxic reagents by reducing the amount of said chemicals in a given space [83-86]. As a result, flow chemistry is a strategic instrument to improve the safety of a process carried on an industrial scale. Indeed, in flow conditions side-reactions and the formation of unwanted, dangerous and toxic products which must be otherwise isolated and separated are drastically reduced [78,87,88].
5. **Scalability and process intensification.** Flow reactors allow to improve the efficiency of a chemical transformation thanks to quicker reaction times and higher productivity obtained per unit of time and volume [89,90].
6. **Cost and energy efficiency.** Cost and energy efficiency are interconnected requirements that every environmentally friendly procedure should satisfy. Under flow conditions it is possible to plan a process scale-up, to enhance mass/heat transfer and to avoid the

purification of intermediates. Moreover, flow methodology could be implemented with *in-line* purification techniques such as micro-distillation and liquid-liquid extraction [88].

7. **Precise reaction parameters control.** Process parameters such as flow rate, pressure and temperature can be much more controlled in flow processes with respect to batch ones. As a result, flow processes are characterized by an outstanding reproducibility [75].
8. **Excellent selectivity and yields.** As described in the point 3, the possibility to screen and optimize various parameters with an easy method in flow conditions leads to achieve high selectivity, conversion and yields [91].

Along with all these advantages in the use of flow processes, unfortunately, flow-chemistry has to face with some challenges such as difficulties in having solids as starting chemicals, by-products or final products. Lastly, commercially available flow reactors still have demanding investment costs [88].

Nevertheless, different companies have exploited flow systems and patented some continuous flow procedures. Recently, Merck showed that through a flow process it is possible to synthesize a drug for the treatment and cure of Alzheimer's at industrial scale. Another recent example of big scale production includes the flow production of ciprofloxacin, an antibiotic [92].

**Equipment for continuous-flow chemistry.** With respect to the development of this Doctoral Thesis, a lab scale single flow hydrogenation reactor has been used. The H-Cube<sup>®</sup> Mini Plus is a powerful, safe and emerging flow reactor which produces *in situ* high pressure hydrogen through the electrolysis of water, allowing to accomplish hydrogenations from 0 to 100 bar and from room temperature to a maximum of 100 °C. The system permits to precisely set selected reactions parameters (temperature, pressure and flow rate).

**Flow-chemistry for biomass/waste valorization and flow-chemistry protocols for preparation of bio-based materials.** In the last decades, the society has begun a challenging shift to a bio- and waste-based circular economy. In this context, the design of catalysts for biomass and waste valorization is a very current topic. Indeed, in the last years, waste and biomass have appeared as renewable and alternative feedstock that can be transformed into high value-added such as chemicals and materials through sustainable and environmentally friendly paths including continuous flow processes [93,94]. In literature, several processes carried out in continuous flow conditions are reported, compounding also transformations of different biomass-derived platform molecules, such as furfural, levulinic acid, xylose, methyl/ethyl levulinate [95-106].

For example, Mika *et al.* [97] have reported the continuous flow synthesis of  $\gamma$ -valerolactone (GVL), which is a key intermediate in the biomass-based economy, from levulinic acid (LA) under 100 bar H<sub>2</sub> at 100°C with 99% conversion and >80% selectivity in most of the cases. Conversion of 83% was achieved using 5% Ru/C CatCart<sup>®</sup>. A significant increase in the conversion up to 98% was further observed adding Bu-DPPDS ligand.

More recently, the above-mentioned researchers have conducted the heterogeneous continuous flow hydrogenation of methyl levulinate and ethyl levulinate to GVL [106]. Indeed, as mentioned before, the valorization and transformation of biomass waste products has taken a key position in reaching the independence from fossil-based products. Therefore, the research on the valorization of biomass has identified novel platform chemicals, which could partially or completely substitute the building blocks currently used in the most known synthetic paths [107]. As a result, several studies have been conducted for the conversion of carbohydrates or lignin-fractions into platform chemicals including levulinic acid [43] or GVL [108]. Catalytic tests were carried out in a H-Cube<sup>®</sup> continuous flow reactor using two different standard 30 mm-long

CatCart<sup>®</sup>, 10%Pd/C and 5% Ru/C. Complete conversions of methyl and ethyl levulinate with 50% of selectivity towards GVL were accomplished with 5%Ru/C CatCart<sup>®</sup> at 100 °C with H<sub>2</sub> pressure fixed at 100 bar using water as solvent.

In 2017, Barta *et al.* have showed the hydrogenation of xylose to xylitol carried out in the same continuous flow hydrogenation reactor, using a Raney nickel catalyst and performing the experiments between 23-130 °C, with H<sub>2</sub> pressure between 20-95 bar and setting the flow rate between 1.5 and 14.5 ml min<sup>-1</sup> [101].

Alternatively, an interesting biomass-derived molecule is benzyl alcohol, which can be aerobically oxidized to benzaldehyde in continuous flow conditions. Benzyl aldehyde is a highly demanded chemical as it is widely used as a flavor in the cosmetic industry or as an ingredient in the pharmaceutical or in the food industry. In the last years, several groups have proposed strategies for the oxidation of benzyl alcohol in flow reactors. Kappe *et al.* achieved up to 42% of selective conversion to benzaldehyde using iron oxide nanoparticles supported on a mesoporous aluminosilicate (Al-SBA-15) and 5 mol% TEMPO as a co-catalyst [96]. Complete conversions were reached by continuous recycling of the mixture through the flow reactor.

Another aerobic alcohol oxidation in flow conditions is the conversion of vanillyl alcohol, a lignin-derived feedstock, into vanillin. The synthesis of this last chemical is of significant interest as vanillin is largely employed in the cosmetic and in the food industries thanks to its aroma.

Semenov *et al.* accomplished the oxidation of vanillyl alcohol under flow conditions using Pt- and Pd-based catalysts immobilized on Sibunit [95]. For platinum-based catalyst, conversions up to 87% and selectivities up to 93% were observed.

Our group has also been involved for some years in the development of flow processes for the valorization of biomass-derived molecules [109-125].

The continuous-flow hydrogenation of a biomass-derived and waste product, methyl levulinate, to GVL was also conducted in the continuous flow reactor Phoenix from ThalesNano<sup>TM</sup> Inc., using a Zr-based metal organic framework, UiO-66 [116]. Within the optimized conditions (0.23 g of catalysts, flow rate 0.2 mL min<sup>-1</sup>, 240 °C, 35 bar of system pressure) 83% of conversion to GVL was obtained, achieving selectivity up to 89%.

Moreover, a series of Ru/TiO<sub>2</sub> catalysts were used for the same application, *i.e.* the continuous flow hydrogenation of industrially derived methyl levulinate to GVL [120]. Tests were carried out in the liquid phase continuous flow reactor Phoenix from ThalesNano<sup>TM</sup> Inc. using *ca.* 300 mg of catalyst. The reaction solutions were prepared by diluting methyl levulinate into 2-propanol, the latter acting as transfer hydrogenated pressure. The best conditions were found to be 0.6 M methyl levulinate, 200 °C, 35 bar of back pressure and 0.3 mL min<sup>-1</sup>. Under these conditions, catalysts 5%Ru/TiO<sub>2</sub> showed remarkable performances (up to 96% of conversion and 98% of selectivity to GVL) and a great stability.

More recently, the selective continuous-flow hydrogenation of 5-hydroxymethylfurfural (5-HMF), a chemical obtained from the dehydration of lignocellulosic C<sub>6</sub> sugars, to 2,5-dimethylfuran (DMF) was carried out using Cu-Pd/RGO (RGO: reduced graphene oxide) [123]. The catalyst displayed outstanding performances with almost full conversion (96%) and very high DMF yield (95%) at the optimized conditions.

Table 3 summarizes all the examples of continuous-flow processes for biomass valorization.

**Table 3** Summary of continuous-flow reactions for biomass and waste valorization.

Catalyst	Application	Reaction conditions	Equipment	Conversion ( <i>C</i> ) Selectivity ( <i>S</i> )	Ref.
5%Ru/C	Hydrogenation of LA to GVL	0.015 mol L <sup>-1</sup> Bu-DPPDS ligand 100 bar H <sub>2</sub> 100 °C	H-Cube® H-Cube Pro™	<i>C</i> = 98.5% <i>S</i> > 99%	[97]
5%Ru/C	Hydrogenation of methyl and ethyl levulinate to GVL	0.1 mol L <sup>-1</sup> substrate in water 100 bar H <sub>2</sub> 100 °C 1 ml min <sup>-1</sup>	H-Cube®	<i>C</i> = 99.9% <i>S</i> = 50%	[106]
Raney-nickel catalyst	Hydrogenation of xylose to xylitol	95 bar H <sub>2</sub> 30 °C 10 ml min <sup>-1</sup>	H-Cube Midi	<i>C</i> > 99.9% <i>S</i> > 99.9	[101]
Fe/Al-SBA15	Oxidation of benzyl alcohol and alkylation of toluene	0.1 mol L <sup>-1</sup> in <i>n</i> -heptane-dioxane 2:1 25 bar O <sub>2</sub> at 5 mL min <sup>-1</sup> 140 °C 0.22 mL min <sup>-1</sup>	H-Cube Pro™	<i>C</i> = 100% <i>S</i> = 95%	[96]
2.3%Pt/Sibunit	Oxidation of vanillyl alcohol to vanillin	Air 1 mol L <sup>-1</sup> NaOH 80 °C	Quartz tube (7 mm diameter)	<i>C</i> = 87.2% <i>S</i> = 93.5%	[95]
UiO-66 (Zr)	Hydrogenation of methyl levulinate to GVL	0.23 g catalyst 35 bar 200 °C 0.2 mL min <sup>-1</sup>	Phoenix ThalesNano Inc.	<i>C</i> = 83% <i>S</i> = 89%	[116]
5%Ru/TiO <sub>2</sub>	Hydrogenation of methyl levulinate to GVL	300 mg catalyst 0.6 M methyl levulinate 35 bar H <sub>2</sub> 100 °C 0.3 ml min <sup>-1</sup>	Phoenix ThalesNano Inc.	<i>C</i> = 96% <i>S</i> = 98%	[120]
10Cu-1Pd/RGO	Hydrogenation of 5-HMF to DMF	15 bar 180 °C 0.2 mL min <sup>-1</sup> 2-propanol	Phoenix ThalesNano Inc.	<i>C</i> = 96% <i>S</i> > 99	[123]

A recent innovative approach in flow chemistry consists in the utilization of biological/natural compounds for the preparation of bio-based materials. In the last years, it has been demonstrated that continuous flow processes have numerous benefits, including faster and safer producers, easy scaling-up and simplification of the system's set-up. So, the field of bio/waste-materials for different applications still have room for improvement in terms of the design and development of synthetic paths using continuous-flow processes or microfluidics. For example, recently, an innovative chitosan-based material was prepared using a procedure employing a microfluidic-flow-step [126].

## **Biomass and waste valorization: case studies**

The following section aims at briefly describing the industrial and biological waste used in the scientific articles included in the Chapter “Results & Discussion”. Specifically, two waste materials are presented, *i.e.* pig bristles and the ceramic-cores of scrap automotive catalytic converters. In both cases, the annual production, the global market and the environmental impact of said waste are illustrated. The state-of-art regarding their reuse and recycling is also described.



## “Everything but the oink!”: pig bristles

“Think globally, act locally”. According to EUROSTAT statistics (European Union countries 28), 252 million pigs were slaughtered in the European Union in 2017. Since each slaughtered pig supplies about one kilogram of pig bristles, about 250 million tons of waste pig bristles are released every year [127-129]. Despite such a large amount, the research for new ways to exploit this industrial waste has not yet received many impulses. Boiled (sterilized) pig bristles are exclusively commercialized for brush factories. However, the production of brushes from pig bristles has always been limited to China. Until the 60s there was also a European brush manufacture which, however, disappeared rapidly due to the increasingly high industrialization of pig farms. In China, until the 80s, each family of farmers raised a dozen pigs and slaughtered about once a month, obtaining delicious meat and excellent quality pig bristles. To understand the value and the importance of the pig in Chinese peasant culture it is sufficient to know that the ideogram that expresses the word "family" is composed of the symbol of the word "home" placed above the symbol of the word "pig", sign of luck and prosperity (Fig. 5).



**Fig. 5** Chinese character for the word “family”.

Looking at the phrase “think globally, act locally”, which urges to recognize that markets are very different worldwide and to consider the health of the entire planet and to act in their own communities and cities [130-132], it

is right to consider that pig bristles are not a sufficiently exploited waste at the European level. Therefore, an improvement in the valorization and in the application of wasted pig bristles in the European Union is necessary and desirable.

**Pig bristles valorization and state-of-art.** In literature, there are only a limited number of studies available on the re-use of waste pig bristles. The few reported papers are limited to the use of pig bristles as food fodder supplements, thanks to the high protein content, and as material for brush industries [128,133-135], while their use as a chemical source is absolutely restricted.

Since the pig bristles are considered a raw material, free of toxic substances, easily-collectable, and accessible on an industrial scale, its valorization and application would really be a good opportunity. Furthermore, this waste is an unexploited source of sulfur and carbon. Moreover, like any commercially available product, sterilized pig bristles could be easily collected and studied on a laboratory scale in order to provide potential paths for the valorization at an industrial scale. Therefore, a very captivating challenge is the valorization of pig bristles to produce chemical materials.

**Composition of pig bristles.** The general chemical composition of pig bristles, almost like human hair, is 45 % of carbon, 28 % of oxygen, 15 % of nitrogen, 6.7% of hydrogen and 5.3% of sulfur [133,136,137]. Moreover, various trace elements are present (Ca, Mg, Sr, B, Al, Si, Na, K, Zn, Cu, Mn, Fe, Ag, Au, Hg, As, Pb, Sd, Ti, W, Mo, I, P, Se). Pig bristles contain primarily keratin ( $\geq 90\%$ ), an insoluble protein packed with cross-linked fibers by disulfide bonds [128,136,138]. Keratin is known for its high mechanical stability, insolubility and recalcitrance to degradation by common proteolytic enzymes such as papain, trypsin, and pepsin [139,140]. Keratin is particularly rich in cysteine (a type of sulfureted aminoacid), which forms disulfide bonds between molecules,

## Introduction

adding rigidity and resistance to the entire structure. Cysteine is the main aminoacid present in keratin (17.5%), followed by serine and glutamic acid, 11.7% and 11.1% respectively. Glycine, threonine and arginine are instead present in smaller percentages (*ca.* 5%) [138].

## “Pedal to the metal!”: scrap automotive catalytic converters

**Catalytic converters market.** According to the statistics, the automobile catalytic converter market will be valued at approximately USD 185 billion by 2022, with an average growth rate (AGR) of *ca.* 3% yearly over the next five years [141], as illustrated in Figure 6.

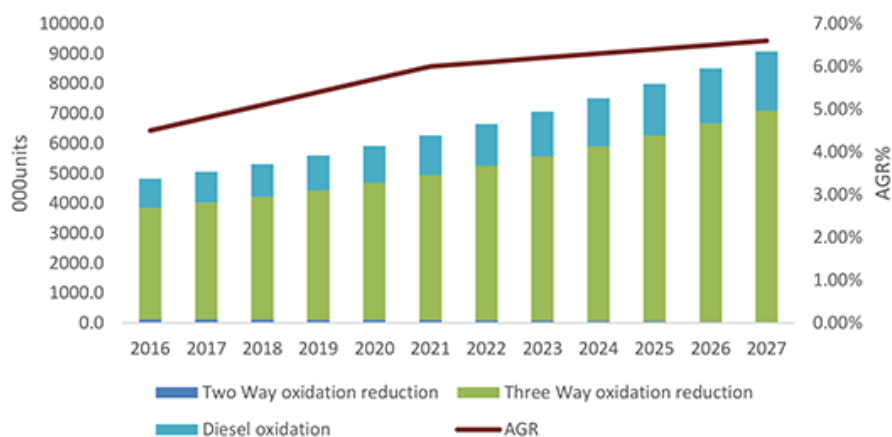


**Fig.6** Representation of global automotive catalytic converter market.

In upcoming years, the catalytic converters marketplace should see noteworthy developments due to an improvement of security measures, and an upgrade in the operational and energy efficiency. Moreover, the increase in manufacturing, selling and the intensification of strict vehicle emission protocols and rules established by governments should complement total marketplace development in the foreseeable future.

Worldwide, the market is partitioned into North America, Europe, Pacific Asia, Latin America, Middle East and Africa (the last three area are also known with the acronym “LAMEA”). Europe has the largest share of the entire catalytic converter market in terms of profits, followed by Pacific Asia and North America. The market of automotive catalytic converters is segmented according to type, noble metal content and geography. It is possible to distinguish between diesel oxidation catalyst, two-way catalytic and three-way

catalytic converters. Automotive catalytic converters can contain, among others, platinum, rhodium or palladium. Finally, catalytic converters can be subdivided according to the place of production, *i.e.* Europe, North America, LAMEA and Pacific Asia.

Every year, end-of-life vehicles (ELVs) generate *ca.* 8-9 million tons of valuable wastes in the European Union alone. The Directive 2000/53/EC, otherwise referred to as "ELV Directive", seeks to dismantle and recycle end-of-life vehicles through more sustainable and environmentally friendly procedures [142,143]. The directive fixes specific targets for recovery, recycling and reuse of ELVs and their components. Between all ELVs valuable waste, around 6 thousand tons of ceramic cores of scrap automotive catalytic converters (CATs) are yearly produced.

**Activity and structure of a catalytic converter.** The principal function of an automotive catalytic converter is to reduce the emissions of cars removing pollutant gases including unburned hydrocarbons ( $C_nH_{2n+2}$ ), carbon monoxides (CO) and nitrogen oxides ( $NO_x$ ) from the automotive exhausted systems.

In catalytic air pollution control, all processes utilize solid heterogeneous catalysts through which gaseous reactants pass. In many industrial reactions, the number of reactant molecules converted to products is directly related to the number of catalytic sites available to the reactants. So, it is a common practice to maximize the number of active sites by dispersing the catalysts on a surface. Maximizing the surface area of the catalytic species such as Pt, Pd, Ni, Fe, Rd and CuO, increases the number of active sites where the catalytic reaction takes place. Therefore, catalytic components are generally dispersed on a high surface area carrier such as alumina, silica or titania. Generally, these carriers are not catalytically active materials, but they play a key role ensuring the durability and the stability of the final catalytic converter. As a result, the catalytic

converter is made of four principal layers or coats [144-146], as illustrated in Figure 7:

1. The first coat is the ceramic monolith which have a honeycomb-structure mainly prepared from synthetic cordierite ( $2\text{MgO}\cdot 2\text{Al}_2\text{O}_3\cdot 5\text{SiO}_2$ ).
2. The wash coat, a high surface area inorganic oxide, containing a complex pore structure, which is a carrier for the catalytic active materials. This structure is used to disperse the materials over a large surface area and is generally made up of  $\text{Al}_2\text{O}_3$ ,  $\text{TiO}_2$ ,  $\text{SiO}_2$ , zeolites or a mixture of aluminum oxide and silicon oxide could be used.
3. A layer made of  $\text{CeO}_2$  or  $\text{CeO}_2\text{-ZrO}_2$ . These oxides are mainly added to promote the storage of oxygen adsorbed from air and needed for the oxidations of exhaust emissions.
4. A coat of precious metals including platinum, rhodium and palladium (PGMs-platinum group metals). In this last coat, other metals such as manganese, iron, nickel and cerium could be also present.

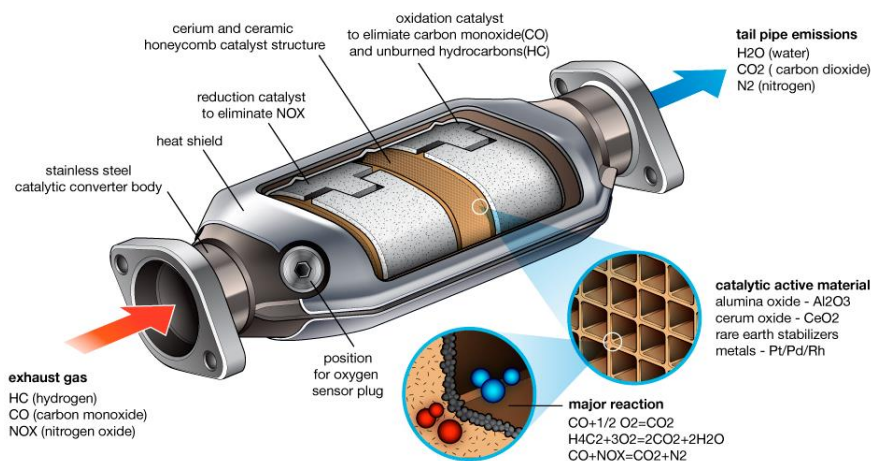


**Fig. 7** Structure of a catalytic converter.

**Precious-metal recovery methods.** Due to the presence of high contents of precious metals such as Pt, Pd and Rh (total PGMs amount between 0.5 and 2 g/kg), scrap catalytic converters derived from ELVs are generally treated in

order to recover and reuse PGMs, after the catalyst has lost its purpose [147]. The recycling of PGMs is vital in terms of the ability to reuse the valuable metals in its content, protecting the environment by decreasing waste and reducing both polluting emissions and electricity consumption. Therefore, numerous protocols have been developed enabling the recycling of PGMs from catalytic converters. The procedures that are normally used include hydrometallurgical and pyrometallurgical methods [145,148-155]. The former ones involve crushing of the spent catalytic converter and its processing with acids in order to dissolve only the ceramic substrate. Instead, pyrometallurgical recovery consists of the melting of the spent CATs, allowing the floating of the support to the top as a waste, while highly dense PGMs get deposited at the bottom of the container. This first step is followed by a chemical process in order to remove the precious metals and by successive purification for reutilization.

However, these methodologies are normally time and energy-consuming as they involve long treatment protocols and highly toxic chemicals in large volumes including inorganic acids [148-152,156-160]. Recent recovery methods, considered more environmentally friendly, are still characterized by very high *E*-factors. Indeed, only noble metals are recovered, while the remaining components are not recycled, generating lots of waste [161,162].

According to literature, R&D is nowadays generally trying to limit the utilization of inorganic acids or to enhance the efficiency of the extraction processes by adding for example chelating agents or peroxides [161,163-166].

**Utilization of scrap catalytic converters as catalysts.** Considering the annual rate of waste catalytic converter and their limited lifetimes, the recovery of this automobile waste avoiding the use of any additional chemical processes is important in terms of both environmental protection and economic efficiency.

However, only a few sporadic studies described the recovery and the reuse of the entire structure of the catalytic converter [167-169].

For example, Kucukislamoglu *et al.* have developed a simple, efficient, safe and economic protocol for the catalytic bath hydrogenation of the olefinic bond of different alkenes to the corresponding alkanes using scrap automotive catalysts, obtaining high product yields [167].

Another possible application of spent automotive three-way catalysts is as active materials for carbon-carbon bond formation reactions such as Heck or in Suzuki-Miyaura cross-couplings [168].

More recently, Genc has tested the activity and the catalytic performance of scrap catalytic converters for nitroarenes reduction in the presence of  $\text{NaBH}_4$  [169]. The automotive catalytic converter is recyclable and selective for the reduction of nitro-groups in the presence of  $-\text{Br}$ ,  $-\text{Cl}$ ,  $-\text{I}$  or  $-\text{CN}$  groups.



## References

1. Gupta, M.; Paul, S.; Gupta, R. General Characteristics and Applications of Microwaves in Organic Synthesis. *Acta Chim. Slov.* **2009**, *56*(4), 749-764.
2. Kappe, C. O.; Dallinger, D.; Murphree, S. S. Practical Microwave Synthesis for Organic Chemistry: Strategies, Instruments, and Protocols. *WILEY-VCH Verlag GmbH & Co. KGaA, Weinheim.* **2009**.
3. Lidstrom, P.; Tierney, J.; Wathey, B.; Westman, J. Microwave assisted organic synthesis - a review. *Tetrahedron.* **2001**, *57*(45), 9225-9283.
4. Sobol, H.; Tomiyasu, K. Milestones of microwaves. *Ieee T. Microw. Theory.* **2002**, *50* (3), 594-611.
5. Osepchuk, J. M. A history of microwave-heating applications. *Ieee T. Microw. Theory.* **1984**, *32* (9), 1200-1224.
6. Caddick, S. Microwave-assisted organic-reactions. *Tetrahedron.* **1995**, *51*(38), 10403-10432.
7. Galema, S. A. Microwave chemistry. *Chem. Soc. Rev.* **1997**, *26*(3), 233-238.
8. Mishra, R. R.; Sharma, A. K. Microwave-material interaction phenomena: Heating mechanisms, challenges and opportunities in material processing. *Compos. Part. A-Appl. S.* **2016**, *81*, 78-97.
9. Chandrasekaran, S.; Ramanathan, S.; Basak, T. Microwave food processing-A review. *Food Res. Int.* **2013**, *52*(1), 243-261.
10. Motasemi, F.; Afzal, M. T. A review on the microwave-assisted pyrolysis technique. *Renew. Sust. Energ. Rev.* **2013**, *28*, 317-330.
11. El Khaled, D.; Novas, N.; Gazquez, J. A.; Manzano-Agugliaro, F. Microwave dielectric heating: Applications on metals processing. *Renew. Sust. Energ. Rev.* **2018**, *82*, 2880-2892.
12. Asomaning, J.; Haupt, S.; Chae, M.; Bressler, D. C. Recent developments in microwave-assisted thermal conversion of biomass for fuels and chemicals. *Renew. Sust. Energ. Rev.* **2018**, *92*, 642-657.
13. Oghbaei, M.; Mirzaee, O. Microwave versus conventional sintering: A review of fundamentals, advantages and applications. *J. Alloy Compd.* **2010**, *494*(1-2), 175-189.
14. Jacob, J.; Chia, L. H. L.; Boey, F. Y. C. Thermal and nonthermal interaction of microwave-radiation with materials. *J. Mater. Sci.* **1995**, *30*(21), 5321-5327.

15. de la Hoz, A.; Diaz-Ortiz, A.; Moreno, A. Microwaves in organic synthesis. Thermal and non-thermal microwave effects. *Chem. Soc. Rev.* **2005**, *34*(2), 164-178.
16. Kappe, C. O. Controlled microwave heating in modern organic synthesis. *Angew. Chem. Int. Edit.* **2004**, *43*(46), 6250-6284.
17. Kappe, C. O. Microwave dielectric heating in synthetic organic chemistry. *Chem. Soc. Rev.* **2008**, *37*(6), 1127-1139.
18. Bassyouni, F. A.; Abu-Bakr, S. M.; Rehim, M. A. Evolution of microwave irradiation and its application in green chemistry and biosciences. *Res. Chem. Intermediat.* **2012**, *38*(2), 283-322.
19. Kokel, A.; Schafer, C.; Torok, B. Application of microwave-assisted heterogeneous catalysis in sustainable synthesis design. *Green Chem.* **2017**, *19*(16), 3729-3751.
20. Estel, L.; Poux, M.; Benamara, N.; Polaert, I. Continuous flow-microwave reactor: Where are we? *Chem. Eng. Process.* **2017**, *113*, 56-64.
21. Horikoshi, S.; Schiffmann, R.; Fukishima, J.; Serpone, N. Microwave Chemical and Materials Processing. *Springer, Singapore.* **2017**.
22. Orsat, V.; Raghavan, G. S. V.; Krishnaswamy, K. Microwave technology for food processing: an overview of current and future applications. Microwave Processing of Foods. *2nd Edition, Elsevier.* **2017**, 100-116.
23. Appleton, T. J.; Colder, R. I.; Kingman, S. W.; Lowndes, I. S.; Read, A. G. Microwave technology for energy-efficient processing of waste. *Appl. Energ.* **2005**, *81*(1), 85-113.
24. Lam, S. S.; Chase, H. A. A Review on Waste to Energy Processes Using Microwave Pyrolysis. *Energies.* **2012**, *5*(10), 4209-4232.
25. Wang, Y. P.; Dai, L. L.; Fan, L. L.; Shan, S. Q.; Liu, Y. H.; Ruan, R. Review of microwave-assisted lignin conversion for renewable fuels and chemicals. *J. Anal. Appl. Pyrol.* **2016**, *119*, 104-113.
26. Ao, W. Y.; Fu, J.; Mao, X.; Kang, Q. H.; Ran, C. M.; Liu, Y.; Zhang, H. D.; Gao, Z. P.; Li, J.; Liu, G. Q.; Dai, J. J. Microwave assisted preparation of activated carbon from biomass: A review. *Renew. Sust. Energ. Rev.* **2018**, *92*, 958-979.
27. Bundhoo, Z. M. A. Microwave-assisted conversion of biomass and waste materials to biofuels. *Renew. Sust. Energ. Rev.* **2018**, *82*, 1149-1177.

## Introduction

28. Calcio Gaudino, E; Cravotto, G.; Manzoli, M.; Tabasso, S. From waste biomass to chemicals and energy via microwave-assisted processes. *Green Chem.* **2019**, *21* (6), 1202-1235.
29. Abubakar, Z.; Salema, A. A.; Ani, F. N. A new technique to pyrolyse biomass in a microwave system: Effect of stirrer speed. *Bioresource Technol.* **2013**, *128*, 578-585.
30. Abioye, A. M.; Ani, F. N. Recent development in the production of activated carbon electrodes from agricultural waste biomass for supercapacitors: A review. *Renew. Sust. Energ. Rev.* **2015**, *52*, 1282-1293.
31. Alvarez, H. M.; Barbosa, D. P.; Fricks, A. T.; Aranda, D. A. G.; Valdes, R. H.; Antunes, O. A. C. Production of piperonal, vanillin, and p-anisaldehyde via solventless supported iodobenzene diacetate oxidation of isosafrol, isoeugenol, and anethol under microwave irradiation. *Org. Process Res. Dev.* **2006**, *10*(5), 941-943.
32. Qi, X. H.; Watanabe, M.; Aida, T. M.; Smith, R. L. Catalytic conversion of fructose and glucose into 5-hydroxymethylfurfural in hot compressed water by microwave heating. *Catal. Commun.* **2008**, *9*(13), 2244-2249.
33. Li, C. Z.; Zhang, Z. H.; Zhao, Z. B. K. Direct conversion of glucose and cellulose to 5-hydroxymethylfurfural in ionic liquid under microwave irradiation. *Tetrahedron Lett.* **2009**, *50* (38), 5403-5405.
34. Weingarten, R.; Cho, J.; Conner, W. C.; Huber, G. W. Kinetics of furfural production by dehydration of xylose in a biphasic reactor with microwave heating. *Green Chem.* **2010**, *12* (8), 1423-1429.
35. Yemis, O.; Mazza, G. Acid-catalyzed conversion of xylose, xylan and straw into furfural by microwave-assisted reaction. *Bioresource Technol.* **2011**, *102*(15), 7371-7378.
36. Guo, F.; Fang, Z.; Zhou, T. J. Conversion of fructose and glucose into 5-hydroxymethylfurfural with lignin-derived carbonaceous catalyst under microwave irradiation in dimethyl sulfoxide-ionic liquid mixtures. *Bioresource Technol.* **2012**, *112*, 313-318.
37. Serrano-Ruiz, J. C.; Campelo, J. M.; Francavilla, M.; Romero, A. A.; Luque, R.; Menendez-Vazquez, C.; Garcia, A. B.; Garcia-Suarez, E. J. Efficient microwave-assisted production of furfural from C-5 sugars in aqueous media catalysed by Bronsted acidic ionic liquids. *Catal. Sci. Technol.* **2012**, *2*(9), 1828-1832.
38. Yang, Y.; Hu, C. W.; Abu-Omar, M. M. Conversion of carbohydrates and lignocellulosic biomass into 5-hydroxymethylfurfural using AlCl<sub>3</sub> center 6H<sub>2</sub>O catalyst in a biphasic solvent system. *Green Chem.* **2012**, *14*(2), 509-513.

39. Yang, Y.; Hu, C. W.; Abu-Omar, M. M. Synthesis of Furfural from Xylose, Xylan, and Biomass Using  $\text{AlCl}_3$  center  $6\text{H}_2\text{O}$  in Biphasic Media via Xylose Isomerization to Xylulose. *Chemsuschem*. **2012**, *5* (2), 405-410.
40. Yemis, O.; Mazza, G. Optimization of furfural and 5-hydroxymethylfurfural production from wheat straw by a microwave-assisted process. *Bioresource Technol.* **2012**, *109*, 215-223.
41. Mukherjee, A.; Dumont, M. J.; Raghavan, V. Review: Sustainable production of hydroxymethylfurfural and levulinic acid: Challenges and opportunities. *Biomass Bioenerg.* **2015**, *72*, 143-183.
42. Yopez, A.; De, S.; Climent, M. S.; Romero, A. A.; Luque, R. Microwave-Assisted Conversion of Levulinic Acid to gamma-Valerolactone Using Low-Loaded Supported Iron Oxide Nanoparticles on Porous Silicates. *Appl. Sci-Basel.* **2015**, *5* (3), 532-543.
43. Antonetti, C.; Licursi, D.; Fulignati, S.; Valentini, G.; Galletti, A. M. R. New Frontiers in the Catalytic Synthesis of Levulinic Acid: From Sugars to Raw and Waste Biomass as Starting Feedstock. *Catalysts.* **2016**, *6* (12), 196.
44. Huang, Y. B.; Yang, T.; Zhou, M. C.; Pan, H.; Fu, Y. Microwave-assisted alcoholysis of furfural alcohol into alkyl levulinates catalyzed by metal salts. *Green Chem.* **2016**, *18* (6), 1516-1523.
45. Li, H.; Fang, Z.; Smith, R. L.; Yang, S. Efficient valorization of biomass to biofuels with bifunctional solid catalytic materials. *Prog. Energ. Combust.* **2016**, *55*, 98-194.
46. Antonetti, C.; Melloni, M.; Licursi, D.; Fulignati, S.; Ribechini, E.; Rivas, S.; Parajo, J. C.; Cavani, F.; Galletti, A. M. R. Microwave-assisted dehydration of fructose and inulin to HMF catalyzed by niobium and zirconium phosphate catalysts. *Appl. Catal. B-Environ.* **2017**, *206*, 364-377.
47. Filiciotto, L.; Balu, A. M.; Romero, A. A.; Rodriguez-Castellon, E.; van der Waal, J. C.; Luque, R. Benign-by-design preparation of humin-based iron oxide catalytic nanocomposites. *Green Chem.* **2017**, *19* (18), 4423-4434.
48. Li, H.; Fang, Z.; Luo, J.; Yang, S. Direct conversion of biomass components to the biofuel methyl levulinate catalyzed by acid-base bifunctional zirconia-zeolites. *Appl. Catal. B-Environ.* **2017**, *200*, 182-191.
49. Rodriguez-Padron, D.; Balu, A. M.; Romero, A. A.; Luque, R. New bio-nanocomposites based on iron oxides and polysaccharides applied to oxidation and alkylation reactions. *Beilstein J. Org. Chem.* **2017**, *13*, 1982-1993.

## Introduction

50. Tukacs, J. M.; Hollo, A. T.; Retfalvi, N.; Csefalvay, E.; Dibo, G.; Havasi, D.; Mika, L. T. Microwave-Assisted Valorization of Biowastes to Levulinic Acid. *Chemistryselect.* **2017**, *2* (4), 1375-1380.
51. Yang, T.; Zhou, Y. H.; Zhu, S. Z.; Pan, H.; Huang, Y. B. Insight into Aluminum Sulfate-Catalyzed Xylan Conversion into Furfural in a  $\gamma$ -Valerolactone/Water Biphasic Solvent under Microwave Conditions. *Chemsuschem.* **2017**, *10*(20), 4066-4079.
52. Delbecq, F.; Wang, Y. T.; Muralidhara, A.; El Ouardi, K.; Marlair, G.; Len, C. Hydrolysis of Hemicellulose and Derivatives-A Review of Recent Advances in the Production of Furfural. *Front. Chem.* **2018**, *6*, 146.
53. Lin, J. Y.; Lai, H. K.; Lin, K. Y. A. Rapid microwave-hydrothermal conversion of lignin model compounds to value-added products via catalytic oxidation using metal organic frameworks. *Chem. Pap.* **2018**, *72*(9), 2315-2325.
54. Mangin, F.; Prinsen, P.; Yopez, A.; Gilani, M.; Xu, G. B.; Len, C.; Luque, R. Microwave assisted benzyl alcohol oxidation using iron particles on furfuryl alcohol derived supports. *Catal. Commun.* **2018**, *104*, 67-70.
55. Marquez-Medina, M. D.; Prinsen, P.; Li, H. K.; Shih, K. M.; Romero, A. A.; Luque, R. Continuous-Flow Synthesis of Supported Magnetic Iron Oxide Nanoparticles for Efficient Isoeugenol Conversion into Vanillin. *Chemsuschem.* **2018**, *11*(2), 389-396.
56. Pineda, A.; Ojeda, M.; Romero, A. A.; Balu, A. M.; Luque, R. Mechanochemical synthesis of supported cobalt oxide nanoparticles on mesoporous materials as versatile bifunctional catalysts. *Micropor. Mesopor. Mat.* **2018**, *272*, 129-136.
57. Sweygens, N.; Harrer, J.; Dewil, R.; Appels, L. A microwave-assisted process for the in-situ production of 5-hydroxymethylfurfural and furfural from lignocellulosic polysaccharides in a biphasic reaction system. *J. Clean. Prod.* **2018**, *187*, 1014-1024.
58. Sweygens, N.; Dewil, R.; Appels, L. Production of Levulinic Acid and Furfural by Microwave-Assisted Hydrolysis from Model Compounds: Effect of Temperature, Acid Concentration and Reaction Time. *Waste Biomass Valori.* **2018**, *9*(3), 343-355.
59. Marquez-Medina, M. D.; Mhadmhan, S.; Balu, A. M.; Romero, A. A.; Luque, R. Post-synthetic Mechanochemical Incorporation of Al-Species into the Framework of Porous Materials: Toward More Sustainable Redox Chemistries. *Acs Sustain. Chem. Eng.* **2019**, *7*(10), 9537-9543.

60. Rao, K. T. V.; Souzanchi, S.; Yuan, Z. S.; Xu, C. B. One-pot sol-gel synthesis of a phosphorylated TiO<sub>2</sub> catalyst for conversion of monosaccharide, disaccharides, and polysaccharides to 5-hydroxymethylfurfural. *New J. Chem.* **2019**, *43*(31), 12483-12493.
61. James, O. O.; Maity, S.; Usman, L. A.; Ajanaku, K. O.; Ajani, O. O.; Siyanbola, T. O.; Sahu, S.; Chaubey, R. Towards the conversion of carbohydrate biomass feedstocks to biofuels via hydroxymethylfurfural. *Energ. Environ. Sci.* **2010**, *3*(12), 1833-1850.
62. van Putten, R. J.; van der Waal, J. C.; de Jong, E.; Rasrendra, C. B.; Heeres, H. J.; de Vries, J. G. Hydroxymethylfurfural, A Versatile Platform Chemical Made from Renewable Resources. *Chem. Rev.* **2013**, *113*(3), 1499-1597.
63. Hu, L.; Lin, L.; Wu, Z.; Zhou, S. Y.; Liu, S. J. Recent advances in catalytic transformation of biomass-derived 5-hydroxymethylfurfural into the innovative fuels and chemicals. *Renew. Sust. Energ. Rev.* **2017**, *74*, 230-257.
64. Xue, Z. M.; Liu, Q. L.; Wang, J. F.; Mu, T. C. Valorization of levulinic acid over non-noble metal catalysts: challenges and opportunities. *Green Chem.* **2018**, *20*(19), 4391-4408.
65. Lange, J. P.; van der Heide, E.; van Buijtenen, J.; Price, R. Furfural-A Promising Platform for Lignocellulosic Biofuels. *ChemSuschem.* **2012**, *5*(1), 150-166.
66. Sanchez, C.; Serrano, L.; Andres, M. A.; Labidi, J. Furfural production from corn cobs autohydrolysis liquors by microwave technology. *Ind. Crop. Prod.* **2013**, *42*, 513-519.
67. <https://www.un.org/sustainabledevelopment/sustainable-development-goals/>.
68. Gomollón-Bel, F. Ten Chemical Innovations That Will Change Our World: IUPAC identifies emerging technologies in Chemistry with potential to make our planet more sustainable. *Chem. Int.* **2019**, *41*(2), 12-17.
69. Akwi, F. M.; Watts, P. Continuous flow chemistry: where are we now? Recent applications, challenges and limitations. *Chem. Commun.* **2018**, *54*(99), 13894-13928.
70. Vaccaro, L.; Lanari, D.; Marrocchi, A.; Strappaveccia, G. Flow approaches towards sustainability. *Green Chem.* **2014**, *16*(8), 3680-3704.
71. Newman, S. G.; Jensen, K. F. The role of flow in green chemistry and engineering. *Green Chem.* **2013**, *15*(6), 1456-1472.
72. Britton, J.; Raston, C. L. Multi-step continuous-flow synthesis. *Chem. Soc. Rev.* **2017**, *46*(5), 1250-1271.

## Introduction

73. Seo, H.; Katcher, M. H.; Jamison, T. F. Photoredox activation of carbon dioxide for amino acid synthesis in continuous flow. *Nat. Chem.* **2017**, *9*(5), 453-456.
74. Wang, S.; Gao, B.; Li, Y.; Creamer, A. E.; He, F. Adsorptive removal of arsenate from aqueous solutions by biochar supported zero-valent iron nanocomposite: Batch and continuous flow tests. *J. Hazard. Mater.* **2017**, *322*, 172-181.
75. Jas, G.; Kirschning, A. Continuous flow techniques in organic synthesis. *Chem Eur. J.* **2003**, *9*(23), 5708-5723.
76. Razzaq, T.; Kappe, C. O. Continuous Flow Organic Synthesis under High-Temperature/Pressure Conditions. *Chem-Asian J.* **2010**, *5*(6), 1274-1289.
77. Yoshida, J. I.; Kim, H.; Nagaki, A. Green and Sustainable Chemical Synthesis Using Flow Microreactors. *Chemsuschem.* **2011**, *4*(3), 331-340.
78. Ley, S. V. On being green: Can flow chemistry help? *Chem. Rec.* **2012**, *12*(4), 378-390.
79. Wiles, C.; Watts, P. Continuous flow reactors: a perspective. *Green Chem.* **2012**, *14*(1), 38-54.
80. Henderson, R. K.; Jimenez-Gonzalez, C.; Constable, D. J. C.; Alston, S. R.; Inglis, G. G. A.; Fisher, G.; Sherwood, J.; Binks, S. P.; Curzons, A. D. Expanding GSK's solvent selection guide - embedding sustainability into solvent selection starting at medicinal chemistry. *Green Chem.* **2011**, *13*(4), 854-862.
81. Stouten, S. C.; Noel, T.; Wang, Q.; Hessel, V. A View Through Novel Process Windows. *Aust. J. Chem.* **2013**, *66*(2), 121-130.
82. Rudolph, J.; Lormann, M.; Bolm, C.; Dahmen, S. A high-throughput screening approach for the determination of additive effects in organozinc addition reactions to aldehydes. *Adv. Synth. Catal.* **2005**, *347*(10), 1361-1368.
83. Hessel, V.; Kralisch, D.; Kockmann, N.; Noel, T.; Wang, Q. Novel Process Windows for Enabling, Accelerating, and Uplifting Flow Chemistry. *Chemsuschem.* **2013**, *6*(5), 746-789.
84. Pastre, J. C.; Browne, D. L.; Ley, S. V. Flow chemistry syntheses of natural products. *Chem. Soc. Rev.* **2013**, *42*(23), 8849-8869.
85. Tsubogo, T.; Ishiwata, T.; Kobayashi, S. Asymmetric Carbon-Carbon Bond Formation under Continuous-Flow Conditions with Chiral Heterogeneous Catalysts. *Angew. Chem. Int. Edit.* **2013**, *52*(26), 6590-6604.

86. Yoshida, J.; Takahashi, Y.; Nagaki, A. Flash chemistry: flow chemistry that cannot be done in batch. *Chem. Commun.* **2013**, *49*(85), 9896-9904.
87. Wegner, J.; Ceylan, S.; Kirschning, A. Flow Chemistry - A Key Enabling Technology for (Multistep) Organic Synthesis. *Adv. Synth. Catal.* **2012**, *354*(1), 17-57.
88. McQuade, D. T.; Seeberger, P. H. Applying Flow Chemistry: Methods, Materials, and Multistep Synthesis. *J. Org. Chem.* **2013**, *78*(13), 6384-6389.
89. Anderson, N. G. Using Continuous Processes to Increase Production. *Org. Process Res. Dev.* **2012**, *16*(5), 852-869.
90. Hessel, V.; Gursel, I. V.; Wang, Q.; Noel, T.; Lang, J. Potential Analysis of Smart Flow Processing and Micro Process Technology for Fastening Process Development: Use of Chemistry and Process Design as Intensification Fields. *Chem. Eng. Technol.* **2012**, *35*(7), 1184-1204.
91. Cambie, D.; Bottecchia, C.; Straathof, N. J. W.; Hessel, V.; Noel, T. Applications of Continuous-Flow Photochemistry in Organic Synthesis, Material Science, and Water Treatment. *Chem. Rev.* **2016**, *116*(17), 10276-10341.
92. Hessel, V. Everything Flows: Continuous Micro-Flow for Pharmaceutical Production. *Chem. Int.* **2018**, *40*(2), 12-16.
93. Ragauskas, A. J.; Williams, C. K.; Davison, B. H.; Britovsek, G.; Cairney, J.; Eckert, C. A.; Frederick, W. J.; Hallett, J. P.; Leak, D. J.; Liotta, C. L.; Mielenz, J. R.; Murphy, R.; Templer, R.; Tschaplinski, T. The path forward for biofuels and biomaterials. *Science*. **2006**, *311* (5760), 484-489.
94. Corma, A.; Iborra, S.; Velty, A. Chemical routes for the transformation of biomass into chemicals. *Chem. Rev.* **2007**, *107*(6), 2411-2502.
95. Tarasov, A. L.; Kustov, L. M.; Bogolyubov, A. A.; Kiselyov, A. S.; Semenov, V. V. New and efficient procedure for the oxidation of dioxybenzylic alcohols into aldehydes with Pt and Pd-based catalysts under flow reactor conditions. *Appl. Catal. A-Gen.* **2009**, *366*(2), 227-231.
96. Obermayer, D.; Balu, A. M.; Romero, A. A.; Goessler, W.; Luque, R.; Kappe, C. O. Nanocatalysis in continuous flow: supported iron oxide nanoparticles for the heterogeneous aerobic oxidation of benzyl alcohol. *Green Chem.* **2013**, *15*(6), 1530-1537.
97. Tukacs, J. M.; Jones, R. V.; Darvas, F.; Dibo, G.; Lezsak, G.; Mika, L. T. Synthesis of gamma-valerolactone using a continuous-flow reactor. *Rsc Adv.* **2013**, *3*(37), 16283-16287.



## Introduction

98. Gemoets, H. P. L.; Su, Y. H.; Shang, M. J.; Hessel, V.; Luque, R.; Noel, T. Liquid phase oxidation chemistry in continuous-flow microreactors. *Chem. Soc. Rev.* **2016**, *45*(1), 83-117.
99. Bizet, B.; Hornung, C. H.; Kohl, T. M.; Tsanaktisidis, J. Synthesis of Imines and Amines from Furfurals Using Continuous Flow Processing. *Aust. J. Chem.* **2017**, *70*(10), 1069-1072.
100. Trombettoni, V.; Bianchi, L.; Zupanic, A.; Porciello, A.; Cuomo, M.; Piermatti, O.; Marrocchi, A.; Vaccaro, L. Efficient Catalytic Upgrading of Levulinic Acid into Alkyl Levulinates by Resin-Supported Acids and Flow Reactors. *Catalysts.* **2017**, *7*(8), 235.
101. Feher, A.; Feher, C.; Rozbach, M.; Racz, G.; Fekete, M.; Hegedus, L.; Barta, Z. Treatments of Lignocellulosic Hydrolysates and Continuous-Flow Hydrogenation of Xylose to Xylitol. *Chem. Eng. Technol.* **2018**, *41*(3), 496-503.
102. Gerardy, R.; Emmanuel, N.; Toupy, T.; Kassin, V. E.; Tshibalonza, N. N.; Schmitz, M.; Monbaliu, J. C. M. Continuous Flow Organic Chemistry: Successes and Pitfalls at the Interface with Current Societal Challenges. *Eur. J. Org. Chem.* **2018**, (20-21), 2301-2351.
103. Moreno-Marrodan, C.; Barbaro, P.; Caporali, S.; Bossola, F. Low-Temperature Continuous-Flow Dehydration of Xylose Over Water-Tolerant Niobia-Titania Heterogeneous Catalysts. *Chemsuschem.* **2018**, *11*(20), 3649-3660.
104. Al-Naji, M.; Puertolas, B.; Kumru, B.; Cruz, D.; Baumel, M.; Schmidt, B.; Tarakina, N. V.; Perez-Ramirez, J. Sustainable Continuous Flow Valorization of gamma-Valerolactone with Trioxane to alpha-Methylene-gamma-Valerolactone over Basic Beta Zeolites. *Chemsuschem.* **2019**, *12*(12), 2628-2636.
105. Hommes, A.; Heeres, H. J.; Yue, J. Catalytic Transformation of Biomass Derivatives to Value-Added Chemicals and Fuels in Continuous Flow Microreactors. *Chemcatchem.* **2019**, *11*, 1-39.
106. Tukacs, J. M.; Sylvester, A.; Kmecz, I.; Jones, R. V.; Ovari, M.; Mika, L. T. Continuous flow hydrogenation of methyl and ethyl levulinate: an alternative route to gamma-valerolactone production. *Roy. Soc. Open Sci.* **2019**, *6*(5), 182233.
107. Bozell, J. J.; Petersen, G. R. Technology development for the production of biobased products from biorefinery carbohydrates-the US Department of Energy's "Top 10" revisited. *Green Chem.* **2010**, *12*(4), 539-554.
108. Horvath, I. T.; Mehdi, H.; Fabos, V.; Boda, L.; Mika, L. T. gamma-Valerolactone - a sustainable liquid for energy and carbon-based chemicals. *Green Chem.* **2008**, *10*(2), 238-242.

109. Balu, A. M.; Pineda, A.; Obermayer, D.; Romero, A. A.; Kappe, C. O.; Luque, R. Versatile low-loaded mechanochemically synthesized supported iron oxide nanoparticles for continuous flow alkylations. *Rsc Adv.* **2013**, *3*(37), 16292-16295.
110. Bermudez, J. M.; Menendez, J. A.; Romero, A. A.; Serrano, E.; Garcia-Martinez, J.; Luque, R. Continuous flow nanocatalysis: reaction pathways in the conversion of levulinic acid to valuable chemicals. *Green Chem.* **2013**, *15*(10), 2786-2792.
111. Itabaiana, I.; Sutili, F. K.; Leite, S. G. F.; Goncalves, K. M.; Cordeiro, Y.; Leal, I. C. R.; Miranda, L. S. M.; Ojeda, M.; Luque, R.; de Souza, R. Continuous flow valorization of fatty acid waste using silica-immobilized lipases. *Green Chem.* **2013**, *15*(2), 518-524.
112. Luque, R.; Campelo, J. M.; Romero, A. A.; Pineda, A.; Ojeda, M.; Yepez, A.; Lastres, C. M.; Franco, A. Continuous flow transformations of platform molecules to valuable chemicals and biofuel precursors. In *245th ACS Meeting*, New Orleans (EEUU), Apr 7-11, **2013**.
113. Zhang, Y. T.; Arancon, R. A. D.; Lam, L. Y. F.; Luque, R. Flow nanocatalysis: innovative methodologies towards green chemical syntheses. *Chim. Oggi.* **2014**, *32*(2), 36-39.
114. Wang, B. J.; Balu, A. M.; Xuan, J.; Gonzalez-Arellano, C.; Bai, Z. S.; Luque, R. Innovative benign-by-design flow chemistry protocols: from bio(nano) materials synthesis to biomass/waste valorisation. *Chim. Oggi.* **2016**, *34*(6A), 58-63.
115. Garcia-Olmo, A. J.; Yepez, A.; Balu, A. M.; Prinsen, P.; Garcia, A.; Maziere, A.; Len, C.; Luque, R. Activity of continuous flow synthesized Pd-based nanocatalysts in the flow hydroconversion of furfural. *Tetrahedron.* **2017**, *73*(38), 5599-5604.
116. Ouyang, W. Y.; Zhao, D. Y.; Wang, Y. T.; Balu, A. M.; Len, C.; Luque, R. Continuous Flow Conversion of Biomass-Derived Methyl Levulinate into gamma-Valerolactone Using Functional Metal Organic Frameworks. *Acs Sustain. Chem. Eng.* **2018**, *6*(5), 6746-6752.
117. Rodriguez-Padron, D.; Puente-Santiago, A. R.; Balu, A. M.; Romero, A. A.; Munoz-Batista, M. J.; Luque, R. Benign-by-Design Orange Peel-Templated Nanocatalysts for Continuous Flow Conversion of Levulinic Acid to N-Heterocycles. *Acs Sustain. Chem. Eng.* **2018**, *6*(12), 16637-16644.
118. Wang, Y. T.; Prinsen, P.; Triantafyllidis, K. S.; Karakoulia, S. A.; Yepez, A.; Len, C.; Luque, R. Batch versus Continuous Flow Performance of Supported Mono- and Bimetallic Nickel Catalysts for Catalytic Transfer Hydrogenation of Furfural in Isopropanol. *Chemcatchem.* **2018**, *10*(16), 3459-3468.

## Introduction

119. Wang, Y. T.; Prinsen, P.; Triantafyllidis, K. S.; Karakoulia, S. A.; Trikalitis, P. N.; Yopez, A.; Len, C.; Luque, R. Comparative Study of Supported Monometallic Catalysts in the Liquid-Phase Hydrogenation of Furfural: Batch Versus Continuous Flow. *Acs Sustain. Chem. Eng.* **2018**, *6* (8), 9831-9844.
120. Xu, C. P.; Ouyang, W. Y.; Munoz-Batista, M. J.; Fernandez-Garcia, M.; Luque, R. Highly Active Catalytic Ruthenium/TiO<sub>2</sub> Nanomaterials for Continuous Production of gamma-Valerolactone. *Chemsuschem.* **2018**, *11* (15), 2604-2611.
121. Zhao, D. Y.; Prinsen, P.; Wang, Y. T.; Ouyang, W. Y.; Delbecq, F.; Len, C.; Luque, R. Continuous Flow Alcoholysis of Furfuryl Alcohol to Alkyl Levulinates Using Zeolites. *Acs Sustain. Chem. Eng.* **2018**, *6* (5), 6901-6909.
122. Lázaro, N.; Franco, A.; Ouyang, W. Y.; Balu, A. M.; Romero, A. A.; Luque, R.; Pineda, A. Continuous-Flow Hydrogenation of Methyl Levulinate Promoted by Zr-Based Mesoporous Materials. *Catalysts.* **2019**, *9* (2), 142.
123. Mhadmhan, S.; Franco, A.; Pineda, A.; Reubroycharoen, P.; Luque, R. Continuous Flow Selective Hydrogenation of 5-Hydroxymethylfurfural to 2,5-Dimethylfuran Using Highly Active and Stable Cu-Pd/Reduced Graphene Oxide. *Acs Sustain. Chem. Eng.* **2019**, *7* (16), 14210-14216.
124. Pfab, E.; Filiciotto, L.; Romero, A. A.; Luque, R. Valorization of Humins-Extracted 5-Methoxymethylfurfural: Toward High Added Value Furanics via Continuous Flow Catalytic Hydrogenation. *Ind. Eng. Chem. Res.* **2019**, *58* (35), 16065-16070.
125. Rodriguez-Padron, D.; Puente-Santiago, A. R.; Balu, A. M.; Munoz-Batista, M. J.; Luque, R. Continuous Flow Synthesis of High Valuable N-Heterocycles via Catalytic Conversion of Levulinic Acid. *Front. Chem.* **2019**, *7*, 103.
126. Xu, J. H.; Xu, X. M.; Zhao, H.; Luo, G. S. Microfluidic preparation of chitosan microspheres with enhanced adsorption performance of copper(II). *Sensor Actuat. B-Chem.* **2013**, *183*, 201-210.
127. ©European Union 1995-2017, EUROSTAT 2017, [http://appsso.eurostat.ec.europa.eu/nui/show.do?dataset=apro\\_mt\\_lspig](http://appsso.eurostat.ec.europa.eu/nui/show.do?dataset=apro_mt_lspig).
128. Gonzalo, M.; Jespersen, C. M.; Jensen, K.; Stoier, S.; Meinert, L. Pig Bristles – An Underestimated Biomass Resource. In *62nd International Congress of Meat Science and Technology*, Bangkok, Thailand, Aug 14 -19, 2016; Elsevier, **2016**.
129. Zuliani, A.; Munoz-Batista, M. J.; Luque, R. Microwave-assisted valorization of pig bristles: towards visible light photocatalytic chalcocite composites. *Green Chem.* **2018**, *20* (13), 3001-3007.

130. Rudie, K.; Wonham, W. M. Think globally, act locally - decentralized supervisory control. *Ieee T. Automat. Contr.* **1992**, *37*(11), 1692-1708.
131. Steel, B. S. Thinking globally and acting locally?: Environmental attitudes, behavior and activism. *J. Environ. Manage.* **1996**, *47*(1), 27-36.
132. Marquis, C.; Battilana, J. Acting globally but thinking locally? The enduring influence of local communities on organizations. *Res. Organ. Behav.* **2009**, *29*, 283-302.
133. Laba, W.; Kopec, W.; Chorazyk, D.; Kancelista, A.; Piegza, M.; Malik, K. Biodegradation of pretreated pig bristles by *Bacillus cereus* B5esz. *Int. Biodeter. Biodegr.* **2015**, *100*, 116-123.
134. Gachango, F. G.; Ekmann, K. S.; Frorup, J.; Pedersen, S. M. Use of pig by-products (bristles and hooves) as alternative protein raw material in fish feed: A feasibility study. *Aquaculture.* **2017**, *479*, 265-272.
135. Laba, W.; Chorazyk, D.; Pudlo, A.; Trojan-Piegza, J.; Piegza, M.; Kancelista, A.; Kurzawa, A.; Zuk, I.; Kopec, W. Enzymatic Degradation of Pretreated Pig Bristles with Crude Keratinase of *Bacillus cereus* PCM 2849. *Waste Biomass Valori.* **2017**, *8*(2), 527-537.
136. Liu, Z. P.; Yu, S. Z.; Xu, X. S. Characteristics of soman diffusion in tissues studied by sticking of pig bristles. *Acta Pharm. Sinic.* **1988**, *9*(6), 526-529.
137. Gumz, W. Influence of origin on the mineral-content of pig bristles. In *13th Seminar on Macroelements and Trace Elements*, Friedrich Schiller Univ, Jena, Germany, Dec 09 -10, 1993.
138. Clay, R. C.; Cook, K.; Routh, J. I. Studies in the composition of human hair. *J. Am. Chem. Soc.* **1940**, *62*, 2709-2710.
139. Lipkowski, A. W.; Gajkowska, B.; Grabowska, A.; Kurzepa, K. Keratin-associated protein micromaterials for medical and cosmetic applications. *Polimery-W.* **2009**, *54*(5), 386-388.
140. Xu, C.; Nasrollahzadeh, M.; Selva, M.; Issaabadi, Z.; Luque, R. Waste-to-wealth: biowaste valorization into valuable bio(nano)materials. *Chem. Soc. Rev.* **2019**, *48*(18), 4791-4822.
141. <https://www.scrapcatalyticconverters.com/we-market-sized-the-autocatalyst-recycling-industry-in-2017/>.
142. Directive 2000/53/EC of the European Parliament and of the Council of 18 September 2000, Official Journal of the European Communities, L269/34. Published: 21st October, **2000**.

## Introduction

143. Hageluken, C. Recycling the Platinum Group Metals: A European Perspective Effective recycling systems for pgm-containing materials will ensure sustainable supply. *Platin. Met. Rev.* **2012**, *56*(1), 29-35.
144. Kaspar, J.; Fornasiero, P.; Hickey, N. Automotive catalytic converters: current status and some perspectives. *Catal. Today.* **2003**, *77*(4), 419-449.
145. Fornalczyk, A.; Saternus, M. Vapour Treatment Method Against Other Pyro- and Hydrometallurgical Processes Applied to Recover Platinum From Used Auto Catalytic Converters. *Acta Metall. Sin-Engl.* **2013**, *26*(3), 247-256.
146. Weng, J. F.; Lu, X. X.; Gao, P. X. Nano-Array Integrated Structured Catalysts: A New Paradigm upon Conventional Wash-Coated Monolithic Catalysts? *Catalysts.* **2017**, *7*(9), 253.
147. Saternus, M.; Fornalczyk, A.; Cebulski, J. Analysis of platinum content in used auto catalytic converter carriers and the possibility of its recovery. *Arch. Metall. Mater.* **2014**, *59*(2), 557-564.
148. Benson, M.; Bennett, C. R.; Harry, J. E.; Patel, M. K.; Cross, M. The recovery mechanism of platinum group metals from catalytic converters in spent automotive exhaust systems. *Resour. Conserv. Recy.* **2000**, *31*(1), 1-7.
149. Barakat, M. A.; Mahmoud, M. H. H. Recovery of platinum from spent catalyst. *Hydrometallurgy.* **2004**, *72*(3-4), 179-184.
150. de Aberasturi, D. J.; Pinedo, R.; de Larramendi, I. R.; de Larramendi, R.; Rojo, T. Recovery by hydrometallurgical extraction of the platinum-group metals from car catalytic converters. *Miner. Eng.* **2011**, *24*(6), 505-513.
151. Jha, M. K.; Lee, J. C.; Kim, M. S.; Jeong, J.; Kim, B. S.; Kumar, V. Hydrometallurgical recovery/recycling of platinum by the leaching of spent catalysts: A review. *Hydrometallurgy.* **2013**, *133*, 23-32.
152. Willner, J.; Fornalczyk, A.; Cebulski, J.; Janiszewski, K. Preliminary studies on simultaneous recovery of precious metals from different waste materials by pyrometallurgical method. *Arch. Metall. Mater.* **2014**, *59*(2), 801-804.
153. Canda, L.; Heput, T.; Ardelean, E. Methods for recovering precious metals from industrial waste. In *International Conference On Applied Sciences (ICAS)*, Military Econ Acad Wuhan, Wuhan, PEOPLES R CHINA, Jun 03-05, **2015**.
154. Dong, H. G.; Zhao, J. C.; Chen, J. L.; Wu, Y. D.; Li, B. J. Recovery of platinum group metals from spent catalysts: A review. *Int. J. Miner. Process.* **2015**, *145*, 108-113.

155. Saguru, C.; Ndlovu, S.; Moropeng, D. A review of recent studies into hydrometallurgical methods for recovering PGMs from used catalytic converters. *Hydrometallurgy*. **2018**, *182*, 44-56.
156. Kim, C. H.; Woo, S. I.; Jeon, S. H. Recovery of platinum-group metals from recycled automotive catalytic converters by carbochlorination. *Ind. Eng. Chem. Res.* **2000**, *39*(5), 1185-1192.
157. Harjanto, S.; Cao, Y.; Shibayama, A.; Naitoh, I.; Nanami, T.; Kasahara, K.; Okumura, Y.; Liu, K.; Fujita, T. Leaching of Pt, Pd and Rh from automotive catalyst residue in various chloride based solutions. *Mater. Trans.* **2006**, *47*(1), 129-135.
158. Baghalha, M.; Gh, H. K.; Mortaheb, H. R. Kinetics of platinum extraction from spent reforming catalysts in aqua-regia solutions. *Hydrometallurgy*. **2009**, *95*(3-4), 247-253.
159. Chen, S.; Shen, S. B.; Cheng, Y.; Wang, H. J.; Lv, B. C.; Wang, F. M. Effect of O<sub>2</sub>, H<sub>2</sub> and CO pretreatments on leaching Rh from spent auto-catalysts with acidic sodium chlorate solution. *Hydrometallurgy*. **2014**, *144*, 69-76.
160. Hasani, M.; Khodadadi, A.; Koleini, S. M. J.; Saeedi, A. H.; Melendez, A. M. Simultaneous leaching of Pt, Pd and Rh from automotive catalytic converters in chloride-containing solutions. In *22nd Colombian Congress of Electrochemistry (CCEQ) / 2nd Symposium on Nanoscience and Nanotechnology (SNN)*, Univ Ind Santander, Bucaramanga, Colombia, Oct 04-07, **2016**.
161. Hodnik, N.; Baldizzone, C.; Polymeros, G.; Geiger, S.; Grote, J. P.; Cherevko, S.; Mingers, A.; Zeradjanin, A.; Mayrhofer, K. J. J. Platinum recycling going green via induced surface potential alteration enabling fast and efficient dissolution. *Nat. Commun.* **2016**, *7*, 13164.
162. Ibrahim, M. Y. S.; Denmark, S. E. Selective extraction of supported Rh nanoparticles under mild, non-acidic conditions with carbon monoxide. *J. Mater. Chem. A*. **2018**, *6*(37), 18075-18083.
163. Cieszynska, A.; Wisniewski, M. Extractive recovery of palladium(II) from hydrochloric acid solutions with Cyphos (R) IL 104. *Hydrometallurgy*. **2012**, *113*, 79-85.
164. Hasegawa, H.; Rahman, I. M. M.; Egawa, Y.; Sawai, H.; Begum, Z. A.; Maki, T.; Mizutani, S. Recovery of the Rare Metals from Various Waste Ashes with the Aid of Temperature and Ultrasound Irradiation Using Chelants. *Water Air Soil Poll.* **2014**, *225*(9), 2112.
165. Gandhi, M. R.; Yamada, M.; Kondo, Y.; Shibayama, A.; Hamada, F. Selective extraction of Pd(II) ions from automotive catalyst residue in Cl<sup>-</sup> media by O-thiocarbamoyl-functionalized thiacalix[n]arenes. *Hydrometallurgy*. **2015**, *151*, 133-140.
166. Fornalczyk, A.; Willner, J.; Gajda, B.; Sedlakova-Kadukova, J. Influence of H<sub>2</sub>O<sub>2</sub> and O<sub>3</sub> on PGM extraction from used car catalysts. *Arch. Metall. Mater.* **2018**, *63*(2), 963-968.

## Introduction

167. Zengin, M.; Genc, H.; Demirci, T.; Arslan, M.; Kucukislamoglu, M. An efficient hydrogenation of various alkenes using scrap automobile catalyst. *Tetrahedron Lett.* **2011**, *52*(18), 2333-2335.
168. Mieczynska, E.; Gniewek, A.; Trzeciak, A. M. Spent automotive three-way catalysts towards C-C bond forming reactions. *Appl. Catal. A-Gen.* **2012**, *421*, 148-153.
169. Genc, H. Efficient reductions of various nitroarenes with scrap automobile catalyst and NaBH<sub>4</sub>. *Catal. Commun.* **2015**, *67*, 64-67.







# Hypothesis & Objectives



The hypotheses and objectives of the current Doctoral thesis are summarized below.

## Hypothesis I

Ag/Ag<sub>2</sub>S heterocomposites have recently emerged as promising catalysts in different applications [1-5], especially in electrocatalysis for the hydrogen evolution reaction (HER) [6,7]. However, the literature relative to the synthesis of these materials reported only energy and time-consuming synthetic protocols [2,5,8,9]. Noteworthy, these procedures use toxic, hazardous and expensive compounds as sulfur sources (*e.g.*, thiols or H<sub>2</sub>S). Therefore, the developing of sustainable and innovative methodologies is necessary.

In this regard, the exploitation of pig bristles, an easily collectable and largely available waste feedstock [10, 11] could be a way to obtain sustainable alternative sources of carbon and sulfur. The industrially abundant residue can be potentially used for a more sustainable synthesis *via* a microwave-assisted protocol.

Indeed, microwave methodology displayed important benefits for the materials synthesis compared to traditional heating processes described in the literature [12,13]. Microwave-assisted processes allow to obtain higher yields reducing reaction times.

## Objective I

A sequence of Ag/Ag<sub>2</sub>S carbon hybrid composites with different Ag(0)/Ag(I) ratios will be firstly synthesized *via* a microwave-assisted protocol changing the different quantities of silver precursor and by fixing the amount of pig bristles. Subsequently, as-synthesized catalysts will be characterized by X-ray diffraction techniques (XRD), scanning electron microscopy with energy

dispersive X-ray analysis (SEM-EDX), N<sub>2</sub> physisorption and X-ray photoelectron spectroscopy (XPS). The catalytic activity of the materials will be explored in the HER performing linear sweep voltammetry. Moreover, the correlation between the electrocatalytic activity of the materials and the ratio between Ag(0) and Ag(I) will be studied. This objective has been achieved and described in detail in the scientific publication “*Microwave-assisted preparation of Ag/Ag<sub>2</sub>S carbon hybrid structures from pig bristles as efficient HER catalysts*”(Journal of Materials Chemistry A, 2018, 6, 21516, Chapter “Results & Discussion”).

## Hypothesis II

Benzaldehyde is a widely used chemical in food, perfumery and pharmaceutical industries, as well as precursor in some chemical processes. Benzyl alcohol is a model molecule of the lignin structure, which can be oxidized to benzaldehyde. Therefore, the catalytic conversion of benzyl alcohol to benzaldehyde is highly attractive and can potentially offer an alternative to the traditional synthetic routes as well as can provide the reactivity and transformation strategies for the valorization of lignocellulose-based biomass [14-20].

Moreover, benzaldehyde could be also obtained through the oxidation of toluene [21]. Since toluene is considered an extremely contaminant compound, its conversion into valuable chemicals such as benzoic acid, benzaldehyde and benzyl alcohol is challenging.

In the last years, zinc sulfide has attracted great attention due to its outstanding photochemical and physical properties [22-27]. However, all described preparation procedures of this material employ highly contaminants or carcinogenic compounds or toxic substances as sulfur sources [2,5,8,9]. In this context, pig bristles, an industrial waste toxic-free feedstock could be

employed as source of sulfur. The use of pig bristles had previously been developed within the group for the preparation of different nanomaterials [28,29]. However, the utilization of toxic solvents and procedures carried out in pressurized tubes were tracking important limits to the synthesis.

Therefore, it will be necessary to develop new procedures and to shift to easier, greener and more efficient conditions. The synthetic protocol involved a simple refluxing procedure in a dilute solution of potassium hydroxide.

## Objective II

A series of three ZnS carbon materials will be prepared via simple refluxing synthesis at different preparation times, *i.e.* 1 hour, 3 hours, 5 hours. After materials preparation, the characterization of the textural and structural properties will be performed using techniques such as adsorption/desorption of N<sub>2</sub>, XRD, XPS and SEM-EDX. Subsequently, the catalytic activity of ZnS will be tested in the liquid-phase oxidation of toluene and benzyl alcohol to benzaldehyde under microwave radiation using H<sub>2</sub>O<sub>2</sub> as green oxidant. Finally, the best catalysts will be used to carry out the stability tests for both reactions. This objective was accomplished in the scientific paper “*A sustainable approach for the synthesis of catalytically active peroxidase-mimic ZnS catalyst*” (ACS Sustainable Chemistry & Engineering, 2019, 7, 1, 1300-1307, Chapter “Results & Discussion”).

## Hypothesis III

The selective hydrogenation of  $\alpha,\beta$ -unsaturated aldehydes has attracted significant interest in the production of fine chemicals, especially for the fragrances and flavoring industries [30]. In particular, the hydrogenation of cinnamaldehyde to various derivatives has been investigated using different

types of catalytic systems to study carbonyl group vs. double carbon bond hydrogenation selectivities [31-33]. The studies proved that the hydrogenation of the C=C bond is favored in terms of both thermodynamic and kinetic effects. As a result, developing materials that preferentially favour C=O bond activation is challenging.

Moreover, the product resulting from the hydrogenation of the carbonyl group of cinnamaldehyde is cinnamyl alcohol, a flavor smelling as hyacinth, widely used in food, drugs and fragrance industries [34-36].

Different types of catalysts have been used to carry out this hydrogenation, mostly containing noble metals supported on porous or carbonaceous materials [37, 38].

In the design of new supported catalysts, the choice of the support is extremely important and criteria such as green credentials and scalability must be considered. Therefore, innovative supports should be very cheap, easily-prepared and with low environmental impact. To this end, the exploitation of ceramic-cores of scrap automotive catalytic converters (CATs) as supports could be a fascinating alternative. Ruthenium-based CATs-supported catalysts could be synthesized using an innovative mechanochemical-assisted procedure and tested in the continuous-flow hydrogenation of cinnamaldehyde.

Indeed, IUPAC has recently included flow chemistry and mechanochemistry between the most emerging technologies that can change our world [39]. Compared to traditional batch processes, flow methods will be more advantageous due to intrinsic benefits including optimization of time screening, minimization of time and waste, energy efficiency, improvement in safety, easy scale-up as well as precise control of process parameters (temperature, pressure and flow rate) [40,41]. On the other hand,

mechanochemistry allows to run very fast reactions, avoiding the use of solvents in the so-called dry milling [42-44].

### Objective III

Different ruthenium-based catalysts will be firstly synthesized using different amounts of Ru salts. The ceramic cores of scrap automotive catalytic converters will be employed as supporting material using a mechanochemically-assisted step followed by a chemical reduction. Subsequently, several Ru catalysts will be prepared *via* the same methodology using different supports including SiO<sub>2</sub>, Al<sub>2</sub>O<sub>3</sub> or activated Al<sub>2</sub>O<sub>3</sub>. The catalysts will be characterized by XRD, SEM-EDX, transmission electron microscopy (TEM), high-resolution transmission electron microscopy (HRTEM), inductively coupled plasma mass spectrometry (ICP-MS), N<sub>2</sub> physisorption and XPS spectroscopy. The catalytic activity of Ru/CATs materials will be tested in the flow hydrogenation of cinnamaldehyde and will be compared with the catalytic performances of the other catalysts. The interactions between ruthenium and CATs will be investigated, studying how they influence the catalytic activity. Various reaction parameters will be studied and optimized such as flow rate, H<sub>2</sub> pressure, temperature and ruthenium loading. The catalytic activity of Ru/CATs will be compared with commercially available hydrogenation catalysts in terms of yield and selectivity. Finally, the long-term stability of the materials will be investigated under the best conditions and the *E*-factor of the protocol will be calculated. All these aspects are developed in the publication entitled “*Efficient Ru-based scrap waste automotive converter catalysts for the continuous-flow selective hydrogenation of cinnamaldehyde*” (Green Chemistry, 2019, 21, 4712-4722, Chapter “Results & Discussion”).



## References

1. Pang, M. L.; Hu, J. Y.; Zeng, H. C. Synthesis, Morphological Control, and Antibacterial Properties of Hollow/Solid Ag<sub>2</sub>S/Ag Heterodimers. *J. Am. Chem. Soc.* **2010**, *132*(31), 10771-10785.
2. Liu, B.; Ma, Z. F. Synthesis of Ag<sub>2</sub>S-Ag Nanoprisms and Their Use as DNA Hybridization Probes. *Small* **2011**, *7*, 1587-1592.
3. Yang, J.; Ying, J. Y. Nanocomposites of Ag<sub>2</sub>S and Noble Metals. *Angew. Chem. Int. Ed.* **2011**, *50*(20), 4637-4643.
4. Ma, X. H.; Zhao, X. Y.; Jiang, X. Y.; Liu, W.; Liu, S. Q.; Tang, Z. Y. Facile Preparation of Ag<sub>2</sub>S/Ag Semiconductor/Metal Heteronanostructures with Remarkable Antibacterial Properties. *Chemphyschem* **2012**, *13*(10), 2531-2535.
5. Sadovnikov, I.; Gusev, A. I. Recent progress in nanostructured silver sulfide: from synthesis and nonstoichiometry to properties. *J. Mater. Chem. A* **2017**, *5*, 17676-17704.
6. Xia, X. H.; Zhao, X. J.; Ye, W. C.; Wang, C. M. Highly porous Ag-Ag<sub>2</sub>S/MoS<sub>2</sub> with additional active sites synthesized by chemical etching method for enhanced electrocatalytic hydrogen evolution. *Electrochim. Acta* **2014**, *142*, 173-181.
7. Basu, M.; Nazir, R.; Mahala, C.; Fageria, P.; Chaudhary, S.; Gangopadhyay, S.; Pande, S. Ag<sub>2</sub>S/Ag Heterostructure: A Promising Electrocatalyst for the Hydrogen Evolution Reaction. *Langmuir* **2017**, *33*(13), 3178-3186.
8. Wang, D. S.; Xie, T.; Peng, Q.; Li, Y. D. Ag, Ag<sub>2</sub>S, and Ag<sub>2</sub>Se nanocrystals: synthesis, assembly, and construction of mesoporous structures. *J. Am. Chem. Soc.* **2008**, *130*(12), 4016-4022.
9. Yang, W. L.; Zhang, L.; Hu, Y.; Zhong, Y. J.; Wu, H. B.; Lou, X. W. Microwave-Assisted Synthesis of Porous Ag<sub>2</sub>S-Ag Hybrid Nanotubes with High Visible-Light Photocatalytic Activity. *Angew. Chem., Int. Ed.* **2012**, *51*(46), 11501-11504.
10. Laba, W.; Kopec, W.; Chorazyk, D.; Kancelista, A.; Piegza, M.; Malik, K. Biodegradation of pretreated pig bristles by *Bacillus cereus* B5esz. *Int. Biodeterior. Biodegrad.* **2015**, *100*, 116-123.
11. Gachango, F. G.; Ekmann, K. S.; Frorup, J.; Pedersen, S. M. Use of pig by-products (bristles and hooves) as alternative protein raw material in fish feed: A feasibility study. *Aquaculture* **2017**, *479*, 265-272.
12. Monzo-Cabrera, J.; Pedreno-Molina, J. L.; Toledo, A. Feedback control procedure for energy efficiency optimization of microwave-heating ovens. *Measurement* **2009**, *42*(8), 1257-1262.

13. Varma, R. S. Journey on greener pathways: from the use of alternate energy inputs and benign reaction media to sustainable applications of nano-catalysts in synthesis and environmental remediation. *Green Chem.* **2014**, *16* (4), 2027-2041.
14. Gritter, R. J.; Dupre, G. D.; Wallace, T. J. Oxidation of benzyl alcohols with manganese dioxide. *Nature.* **1964**, *202*(492), 179-181.
15. Yang, Z. J.; Ji, H. B. Synergistic effect of hydrogen bonding mediated selective synthesis of benzaldehyde in water. *Chin.J. Catal.* **2014**, *35* (4), 590-598.
16. Colmenares J. C.; Ouyang W.; Ojeda M.; Kuna E.; Chernyayeva O.; Lisovytskiy D.; De S.; Luque R.; Balu A. M. Mild ultrasound-assisted synthesis of TiO<sub>2</sub> supported on magnetic nanocomposites for selective photo-oxidation of benzyl alcohol. *Appl. Catal. B.* **2016**, *183*, 107-112.
17. Magdziarz A.; Colmenares J. C.; Chernyayeva O.; Kurzydłowski K.; Grzonka J. Iron-Containing Titania Photocatalyst Prepared by the Sonophotodeposition Method for the Oxidation of Benzyl Alcohol. *Chemcatchem.* **2016**, *8* (3), 536-539.
18. Magdziarz A.; Colmenares J. C.; Chernyayeva O.; Lisovytskiy D.; Grzonka J.; Kurzydłowski K.; Freindl K.; Korechi J. Insight into the synthesis procedure of Fe<sup>3+</sup>/TiO<sub>2</sub>-based photocatalyst applied in the selective photo-oxidation of benzyl alcohol under sun-imitating lamp. *Ultrason. Sonochem.* **2017**, *38*, 189-196.
19. Ouyang W.; Reina J. M.; Kuna E.; Yopez A.; Balu A. M.; Romero A. A.; Colmenares J. C.; Luque R. Wheat bran valorisation: Towards photocatalytic nanomaterials for benzyl alcohol photo-oxidation. *J. Environ. Manage.* **2017**, *203*(2), 768-773.
20. Zhu, L.; Xu, X. H.; Zheng, F. P. Synthesis of benzaldehyde by Swern oxidation of benzyl alcohol in a continuous flow microreactor system. *Turk. J. Chem.* **2018**, *42*(1), 75-85.
21. Borgaonkar, H. V.; Raverkar, S. R.; Chandalla, S. B. Liquid-phase oxidation of toluene to benzaldehyde by air. *Ind. Eng. Chem. Prod. Res. Dev.* **1984**, *23* (3), 455-458.
22. Fox, M. A.; Dulay, M. T. Heterogeneous photocatalysis. *Chem. Rev.* **1993**, *93*(1), 341-357.
23. Fang, X. S.; Bando, Y.; Gautam, U. K.; Ye, C.; Golberg, D. Inorganic semiconductor nanostructures and their field-emission applications. *J. Mater. Chem.* **2008**, *18*(5), 509-522.
24. Chen, D. G.; Huang, F.; Ren, G. Q.; Li, D. S.; Zheng, M.; Wang, Y. J.; Lin, Z. ZnS nano-architectures: photocatalysis, deactivation and regeneration. *Nanoscale.* **2010**, *2* (10), 2062-2064.

## Hypothesis & Objectives

25. Fang, X. S.; Zhai, T. Y.; Gautam, U. K.; Li, L.; Wu, L. M.; Yoshio, B.; Golberg, D. ZnS nanostructures: From synthesis to applications. *Prog. Mater. Sci.* **2011**, *56*(2), 175-287.
26. Ashkarran, A. A. Absence of photocatalytic activity in the presence of the photoluminescence property of Mn-ZnS nanoparticles prepared by a facile wet chemical method at room temperature. *Mater Sci. Semicond. Process.* **2014**, *17*, 1-6.
27. Ummartyotin, S.; Infahsaeng, Y. A comprehensive review on ZnS: From synthesis to an approach on solar cell. *Renewable Sustainable Energy Rev.* **2016**, *55*(C), 17-24.
28. Zuliani, A.; Munoz-Batista, M. J.; Luque, R. Microwave-assisted valorization of pig bristles: towards visible light photocatalytic chalcocite composites. *Green Chem.* **2018**, *20*(13), 3001-3007.
29. Cova, C. M.; Zuliani, A.; Puente-Santiago, A. R.; Caballero, A.; Munoz-Batista, M. J.; Luque, R. Microwave-assisted preparation of Ag/Ag<sub>2</sub>S carbon hybrid structures from pig bristles as efficient HER catalyst. *J. Mater. Chem. A.* **2018**, *6*, 21516-21523.
30. Wang, X.; Hu, W.; Deng, B.; Liang, X. Selective hydrogenation of citral over supported Pt catalysts: insight into support effects. *J. Nanopart. Res.* **2017**, *19*, 153.
31. Gallezot, P.; Richard, D. Selective Hydrogenation of  $\alpha,\beta$ -Unsaturated Aldehydes. *Catal. Rev. Sci. Eng.* **1998**, *40*(1,2), 81-126.
32. Loffreda, D.; Delbecq, F.; Vigne, F.; Sautet, P. Chemo-Regioselectivity in Heterogeneous Catalysis: Competitive Routes for C=O and C=C Hydrogenations from a Theoretical Approach. *J. Am. Chem. Soc.* **2006**, *128*(4), 1316-1323.
33. Bertero, N. M.; Trasarti, A. F.; Moraweck, B.; Borgna, A.; Marchi, A. J. Selective liquid-phase hydrogenation of citral over supported bimetallic Pt-Co catalysts. *Appl. Catal. A.* **2009**, *358*(1), 32-41.
34. Tian, Z. M.; Xiang, X.; Xie, L. S.; Li, F. Liquid-Phase Hydrogenation of Cinnamaldehyde: Enhancing Selectivity of Supported Gold Catalysts by Incorporation of Cerium into the Support. *Ind. Eng. Chem. Res.* **2013**, *52*(1), 288-296.
35. Plessers, E.; De Vos, D. E.; Roeyfaers, M. B. J. Chemoselective reduction of  $\alpha,\beta$ -unsaturated carbonyl compounds with UiO-66 materials. *J. Catal.* **2016**, *340*, 136-143.
36. Chen, S. J.; Meng, L.; Chen, B. X.; Chen, W. Y.; Duan, X. Z.; Huang, X.; Zhang, B. S.; Fu, H. B.; Wan, Y. Poison Tolerance to the Selective Hydrogenation of Cinnamaldehyde in Water over an Ordered Mesoporous Carbonaceous Composite Supported Pd Catalyst. *ACS Catal.* **2017**, *7*(3), 2074-2087.

37. Wang, Y.; Rong, Z. M.; Wang, Y.; Zhang, P.; Wang, Y.; Qu, J. P. Ruthenium nanoparticles loaded on multiwalled carbon nanotubes for liquid-phase hydrogenation of fine chemicals: An exploration of confinement effect. *J. Catal.* **2015**, *329*, 95-106.
38. Wang, Y.; Rong, Z. M.; Wang, Y.; Qu, Y. P. Ruthenium nanoparticles loaded on functionalized graphene for liquid-phase hydrogenation of fine chemicals: Comparison with carbon nanotube. *J. Catal.* **2016**, *333*, 8-16.
39. Gomollón-Bel, F. Ten Chemical Innovations That Will Change Our World: IUPAC identifies emerging technologies in Chemistry with potential to make our planet more sustainable. *Chem. Int.* **2019**, *41*(2), 12-17.
40. Akwi, F. M.; Watts, P. Continuous flow chemistry: where are we now? Recent applications, challenges and limitations. *Chem. Commun.* **2018**, *54*(99), 13894-13928.
41. Vaccaro, L.; Lanari, D.; Marrocchi, A.; Strappaveccia, G. Flow approaches towards sustainability. *Green Chem.* **2014**, *16*(8), 3680-3704.
42. James, S. L.; Adams, C. J.; Bolm, C.; Braga, D.; Collier, P.; Friscic, T.; Grepioni, F.; Harris, K. D. M.; Hyett, G.; Jones, W.; Krebs, A.; Mack, J.; Maini, L.; Orpen, A. G.; Parkin, I. P.; Shearouse, W. C.; Steed, J. W.; Waddell, D. C. Mechanochemistry: opportunities for new and cleaner synthesis. *Chem. Soc. Rev.* **2012**, *41*(1), 413-447.
43. Xu, C. P.; De, S.; Balu, A. M.; Ojeda, M.; Luque, R. Mechanochemical synthesis of advanced nanomaterials for catalytic applications. *Chem. Commun.* **2015**, *51*, 6698-6713.
44. Munoz-Batista, M. J.; Rodriguez-Padron, D.; Puente-Santiago, A. R.; Luque, R. Mechanochemistry: Toward Sustainable Design of Advanced Nanomaterials for Electrochemical Energy Storage and Catalytic Applications. *ACS Sustain. Chem. Eng.* **2018**, *6*(8), 9530-9544.



# Results & Discussion



# Microwave-assisted preparation of Ag/Ag<sub>2</sub>S carbon hybrid structures from pig bristles as efficient HER catalysts

Camilla Maria Cova,<sup>a</sup> Alessio Zuliani,<sup>a</sup> Alain R. Puente Santiago,<sup>a</sup> Alvaro Caballero,<sup>b</sup> Mario J. Muñoz-Batista<sup>a</sup> and Rafael Luque<sup>\*ac</sup>

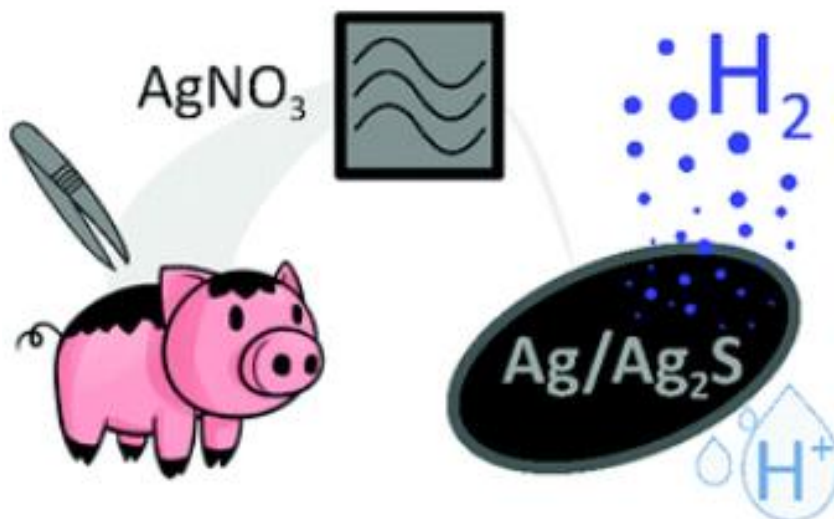
<sup>a</sup>Departamento de Química Orgánica, Universidad de Córdoba, Edificio Marie-Curie (C-3), Ctra Nnal IV-A, Km 396, Córdoba, Spain. E-mail: rafael.luque@uco.es

<sup>b</sup>Departamento de Química Inorgánica e Ingeniería Química, Campus de Rabanales, Edificio Marie Curie (C-3), Ctra Nnal IV-A, Km 396, E14014, Córdoba, Spain

<sup>c</sup>Peoples Friendship University of Russia (RUDN University), 6 Miklukho-Maklaya Str. Moscow, 117198, Russia

DOI: 10.1039/c8ta06417b

## Graphical abstract



Reproduced by permission of The Royal Society of Chemistry, link to publication:  
<https://pubs.rsc.org/en/content/articlelanding/2018/ta/c8ta06417b#!divAbstract>



## Abstract

Ag/Ag<sub>2</sub>S hybrid structures have recently attracted significant interest due to their high chemical and thermal stability, in addition to their unique optical and electrical properties. However, their standard synthetic protocols have important drawbacks including long term and harsh reaction conditions and the utilization of highly toxic sulfur precursors. Herein, an innovative, simple one-pot green approach for the synthesis of Ag/Ag<sub>2</sub>S carbon hybrid structures is reported. The procedure involves a one-step microwave-assisted step using ethylene glycol as solvent and reducing agent, pig bristles as a sulphur and carbon source and silver nitrate as a metal precursor. Different amounts of silver nitrate were employed in order to investigate the synthetic mechanism for the formation of zerovalent silver over silver sulphide nanoparticles, producing three different samples. The materials were characterized by XRD, SEM, EDX, N<sub>2</sub> physisorption and XPS spectroscopy. Aiming to prove the efficiency of the as-synthesized compounds, their electrocatalytic activities were explored in the hydrogen evolution reaction (HER) performing linear sweep voltammetry.

## Introduction

Environmental and economic metrics are becoming increasingly and equally important in the design of new materials. Currently, most industrially available compounds are derived from non-renewable sources, following the so-defined linear economy. However, the rising costs of gas and crude oil and more importantly the drive towards a more sustainable future utilisation of low toxicity reagents is pushing research towards the valorisation of renewable

sources through sustainable synthetic processes.<sup>1</sup> In this context, meeting the principles of green chemistry can be considered as the key to the sustainable design of innovative materials.<sup>2-4</sup>

In the last few decades, different metal chalcogenides have attracted interest because of their unique physical and chemical properties that make them suitable in diverse areas ranging from electronics to biomedicine. These materials include copper sulphide (Cu<sub>2</sub>S), silver sulphide (Ag<sub>2</sub>S), nickel sulphide (NiS), lead sulphide (PbS), cadmium sulphide (CdS) and mercury sulphide (HgS).<sup>5-7</sup> Silver sulphide emerged as an excellent material for the preparation of metal-semiconductor heterostructures.<sup>8,9</sup> These heterostructures may exhibit a behaviour not limited to the combination of the properties of the separated components, but also the synergetic effects of the two constituents.<sup>10</sup> For example, Ag/Ag<sub>2</sub>S heterostructures have attracted special attention as antibacterial agent, biosensing probes and photocatalysts.<sup>11,12</sup> The Ag/Ag<sub>2</sub>S heterostructures have also been proposed as efficient catalysts for the hydrogen evolution reaction (HER).<sup>13,14</sup> Hydrogen is in fact a promising candidate as an alternative green energy source that can be produced *via* water splitting. Consequently, the development of suitable, low cost, high performance catalysts for hydrogen evolution reactions (HER) is of great importance and practical needs. However, despite the reported scope for the production of green hydrogen as an alternative energy source, the synthesis of Ag/Ag<sub>2</sub>S materials entails some sustainability restrictions. All reported synthetic protocols for these materials are normally time and energy consuming.<sup>12</sup> Most importantly, these syntheses involve the utilization of expensive and toxic sulphur sources including highly hazardous compounds such as H<sub>2</sub>S, thiols or Na<sub>2</sub>S and less aggressive (but still toxic) silver thiol salts.<sup>8,15,16</sup>

Based on recent endeavours from our group in microwave chemistry and biomass valorisation, herein we report a sustainable and innovative one-step synthesis of pig bristles-derived Ag/Ag<sub>2</sub>S carbon hybrid structures *via* a microwave-assisted reaction.<sup>17-19</sup> The synthesized material exhibited a high performance as a catalyst for the hydrogen evolution reaction (HER). In this way, the designed nanohybrid material follows the principles of circular economy, being derived from biowaste (pig bristles), also being used as a catalyst for the sustainable production of hydrogen. Pig bristles are indeed an unexploited waste source of sulphur and carbon. Every year ~225k tons of wasted pig bristles are produced only in EU slaughterhouses. However, the few reports available about pig bristles valorisation are limited to their utilization as fodder supplements and materials for brushes.<sup>20,21</sup>

The preparation of Ag/Ag<sub>2</sub>S involved a simple microwave assisted reaction. Microwave synthetic protocols show several advantages compared to conventional heating procedures. For example, they allow reactions to proceed faster, obtaining higher yields with potentially switchable selectivities.<sup>22-24</sup> Ethylene glycol (common solvent used as an antifreeze agent in the automotive industry) was additionally employed as a solvent and reducing agent. Wasted pig bristles were used as a carbon and sulphur source while silver sulphide was employed as a metal precursor. In order to investigate the formation of silver(0) over silver(I) sulphide, the reaction was carried out using different quantities of silver precursor and a fixed amount of pig bristles, resulting in a sequence of three materials with varying Ag/Ag<sub>2</sub>S ratios. The hybrid nanostructures were characterized by XRD, N<sub>2</sub> physisorption, SEM, EDX and XPS spectroscopy.

The materials were tested as catalysts for the hydrogen evolution reaction (HER). Recently Ren *et al.* reported the HER activity of porous Ag<sub>2</sub>S/CuS generating 10 mA cm<sup>-2</sup> by supplying ~0.2 V in 0.5 M H<sub>2</sub>SO<sub>4</sub>.<sup>25</sup> Using the same electrolyte solution, Basu *et al.* reported the HER activity of the Ag/Ag<sub>2</sub>S

nanostructures with a current density of  $10 \text{ mA cm}^{-2}$  upon application of  $-0.199 \text{ V}$  potential.<sup>14</sup>

Herein, the best sample allowed the production of  $10 \text{ mA cm}^{-2}$  operating at  $-0.190 \text{ V}$  potential, one of the lowest applied potential reported in literature for these types of heterostructures.

## Experimental

### Materials

Ethylene glycol ( $\text{HOCH}_2\text{CH}_2\text{OH}$ , 99.9%), silver nitrate ( $\text{AgNO}_3$ ), acetone ( $\text{CH}_3\text{COCH}_3$ ), sulfuric acid ( $\text{H}_2\text{SO}_4$ , 95-97%) and ethanol ( $\text{CH}_3\text{CH}_2\text{OH}$ , 99.5%) were purchased from Sigma-Aldrich Inc., St. Louis, MO, USA. All reagents were used without any further purification.

### Synthesis of Ag/Ag<sub>2</sub>S

A sequence of three different Ag/Ag<sub>2</sub>S carbon hybrid structures with different Ag(0)/Ag(I) ratios was synthesized. The materials were prepared by modifying a methodology recently developed in our group for the synthesis of Cu<sub>2</sub>S.<sup>18</sup> In a typical procedure, the correct amount of silver nitrate (340-2040 mg, 2-12 mmol) was dissolved in 20 mL of ethylene glycol in a 50 mL Teflon microwave tube under vigorous stirring. Sequentially, 1.5 g of pig bristles (cut into pieces of  $\sim 0.5 \text{ cm}$ ) were added. The mixture was kept at room temperature under magnetic stirring (700 rpm) for 10 min. Successively, the Teflon tube was closed and inserted into a Milestone Ethos D microwave reactor (Milestone Srl, Italy). The tube was subjected to microwave irradiation at 500 W for 4 min. In order to avoid any unwanted decomposition of ethylene glycol, the reaction time never exceeded 4 min, and the microwave reactor was set at 200 °C as the maximum external temperature (Infra-Red temperature control) and 60 °C as the maximum internal temperature (a fiber optic cable was inserted into the

reference tube) and all tubes were equipped with pressure safe valves. After the reaction, the mixture was cooled down to room temperature for ~2 hours. The homogeneous dark precipitate was filtrated and washed several times with distilled water, ethanol and acetone. The material was finally oven-dried at 100 °C for 24 hours.

### **Material characterization**

Ag/Ag<sub>2</sub>S carbon hybrid composites were characterized by scanning electron microscopy (SEM), powder X-ray diffraction (XRD) and X-ray photoelectronic spectroscopy (XPS).

Scanning electron microscopy images were recorded using a JEOL JSM-6300 scanning microscope (JEOL Ltd., Peabody, MA, USA) equipped with Energy-dispersive X-ray spectroscopy (EDX) at 15 kV at the Research Support Center (SCAI) from the University of Cordoba.

Powder X-ray diffraction (XRD) patterns were recorded using a Bruker D8 DISCOVER A25 diffractometer (PanAnalytic/Philips, Lelyweg, Almelo, The Netherlands) with CuK $\alpha$  ( $\lambda = 1.5418 \text{ \AA}$ ) radiation. Wide angle scanning patterns were collected over a  $2\theta$  range from 10° to 80° with a step size of 0.018° and counting time of 5 s per step.

The textural properties of the materials were determined by N<sub>2</sub> physisorption using a Micromeritics ASAP 2020 automated system (Micromeritics Instrument Corporation, Norcross, GA, USA) with the Brunauer-Emmet-Teller (BET) and the Barrett-Joyner-Halenda (BJH) methods. Prior to analysis, the samples were outgassed for 24 h at 100 °C under vacuum ( $P_0 = 10^{-2} \text{ Pa}$ ) and subsequently analysed.

XPS studies were performed at the Central Service of Research Support (SCAI) of the University of Cordoba, using an ultrahigh vacuum (UHV) multipurpose surface analysis system Specs<sup>TM</sup>. The experiments were carried

out at pressures  $<10^{-10}$  mbar, using a conventional X-ray source (XR-50, Specs, Mg-K $\alpha$ ,  $h\nu = 1253.6$  eV,  $1$  eV =  $1.603 \times 10^{-19}$  J) in a “stop and go” mode. The samples were deposited on a sample holder using a double sided adhesive tape, and afterwards evacuated overnight under vacuum ( $<10^{-6}$  mbar). Spectra were collected at room temperature (pass energy: 25 and 10 eV, step size: 1 and 0.1 eV) with a Phoibos 150-MCD energy detector. The deconvolutions of the obtained curves and elemental quantification were carried out using the XPS CASA program.

### **Preparation of the electrodes**

Prior to coating, 10 x 10 mm ITO glasses were washed following a standard procedure. Firstly, the glasses were washed with distilled water and soap. Sequentially, the electrodes were washed in an US bath with deionized water, ethanol and acetone. Ag/Ag<sub>2</sub>S/ITO electrodes were prepared by dispersing 1 mg of each sample into 1 mL of ethanol and by drop casting the mixture (90  $\mu$ L) over the ITO surfaces. The geometric area of the electrode and the electrochemical active surface area (ECSA) were 0.80 cm<sup>2</sup> and 2 cm<sup>2</sup> respectively. The electrochemical active surface area was determined by measuring the non-faradaic capacitive current with double-layer charging at a potential of 0.2 V, where non electrocatalytic contributions were observed.<sup>26</sup>

### **Electrochemical measurement**

Linear-sweep voltammetry measurements were performed in a three-electrode electrochemical cell Potentiostat/Galvanostat Autolab (Solartron1286). 50 mL of a 0.5 M H<sub>2</sub>SO<sub>4</sub> aqueous solution was employed as the electrolyte. Ag/AgCl was used as the reference electrode; a Pt substrate was used as the counter electrode and the different Ag/Ag<sub>2</sub>S/ITO electrodes as the working electrodes. It should be pointed out that the area of the Pt substrate was at least ten times higher than the geometrical WE areas with the objective to avoid the deposition

of Pt nanodots on the Ag/Ag<sub>2</sub>S carbon hybrid structures through the formation of large energy barrier.<sup>27</sup> All the electrochemical experiments were performed by applying a potential ranging from 0.2 V to -0.64 V *vs* Ag/AgCl at a scan rate of 2 mV s<sup>-1</sup>.

## Results and discussion

### Synthesis of Ag/Ag<sub>2</sub>S

The synthetic protocol for the production of Ag/Ag<sub>2</sub>S carbon hybrid composites allowed the exploitation of wasted pig bristles as a non-toxic and renewable source of sulphur and carbon as opposed to toxic and hazardous thiols, hydrogen and sodium sulphides<sup>28-30</sup> as shown in Fig. 1. The synthetic procedure involves two different reaction pathways. On one hand, the silver ions were reduced to zerovalent silver. On the other hand, the silver ions reacted with sulphur (released from the pig bristles) in order to form Ag<sub>2</sub>S. For the reduction of silver ions, we resorted to the oxidation of ethylene glycol. This redox reaction is in fact widely known and has been proved to be a highly efficient procedure for the reduction of silver.<sup>31</sup> As shown in the upper arrow in Fig. 1, the proposed reaction mechanism involves the reduction of Ag(I) to Ag(0) and the oxidation of ethylene glycol to glycolaldehyde (2-hydroxyl-acetaldehyde). Additional details about the reaction mechanism and GC-MS analysis can be found in a precedent work where ethylene glycol was used to reduce Ni<sup>2+</sup> to metallic Nickel in a similar microwave-assisted approach.<sup>17</sup>

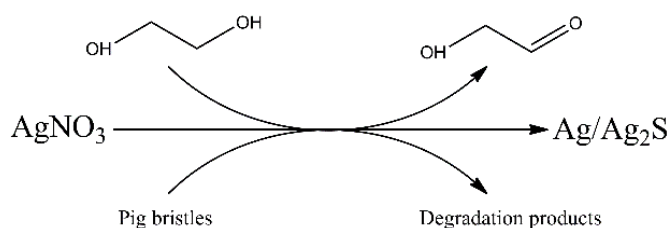


**Fig. 1** Schematic illustration of the synthesis of Ag/Ag<sub>2</sub>S.

At the same time, the silver ions underwent a competitive reaction for the formation of silver sulphide. This reaction involved the rapid degradation of pig bristles *via* microwave heating and the release of sulphur. Pig bristles are in fact sulphur-rich derived from keratin-containing aminoacids (*e.g.* methionine, cysteine and cysteic acid).<sup>30</sup> The total amount of sulphur in pig bristles has been previously quantified to be *ca.* 5 wt% in average.<sup>20,31</sup> The rapid microwave heating and the quick increase of pressure in the reaction tube favoured the fast decomposition of the aminoacids and the release of sulphur. Sequentially, silver sulphide was formed due to the reaction between Ag(I) and S<sup>2-</sup>. In this step, the particles self-aggregated to minimize the surface energy, binding together with pig bristle residual carbon, as shown in the SEM images and as confirmed by XPS analysis.

As summarized in Table 1, three different samples were prepared, using the same amount of pig bristles, and varying silver nitrate concentrations. The hybrid materials were denoted 1.4Ag/Ag<sub>2</sub>S, 0.5Ag/Ag<sub>2</sub>S and 0.2Ag/Ag<sub>2</sub>S, indicating the wt ratio between AgNO<sub>3</sub> and pig bristle in the starting mixture. The weight ratio limit of 1.4 between AgNO<sub>3</sub> and pig bristles was determined due to a practical reason. In fact, all the samples produced with increased amounts of silver nitrate were found to be considerably inhomogeneous, and therefore useless for HER reactions.

**Table 1** Pig bristles and silver nitrate used for the three different samples

Sample	Pig bristles/g	AgNO <sub>3</sub> /g	AgNO <sub>3</sub> /pig bristles
0.2 Ag/Ag <sub>2</sub> S	1.5	0.34	0.2
0.5 Ag/Ag <sub>2</sub> S	1.5	0.75	0.5
1.4 Ag/Ag <sub>2</sub> S	1.5	2.04	1.4

In order to determine the influence of microwave heating in the formation of Ag/Ag<sub>2</sub>S, different trials using conventional heating were carried out in an



open vessel for safety issues.<sup>32</sup> In fact, due to possible degradation of ethylene glycol after long heating times, the utilization of an autoclave was avoided. In all experiments, the formation of pure silver was completed before the degradation of pig bristles took place, resulting in a visibly heterogeneous precipitate, not suitable for an electrochemical cell.

### Materials characterization

The morphology of the Ag/Ag<sub>2</sub>S carbon hybrid structures was investigated by SEM and EDX analyses. Fig. 2 shows the SEM images for the three samples.

All the samples exhibited a coral-like homogeneous morphology where carbon derived from pig bristles is aggregated with Ag/Ag<sub>2</sub>S. Fig. 3 shows the cross-sectional images of SEM for 1.4Ag/Ag<sub>2</sub>S.

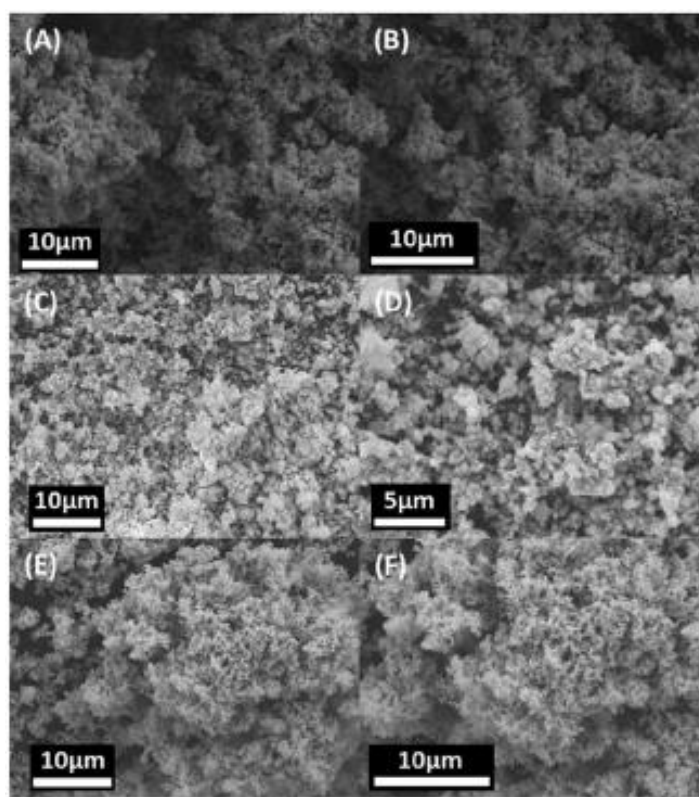


**Fig. 2** SEM images of the three different Ag/Ag<sub>2</sub>S carbon heterostructures. (A) and (B) 1.4Ag/Ag<sub>2</sub>S; (C) and (D) 0.5Ag/Ag<sub>2</sub>S; (E) and (F) 0.2Ag/Ag<sub>2</sub>S.

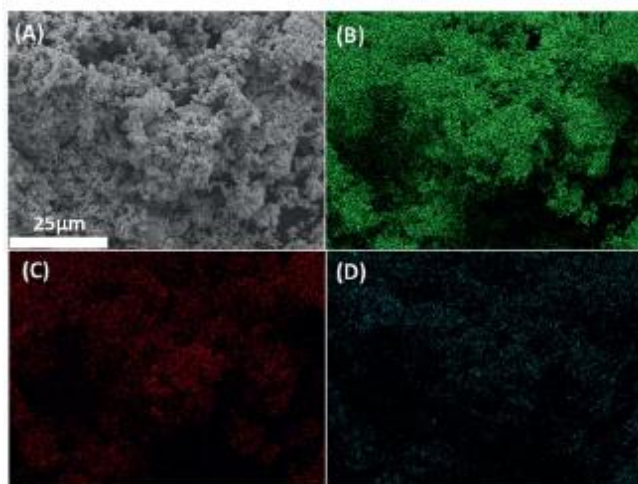


**Fig. 3** SEM images with mapping analysis of (a) 1.4Ag/Ag<sub>2</sub>S carbon hybrid structure. (b) Silver; (c) Carbon; (d) Sulphur.

Remarkably, silver, sulphur and carbon were found to be nicely distributed in the material, confirming the homogeneous conditions of the synthesis (please see Fig. S1† for 0.5Ag/Ag<sub>2</sub>S and 0.2Ag/Ag<sub>2</sub>S mapping).

EDX-mapping micrographs detected the presence of carbon, sulphur and silver. The atomic percentage of S, Ag and C of the three different samples are shown in Table 2. Except for oxygen, found in the atomic percentage of ~ 8% in all the samples, and most likely absorbed as CO<sub>2</sub>, no other elements were detected in EDX analysis, indicating the high purity of the samples.

**Table 2** EDX data of the three different samples

Sample	S / Atomic %	Ag / Atomic %	C / Atomic %
0.2 Ag/Ag <sub>2</sub> S	28.7	33.8	29.4
0.5 Ag/Ag <sub>2</sub> S	12.9	40.2	37.4
1.4 Ag/Ag <sub>2</sub> S	6.4	53.6	32.1

The phase purity and crystallinity of the synthesized Ag/Ag<sub>2</sub>S carbon hybrid composites were subsequently investigated by XRD analysis. As shown in Fig. 4, XRD patterns for all the different samples show the presence of both

Ag<sub>2</sub>S and Ag crystals. All the diffraction peaks nicely match with the lattice planes of Ag<sub>2</sub>S along with cubic Ag crystals. Most intense diffraction peaks of the sample 1.4Ag/Ag<sub>2</sub>S could be observed at  $2\theta$  values of 37.65°, 43.95°, 64.04° and 77.15°, correspondingly indexed to (1 1 1), (2 0 0), (2 2 0) and (3 1 1) planes of silver with cubic structure (JCPDS 01-087-0597).<sup>33</sup> The peaks of the same sample at  $2\theta$  values of 28.49°, 31.07°, 33.14°, 34.25°, 36.19°, 40.31°, 52.87° and 63.85° could be indexed to (0 2 1), (-3 1 1), (1 2 1), (2 2 0), (0 2 2), (-1 3 0), (0 0 4) and (-6 0 1) planes of silver sulphide (JCPDS 00-009-0422).<sup>34</sup> No other impurity peaks detected through XRD also suggested high purity of the materials (for a complete list of the peaks and the assigned planes of all the samples, please see Table S1†).

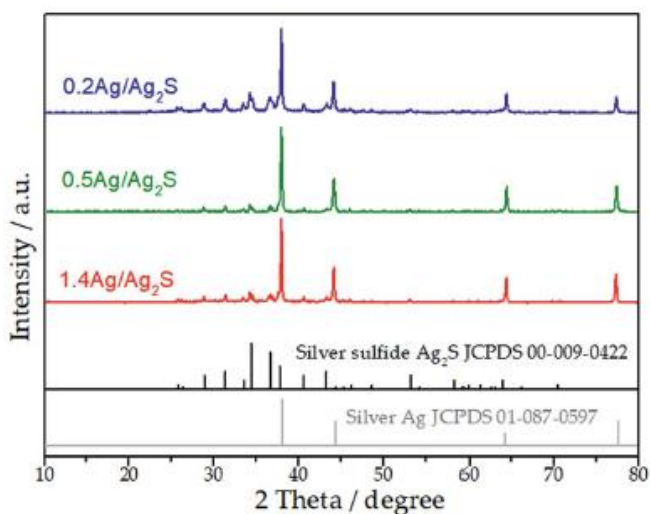


**Fig. 4** XRD pattern of Ag/Ag<sub>2</sub>S hybrid materials.

Brunauer–Emmett–Teller (BET) physisorption was carried out in order to determine the specific surface area of the materials using nitrogen adsorption–desorption measurements. BET surface areas were found to be  $\sim 20 \text{ m}^2 \text{ g}^{-1}$  for all the samples, with the isotherms clearly pointing to the formation of non-porous materials, confirming SEM analysis (please see Fig. S2† for the isotherm of sample 1.4Ag/Ag<sub>2</sub>S).

In order to obtain additional information on the surface for the composite samples, XPS analysis of C 1s, Ag 3d and NNM and S 2p were carried out. C 1s shows no difference in C species through the series, with the reference peak at the same position (please see Fig. 5(A) for the analysis of C 1s) used for calibration *ca.* 284.6 eV (C-C). Ag 3d<sub>5/2</sub> and Ag 3d<sub>3/2</sub> contributions were analysed considering both Ag(0) and Ag(I), as presented in Fig. 5(B) and Table 3. The literature shows certain ambiguity over the binding energy values of Ag(0) and Ag(I) ions due to the very similar peak position detected. In fact, several references have reported Ag 3d<sub>5/2</sub> in the range of 367.9-368.4 eV and 367.6-368.5 eV for Ag(0) and Ag(I), respectively.<sup>35-39</sup> The clear shift through the series and the analysis of Ag MNN level allowed the following assignment. The contribution at *ca.* 367.9 (Ag 3d<sub>5/2</sub>) and 373.8 (Ag 3d<sub>3/2</sub>) eV may be assigned to Ag(0) species,<sup>40,41</sup> while the peaks at *ca.* 368.6 and 374.7 eV may be attributed to those of Ag 3d<sub>5/2</sub> and Ag 3d<sub>3/2</sub> of the Ag(I) ions in Ag<sub>2</sub>S.<sup>35,40</sup> These hypotheses are also confirmed by the S 2p XPS region (Fig. 5(C)). The values of *ca.* 161.5 eV and 163.0 eV are in agreement with S 2p<sub>3/2</sub> and S 2p<sub>1/2</sub> for Ag<sub>2</sub>S from previous reports (Table 3).<sup>35,40</sup> As it can be seen in Table 3 and Fig. 5(B) and (C), the signal enhancement for sulphur can be unambiguously associated with a higher S concentration and consequently with a higher concentration of Ag<sub>2</sub>S. In addition, quantitative analysis confirmed the dominant presence of metallic silver for 1.4Ag/Ag<sub>2</sub>S while a higher superficial concentration of Ag<sub>2</sub>S was obtained in the samples 0.5Ag/Ag<sub>2</sub>S and 0.2Ag/Ag<sub>2</sub>S, which is in good agreement with the XRD results (Table 3). The ratio between the two Ag species varies along the series. Interestingly, Ag(0)/Ag(I) showed a roughly linear trend suggesting the possibility to control and fine-tune Ag(0)/Ag(I) ratios in the novel synthetic protocol (Fig.5(D) and (E)). Finally, as it is represented in Fig. 5(E), the ratio Ag/S as function of the pig bristle (pb)/Ag

precursor ratio (wt) showed similar values in comparison to those obtained by EDX (Table 1) while, as expected, the Ag(I)/S ratio presented a relatively constant value (*ca.* 2) for all the samples (see Table 3 for details).

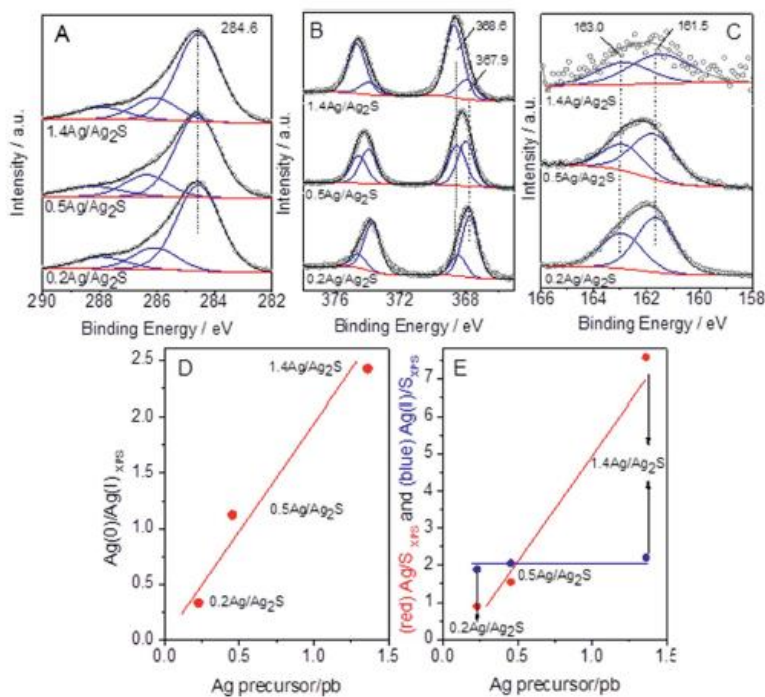


**Fig. 5** (A) C 1s, (B) Ag 3d, (C) S 2p of the  $x\text{Ag}/\text{Ag}_2\text{S}$  samples; (D-E) XPS ratios obtained by XPS vs. pig bristle (pb)/Ag precursor ratio (wt ratio).

**Table 3** XPS Data for the Ag/Ag<sub>2</sub>S samples

Sample	Position/eV						
	Ag 3d <sub>5/2</sub>		S 2p <sub>3/2</sub>	C 1s	Ag(0)/Ag(I)	Ag/S	Ag(I)/S
Ag(0)	Ag(I)						
0.2Ag/Ag <sub>2</sub> S	367.9	368.5	161.5	284.6	0.3	0.9	1.9
0.5Ag/Ag <sub>2</sub> S	367.9	368.6	161.6	284.6	1.0	1.5	2.1
1.4Ag/Ag <sub>2</sub> S	367.9	368.7	161.5	284.6	2.4	7.6	2.2

### Electrochemical hydrogen evolution

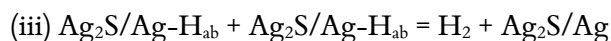
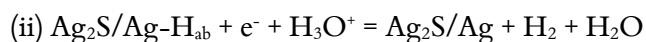
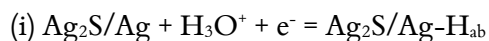
Ag/Ag<sub>2</sub>S/ITO electrodes were subsequently prepared and tested for electrochemical activity in the hydrogen evolution reaction (HER) using linear sweep voltammetry (LSV) experiments in 0.5 M of H<sub>2</sub>SO<sub>4</sub> at a scan rate of

2 mV s<sup>-1</sup>. Potentials were measured vs. the Ag/AgCl electrode and reported against the reversible hydrogen electrode (RHE). Fig. 6(A) shows the electrocatalytic performances towards hydrogen evolution in acid media of 0.2Ag/Ag<sub>2</sub>S, 0.5Ag/Ag<sub>2</sub>S and 1.4Ag/Ag<sub>2</sub>S composites respectively. Notably, 0.5Ag/Ag<sub>2</sub>S and 1.4Ag/Ag<sub>2</sub>S hybrid materials can generate a current density of *ca.* 37 mA cm<sup>-2</sup> and *ca.* 110 mA cm<sup>-2</sup> at -0.6 V respectively, while the 0.2Ag/Ag<sub>2</sub>S sample shows a negligible electrocatalytic response. It should be pointed out that the current densities in the Fig. 6(A) and (B) were calculated from the geometric area of the electrodes. Additional plots of the current density normalized to the electrochemical surface area of the catalyst are provided in the ESI (Fig. S3<sup>†</sup>). Importantly, at a scan rate of 2 mV s<sup>-1</sup>, the sample 0.5Ag/Ag<sub>2</sub>S required an overpotential of 370 mV to produce a current density of 10 mA cm<sup>-2</sup> whereas the sample 1.4Ag/Ag<sub>2</sub>S could successfully generate 10 mA cm<sup>-2</sup> at a -190 mV potential. This value surpassed the electrocatalytic activity of the Ag<sub>2</sub>S/CuS which exhibited, to the best of our knowledge, among the hybrid catalysts constructed from Ag, the best activity with demand for an overpotential to deliver 10 mA cm<sup>-2</sup> (193 mV).<sup>25</sup> Therefore, the aforementioned findings constitute, to date, one of the lowest applied potentials reported in literature for these types of materials.<sup>13,14,25,42</sup> Interestingly, the increase of the current density followed a pronounced linear trend with respect to the Ag(0)/Ag(I) ratio (Fig. 6(D)), suggesting that the content of Ag(0) at the heterostructure surfaces controls the electrocatalytic yields of the hydrogen evolution process. Recently, the improvement of the electrocatalytic performances of the Ag/Ag<sub>2</sub>S heterostructures towards hydrogen production has been ascribed to differences in the microstructures. Indeed, these differences can in turn modulate the number of hydrogen anions adsorbed at the composites surfaces and therefore the current densities involved in the

electrocatalytic processes.<sup>14</sup> All the synthesized samples have a similar microstructure and surface area. Considering that the anchorage of the hydrogen anions on the metallic silver surfaces is the first step of the HER process (see mechanism below), it is conceivable to think that increasing silver contents, therefore of the metallic silver surface, provide more catalytic active sites, effectively improving hydrogen production.

The evaluation of the Tafel slopes is a useful tool to get insights on mechanistic pathways for the HER processes. Fig. 6(C) depicts the Tafel slopes for 0.5Ag/Ag<sub>2</sub>S and 1.4Ag/Ag<sub>2</sub>S composites. The Tafel slope obtained for 1.4Ag/Ag<sub>2</sub>S (150 mV dec<sup>-1</sup>) exhibits a comparatively lower value to that obtained for 0.5Ag/Ag<sub>2</sub>S (240 mV dec<sup>-1</sup>), indicating a remarkable enhancement in the kinetics of the catalytic process of 1.4Ag/Ag<sub>2</sub>S as the electrocatalyst. These results strongly confirm the superior catalytic performance of 1.4Ag/Ag<sub>2</sub>S towards the HER.

The proposed mechanism for the HER processes in an acidic medium consists of two steps (i) the Volmer step, (ii) the desorption step or Heyrovsky process and (iii) the recombination step or Tafel step.<sup>43</sup>



It is worth to note that the rate-determining step of the HER for 1.4Ag/Ag<sub>2</sub>S is the Volmer step due to its Tafel slope being closer to 120 mV dec<sup>-1</sup> rather than 40mV dec<sup>-1</sup>.

Importantly, since the rate-limiting step of 1.4Ag/Ag<sub>2</sub>S for the HER is the anchorage of hydrogen anions onto the catalytically active metallic Ag sites, larger amounts of metallic Ag in the composite surfaces consequently improve the electrocatalytic efficiency in terms of hydrogen production. In addition, the high content of carbon in all the samples most likely improved the catalytic

activity. Indeed, carbon itself is inert carbon itself is inert for the hydrogen evolution reaction. However, as reported by Zhou *et al.* and by Zhang *et al.*, the catalytic activity of carbon can be improved by the introduction of transition metal nanoparticles in order to modify the electronic properties of carbon and create new active sites for the HER.<sup>44,45</sup> Considering that, as reported in EDX analysis (please see Table 2) all the materials showed a similar content of carbon ( $\sim 30$  atomic%), the effect of carbon was comparable in all the HER reactions.

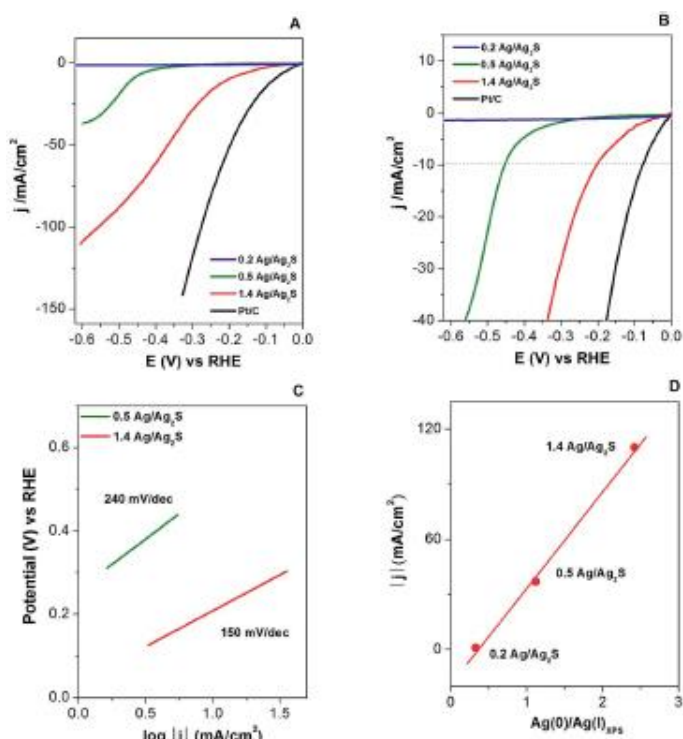


**Fig. 6** (A,B) LSV curves for 0.2Ag/Ag<sub>2</sub>S, 0.5Ag/Ag<sub>2</sub>S, 1.4Ag/Ag<sub>2</sub>S and commercial Pt/C with a scan rate of 2 mV s<sup>-1</sup> for the HER; (C) Tafel plots for 0.5Ag/Ag<sub>2</sub>S and 1.4Ag/Ag<sub>2</sub>S carbon-hybrid composites respectively; (D) current densities vs. Ag(0)/Ag(I) ratio determined by XPS.



## Conclusions

A sequence of Ag/Ag<sub>2</sub>S carbon hybrid composites were synthesized using pig bristles as a source of sulphur and silver nitrate under microwave irradiation. The presence of both phases, metallic silver and silver sulphide, was demonstrated by XRD analysis, which clearly showed diffraction peaks relative to Ag and Ag<sub>2</sub>S. A ratio between the concentration on the surface of the two different oxidation states of Ag (*i.e.* Ag(0) and Ag(I)) could be found from the XPS results. This Ag(0)/Ag(I) ratio shows a linear dependence as a function of the pig bristle/silver precursor. The materials were tested in the electrocatalytic hydrogen evolution reaction, with the most active sample (1.4Ag/Ag<sub>2</sub>S), allowing the production of 10 mA cm<sup>-2</sup> operating at -0.190 V potential. Such a value is one of the lowest applied potentials reported in the literature for Ag/Ag<sub>2</sub>S hybrid compounds in the HER. Importantly, the synthetic protocol is simple, sustainable and allows the valorisation of a waste feedstock (pig bristle) for the design of highly active electrocatalytic materials. The catalytic activity of the materials was found to linearly depend on the ratio between Ag(0) and Ag(I) which can be easily fine-tuned in the microwave-assisted methodology, pointing to a potentially tunable synthetic protocol depending on the target applications (*i.e.* electrosynthesis of biomass-derived molecules) that will be additionally reported in due course.

## Conflicts of interest

There are no conflicts to declare.

## Acknowledgements

This project has received funding from the European Union's Horizon 2020 research and innovation programme under the Marie Skłodowska-Curie grant agreement No 721290. This publication reflects only the author's view,

exempting the Community from any liability. Project website: <http://cosmic-etn.eu/>. M.J.M-B thanks MINECO for the award of postdoctoral JdC contract (FJCI-2016-29014). The publication has been prepared with support from the RUDN University program 5-100.

## Notes and references

- 1 C. O. Tuck, E. Perez, I. T. Horvath, R. A. Sheldon and M. Poliakoff, *Science*, 2012, **337**, 695-699.
- 2 P. Anastas and N. Eghbali, *Chem. Soc. Rev.*, 2010, **39**, 301-312.
- 3 P. Gallezot, *Chem. Soc. Rev.*, 2012, **41**, 1538-1558.
- 4 R. A. Sheldon, *Green Chem.*, 2017, **19**, 18-43.
- 5 S. Santner, J. Heine and S. Dehnen, *Angew. Chem., Int. Ed.*, 2016, **55**, 876-893.
- 6 Y. Xu, Y. Huang and B. Zhang, *Inorg. Chem. Front.*, 2016, **3**, 591-615.
- 7 N. Jiang, Q. Tang, M. L. Sheng, B. You, D. E. Jiang and Y. J. Sun, *Catal. Sci. Technol.*, 2016, **6**, 1077-1084.
- 8 B. Liu and Z. F. Ma, *Small*, 2011, **7**, 1587-1592.
- 9 M. L. Pang, J. Y. Hu and H. C. Zeng, *J. Am. Chem. Soc.*, 2010, **132**, 10771-10785.
- 10 J. Yang and J. Y. Ying, *Angew. Chem., Int. Ed.*, 2011, **50**, 4637-4643.
- 11 X. H. Ma, Y. Y. Zhao, X. Y. Jiang, W. Liu, S. Q. Liu and Z. Y. Tang, *Chemphyschem*, 2012, **13**, 2531-2535.
- 12 S. I. Sadovnikov and A. I. Gusev, *J. Mater. Chem. A*, 2017, **5**, 17676-17704.
- 13 X. H. Xia, X. J. Zhao, W. C. Ye and C. M. Wang, *Electrochim. Acta*, 2014, **142**, 173-181.
- 14 M. Basu, R. Nazir, C. Mahala, P. Fageria, S. Chaudhary, S. Gangopadhyay and S. Pande, *Langmuir*, 2017, **33**, 3178-3186.
- 15 W. L. Yang, L. Zhang, Y. Hu, Y. J. Zhong, H. B. Wu and X. W. Lou, *Angew. Chem., Int. Ed.*, 2012, **51**, 11501-11504.
- 16 D. S. Wang, T. Xie, Q. Peng and Y. D. Li, *J. Am. Chem. Soc.*, 2008, **130**, 4016-4022.

## Results & Discussion

- 17 A. Zuliani, A. M. Balu and R. Luque, *ACS Sustainable Chem. Eng.*, 2017, **5**, 11584-11587.
- 18 A. Zuliani, M. J. Munoz-Batista and R. Luque, *Green Chem.*, 2018.
- 19 A. Yopez, S. De, M. S. Climent, A. A. Romero and R. Luque, *Appl. Sci.*, 2015, **5**, 532-543.
- 20 Laba, W. Kopec, D. Chorazyk, A. Kancelista, M. Piegza and K. Malik, *Int. Biodeterior. Biodegrad.*, 2015, **100**, 116-123.
- 21 F. G. Gachango, K. S. Ekmann, J. Frorup and S. M. Pedersen, *Aquaculture*, 2017, **479**, 265-272.
- 22 J. B. Bariwal, D. S. Ermolat'ev and E. V. Van der Eyeken, *Chem.-Eur. J.*, 2010, **16**, 3281-3284.
- 23 J. Monzo-Cabrera, J. L. Pedreno-Molina and A. Toledo, *Measurement*, 2009, **42**, 1257-1262.
- 24 R. S. Varma, *Green Chem.*, 2014, **16**, 2027-2041.
- 25 H. T. Ren, W. C. Xu, S. L. Zhu, Z. D. Cui, X. J. Yang and A. Inoue, *Electrochim. Acta*, 2016, **190**, 221-228.
- 26 J. Kibsgaard, C. Tsai, K. Chan, J. D. Benck, J. K. Norskov, F. Abild-Pedersen and T. F. Jaramillo, *Energy Environ. Sci.*, 2015, **8**, 3022-3029.
- 27 R. Chen, C. J. Yang, W. Z. Cai, H. Y. Wang, J. W. Miao, L. P. Zhang, S. L. Chen and B. Liu, *Acs Energy Lett.*, 2017, **2**, 1070-1075.
- 28 W. L. Ong, Y. F. Lim, J. L. T. Ong and G. W. Ho, *J. Mater. Chem. A*, 2015, **3**, 6509-6516.
- 29 S. I. Sadovnikov and A. I. Gusev, *J. Nanopart. Res.*, 2016, **18**.
- 30 R. Vogel, P. Hoyer and H. Weller, *J. Phys. Chem.*, 1994, **98**, 3183-3188.
- 31 Y. G. Sun, Y. D. Yin, B. T. Mayers, T. Herricks and Y. N. Xia, *Chem. Mater.*, 2002, **14**, 4736-4745.
- 32 F. Lees, *Lees' Loss Prevention in the Process Industries: Hazard Identification, Assessment and Control*, Butterworth-Heinemann, 2012.
- 33 Q. Zhang, Y. Huang, L. F. Xu, J. J. Cao, W. K. Ho and S. C. Lee, *ACS Appl. Mater. Interfaces*, 2016, **8**, 4165-4174.
- 34 P. J. Wu, J. W. Yu, H. J. Chao and J. Y. Chang, *Chem. Mater.*, 2014, **26**, 3485-3494.
- 35 G. X. Zhu, C. L. Bao, Y. J. Liu, X. P. Shen, C. Y. Xi, Z. Xu and Z. Y. Ji, *Nanoscale*, 2014, **6**, 11147-11156.
- 36 W. G. Fan, S. Jewell, Y. Y. She and M. K. H. Leung, *Phys. Chem. Chem. Phys.*, 2014, **16**, 676-680.

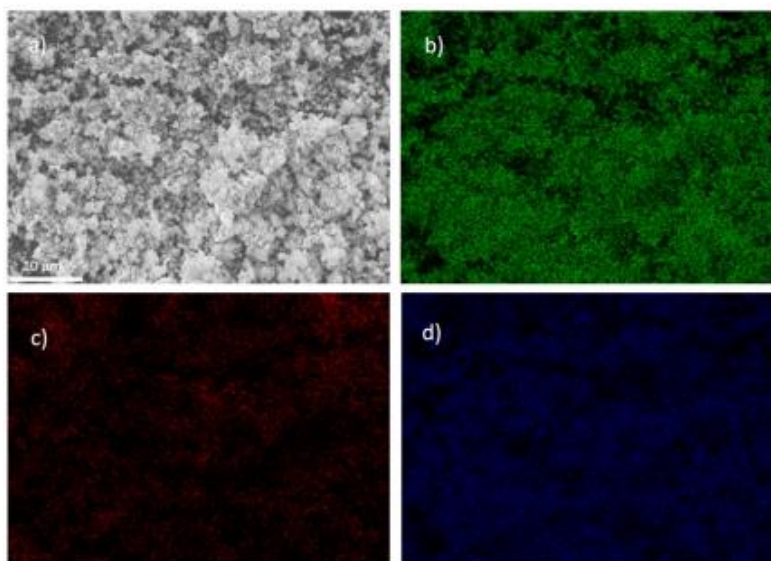
- 37 C. S. Xing, Y. Zhang, Z. D. Wu, D. L. Jiang and M. Chen, *Dalton Trans.*, 2014, **43**, 2772-2780.
- 38 D. Dutta, R. Hazarika, P. D. Dutta, T. Goswami, P. Sengupta and D. K. Dutta, *RSC Adv.*, 2016, **6**, 85173-85181.
- 39 F. Sastre, M. J. Munoz-Batista, A. Kubacka, M. Fernandez-Garcia, W. A. Smith, F. Kapteijn, M. Makkee and J. Gascon, *ChemElectroChem*, 2016, **3**, 1497-1502.
- 40 J. L. Wang, H. Feng, K. M. Chen, W. L. Fan and Q. Yang, *Dalton Trans.*, 2014, **43**, 3990-3998.
- 41 A. M. Ferraria, A. P. Carapeto and A. M. B. do Rego, *Vacuum*, 2012, **86**, 1988-1991.
- 42 X. Q. Ji, B. P. Liu, X. Ren, X. F. Shi, A. M. Asiri and X. P. Sun, *ACS Sustainable Chem. Eng.*, 2018, **6**, 4499-4503.
- 43 B. E. Conway and B. V. Tilak, *Electrochim. Acta*, 2002, **47**, 3571-3594.
- 44 W. Zhou, J. Jia, L. Yang, D. Hou, G. Li and S. Chen, *Nano Energy*, 2016, **28**, 29-43.
- 45 L. Zhang, J. Xiao, H. Wang and M. Shao, *ACS Catal.*, 2017, **7**, 7855-7865.

## Supporting Information

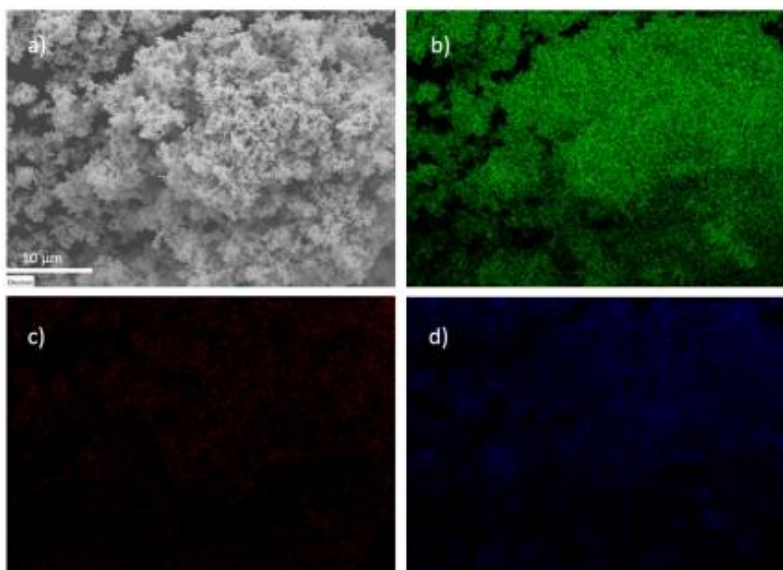
### Microwave-assisted preparation of Ag/Ag<sub>2</sub>S carbon hybrid structures from pig bristles as efficient HER catalysts

Camilla Maria Cova, Alessio Zuliani, Alain R. Puente Santiago, Alvaro Caballero, Mario J. Muñoz-Batista and Rafael Luque\*

Fig. S.1 SEM Mapping of samples 0.5Ag/Ag<sub>2</sub>S and 0.2Ag/Ag<sub>2</sub>S



SEM images with mapping analysis of 0.5Ag/Ag<sub>2</sub>S carbon hybrid structure (a)  
Distribution of Silver (b), Carbon (c) and Sulphur (d)



SEM images with mapping analysis of 0.2Ag/Ag<sub>2</sub>S carbon hybrid structure (a) Distribution of Silver (b), Carbon (c) and Sulphur (d)

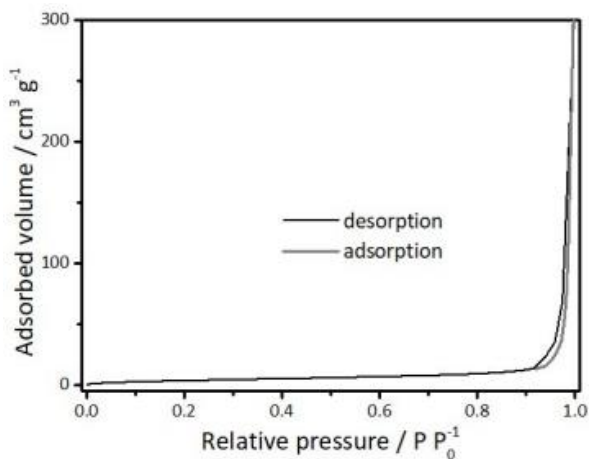
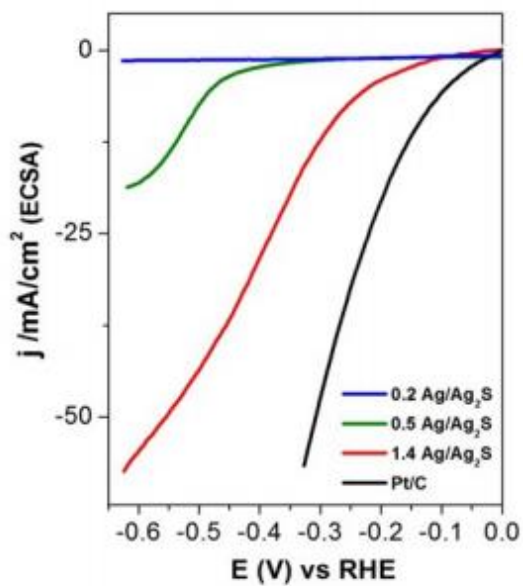
Table S.1 Complete list of XRD peaks of the different materials

1.4Ag/Ag <sub>2</sub> S			Silver, 01-087-0597				Silver sulphide, 00-009-0422							
Pos. [°2Th.]	Intensity		h	k	l	d	Pos. [°2Th.]	Intensity	h	k	l	d	Pos. [°2Th.]	Intensity
1	25,4437	2,1							0	0	2	3,4500	25,347	10
2	28,4983	4,67							0	2	1	3,0900	28,871	30
3	31,0469	5,7							-					
4	33,9065	8,52							3	1	1	2,8500	31,362	40
5	34,2556	3,89							1	2	1	2,6700	33,537	20
6	36,1951	2,54							2	2	0	2,6000	34,467	100
7	37,6559	100							0	2	2	2,4500	36,65	80
8	40,2972	4,24	1	1	1	2,35917	38,115	100	4	0	2	2,3800	37,768	50
9	43,8532	39,19							1	3	0	2,2200	40,606	30
10	45,7315	2,93							-					
11	47,3466	1,03							1	2	3	2,0900	43,254	40
12	48,2896	1,52	2	0	0	2,0431	44,229	45,7	2	1	2	2,0000	45,306	5
13	52,8359	2,63							-					
14	57,8335	0,48							4	2	2	1,9610	47,259	10
15	59,3723	0,41							4	1	4	1,8700	48,652	10
16	63,3254	2,2							0	0	4	1,7190	53,245	30
17	64,0454	30,33	2	2	0	1,44469	64,443	22,5	5	0	0	1,5800	58,357	20
18	69,4916	0,45							3	3	1	1,5560	59,346	10
19	70,2608	0,83							2	4	1	1,4750	62,965	5
20	77,0372	31,11	3	1	1	1,23204	77,397	22,2	6	0	1	1,4550	63,932	20
									5	2	5	1,4120	66,123	5
									3	4	1	1,3360	70,42	10

## Results & Discussion

0.5Ag/Ag <sub>2</sub> S			Silver, 01-087-0597				Silver sulphide, 00-009-0422							
Pos. [°2Th.]	Intensity		h	k	l	d	Pos. [°2Th.]	Intensity	h	k	l	d	Pos. [°2Th.]	Intensity
1	25,8548	3,35							0	0	2	3,4500	25,347	10
2	28,8994	6,06							0	2	1	3,0900	28,871	30
3	31,4425	8,38							-					
4	33,5304	5,09							3	1	1	2,8500	31,362	40
5	34,6601	12,02							1	2	1	2,6700	33,537	20
6	36,05	7,9							2	2	0	2,6000	34,467	100
7	37,55	100							0	2	2	2,4500	36,65	80
8	40,6724	5,38	1	1	1	2,35917	38,115	100	-					
9	43,3417	5,67							4	0	2	2,3800	37,768	50
10	45,3191	1,7							-					
11	46,1077	1,84							1	3	0	2,2200	40,606	30
12	48,67	1							-					
13	53,2118	2,51							1	2	3	2,0900	43,254	40
14	58,2365	0,55	2	0	0	2,0431	44,229	45,7	2	1	2	2,0000	45,306	5
15	59,5443	0,13							-					
16	62,4927	0,69							4	2	2	1,9610	47,259	10
17	64,3947	29,41							-					
18	65,98	1,47							4	1	4	1,8700	48,652	10
19	70,4506	0,18							0	0	4	1,7190	53,245	30
20	77,3515	33,3							5	0	0	1,5800	58,357	20
									3	3	1	1,5560	59,346	10
									2	4	1	1,4750	62,965	5
									-					
			2	2	0	1,44469	64,443	22,5	6	0	1	1,4550	63,932	20
									-					
									5	2	5	1,4120	66,123	5
									3	4	1	1,3360	70,42	10
			3	1	1	1,23204	77,397	22,2						

0.2Ag/Ag <sub>2</sub> S			Silver, 01-087-0597				Silver sulphide, 00-009-0422							
Pos. [°2Th.]	Intensity		h	k	l	d	Pos. [°2Th.]	Intensity	h	k	l	d	Pos. [°2Th.]	Intensity
1	25,6166	4,47							0	0	2	3,4500	25,347	10
2	28,6975	7,62							0	2	1	3,0900	28,871	30
3	31,2633	12,03							-					
4	33,3086	4,96							3	1	1	2,8500	31,362	40
5	34,1344	19,04							1	2	1	2,6700	33,537	20
6	36,4339	9,35							2	2	0	2,6000	34,467	100
7	37,8899	100							0	2	2	2,4500	36,65	80
8	40,4984	6,86							-					
9	43,2104	7,1							4	0	2	2,3800	37,768	50
10	45,3012	0,68							-					
11	45,9691	3,39	1	1	1	2,35917	38,115	100	1	3	0	2,2200	40,606	30
12	48,5474	2,28							-					
13	53,0746	3,53							1	2	3	2,0900	43,254	40
14	58,1157	1,43							2	1	2	2,0000	45,306	5
15	59,8648	1,63	2	0	0	2,0431	44,229	45,7	-					
16	62,3952	1,43							4	2	2	1,9610	47,259	10
17	64,2486	21,78							-					
18	66,05	1,24							4	1	4	1,8700	48,652	10
19	72,1161	1,05							0	0	4	1,7190	53,245	30
20	77,2383	18,43							5	0	0	1,5800	58,357	20
									3	3	1	1,5560	59,346	10
									2	4	1	1,4750	62,965	5
									-					
			2	2	0	1,44469	64,443	22,5	6	0	1	1,4550	63,932	20
									-					
									5	2	5	1,4120	66,123	5
									3	4	1	1,3360	70,42	10
			3	1	1	1,23204	77,397	22,2						

Fig. S.2 N<sub>2</sub> adsorption-desorption isotherm of 1.4Ag/Ag<sub>2</sub>SFig. S.3 LSV curves for 0.2Ag/Ag<sub>2</sub>S, 0.5Ag/Ag<sub>2</sub>S, 1.4Ag/Ag<sub>2</sub>S and commercial Pt/C normalized by the electrochemical active surface area (ECSA)



# A sustainable approach for the synthesis of catalytically active peroxidase-mimic ZnS catalysts

Camilla M. Cova,<sup>†</sup> Alessio Zuliani,<sup>†</sup> Mario J. Muñoz-Batista,<sup>†</sup> and Rafael Luque<sup>\*,†,‡</sup>

<sup>†</sup>*Departamento de Química Orgánica, Universidad de Córdoba, Edificio Marie-Curie (C-3), Ctra Nnal IV-A, Km 396, Córdoba, Spain*

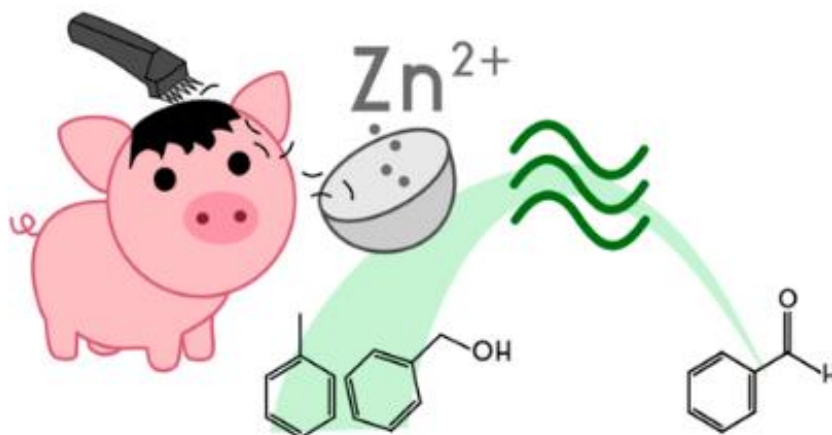
<sup>‡</sup>*Peoples Friendship University of Russia (RUDN University), 6 Miklukho-Maklaya str., 117198, Moscow, Russia*

Corresponding Author: q62alsor@uco.es (R. Luque)

DOI: 10.1021/acssuschemeng.8b04968

KEYWORDS: Zinc sulfide, Pig bristles, Microwave chemistry, Selective oxidations

## Graphical abstract



Adapted with permission from ACS Sustain. Chem. Eng., 2019, 7 (1), 1300-1307.  
Copyright 2019 American Chemical Society

## Abstract

Zinc sulfides are emerging as promising catalysts in different fields such as photochemistry or organic synthesis. Nevertheless, the synthesis of ZnS compounds normally requires the utilization of toxic sulfur precursors, e.g., thiourea which is a contaminant and carcinogenic agent. As a result, new green and sustainable synthetic methodologies are needed. Herein, an innovative, simple, and cheap approach for the synthesis of ZnS carbon composites is reported. Zinc acetate dihydrate was employed as metal precursor while wasted pig bristles were employed as carbon and sulfur source. The phase and the morphology of the compounds were analyzed by XRD, XPS, SEM and EDX and the surface area was determined by nitrogen physisorption. ZnS carbon materials showed remarkable peroxidase-like catalytic activity for two different model reactions: the liquid-phase selective oxidation of benzyl alcohol and toluene to benzaldehyde (conversions up to 63% and 29% and selectivities up to 86% and 87%, respectively) using hydrogen peroxide as oxidant under microwave irradiation.

## Introduction

Zinc sulfide has been studied as an important compound due to its unique physical and photochemical properties.<sup>1-3</sup> It has demonstrated an extraordinary versatility and potentiality for different applications including light-emitting diodes (LEDs), electroluminescence, infrared windows, sensors, lasers, and biodevices.<sup>4-6</sup> Additionally, ZnS possesses many interesting characteristics such as excellent transport properties, an intrinsically *n*-type semiconductivity, good

thermal stability, high electronic mobility, nontoxicity, water insolubility, and low-production costs.<sup>4-7</sup>

All reported synthetic protocols for ZnS preparation involve the utilization of highly toxic sulfur sources including extremely hazardous compounds such as H<sub>2</sub>S, or Na<sub>2</sub>S as well as thioureas, highly contaminant and carcinogenic agents.<sup>8-10</sup> New green and low-toxicity sulfur sources are therefore required for sustainable development. In this context, pig bristles represent a cheap and largely available source of sulfur (and carbon). Pig bristles are considered as a waste toxic-free feedstock, easily collectable and accessible at industrial scale. In fact, ca. ~225k tons of wasted pig bristles are yearly produced only in European slaughterhouses.<sup>11</sup> However, only a few works to date are available on the reutilization/use of pig bristles as fodder supplements, while their valorisation as chemical source is extremely limited.<sup>11-13</sup>

Herein, a simple and innovative synthesis of ZnS carbon composites derived from wasted pig bristles is reported. The synthetic procedure involved a facile heating step in a diluted aqueous solution of potassium hydroxide. Wasted pig bristles were employed as sulfur and carbon source while zinc acetate dihydrate was used as metal source. The material was characterized by XPS, XRD, N<sub>2</sub> physisorption, SEM and EDX, demonstrating the successful formation of zinc sulfides carbon compounds.

In order to validate the practical application of the new material, ZnS carbon composites were tested as catalysts in two different model reactions: the selective oxidation of benzyl alcohol and toluene to benzaldehyde. Among all known oxidative transformations, the selective oxidations of alcohols to the corresponding carbonyl compounds have gained attention due to their broad range of industrial applications.<sup>14, 15</sup> Specifically, the conversion of benzyl alcohol to benzaldehyde has attracted significant interest since benzaldehyde is a widely used chemical in food, pharmaceutical, and perfumery industries as

well as building block in other chemical industries.<sup>16-22</sup> For example, benzaldehyde is commonly used as a flavor and fragrance agent tasting of almond, peach, marzipan, and pistachio. In addition, benzaldehyde can be also synthesized via toluene oxidation.<sup>23</sup> Considering that toluene is classified as a highly pollutant chemical, its oxidation to beneficial chemicals products, i.e., benzyl alcohol, benzaldehyde, benzoic acid, and benzoate is extremely attractive.<sup>24,25</sup> For example, benzoic acid is industrially obtained from toluene using (thermally driven) Co-based catalyzed reactions.<sup>26</sup>

ZnS carbon compounds were particularly tested in fast microwave-assisted reactions, using only hydrogen peroxide as oxidant. Less aggressive oxidants such as hydrogen peroxide (H<sub>2</sub>O<sub>2</sub>) and molecular oxygen (O<sub>2</sub>) are nowadays employed aiming to scale up oxidation processes,<sup>14</sup> whereas, in the past, the scale up of the oxidation reactions has been very limited due to the use of heavy metals (e.g., chromium, manganese and permanganate derivatives).<sup>27-30</sup> In addition, the utilization of hydrogen peroxide allows the minimization of chemical waste in these catalytic processes, as water is the only reaction side product.

## Materials and methods

### Materials

Zinc acetate dihydrate (Zn(CH<sub>3</sub>COOH)<sub>2</sub>·2H<sub>2</sub>O), potassium hydroxide (KOH), acetone (CH<sub>3</sub>COCH<sub>3</sub>), ethanol (CH<sub>3</sub>CH<sub>2</sub>OH, 99.8%) acetonitrile (CH<sub>3</sub>CN, 99.8%), benzyl alcohol (C<sub>6</sub>H<sub>5</sub>CH<sub>2</sub>OH, 99.8%), toluene (C<sub>7</sub>H<sub>8</sub>, 99.8%) and hydrogen peroxide (H<sub>2</sub>O<sub>2</sub>, 30% v/v) were purchased from Sigma-Aldrich Inc., St. Louis, MO, USA. All reagents were used without any further purification.

### **Synthesis of ZnS carbon catalysts**

A sequence of three ZnS carbon structures characterized by different synthesis times were prepared. In a typical procedure, the correct amount of zinc acetate dihydrate (850 mg, 3.8 mmol) was dissolved in 200 mL of 1.0 M KOH solution in a 250 mL round flask equipped with a stirring bar and a reflux condenser. Sequentially, 1.5 g of pig bristles (cut in pieces of ~5 mm) were added. The mixture was kept at room temperature under vigorous magnetic stirring (800 rpm) for 10 min before starting the reaction. The mixture was then heated at reflux in an oil bath. After completing the reaction, the solution was naturally cooled down to r.t. and the light-brown precipitate was filtrated and washed several times with acetone and ethanol. Finally, the material was oven-dried at 100 °C for 24 h. Three different samples were produced by setting the heating time for 1 h, 3 h, and 5 h. The samples were denoted ZnS-1h, ZnS-3h, and ZnS-5h respectively.

### **Material characterization**

ZnS carbon composites were characterized by scanning electron microscopy (SEM), energy dispersive X-ray Analysis (EDX), powder X-ray diffraction (XRD), N<sub>2</sub> physisorption, and X-ray photoelectronic spectroscopy (XPS).

Scanning electron microscopy images were recorded with a JEOL JSM-6300 scanning microscope (JEOL Ltd., Peabody, MA, USA) equipped with energy-dispersive X-ray spectroscopy (EDX) of 15 kV at the Research Support Service Center (SCAI) from University of Cordoba.

Powder X-ray diffraction (XRD) patterns were recorded using a Bruker D8 DISCOVER A25 diffractometer (PanAnalytic/Philips, Lelyweg, Almelo, The Netherlands) using Cu K $\alpha$  ( $\lambda = 1.5418 \text{ \AA}$ ) radiation. Wide angle scanning patterns were collected over a  $2\theta$  range from 10° to 80° with a step size of 0.018° and counting time of 5 s per step.

Textural properties of the samples were determined by N<sub>2</sub> physisorption using a Micromeritics ASAP 2020 automated system (Micromeritics Instrument Corporation, Norcross, GA, USA) with the Brunauer-Emmet-Teller (BET) and the Barret-Joyner-Halenda (BJH) methods. Prior to analysis, the samples were outgassed for 24 h at 100 °C under vacuum ( $P_0 = 10^{-2}$  Pa) and subsequently analyzed.

XPS studies were performed at the Central Service of Research Support (SCAI) of the University of Cordoba, using an ultrahigh vacuum (UHV) multipurpose surface analysis system Specs. The experiments were carried out at pressures  $<10^{-10}$  mbar, using a conventional X-ray source (XR-50, Specs, Mg-K $\alpha$ ,  $h\nu = 1253.6$  eV,  $1 \text{ eV} = 1.603 \times 10^{-19}$  J) in a “stop and go” mode. The samples were deposited on a sample holder using a double sided adhesive tape, and afterward evacuated overnight under vacuum ( $<10^{-6}$  mbar). Spectra were collected at room temperature (pass energy: 25 and 10 eV, step size: 1 and 0.1 eV) with a Phoibos 150-MCD energy detector. The deconvolutions of the obtained curves and element quantification were carried out using XPS CASA program.

### **Catalytic activity**

The oxidation tests were performed following a procedure optimized in a previous work.<sup>31</sup> Briefly, 25 mg of catalyst, 0.1 mL of benzyl alcohol (0.95 mmol) or 0.1 mL of toluene (0.94 mmol), 0.25 mL of hydrogen peroxide (30% v/v) and 2 mL of acetonitrile as solvent. Blank tests were run in the absence of the catalysts. Both microwave-assisted oxidations were carried out in a CEM-Discover microwave reactor, equipped with a PC-controlled interface. The mixtures were irradiated for 45 min, withdrawing aliquots for GC-FID analysis every 15 min. The experiments were performed in closed vessels. The "discover" method was used under pressure, allowing the control

of the irradiation power, the temperature, and the pressure. The reactions were stirred and heated with microwave irradiation fixing the temperature at 120 °C by an infrared probe. The autogenous pressure ranged from 3.5 to 8 bar.

### **Product analysis**

The filtrates collected from the reaction mixtures were analysed by GC, using an Agilent 19091J-413 GC model equipped with a Supelco 2-8047-U (30 m x 0.32 mm x 0.25µm i.d.) capillary column and an FID detector. The temperature of the column was ramped at 25 °C min<sup>-1</sup> to 25 °C (1 min hold time), then at 25 °C min<sup>-1</sup> to 250 °C (5 min hold time) and finally to 300 °C at 20 °C min<sup>-1</sup> (10 min hold time). The nitrogen gas flow was set at 1.3 mL min<sup>-1</sup>.

## **Results and discussion**

### **Synthesis of ZnS carbon composites**

A simple, fast, and cheap methodology is shown for the synthesis of ZnS carbon structures using wasted pig bristles as carbon and sulfur source. As reported by Gonzalo et al., pig bristles are carbon- and sulfur-rich wastes largely produced in most industrialized countries, generally burnt as waste or partially reused in brush industries or as food fodder supplement.<sup>12,13,32</sup> The sulfur contained in pig bristles is mainly derived from keratin, an insoluble protein containing disulfide bonds as well as from amino acids such as cysteine, methionine, and cysteic acid.<sup>33</sup> Due to similarities with human hair, the total amount of sulfur contained in pig bristles has been reported to be ca. 5% wt.<sup>34</sup> However, contrary to human hair, which production is also vast but distributed in the numerous barber shops, pig bristles are produced in large quantities in slaughterhouses and can be easily collected at industrial scale. As illustrated in Figure 1, the new synthesis involved a unique step where a mixture of pig

bristles, zinc acetate dihydrate and a solution 1.0 M of potassium hydroxide where heated up under reflux conditions.

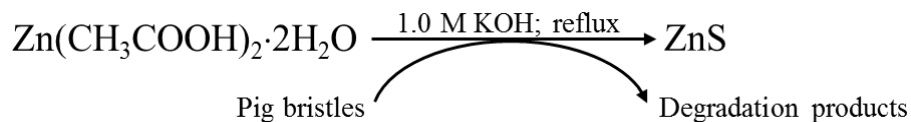


**Figure 1.** Schematic illustration of the preparation of ZnS.

The synthesis is adapted from a previously reported protocol for the preparation of  $\text{Cu}_2\text{S}$ , where the solvent solution, made of ethylene glycol and  $\text{NaOH}$ , has been substituted with a less hazardous and easier to manipulate dilute aqueous solution of  $\text{KOH}$ .<sup>11</sup> Ethylene glycol is indeed a suspicious carcinogenic agent and can explosively degrade when heated up with  $\text{NaOH}$ . The aqueous basic solution of  $\text{KOH}$  was employed in order to accelerate and facilitate the decomposition of pig bristles and the release of sulfur via keratin hydrolysis.<sup>35</sup> Without the basic solution, the thermal degradation would require higher temperature and processing time. In fact, keratin and amino acids present in proteins start to thermally degrade above  $150\text{ }^\circ\text{C}$ , and release sulfur up to  $300\text{ }^\circ\text{C}$ .<sup>36</sup>

When the mixture was heated up, the pig bristles started to decompose and the dissolved  $\text{Zn}^{2+}$  ions bind with sulfur. During this step, the particles self-aggregate in order to minimize the surface energy, incorporating the residual carbon, and forming homogeneous ZnS carbon structures. Three different samples were prepared, using the same amount of pig bristles and zinc acetate dihydrate and heating up the reaction mixture for different time, respectively 1 h, 3 h, and 5 h. The zinc sulfide carbon materials were denoted as ZnS-1h, ZnS-3h, and ZnS-5h.



### Materials characterization

The morphology of ZnS carbon structures was investigated by SEM and EDX analyses. Figure 2 shows SEM images for the three ZnS carbon materials. All samples exhibited a “coral-like” homogeneous morphology where the carbon derived from the degradation of pig bristles was aggregated with ZnS.

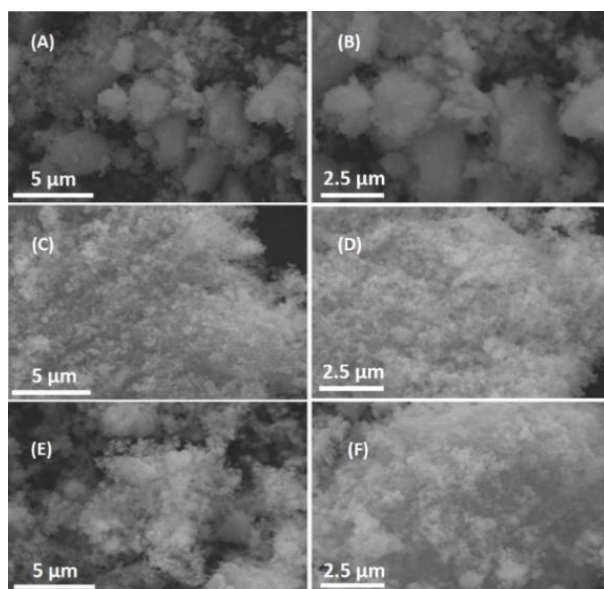


**Figure 2.** SEM images of the three different ZnS composites. (A, B) ZnS-1h; (C, D) ZnS-3h; (E, F) ZnS-5h.

EDX mapping were reported in order to demonstrate the distribution of catalytically active sites, as reported in Figure 3 for sample ZnS-3h.<sup>37</sup> Remarkably, zinc, sulfur, and carbon were found to be well distributed in the material, confirming the homogeneous conditions of the synthesis, and the presence of active sites over all the catalyst surface (please see Figure S1 and S2 for ZnS-1h and ZnS-5h EDX mapping).

EDX-mapping micrographs showed the presence of carbon, sulfur, and zinc, indicating the high purity of the materials. The phase purity and crystallinity of synthesized ZnS carbon composites were subsequently investigated by XRD analysis.

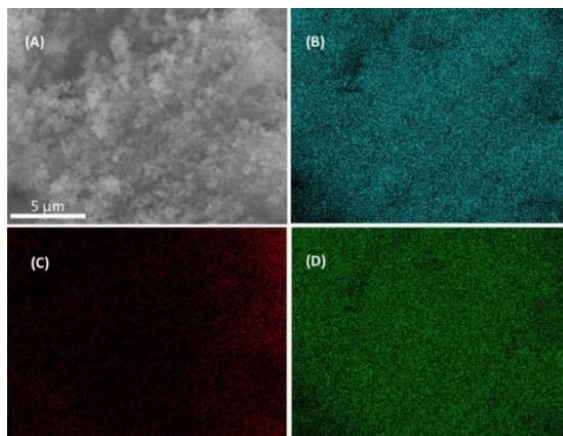


**Figure 3.** SEM images of ZnS-3h with mapping analysis of (A) ZnS carbon structure, (B) zinc, (C) carbon, and (D) sulfur.

As shown in Figure 4, XRD patterns for all different samples showed the presence of zinc sulfide. The diffraction peaks at  $29.04^\circ$ ,  $48.38^\circ$ , and  $57.42^\circ$  could be indexed to the (1 1 1), (2 2 0) and (3 1 1) planes of cubic zinc sulfide (JCPDS 01-080-0020).<sup>38</sup> No other impurity peaks detected through XRD also suggested high purity in the materials. In addition, the width of the most intense peaks at half height measured almost the same for the three patterns, indicating similar dimensions of the particles in all the samples, according to Scherrer's equation.<sup>39</sup>

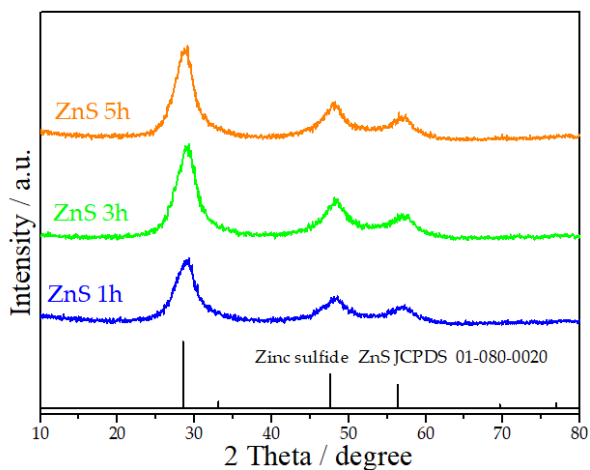


**Figure 4.** XRD patterns for ZnS carbon composites.

The samples were thus subjected to an XPS study. Figure 5 shows plots of high-resolution spectra concerning C 1s, Zn 2p and S 2p regions. A summary of the fitting position values for the different elements mentioned as well as the surface atomic ratios (C/Zn) is presented in Table 1. In agreement with XRD analysis, the presence of a defined ZnS structure was successfully observed for all synthesized ZnS materials. In particular, both Zn 2p and S 2p core level spectra do not display significant modifications with synthesis time (middle and right panels of Figure 5). Zn 2p shows two strong peaks at ca. 1021.5 and 1044.8 eV, assigned to the binding energies of Zn 2p<sub>3/2</sub> and Zn 2p<sub>1/2</sub>, respectively, indicating the existence of Zn(II) and discarding the possible presence of oxidized minority species.<sup>40,41</sup> The value of ca. 161.2 eV is in good agreement with the S 2p<sub>3/2</sub> typical value for ZnS.<sup>40</sup> In contrast, a significant difference can be observed for C 1s XPS region. All samples show the dominant typical C-C contribution at 284.6 eV (C2) corresponding to adventitious C. However certain differences were detected for the other C-related species as can be seen in the left panel of Figure 5 and Table 1.

**Table 1.** XPS Data for ZnS samples

Sample	position					
	Zn 2p <sub>3/2</sub> (eV)	S 2p <sub>3/2</sub> (eV)	C 1s (eV)			C/Zn
			C1	C2	C3	
ZnS-1h	1021.5	161.1	288.3	284.6	281.2	3.6
Zns-3h	1021.6	161.2	287.4	284.6	279.9	3.5
ZnS-5h	1021.5	161.2	287.5	284.6		2.2

Carbon species evolve over the time of synthesis. The contribution located around 287 eV (C1), typically attributed to C-O, shifts to less binding energy when higher reaction times were used. The evolution of carbon species is even more evident for the contribution situated at less energy respect to C-C bond

(C3). These unexpected contributions were detected at 281.2 and 279.9 for ZnS-1h and ZnS-3h, respectively, and could be associated with an interaction between C and Zn species. The detected modifications of carbon-related species on the surface of ZnS have also certain influence on the final carbon content of the samples. C/Zn ratio indicated that cleaner carbon samples can be obtained using longer reaction times. This fact had a relative influence on the final catalytic properties through the series as discussed in further sections.

Physisorption experiments were carried out in order to determine the specific surface area of the materials by nitrogen adsorption-desorption measurements. The samples were observed to be low porous materials with surface areas of 50 m<sup>2</sup>/g, 53 m<sup>2</sup>/g, and 57 m<sup>2</sup>/g for ZnS-1h, ZnS-3h, and ZnS-5h, respectively. The so-obtained values showed a linear and small increment of the surface area increasing the reaction time. This relation can be correlated to the lower content of carbon observed in XPS analysis (Table 1). In addition, the values obtained for samples ZnS-1h and ZnS-3h were similar, in good agreement with the stabilization of carbon species described in XPS analysis. The maximum value obtained for ZnS-5h confirmed the production of a material with more active sites on the surface.

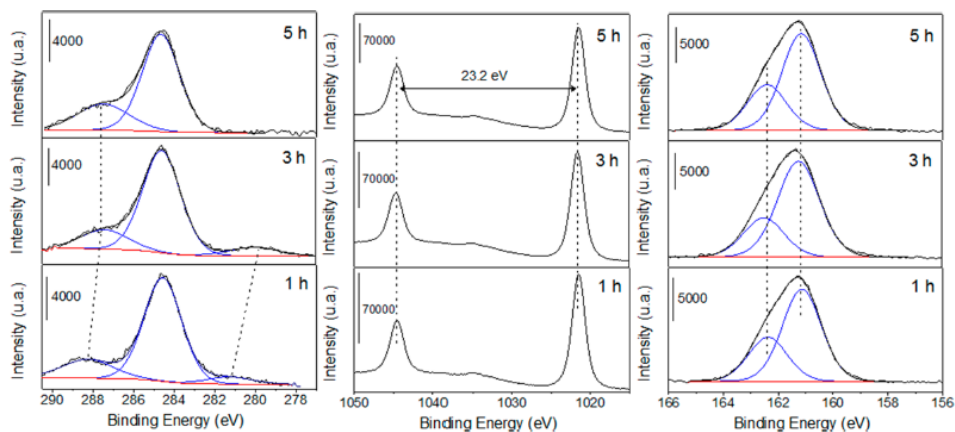
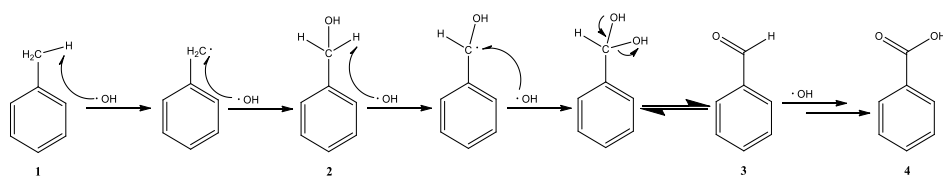


**Figure 5.** XPS patterns for ZnS carbon composites.

### Catalytic activity

The catalytic activity of the materials has been investigated in two different reactions: the selective liquid-phase oxidation of benzyl alcohol and toluene to benzaldehyde. ZnS has been recently demonstrated to exhibit peroxidase-like activities for the degradation of  $\text{H}_2\text{O}_2$  into hydroxyl radicals ( $\cdot\text{OH}$ ), which act as oxidants for toluene and benzyl alcohol.<sup>42</sup> The reported mechanism for the oxidation of toluene **1** and benzyl alcohol **2** to benzaldehyde **3** is illustrated in Scheme 1.<sup>43</sup> The only detectable side product of the reaction was benzoic acid **4**. No other products were detected. The results were confirmed by a carbon balance (>95 % in all tests).



**Scheme 1.** Proposed Mechanism for Toluene and Benzyl Alcohol Oxidation

The oxidation reaction of benzyl alcohol was carried out using the three ZnS carbon composites as heterogeneous catalysts. Results reported in Table 2 show that conversions observed were ca. ~60-65% for all ZnS carbon materials after 15 min of microwave irradiation. Within the same time, the selectivity was observed to be 70%, 85%, and 87% for samples ZnS-1h, ZnS-3h, and ZnS-5h, respectively. In terms of conversion, an increase of the reaction time to 30 and 45 min did not have any influence in reaction yields. Most importantly, the selectivity dropped to 64% for ZnS-1h, 82% for ZnS-3h, and 84% for ZnS-5h. On the basis on these data, all catalysts exhibited an almost identical conversion while the best selectivity was observed after 15 min employing ZnS-5h catalyst, most probably due to the larger surface area ( $57\text{g}/\text{m}^2$  vs  $50\text{g}/\text{m}^2$  of ZnS-1h). Hypothetically, the higher surface area facilitated the rapid decomposition of  $\text{H}_2\text{O}_2$  into hydroxyl radicals, which

directly oxidized benzyl alcohol. A lower surface area (ZnS-1h) would have taken more time to decompose hydrogen peroxide; therefore, more benzyl alcohol could have been already oxidized to benzaldehyde and sequentially to benzoic acid, reducing the selectivity. In addition, sample ZnS-5h exhibited a lower C/Zn surface ratio, indicating that more active zinc sulfide sites were accessible for the degradation of hydrogen peroxide using this catalyst.

**Table 2.** Conversion and Selectivity Results for the Oxidation of Benzyl Alcohol.

Sample	15 min		30 min		45 min	
	conversion /%	selectivity /%	conversion /%	selectivity /%	conversion /%	selectivity /%
BLANK	<15	55.4	<15	53.8	<15	52.1
ZnS-1h	63.0	70.2	63.8	65.0	64.0	64.1
ZnS-3h	62.6	85.1	62.7	83.2	63.0	82.1
ZnS-5h	62.7	87.1	63.1	85.8	63.4	84.3

The stability of the catalysts was studied using the most active material ZnS-5h. The catalyst was reused up to 4 times and the activity and selectivity to benzyl aldehyde was found to be almost identical to that of the fresh catalyst as shown in Figure 6 (for the numeric data, please see Table S1).

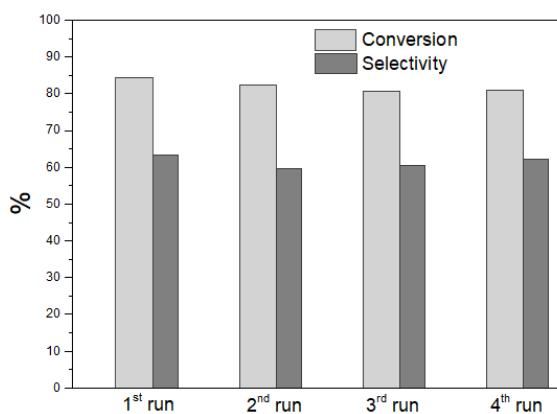


**Figure 6.** Schematic representation of conversion and selectivity of the most active catalyst up to the 4th run of the oxidation of benzyl alcohol.

The results of the oxidation of toluene to benzaldehyde are reported in Table 3. After 15 min of reaction, the best result was obtained with ZnS-5h (19%), while the selectivity was approximately the same value (around 90%) for all three zinc sulfide carbon materials. After 30 min, an increase of conversion up to 29% with ZnS-5h was observed, while the conversion with ZnS-1h and ZnS-3h remained unchanged. On the other hand, the selectivity did not improve for any catalyst. After 45 min, the values of conversion and selectivity were equal to those obtained after 30 min, confirming that the reaction was not proceeding.

On the basis of these considerations, the most active catalyst was ZnS-5h, which again showed the best results after 30 min reaction. Such optimum behavior could be again explained in terms of the higher surface area and higher Zn/C ratio for ZnS-5h.

**Table 3.** Conversion and Selectivity Results for the Oxidation of Toluene.

Sample	15 min		30 min		45 min	
	conversion /%	selectivity /%	conversion /%	selectivity /%	conversion /%	selectivity /%
BLANK	<5	~50	<5	~50	<5	~50
ZnS-1h	7.3	94.1	8.2	89.0	9.2	88.8
ZnS-3h	11.3	88.1	12.1	90.7	12.6	88.1
ZnS-5h	18.8	89.6	28.6	89.8	28.5	86.7

The stability tests were carried out using ZnS-5h. The catalyst was reused up to 4 times without any appreciable losses of activity or selectivity to benzaldehyde, as shown in Figure 7.

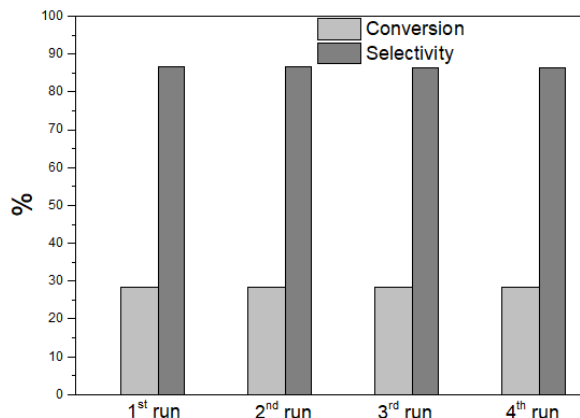


**Figure 7.** Schematic representation of conversion and selectivity to benzyl aldehyde for the most active catalyst up to 4th run for the oxidation of toluene (for the numeric data, please see Table S2).

## Conclusions

A simple, effective, and sustainable methodology has been reported for the preparation of ZnS carbon composites. The materials were synthesized using wasted pig bristles as sulfur and carbon source and zinc acetate dihydrate as zinc precursor. The materials were synthesized using a one step protocol where pig bristles and zinc acetate dihydrate were heated up in an aqueous diluted solution of KOH. The presence of zinc sulfide phases was demonstrated by XRD and XPS analysis, while the surface area was investigated via SEM, EDX, and N<sub>2</sub> physisorption. The synthesis is a clear example of an easy and sustainable valorization of wasted pig bristles. The protocol can track new paths for substituting sulfur toxic sources with harmless pig bristles.

In addition, the so-produced ZnS carbon materials showed remarkably activity as catalysts for two different oxidation reactions: the oxidation of benzyl alcohol to benzaldehyde and the oxidation of toluene to benzaldehyde. The oxidation of benzyl alcohol plays an important role in the chemical industry, while the oxidation of toluene is extremely captivating as it solves the



problem of removing a pollutant through the production of value-added benzyl aldehyde. For both reactions, the most active sample was ZnS-5h, reaching the oxidation of benzyl alcohol up to 63% with 86% selectivity and the oxidation of toluene up to 29% with 87% selectivity.

## Supporting Information

Additional materials characterizations and data of the reuse of the catalysts.

## Notes

The authors declare no competing financial interest.

## Acknowledgments

This project has received funding from the European Union's Horizon 2020 research and innovation programme under the Marie Skłodowska-Curie grant agreement No 721290. This publication reflects only the author's view, exempting the Community from any liability. Project website: <http://cosmic-etn.eu/>. M.J.M-B also thanks MINECO for the award of postdoctoral JdC contract (FJCI-2016-29014). The publication has been prepared with support of RUDN University program 5-100.

## References

- (1) Fox, M. A.; Dulay, M. T. Heterogeneous photocatalysis. *Chem. Rev.* **1993**, *93*(1), 341-357.
- (2) Fang, X. S.; Bando, Y.; Gautam, U. K.; Ye, C.; Golberg, D. Inorganic semiconductor nanostructures and their field-emission applications. *J. Mater. Chem.* **2008**, *18*(5), 509-522.
- (3) Ummartyotin, S.; Infahsaeng, Y. A comprehensive review on ZnS: From synthesis to an approach on solar cell. *Renewable Sustainable Energy Rev.* **2016**, *55*, 17-24.
- (4) Fang, X. S.; Zhai, T. Y.; Gautam, U. K.; Li, L.; Wu, L. M.; Yoshio, B.; Golberg, D. ZnS nanostructures: From synthesis to applications. *Prog. Mater. Sci.* **2011**, *56*(2), 175-287.
- (5) Chen, D. G.; Huang, F.; Ren, G. Q.; Li, D. S.; Zheng, M.; Wang, Y. J.; Lin, Z. ZnS nano-architectures: photocatalysis, deactivation and regeneration. *Nanoscale* **2010**, *2*(10), 2062-2064.

- (6) Ashkarran, A. A. Absence of photocatalytic activity in the presence of the photoluminescence property of Mn-ZnS nanoparticles prepared by a facile wet chemical method at room temperature. *Mater Sci. Semicond. Process.* **2014**, *17*, 1-6.
- (7) Zhang, H. L.; Wei, B.; Zhu, L.; Yu, J. H.; Sun, W. J.; Xu, L. L. Cation exchange synthesis of ZnS-Ag<sub>2</sub>S microspheric composites with enhanced photocatalytic activity. *Appl. Surf. Sci.* **2013**, *270*, 133-138.
- (8) Vostrikov, A. A.; Fedyaeva, O. N.; Sokol, M. Y.; Shatrova, A. V. Synthesis of zinc sulfide nanoparticles during zinc oxidization by H<sub>2</sub>S and H<sub>2</sub>S/H<sub>2</sub>O supercritical fluids. *Tech. Phys. Lett.* **2014**, *40*(12), 1057-1060.
- (9) Liu, J.; Ma, J. F.; Liu, Y.; Song, Z. W.; Sun, Y.; Fang, J. R.; Liu, Z. S. Synthesis of ZnS nanoparticles via hydrothermal process assisted by microemulsion technique. *J. Alloys Compd.* **2009**, *486* (1-2), L40-L43.
- (10) Biswas, S.; Kar, S.; Chaudhuri, S. Synthesis and characterization of zinc sulfide nanostructures. *Synth. React. Inorg., Met.-Org., Nano-Met. Chem.* **2006**, *36*(1), 33-36.
- (11) Zuliani, A.; Munoz-Batista, M. J.; Luque, R. Microwave-assisted valorization of pig bristles: towards visible light photocatalytic chalcocite composites. *Green Chem.* **2018**, *20*, 3001.
- (12) Gachango, F. G.; Ekmann, K. S.; Frorup, J.; Pedersen, S. M. Use of pig by-products (bristles and hooves) as alternative protein raw material in fish feed: A feasibility study. *Aquaculture.* **2017**, *479*, 265-272.
- (13) Laba, W.; Kopec, W.; Chorazyk, D.; Kancelista, A.; Piegza, M.; Malik, K. Biodegradation of pretreated pig bristles by *Bacillus cereus* B5esz. *Int. Biodeterior. Biodegrad.* **2015**, *100*, 116-123.
- (14) Matsumoto, T.; Ueno, M.; Wang, N.; Kobayashi, S. Recent advances in immobilized metal catalysts for environmentally benign oxidation of alcohols. *Chem.-Asian J.* **2008**, *3*(2), 196-214.
- (15) Pineda, A.; Balu, A. M.; Campelo, J. M.; Romero, A. A.; Carmona, D.; Balas, F.; Santamaria, J.; Luque, R. A Dry Milling Approach for the Synthesis of Highly Active Nanoparticles Supported on Porous Materials. *Chemsuschem* **2011**, *4*(11), 1561-1565.
- (16) Gritter, R. J.; Dupre, G. D.; Wallace, T. J. Oxidation of benzyl alcohols with manganese dioxide. *Nature* **1964**, *202*(492), 179-181.
- (17) Yang, Z. J.; Ji, H. B. Synergistic effect of hydrogen bonding mediated selective synthesis of benzaldehyde in water. *Chin.J. Catal.* **2014**, *35*(4), 590-598.

## Results & Discussion

(18) Zhu, L.; Xu, X. H.; Zheng, F. P. Synthesis of benzaldehyde by Swern oxidation of benzyl alcohol in a continuous flow microreactor system. *Turk. J. Chem.* **2018**, *42*(1), 75-85.

(19) Colmenares J. C.; Ouyang W.; Ojeda M.; Kuna E.; Chernyayeva O.; Lisovytskiy D.; De S.; Luque R.; Balu A. M. Mild ultrasound-assisted synthesis of TiO<sub>2</sub> supported on magnetic nanocomposites for selective photo-oxidation of benzyl alcohol. *Appl. Catal., B.* **2016**, *183*, 107-112.

(20) Magdziarz A.; Colmenares J. C.; Chernyayeva O.; Kurzydłowski K.; Grzonka J. Iron-Containing Titania Photocatalyst Prepared by the Sonophotodeposition Method for the Oxidation of Benzyl Alcohol. *Chemcatchem.* **2016**, *8*, 536-539.

(21) Magdziarz A.; Colmenares J. C.; Chernyayeva O.; Lisovytskiy D.; Grzonka J.; Kurzydłowski K.; Freindl K.; Korechi J. Insight into the synthesis procedure of Fe<sup>3+</sup>/TiO<sub>2</sub>-based photocatalyst applied in the selective photo-oxidation of benzyl alcohol under sun-imitating lamp. *Ultrason. Sonochem.* **2017**, *38*, 189-196.

(22) Ouyang W.; Reina J. M.; Kuna E.; Yopez A.; Balu A. M.; Romero A. A.; Colmenares J. C.; Luque R. Wheat bran valorisation: Towards photocatalytic nanomaterials for benzyl alcohol photo-oxidation. *J. Environ. Manage.* **2017**, *203*, 768-773.

(23) Borgaonkar, H. V.; Raverkar, S. R.; Chandalla, S. B. Liquid-phase oxidation of toluene to benzaldehyde by air. *Ind. Eng. Chem. Prod. Res. Dev.* **1984**, *23*(3), 455-458.

(24) Wang, Y.; Li, H. R.; Yao, J.; Wang, X. C.; Antonietti, M. Synthesis of boron doped polymeric carbon nitride solids and their use as metal-free catalysts for aliphatic C-H bond oxidation. *Chem. Sci.* **2011**, *2*(3), 446-450.

(25) Andrews, L. S.; Lee, E. W.; Witmer, C. M.; Kocsis, J. J.; Snyder, R. Effects of toluene on metabolism, disposition and hematopoietic toxicity of benzene-H-3. *Biochem. Pharmacol.* **1977**, *26*(4), 293-300.

(26) Yuan, Z. H.; Chen, B. Z.; Zhao, J. S. Controllability analysis for the liquid-phase catalytic oxidation of toluene to benzoic acid. *Chem. Eng. Sci.* **2011**, *66*(21), 5137-5147.

(27) He, A.; Zhang, J.; Zheng, W. J.; Huang, C.; Zhang, C. H.; Huang, L. H.; Lou, J. D. Rapid oxidation of alcohols to aldehydes and ketones with chromium trioxide catalyzed by kieselguhr under solvent-free conditions. *Res. Chem. Intermed.* **2013**, *39*(3), 1015-1020.

(28) Shaabani, A.; Mirzaei, P.; Lee, D. G. The beneficial effect of manganese dioxide on the oxidation of organic compounds by potassium permanganate. *Catal. Lett.* **2004**, *97*(3-4), 119-123.

- (29) Chang, C. K.; Sheldon, R.A.; Kochi, J.K. Metal-catalyzed oxidations of organic-compounds. *J. Am. Chem. Soc.* **1983**, *105*(11), 3749-3749.
- (30) Gonzalo, M.; Jespersen, C. M.; Jensen, K.; Støier, S.; Meinert, L. Pig Bristles – An Underestimated Biomass Resource. In *62nd International Congress of Meat Science and Technology*, Bangkok, Thailand, Aug 1-19, 2016; Elsevier, 2016.
- (31) Mangin, F.; Prinsen, P.; Yopez, A.; Gilani, M.; Xu, G. B.; Len, C.; Luque, R. Microwave assisted benzyl alcohol oxidation using iron particles on furfuryl alcohol derived supports. *Catal. Commun.* **2018**, *104*, 67-70.
- (32) Dey, S. K.; Mukherjee, A. Catechol oxidase and phenoxazinone synthase: Biomimetic functional models and mechanistic studies. *Coord. Chem. Rev.* **2016**, *310*, 80-115.
- (33) Clay, R. C.; Cook, K.; Routh, J. I. Studies in the Composition of Human Hair. *J. Am. Chem. Soc.* **1940**, *62*, 2709.
- (34) Rechiche, O.; Plowman, J. E.; Harland, D. P.; Lee, T. V.; Lott, J. S. Expression and purification of high sulfur and high glycine-tyrosine keratin-associated proteins (KAPs) for biochemical and biophysical characterization. *Protein Expression Purif.* **2018**, *146*, 34-44.
- (35) Brebu, M.; Spiridon, I. Thermal degradation of keratin waste. *J. Anal. Appl. Pyrolysis* **2011**, *91*(2), 288-295.
- (36) Yeh, C. Y.; Lu, Z. W.; Froyen, S.; Zunger, A. Zinc-blende-wurtzite polytypism in semiconductors. *Phys. Rev. B: Condens. Matter Mater Phys.* **1992**, *46*(16), 10086-10097.
- (37) Otto, T. N.; et al. Catalyst Characterization with FESEM/EDX by the Example of Silver-Catalyzed Epoxidation of 1,3-Butadiene. In *Scanning Electron Microscopy*; Kazmiruk, V., Ed.; IntechOpen: London, 2012.
- (38) *Criteria for a Recommended Standard: Occupational exposure to Sodium Hydroxide*; DHHS Publication Number 76-105; NIOSH, 1975.
- (39) Xu, X.; Hu, L.; Gao, N.; Liu, S.; Wageh, S.; Al-Ghamdi, A.A.; Alshahrie, A.; Fang, X. Controlled Growth from ZnS Nanoparticles to ZnS–CdS Nanoparticle Hybrids with Enhanced Photoactivity. *Adv. Funct. Mater.* **2015**, *25*(3), 445-454.
- (40) Yu, J. G.; Zhang, J.; Liu, S. W. Ion-Exchange Synthesis and Enhanced Visible-Light Photoactivity of CuS/ZnS Nanocomposite Hollow Spheres. *J. Phys. Chem. C* **2010**, *114*(32), 13642-13649.

## Results & Discussion

(41) Wanger, C. D.; Riggs, W. M.; Davis, L. E.; Moulder, J. F.; Muilenberg G. E. Handbook of x-ray photoelectron spectroscopy: A reference book of standard data for use in X-ray photoelectron spectroscopy; Perkin-Elmer Corp.: Eden Prairie, MN, 1979.

(42) Ding, Y. Y.; Sun, L. F.; Jiang, Y. L.; Liu, S. X.; Chen, M. X.; Chen, M. M.; Ding, Y. N.; Liu, Q. Y. A facile strategy for the preparation of ZnS nanoparticles deposited on montmorillonite and their higher catalytic activity for rapidly colorimetric detection of H<sub>2</sub>O<sub>2</sub>. *Mat. Sci. Eng., C*. **2016**, *67*, 188-194.

(43) Ramu, R.; Wanna, W. H.; Janmanchi, D.; Tsai, Y. F.; Liu, C. C.; Mou, C. Y.; Yu, S. S. F. Mechanistic study for the selective oxidation of benzene and toluene catalyzed by Fe(ClO<sub>4</sub>)<sub>2</sub> in an H<sub>2</sub>O<sub>2</sub>-H<sub>2</sub>O-CH<sub>3</sub>CN system. *Mol. Catal.* **2017**, *441*, 114-121.

## Supporting Information

### A sustainable approach for the synthesis of catalytically active peroxidase-mimic ZnS catalysts

Camilla M. Cova<sup>a</sup>, Alessio Zuliani<sup>a</sup>, Mario J. Muñoz-Batista<sup>a</sup> and Rafael Luque<sup>a, b\*</sup>

<sup>a</sup>*Departamento de Química Orgánica, Universidad de Córdoba, Edificio Marie-Curie (C-3), Ctra Nnal IV-A, Km 396, Córdoba, Spain*

<sup>b</sup>*Peoples Friendship University of Russia (RUDN University), 6 Miklukho-Maklaya str., 117198, Moscow, Russia*

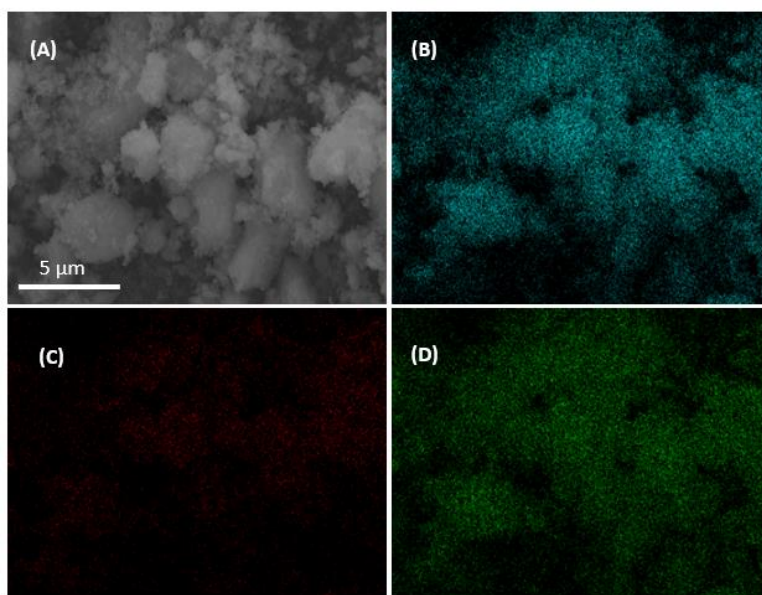


**Figure S1.** SEM images with mapping analysis of ZnS-1h carbon material (A) Distribution of Zinc (B), Carbon (C) and Sulphur (D).

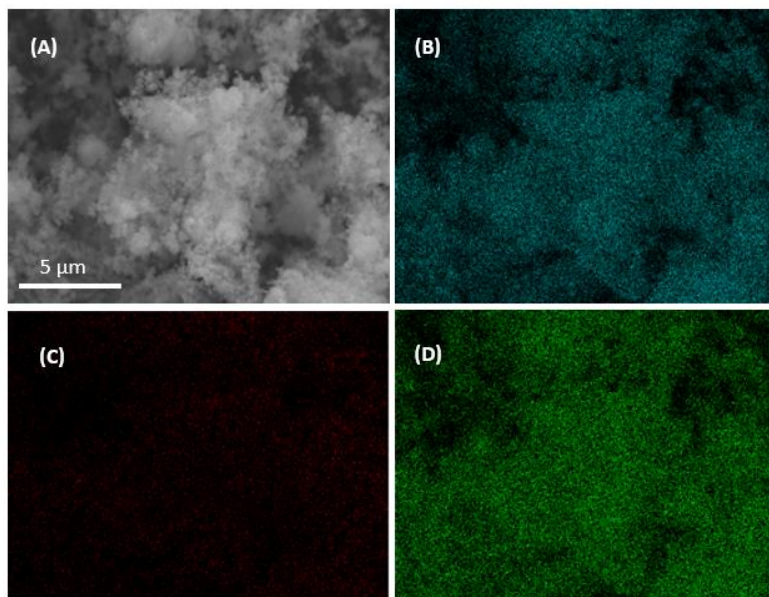


**Figure S2.** SEM images with mapping analysis of ZnS-5h carbon material (A) Distribution of Zinc (B), Carbon (C) and Sulphur (D).

**Table S1.** Stability results for ZnS-5h for the oxidation of benzyl alcohol.

Sample	1 <sup>st</sup> run	2 <sup>nd</sup> run	3 <sup>rd</sup> run	4 <sup>th</sup> run
Conversion	63.4	59.6	60.4	62.2
Selectivity	84.3	82.4	80.7	81.0

**Table S2.** Stability results for ZnS-5h for the oxidation of toluene.

Sample	1 <sup>st</sup> run	2 <sup>nd</sup> run	3 <sup>rd</sup> run	4 <sup>th</sup> run
Conversion	28.5	28.4	28.5	28.3
Selectivity	86.7	86.6	86.4	86.4

# Efficient Ru-based scrap waste automotive converter catalysts for the continuous-flow selective hydrogenation of cinnamaldehyde

Camilla Maria Cova,<sup>a</sup> Alessio Zuliani,<sup>a</sup> Mario J. Muñoz-Batista<sup>\*a</sup> and Rafael Luque<sup>\*a,b</sup>

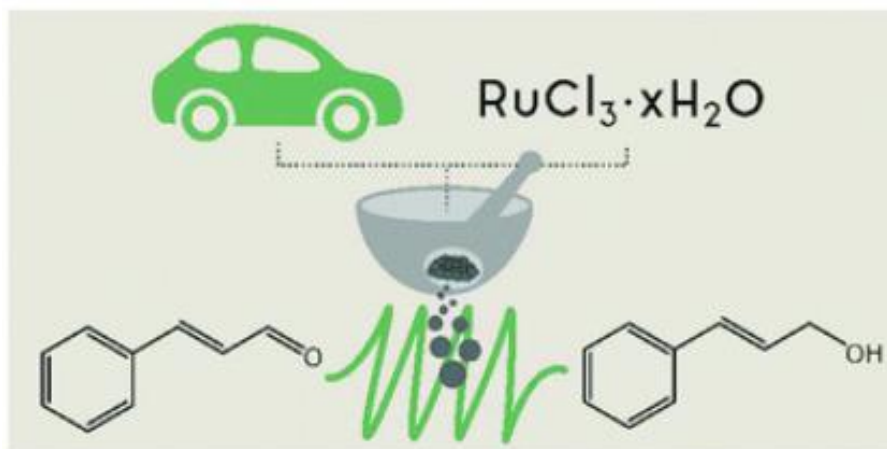
<sup>a</sup>Departamento de Química Orgánica, Universidad de Córdoba, Edificio Marie-Curie (C-3), Ctra Nnal IV-A, Km 396, Córdoba, Spain. E-mail: rafael.luque@uco.es

<sup>b</sup>Departamento de Química Inorgánica e Ingeniería Química, Campus de Rabanales, Edificio Marie Curie (C-3), Ctra Nnal IV-A, Km 396, E14014, Córdoba, Spain

<sup>b</sup>Peoples Friendship University of Russia (RUDN University), 6 Miklukho-Maklaya Str. Moscow, 117198, Russia

DOI: 10.1039/C9GC01596E

## Graphical abstract



Reproduced by permission of The Royal Society of Chemistry, link to publication:

<https://pubs.rsc.org/en/content/articlelanding/2019/gc/c9gc01596e#1divAbstract>



## Abstract

The selective, efficient and sustainable continuous flow hydrogenation of a  $\alpha,\beta$ -unsaturated aldehyde, *i.e.* cinnamaldehyde, to the corresponding unsaturated alcohol, *i.e.* cinnamyl alcohol, using a novel catalyst based on Ru-containing scrap waste automotive converters is reported. The catalyst was prepared by recycling and upgrading waste ceramic-cores of scrap automotive catalytic converters as supporting materials. Ruthenium was incorporated into the ceramic structures using a simple, fast and solventless mechano-chemically assisted procedure followed by a chemical reduction step. Different catalysts were prepared with varying Ru contents. The materials were characterized by XRD, N<sub>2</sub> physisorption, XPS, TEM, HRTEM and SEM/mapping analyses. Compared to Ru supported over most studied silica and alumina supports, the new system displayed an outstanding catalytic performance under continuous-flow conditions in terms of conversion and selectivity and a remarkable stability with time-on-stream, demonstrating a synergistic action between Ru and the waste catalytic converter support. A Ru loading of 10 wt% provided the optimum results, including a cinnamaldehyde conversion of up to 95% with a selectivity to cinnamyl alcohol of 80%.

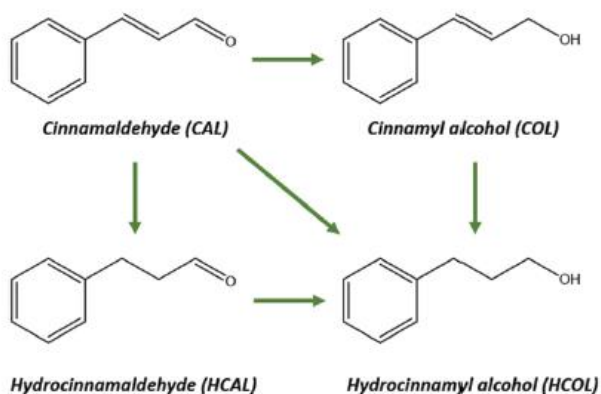
## Introduction

Chemoselectivity is the bedrock of catalytic processes since it involves the activation of specific functional groups within more complex starting reactants. The chemoselective hydrogenation of  $\alpha,\beta$ -unsaturated aldehydes represents a critical step in the synthetic preparation of chemicals for the pharmaceutical and flavour/fragrance industries. For example, citral, an  $\alpha,\beta$ -unsaturated aldehyde extracted from plants, can be selectively hydrogenated to geraniol, a commonly

used fragrance tasting peach, raspberry, grapefruit and red apple.<sup>1-5</sup> In general, the chemoselective hydrogenation of  $\alpha,\beta$ -unsaturated aldehydes has been widely investigated from a mechanistic point using different catalytic systems.<sup>6-8</sup> The results demonstrated that the activation of the double carbon bond is kinetically and thermodynamically favoured, leading to the formation of saturated aldehydes.<sup>1,9-11</sup> However, the less-favoured unsaturated alcohols ( $\Delta E \sim 35 \text{ kJ mol}^{-1}$  less favoured)<sup>12</sup> are of high value and broadly employed in industry.<sup>10,13-15</sup> As a consequence, designing of catalytically active materials that preferentially hydrogenate the carbonyl bond within yields is a captivating yet significant challenge still nowadays.

A largely investigated reaction for the selective hydrogenation of  $\alpha,\beta$ -unsaturated aldehydes is the hydrogenation of cinnamaldehyde (CAL) to cinnamyl alcohol (COL). COL is a fragrance smelling as hyacinth with balsamic and spicy notes widely used in perfumes, drugs and food formulations.<sup>16-18</sup>

As illustrated in Scheme 1, besides COL, the other principal products of the hydrogenation of cinnamaldehyde include hydrocinnamaldehyde (HCAL) and hydrocinnamyl alcohol (HCOL).<sup>19-21</sup>



**Scheme 1** Reaction pathways in the hydrogenation of cinnamaldehyde (CAL: cinnamaldehyde; COL: cinnamyl alcohol; HCAL: hydrocinnamaldehyde; HCOL: hydrocinnamyl alcohol).

Most studied chemoselective heterogeneous catalysts for the hydrogenation of CAL to COL are based on supported ruthenium compounds.<sup>22–25</sup> In particular, significant conversion and selectivity values have been reported using ruthenium supported on porous alumina<sup>26</sup> or silica.<sup>27</sup> More recently, also different carbon materials such as graphene,<sup>28</sup> carbon nanotubes,<sup>22,29,30</sup> activated carbons<sup>31,32</sup> or mesoporous carbons<sup>33</sup> have been reported as efficient supporting materials. The choice of an appropriate supporting material is of primary importance since its intrinsic properties and, more importantly, the interaction between the metals and the support can deeply modify the reaction selectivity, as reported by Leng *et al.*<sup>34</sup> Firstly, a lower metal dispersion generally boosts the selectivity to COL. Furthermore, an enhanced charge transfer between the metal and the support material can also lead to an improvement in selectivity to COL. Finally, the presence of metallic promoters or additional Lewis acid properties could also improve the selectivity to COL.

Important features that should always be considered in the development of novel supporting materials include the scalability and the green credentials of the reaction. Therefore, new supporting materials should be inexpensive, should be easily synthesized and should have a low environmental impact.

With these aims, exploitation of largely produced waste can offer almost unlimited opportunities. In 2016, *ca.* 6 million end-of-life vehicles were registered in the European Union alone, generating approximately 6 thousand tons of ceramic-cores of scrap automotive catalytic converters (CATs). Scrap CATs are normally recycled and treated in order to recover platinum-group metals (PGMs). However, these procedures are normally highly toxic and time-consuming and generate lots of waste.<sup>35–40</sup> In addition, also the latest procedures with environmentally friendly characteristics still have a very high

*E*-factor, as only the PMGs are recovered, while the remaining matrix is waste.<sup>41</sup>

Herein, novel Ru catalysts supported on scrap waste CATs with a high catalytic activity (up to 95% conversion) and selectivity (up to 80%) for the hydrogenation of CAL to COL are reported. To the best of our knowledge, no similar studies were previously carried out on the use of these systems as sustainable catalyst supports. Ru-based catalysts were prepared *via* a fast and simple procedure involving a mechanochemical step followed by a chemical reduction. The catalysts were tested in the hydrogenation of CAL to COL using a continuous flow system to test not only the activity and selectivity of the systems but also their stability with time-on-stream. Remarkably, IUPAC has identified flow chemistry and mechanochemistry among the “top ten chemical innovations that will change our world” and defined them as “emerging technologies with potential to make our planet sustainable”.<sup>42</sup> Indeed, continuous flow systems can offer several advantages including the use of small amounts of solvents and chemical reagents, reduced reaction times, improved selectivity and increased yields.<sup>43,44</sup> On the other hand, mechanochemical protocols allow us to carry out reactions easily and quickly, with a high reproducibility, avoiding, in most cases, solvent utilization. As a result, mechanochemistry can be pointed as an overall highly relevant environmentally friendly technique.<sup>45–47</sup>

## Experimental sections

Ruthenium(III)-chloride hydrate ( $\text{RuCl}_3 \cdot x\text{H}_2\text{O}$ ), sodium borohydride ( $\text{NaBH}_4$ , 99%), *trans*-cinnamaldehyde ( $\text{C}_9\text{H}_8\text{O}$ , 99%) and ethanol ( $\text{CH}_3\text{CH}_2\text{OH}$ , 99.5%) were purchased from Sigma-Aldrich Inc., St Louis, MO, USA. Acetonitrile ( $\text{CH}_3\text{CN}$ , 99.9%), silica Gel 60 (63–200 microns), aluminium

oxide (basic), and aluminium oxide activated (acidic) were purchased from PanReac Química, Barcelona, Spain. All reagents were used without any further purification.

### Synthesis

Prior to the utilization as supporting materials, the ceramic cores of scrap automotive catalytic converters (CATs), kindly donated by the company PROVALUTA S.L., were washed and dried. Specifically, 50 g of CATs was dispersed in 100 mL of distilled water and put in an ultrasonic bath for 2 hours. Sequentially, the powders were filtered and dried in a 100 °C oven (the resulting powder was denoted as CC0, unreduced support).

A number of supported Ru catalysts were synthesized (supporting materials: CC0, SiO<sub>2</sub>, Al<sub>2</sub>O<sub>3</sub> activated or Al<sub>2</sub>O<sub>3</sub>) by a mechanochemically assisted method followed by a chemical reduction. In a typical synthesis, the supporting powder (2 g) and the correct amount of ruthenium salt, RuCl<sub>3</sub>·xH<sub>2</sub>O, (456 mg for 10 wt%; 228 mg for 5 wt%, 114 mg for 2.5 wt% and 45 mg for 1 wt%) were mixed together in a 125 mL stainless steel milling jar equipped with eighteen 5 mm diameter stainless steel balls. The powders were ground in a Retsch PM100 planetary ball mill at 350 rpm for 15 min, changing the direction of rotation every 2'30". Upon milling, the resulting homogenous powders were chemically reduced using NaBH<sub>4</sub> (4 eq.) and EtOH (20 mL) as solvents. The reduced catalysts were filtered and washed with water (5 mL) and ethanol (5 mL). Finally, the resulting powders were oven-dried at 100 °C for 24 hours. Samples were named 10%Ru/CC, 5%Ru/CC, 2.5%Ru/CC, 1%Ru/CC, 0%Ru/CC (0%Ru/CC has no ruthenium content, standing for reduced CC0), 10%Ru/SiO<sub>2</sub>, 10%Ru/Al<sub>2</sub>O<sub>3</sub> activated and 10%Ru/Al<sub>2</sub>O<sub>3</sub>. CC0 corresponds to the unreduced/untreated scrap CAT.

### Catalyst characterization

Powder X-ray diffraction (XRD) patterns were obtained with a Bruker D8 DISCOVER A25 diffractometer (PanAnalytic/Philips, Lelyweg, Almelo, The Netherlands) using  $\text{CuK}\alpha$  ( $\lambda = 1.5418 \text{ \AA}$ ) radiation. Wide angle scanning patterns were collected over a  $2\theta$  range from  $10^\circ$  to  $80^\circ$  with a step size of  $0.018^\circ$  and counting time of 5 s per step.

Textural properties of the samples were determined by  $\text{N}_2$  physisorption using a Micromeritics ASAP 2020 automated system (Micromeritics Instrument Corporation, Norcross, GA, USA) using the Brunauer-Emmett-Teller (BET) and the Barrett-Joyner-Halenda (BJH) methods. The samples were outgassed for 24 h at  $100^\circ\text{C}$  under vacuum ( $P_0 = 10^{-2} \text{ Pa}$ ) and subsequently analysed.

Scanning electron microscopy images were recorded with a JEOL JSM-6300 scanning microscope (JEOL Ltd, Peabody, MA, USA) equipped with energy-dispersive X-ray spectroscopy (EDX) at 15 kV at the Research Support Service Center (SCAI) from the University of Cordoba.

TEM images were recorded in a JEOL 1200 equipped with energy-dispersive X-ray spectroscopy (EDX), at the Research Support Service Center (SCAI) from Universidad de Cordoba. Prior to analysis, samples were prepared by suspension in EtOH, assisted by sonication and followed by deposition on a copper grid.

HRTEM images were recorded in a FEI TITAN<sup>3</sup> (CEOS Company) equipped with a SuperTwin<sup>®</sup> objective lens and a CETCOR Cs-objective corrector (CEOS Company) at the Laboratorio de Microscopias Avanzadas of the Instituto de Aragon, at the University of Zaragoza (Spain).

XPS studies were performed at the Central Service of Research Support (SCAI) of the University of Cordoba, using an ultrahigh vacuum (UHV)

multipurpose surface analysis system (Specs™). The experiments were carried out at pressures  $<10^{-10}$  mbar, using a conventional X-ray source (XR-50, Specs, Mg-K $\alpha$ ,  $h\nu = 1253.6$  eV,  $1 \text{ eV} = 1.603 \times 10^{-19}$  J) in the “stop and go” mode. The samples (4 mm  $\times$  4 mm pellets, 0.5 mm thick) were evacuated overnight under vacuum ( $<10^{-6}$  mbar). Spectra were collected at room temperature (pass energy: 25 and 10 eV, step size: 1 and 0.1 eV) with a Phoibos 150-MCD energy detector. The deconvolutions of the curves and the elements quantifications were obtained using XPS CASA software.

### Catalytic experiments

Catalytic performances of the catalysts were evaluated under liquid phase continuous flow conditions in an H-Cube Mini Plus™ flow hydrogenation reactor. The materials were packed ( $\sim 0.2$  g of catalyst per cartridge) in 30 mm-long ThalesNano CatCarts. Initially, the reactor was washed with methanol and acetonitrile ( $0.3 \text{ mL min}^{-1}$  flow, 20 min for each solvent). Sequentially, a solution of 0.1 M cinnamaldehyde in acetonitrile was pumped through and the reaction conditions were optimized based on previous studies from the group ( $90 \text{ }^\circ\text{C}$ , 30 bar,  $0.1 \text{ mL min}^{-1}$ ). The required hydrogen was generated *in situ* during the reaction by water electrolysis in the H-Cube equipment. The reactions were performed for 120 min, collecting samples every 15 min for further analysis. Samples collected at “0 min” were considered as first outcomes under operative reaction conditions passed through the cartridge.

The conversion and selectivity were analyzed by gas chromatography (GC) in an Agilent 6890N gas chromatograph ( $60 \text{ mL min}^{-1}$  N<sub>2</sub> carrier flow, 20 psi column top head pressure) using a flame ionization detector (FID). A capillary column, HP-5 (30 m  $\times$  0.32 mm  $\times$  0.25  $\mu\text{m}$ , Agilent Technologies Inc.), was employed. Calibration curves were obtained with an internal

standard method using octane as the standard. Standard solutions of cinnamaldehyde (from 0.005 to 0.1 M) and 0.1 M octane in CH<sub>3</sub>CN were analyzed by GC to give linear regressions with  $R^2 > 0.999$ . In addition, the collected liquid fractions were analyzed by GC-MS—using the Agilent 7820A GC/5977B High Efficiency Source (HES) MSD—in order to identify the obtained products.

## Results and discussion

### Characterization of Ru/catalytic converter systems

The novel catalysts were characterized by XRD, TEM, HRTEM, SEM/mapping, N<sub>2</sub> physisorption and XPS. As illustrated in Fig. 1, the washing of the starting CATs for the preparation of CC resulted in increasing the diffraction peaks of the samples. This demonstrated that a great portion of the amorphous carbon adsorbed on the surfaced was successfully removed. Considering samples CC0 (unreduced support), 0%Ru/CC (reduced CC0) and 10%Ru/CC, the most intense diffraction peaks observed at  $2\theta$  values of 21.72°, 28.49° and 54.67° could be indexed to the (1 0 0), (0 1 1), and (2 0 2) planes of SiO<sub>2</sub> with a hexagonal structure (JCPDS 00-023-0961), one of the major component of CATs.<sup>48</sup>

In fact, an automotive catalytic converter generally consists of four main structures:<sup>49</sup>

(1) The catalyst core or substrate, which consists of a ceramic monolith (defined as inner ceramic). The monolith has a honeycomb structure mainly made of cordierite (2MgO·2Al<sub>2</sub>O<sub>3</sub>·5SiO<sub>2</sub>).

(2) The wash coat, which is a carrier for the catalytic material and is used to disperse the materials over a large surface area. Al<sub>2</sub>O<sub>3</sub>, TiO<sub>2</sub>, SiO<sub>2</sub>, or a mixture of alumina and silica can be used.

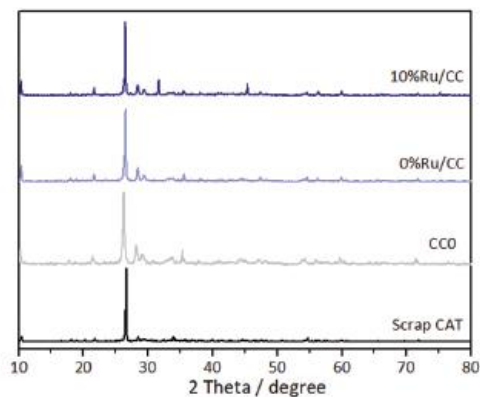


(3)  $\text{CeO}_2$  or  $\text{CeO}_2\text{-ZrO}_2$ . These oxides are mainly added to promote the storage of oxygen adsorbed from air and needed for the oxidations of exhaust emission.

(4) Noble metals such as platinum, palladium and rhodium. Other metals such as iron, manganese, nickel and cerium are also present.

As a consequence of this complexity, all remaining diffraction peaks could hardly be assigned in any case due to their low diffraction line intensities. ICP-MS of the CC0 unreduced support also detected Si, Al, Mg, Fe and Ce as main components while also minor components such as Ti, Zn, Zr and Pt were revealed. (For detailed ICP-MS analysis, please see ESI, Table S1.†).

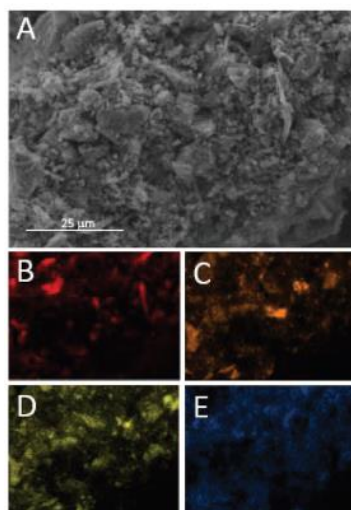
The XRD patterns of 10%Ru/CC, and the XRD patterns of 10%Ru/SiO<sub>2</sub>, 10%Ru/Al<sub>2</sub>O<sub>3</sub> and 10%Ru/Al<sub>2</sub>O<sub>3</sub> activated, did not show any appreciable peaks that could be indexed to ruthenium. (Please see ESI Fig. S1† for the complete XRD patterns.) The presence of Ru was subsequently confirmed by TEM, HRTEM, SEM/mapping and XPS analysis.



**Fig. 1** XRD patterns for 10%Ru/CC, 0%Ru/CC, CC0 and ceramic-core of the scrap catalytic converter.

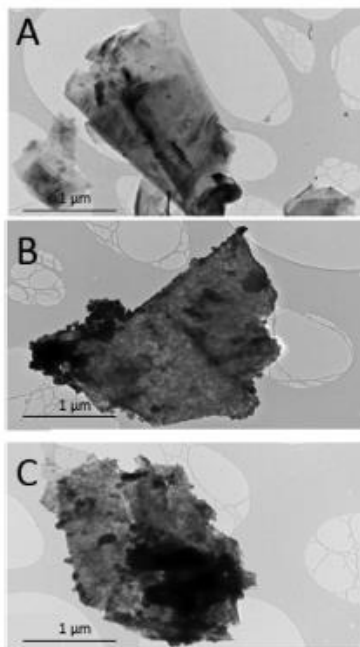
Fig. 2 shows SEM images and SEM/mapping of sample 10%Ru/CC. In Fig. 2A it is possible to visualize flake structures derived from the smashed ceramic honeycomb. Fig. 2B, C and D show the EDX-mapping of the major

components of the CC support, *i.e.* C, Si and Al. The inhomogeneous carbon distribution is a consequence of the ball milling treatment: initially, carbon was almost exclusively located on the CAT surface, while it was mixed with all other components after ball milling. Si and Al were homogeneously distributed over the catalyst surface, as they are elements both present in the catalyst core and in the wash coat. Remarkably, as illustrated in Fig. 2E, Ru was homogeneously distributed over all the catalyst surface. (Fig. S2 ESI,† SEM/mapping of all samples.)



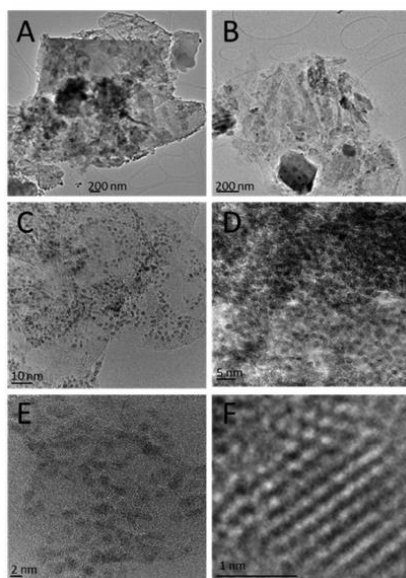
**Fig. 2** (A) SEM image of the 10%Ru/CC catalyst with mapping analysis of (B) carbon; (C) silicon; (D) aluminium and (E) ruthenium.

Fig. 3 shows TEM images of scrap automotive catalytic converters (CATs) and of the 10%Ru/CC catalyst before and after the catalytic tests. TEM images of the 10%Ru/CC catalyst (Fig. 3B and C) showed that ruthenium particles were successfully supported on the catalytic converter surface. In particular, several darker areas, clearly associated with the ruthenium-oxide counterpart, were observed and confirmed by EDX analysis. Despite some significant agglomeration taking place (Fig. 3C), the materials were proved to be highly active and stable under the investigated reaction conditions.



**Fig. 3** TEM images of the CATs (A), 10%Ru/CC catalyst (B) and 10%Ru/CC catalysts after the stability test (C).

In order to better analyse the morphology and Ru content of 10%Ru/CC, additional HRTEM images were taken as illustrated in Fig. 4.



**Fig. 4** HRTEM images of 10%Ru/CC. F corresponds to a single Ru nanoparticle.

The images showed the smashed structure of CATs (Fig. 4A and B) and the presence of Ru nanoparticles, also in some agglomerated forms (Fig. 4C and D). The dimension of the individual Ru nanoparticles was found to be *ca.* 2 nm in diameter (Fig. 4E). The *d*-spacing of some of the ruthenium crystals ranged from 0.20 to 0.21, which can be associated with the (101) and (002) planes of RuO<sub>2</sub>. (For additional images, please see ESI, Fig. S3.†)

In order to determine the specific surface area of the catalyst, Brunauer-Emmett-Teller (BET) physisorption was carried out by nitrogen adsorption-desorption measurements. Table 1 lists the results of the analysis. The data demonstrated that the catalysts were essentially nonporous (type III isotherm), in good agreement with the SEM images. After the addition of ruthenium, a slight increase in surface area was observed. This could be related to the ball-milling addition of the ruthenium precursor which was deposited on the surface of the catalytic converter as small nanoparticles, increasing the surface area. After metal reduction, these particles were reduced in dimensions so that a further surface area increment was detected. (Please see the isotherm graph in the ESI, Fig. S4.†).

**Table 1** Textural properties of key synthesized catalysts

Sample	Surface area/m <sup>2</sup> g <sup>-1</sup>
CC0 (unreduced support)	13
10%Ru/CC <sup>a</sup>	16
10%Ru/CC	21

<sup>a</sup>Before chemical reduction

The interaction of Ru entities and the CC support was also studied by XPS. As analysed in previous work, Ru-containing catalysts exhibit complex spectra. On the one hand, the fitting of the Ru 3d core level can be achieved using several asymmetric line shape; on the other hand, a strong overlapping effect from close enough peak positions can be encountered between carbon

and ruthenium contributions.<sup>50,51</sup> Such overlapping can be observed in Fig. 5A. The Ru 3d XPS region showed a separate band at 280.7 eV, which can be associated with a dominant Ru(IV) oxidation state on the surface.<sup>50</sup> Position and shape of this contribution were pretty similar to those obtained for the 10%Ru/SiO<sub>2</sub> reference (Fig. 5A). However, clear differences concerning the C component were observed. C 1s, with a reference peak at 284.6 eV (C–C), confirmed that adventitious C remained in the structure of the CC support after the washing treatments and further functionalization with Ru.

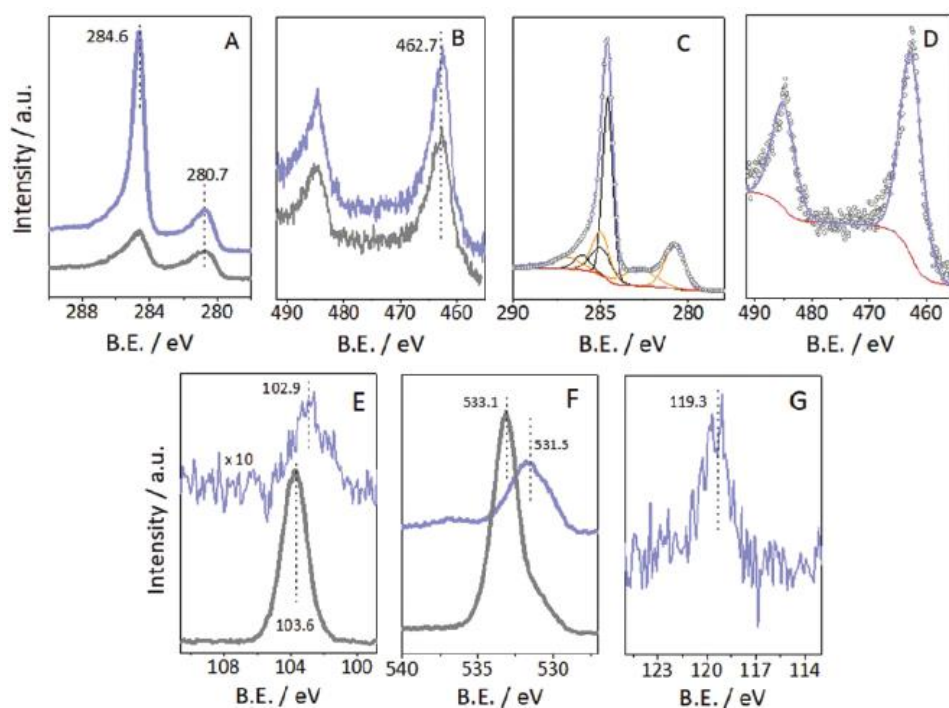
A detailed analysis of the region is presented in Fig. 5C for the 10%Ru/CC sample. The fitting procedure followed the recommendations given by Morgan.<sup>50</sup>

Fig. 5C shows the lines at 284.7 eV ( $3d_{5/2}$ ) and 284.0 eV ( $3d_{3/2}$ ) associated, as aforementioned, with RuO<sub>2</sub>.<sup>50,51</sup> In addition, satellites 1.9 eV above each Ru (3d) signal and line shape equivalent to the parent peak and a spin-orbit splitting of 4.17 eV for photoelectron peaks and satellites with an area ratio of 0.67 must be considered.<sup>50</sup> The existence of dominant oxidized ruthenium was confirmed by the Ru 3p XPS region.

As observed in Fig. 5B and D, the binding energy values associated with the Ru  $3d_{3/2}$  peak were both (10%Ru/CC and 10%Ru/SiO<sub>2</sub>) above 462.7 eV, characteristic of Ru(IV).<sup>52,53</sup> Identification of other elements constituting the CC structure and silica support was also carried out. Fig. 5E, F and G show the Si 2p, O 1s and Al 2s XPS regions. The values of *ca.* 103.6 eV and 533.1 eV agree with Si 2p and O 1s of SiO<sub>2</sub>, respectively.<sup>54</sup> Nonetheless, all Si 2p, O 1s and Al 2s showed a low binding energy shift in comparison with pure aluminosilicate compounds,<sup>55</sup> which could be associated with an electronic effect due to the presence of multiple Si-metals and O-metals (Ce, Zr, Fe, *etc.*) interactions in the CC support.

However, no clear evidence of charge transfer enhancement and its relation with the activity and selectivity could be claimed from this result,<sup>34</sup> and new experiments such as *in situ* synchrotron X-ray absorption spectroscopy must be considered to prove this singular interaction.

Finally, the 10%Ru/CC catalyst was characterized by XPS analysis after the stability test, showing no appreciable differences compared with the fresh (unused) catalyst.

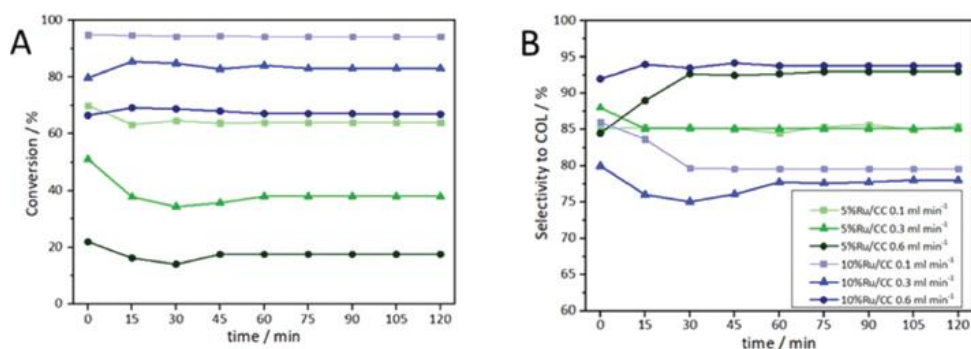


**Fig. 5** XPS analysis of 10%Ru/CC (light blue) and 10%Ru/SiO<sub>2</sub> (grey) samples. (A) C 1s and Ru 3d. (B) Ru 3p. (C) Representative example (10%Ru/CC) of the fitting procedure of the C 1s (black) and Ru 3d (orange) XPS regions. (D) Representative example (10%Ru/CC) of the fitting procedure of the Ru 3p XPS region. (E) Si 2p. (F) O 1s and (G) Al 2s.

### Catalytic tests

**Influence of flow rate.** The effect of flow rate on the hydrogenation of CAL was initially investigated using 5%Ru/CC and 10%Ru/CC. Previously

optimised operating conditions of 90 °C temperature under 30 bar H<sub>2</sub> pressure were selected as starting conditions.<sup>56</sup> Acetonitrile was chosen as the solvent due to the less aggressive toxic and pollutant characteristics<sup>57</sup> and being the optimum solvent for the hydrogenation of CAL in previous work from the group.<sup>58</sup> Other solvents including isopropanol, ethanol and water were discharged due to relevant problems in flow conditions such as cartridge blockage and pressure drop issues. Fig. 6 displays the results in terms of conversion and selectivity to COL operating at flow rates of 0.1, 0.3 and 0.6 mL min<sup>-1</sup>. Steady state conditions were observed for all catalysts after 45' of reactions.

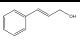
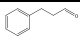
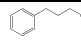


**Fig. 6** Influence of flow rate on CAL conversion (A) and COL selectivity (B). Reaction conditions:  $p = 30$  bar H<sub>2</sub>;  $T = 90$  °C.

Table 2 summarizes the results in average under steady-state conditions. Main products include COL, CAL and HCAL. Other products (reported together as “others”) include  $\beta$ -methylstyrene, propylbenzene and ring hydrogenation products.<sup>58</sup> While a higher content of Ru provided a higher conversion (Fig. 6A and Table 2), the correlation between Ru% and selectivity to COL was not obvious. Reduced Ru content corresponded to an increased selectivity to COL of *ca.* 5–10% at a flow rate of 0.1 mL min<sup>-1</sup> and 0.3 mL min<sup>-1</sup>. As HCAL was not observed (Table 2), although there is no experimental evidence, the most probable hypothesis is that CAL was initially hydrogenated

to COL, which was subsequently hydrogenated to HCOL. This supposition could be further supported by the observed selectivity to COL at higher flow rates (*e.g.* 0.6 mL min<sup>-1</sup>). Higher flux prevented a longer contact between COL and the catalyst, avoiding the sequential hydrogenation to HCOL. In order to better analyse the selective hydrogenation to COL, the flow rate of 0.1 mL min<sup>-1</sup> was further selected (Table 2).

**Table 2** Reaction parameters and conversion and selectivity values under steady state conditions for the reaction carried out at different flow rates

Catalyst	Flow rate mL min <sup>-1</sup>	$\tau^a$ /min	Conversion /%	Selectivity/%				COL yield /%
				 COL	 HCOL	 HCOL	Others	
BLANK	0.1	3	<3%	-	-	-	-	-
10%Ru/CC	0.1	3	94.4	80.1	-	8.8	11.1	75.6
10%Ru/CC	0.3	1.5	84.8	74.2	-	6.1	19.7	62.9
10%Ru/CC	0.6	0.7	64.8	93.4	-	-	6.6	60.5
5%Ru/CC	0.1	3	64.0	85.1	-	5.1	9.8	54.5
5%Ru/CC	0.3	1.5	38.0	85.0	-	3.8	11.2	32.3
5%Ru/CC	0.6	0.7	19.9	92.2	-	-	7.8	18.3

<sup>a</sup>Residence time = Catcarts volume/flow rate.

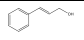
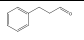
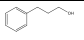
**Influence of H<sub>2</sub> pressure and temperature.** The influence of H<sub>2</sub> pressure and temperature on the hydrogenation of CAL was further studied using 10%Ru/CC. A set of experiments were carried out fixing the reaction temperature at 90°C and varying the H<sub>2</sub> pressure (from 10 to 40 bar). Steady state conditions were observed for all trials after 45 min of reaction (*ca.* 2 min residence time).

Table 3 summarizes the average results under steady-state conditions. Remarkably, the selectivities to the main different products gave almost the same values. However, a higher pressure provided a higher conversion, reaching a maximum at 30 bar of H<sub>2</sub> pressure. The experiment conducted at 40 bar of H<sub>2</sub> pressure gave almost identical results. As a result, the 30 bar H<sub>2</sub>



pressure value was selected as the optimum reaction pressure, in order to minimize the energy consumption.

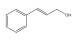
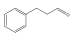
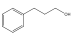
**Table 3** Reaction parameters and conversion and selectivity values under steady state conditions for the reaction carried out at different H<sub>2</sub> pressures

Catalyst	Pressure /bar	Temperature /°C	Conversion /%	Selectivity/%				COL yield /%
							Others	
				COL	HCAL	HCOL		
10%Ru/CC	10	90	38.2	84.1	-	6.7	9.2	32.1
10%Ru/CC	20	90	66.4	82.7	-	7.0	10.3	54.9
10%Ru/CC	30	90	94.4	80.1	-	8.8	11.1	75.6
10%Ru/CC	40	90	95.1	79.9	-	9.2	10.9	75.9

Successively, a series of experiments were carried out operating at 30 bar H<sub>2</sub> pressure and changing the reaction temperature. The trials were performed at 50, 70 and 90 °C. 90 °C was selected as the maximum reaction temperature in order to operate avoiding any damage and blockage of the instrument (H-Cube can operate maximum at 100 °C). Results under steady-state conditions are presented in Table 4.

A higher temperature provided a higher conversion and a higher selectivity to COL. Based on these results (94% of conversion and 80% of selectivity to COL), 90 °C was selected as the optimum reaction temperature.

**Table 4** Reaction parameters and conversion and selectivity values under steady state conditions for the reaction carried out at different temperatures

Catalyst	Pressure /bar	Temperature /°C	Conversion /%	Selectivity/%				COL Yield /%
							Others	
				COL	HCAL	HCOL		
10%Ru/CC	30	50	78.3	68.9	-	16.6	14.5	53.9
10%Ru/CC	30	70	85.6	74.2	-	11.4	12.4	63.5
10%Ru/CC	30	90	94.4	80.1	-	8.8	11.1	75.6

**Effect of Ruthenium loading.** Sequentially, operating under the optimized flow rate of 0.1 mL min<sup>-1</sup>, the selective hydrogenation of CAL was investigated

as a function of metal loading. As illustrated in Fig. 7, optimum conversion values were observed at higher Ru contents, with very low conversion values obtained for Ru loadings below 5% Ru.

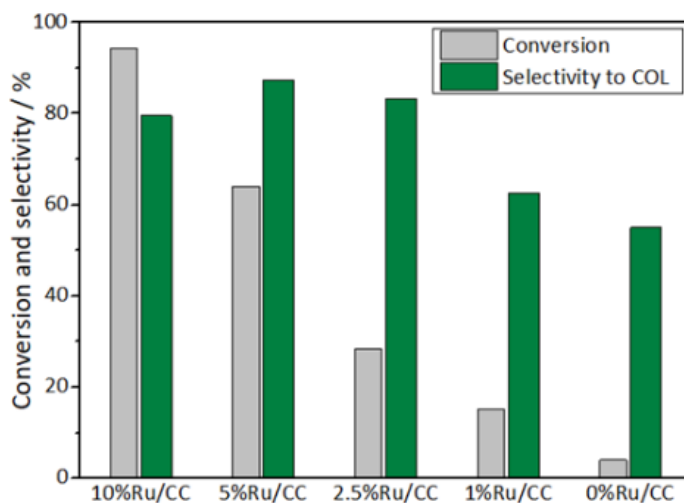


**Fig. 7** CAL conversion and COL selectivity average under steady state conditions (TOS = 120 min) for different Ruthenium loadings over the CC supporting material. Reaction conditions:  $p = 30$  bar  $H_2$ ;  $T = 90^\circ C$ ; flow rate =  $0.1$  ml  $min^{-1}$ .

In addition, the selectivity to COL increased by increasing the Ru content, reaching a maximum for 5%Ru/CC. As previously described, sample 10%Ru/CC showed a slightly low selectivity to COL due to further hydrogenation to HCOL (Table 2). Although catalyst 5%Ru/CC showed the best performance in terms of selectivity, 10%Ru/CC was selected for sequential tests due to the optimum product yield (75% vs. 54% for 5%Ru/CC, Table 2).

Remarkably, the CC (reduced) support material showed some catalytic activity also before the addition of Ru, while CC0 (support not reduced) showed no catalytic activity. This can be explained in terms of the content of noble metals in the supporting material: after the recovery and the washing of the ceramic from scrap automotive catalytic converters, noble metals (Pt, Pd, Rh) present in trace quantities in CATs were also reduced during the reduction

of Ru, reactivating the metallic sites. As described by Gallezot and Richard,<sup>9</sup> Pt is highly selective to the carbonyl group, while Pd to the olefinic bond, explaining the selectivity to COL of the 1%Ru/CC and reduced CC samples of around 62% and 50%, respectively (ESI, see Table S2† for all selectivity and yield data).

**Influence of the supporting material.** In order to investigate and demonstrate the positive influence of the CC supporting material on the catalytic activity, different catalysts (10%Ru loading) were prepared using standard supporting materials including SiO<sub>2</sub>, acidic Al<sub>2</sub>O<sub>3</sub> activated and commercial Al<sub>2</sub>O<sub>3</sub>. As illustrated in Fig. 8 and Table 5, the conversion obtained for 10%Ru/CC was remarkably superior to that of all additionally investigated supports. The most active alternative catalyst, 10%Ru/SiO<sub>2</sub>, exhibited a conversion of CAL up to 68.4%, but with a low selectivity to COL (32.4%).

On the other hand, the acidic properties of activated Al<sub>2</sub>O<sub>3</sub> enhanced the hydrogenation reaction of CAL, but with a low selectivity to COL. Furthermore, such acidity was slowly deactivated in time, reducing the catalytic activity of the catalysts to the same of standard Al<sub>2</sub>O<sub>3</sub>. This comparison also demonstrated that Ru/CC catalysts could hydrogenate the aldehyde of the  $\alpha,\beta$ -unsaturated aldehyde, while the olefinic bond was hydrogenated only when the compound was in the form of the  $\alpha,\beta$ -unsaturated alcohol. As a consequence, the high activity and selectivity of 10%Ru/CC could be explained in terms of enhanced charge transfer between the metal and the support material (as also indicated and found by XPS analysis) and by the presence of traces of metallic promoters present in the scrap waste CC (mainly Fe, Ce, Zr, Ti, Zn, Pt, Mg and Pd).

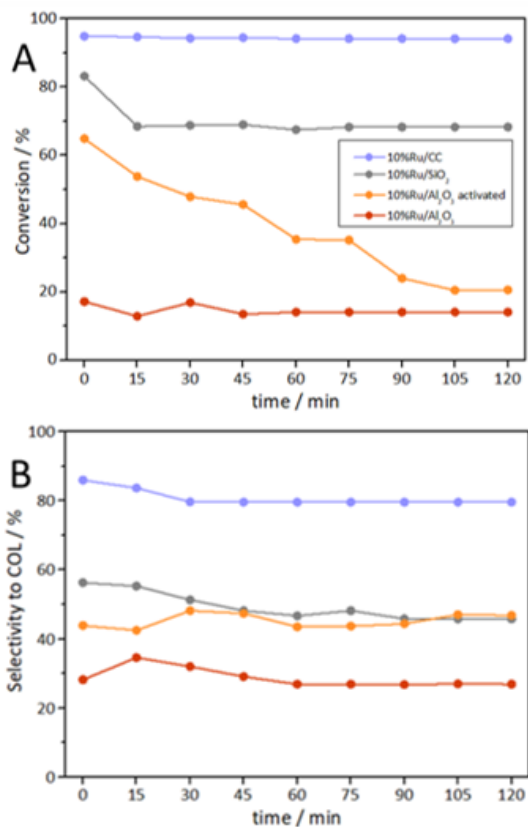


**Fig. 8** CAL conversion (A) and COL selectivity (B) using different catalysts. Reaction conditions:  $p = 30$  bar  $H_2$ ;  $T = 90^\circ C$ ; flow rate =  $0.1$  mL  $min^{-1}$ .

**Table 5** CAL conversion and COL selectivity average at stationary state (TOS = 120 min) for different supporting materials

Catalyst	Conversion /%	Selectivity/%			Yield to COL/%
		COL	HCOL	Others	
10%Ru/CC	78.3	68.9	16.6	14.5	53.9
Blank	<5	-	-	-	-
10%Ru/CC	94.4	79.7	9.2	11.1	75.2
10%Ru/SiO <sub>2</sub>	68.4	47.4	2.4	47.8	32.4
10%Ru/Al <sub>2</sub> O <sub>3</sub> activated <sup>a</sup>	20.5	45.3	3.4	34.2	9.3
10%Ru/Al <sub>2</sub> O <sub>3</sub>	14.2	28.7	0	37.0	4.1

<sup>a</sup> Stationary state reached after 105 min.

**Comparison with commercially available hydrogenation catalysts.** The catalytic activity of the synthesized scrap-based catalysts was eventually compared with commercially available 5%Pd/C and 5%Ru/C systems, as shown in Fig. 9.

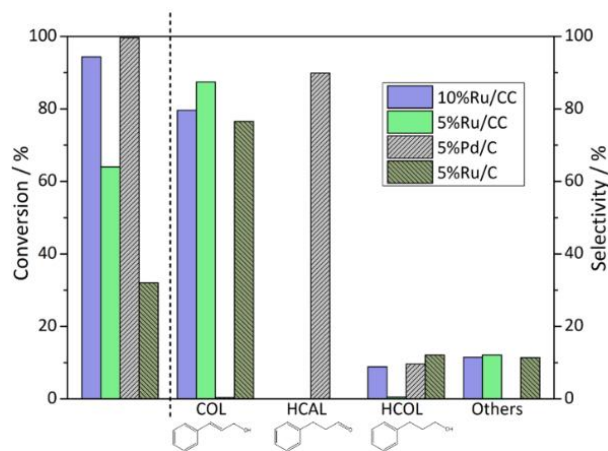


**Fig. 9** CAL conversion (A) and COL, HCAL, HCOL selectivity average in the stationary state (TOS = 120 min) comparing 10%Ru/CC and 5%Ru/CC with commercially available 5%Pd/C and 5%Ru/C. Reaction conditions:  $p = 30$  bar  $H_2$ ;  $T = 90^\circ C$ ; flow rate =  $0.1$  mL  $min^{-1}$ .

For a complete comparison, also sample 5%Ru/CC was considered, in order to relate the same weight amount of the metal loaded. As illustrated in Fig. 9, 5%Pd/C was highly active for the hydrogenation, exhibiting an almost complete conversion of CAL under the investigated reaction conditions. Comparably, 5%Ru/CC and 10%Ru/CC were significantly less active. However, Pd was found to be selective to the reduction of the double bond of the  $\alpha,\beta$ -unsaturated aldehyde, favouring the production of HCAL, which was sequentially hydrogenated to HCOL. On the other hand, the Ru/CC catalysts were highly selective to the carbonyl group of CAL. The conversion obtained with 5%Ru/CC was remarkably superior to that of the 5%Ru/C commercial

catalyst (Fig. 9), demonstrating again the positive influence of the catalytic converter supporting material on the catalytic activity.

**Stability of the catalyst.** The long term stability of 10%Ru/CC was investigated under optimum continuous flow conditions. The reaction was performed for a 10 hours TOS. No relevant changes in conversion of CAL and selectivity to COL demonstrated a good stability of the catalyst under the investigated conditions, as shown in Fig. 10, further supported by almost negligible Ru leaching (<10 ppm in the filtrate after 10 h reaction) as determined by ICP-MS.

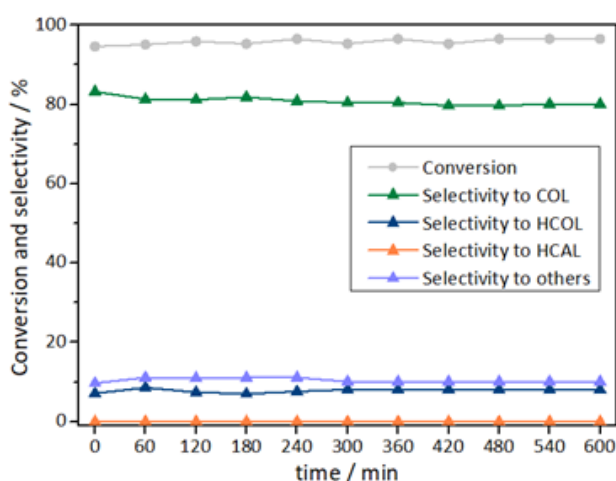


**Fig. 10** Stability test of sample 10%Ru/CC. Reaction conditions:  $p = 30$  bar  $H_2$ ;  $T = 90^\circ C$ ; flow rate =  $0.1$  mL  $min^{-1}$ .

**E-Factor.** In order to validate the green credentials of the proposed methodology, the  $E$ -factor of 10%Ru/CC was calculated and compared to catalysts previously described for the same application.<sup>58-60</sup>  $E$ -factor was calculated as reported by R. Sheldon:<sup>61</sup>

$$E\text{-factor} = (\text{total waste/kg})/(\text{product/kg})$$

While 10%Ru/CC had an  $E$ -factor of 24 (which corresponds to the industrial segment of fine chemicals), our previously reported Pd system had an

*E*-factor of 140 (mostly due to the synthesis of the supporting material SBA-15).<sup>58</sup> Other catalysts, such as Cu–Ni–AAPTMS@GO and CeO<sub>2</sub>–ZrO<sub>2</sub> composites supported Pt nanoparticles, have *E*-factors of <350 and <250, respectively.<sup>59-60</sup>

## Conclusions

Ruthenium-based catalysts supported on ceramic-cores of scrap automotive catalytic converters were efficiently synthesized by a mechanochemical approach followed by a chemical reduction. The interaction between Ru and the recycled catalytic converter strongly influenced the catalytic performances of ruthenium. Such catalytic response could be associated with an enhancement of charge transfer and the presence of noble metal particles. Synthesized catalysts were tested in the selective conversion of CAL to COL in continuous flow conditions. A complete analysis of the reaction was performed changing the flow rate and metal loading catalysts. In order to prove the effective influence of the catalytic converter support on the conversion of CAL, different catalysts were prepared using same Ru-loading on standard supporting materials.

In conclusion, a Ru loading of 10 wt% allowed the best catalytic performance, including the conversion of CAL up to 95%, with selectivity to COL up to 80%.

This work opens to the possibility for reusing scrap automotive catalytic converters as efficient support materials (for catalyst design) and even as catalysts, to be reported in due course.

## Conflicts of interest

The authors declare no conflicts of interest.

## Acknowledgements

The authors thank Mr. Rafael Ángel Gómez Haro and Provaluta España Reciclaje de Metales, S.L., Córdoba (ES), for the supply of scrap automotive catalytic converters. The authors thank Prof. Victor Sebastian, from the University of Zaragoza, for the HRTEM studies conducted at the Laboratorio de Microscopias Avanzadas, Instituto de Nanociencia de Aragon, Universidad de Zaragoza, Spain. This project has received funding from the European Union's Horizon 2020 research and innovation programme under the Marie Skłodowska-Curie grant agreement No 721290. This publication reflects only the author's view, exempting the Community from any liability. Project website: <http://cosmic-etn.eu/>. The publication has been prepared with support from RUDN University program 5-100.

## References

1. N. M. Bertero, A. F. Trasarti, B. Moraweck, A. Borgna and A. J. Marchi, *Appl. Catal., A*, 2009, **358**, 32-41.
2. R. Malathi and R. P. Viswanath, *Appl. Catal., A*, 2001, **208**, 323-327.
3. C. Milone, M. L. Tropeano, G. Gulino, G. Neri, R. Ingoglia and S. Galvagno, *Chem. Commun.*, 2002, 868-869.
4. U. K. Singh and M. A. Vannice, *J. Catal.*, 2001, **199**, 73-84.
5. X. Wang, W. Hu, B. Deng and X. Liang, *J. Nanopart. Res.*, 2017, **19**, 153.
6. Y. Zhu, H. F. Qian, B. A. Drake and R. C. Jin, *Angew. Chem. Int. Ed.*, 2010, **49**, 1295-1298.
7. A. B. Merlo, B. F. Machado, V. Vetere, J. L. Faria and M. L. Casella, *Appl. Catal., A*, 2010, **383**, 43-49.
8. L. He, F. J. Yu, X. B. Lou, Y. Cao, H. Y. He and K. N. Fan, *Chem. Commun.*, 2010, **46**, 1553-1555.
9. P. Gallezot and D. Richard, *Catal. Rev. Sci. Eng.*, 1998, **40**, 81-126.
10. P. Maki-Arvela, J. Hajek, T. Salmi and D. Y. Murzin, *Appl. Catal., A*, 2005, **292**, 1-49.



## Results & Discussion

11. D. Loffreda, F. Delbecq, F. Vigne and P. Sautet, *J. Am. Chem. Soc.*, 2006, **128**, 1316-1323.
12. C. J. Kliewer, M. Bieri and G. A. Somorjai, *J. Am. Chem. Soc.*, 2009., **131**, 9958-9966.
13. W. Koo-amornpattana and J. M. Winterbottom, *Catal. Today*, 2001, **66**, 277-287.
14. J. J. Shi, R. F. Nie, P. Chen and Z. Y. Hou, *Catal. Commun.*, 2013, **41**, 101-105.
15. J. J. Shi, M. Y. Zhang, W. C. Du, W. S. Ning and Z. Y. Hou, *Catal. Sci. Technol.*, 2015, **5**, 3108-3112.
16. Z. M. Tian, X. Xiang, L. S. Xie and F. Li, *Ind. Eng. Chem. Res.*, 2013, **52**, 288-296.
17. S. J. Chen, L. Meng, B. X. Chen, W. Y. Chen, X. Z. Duan, X. Huang, B. S. Zhang, H. B. Fu and Y. Wan, *ACS Catal.*, 2017, **7**, 2074-2087.
18. E. Plessers, D. E. De Vos and M. B. J. Roeffaers, *J. Catal.*, 2016, **340**, 136-143.
19. A. Y. Hammoudeh, S. M. Sa'ada and S. S. Mahmoud, *Jordan J. Chem.*, 2007, **2**, 53-67.
20. Y. J. Zhu and F. Zaera, *Catal. Sci. Technol.*, 2014, **4**, 3390-3390.
21. J. Hajek, N. Kumar, P. Maki-Arvela, T. Salmi, D. Y. Murzin, I. Paseka, T. Heikkila, E. Laine, P. Laukkanen and J. Vayrynen, *Appl. Catal., A*, 2003, **251**, 385-396.
22. J. M. Planeix, N. Coustel, B. Coq, V. Brotons, P. S. Kumbhar, R. Dutartre, P. Geneste, P. Bernier and P. M. Ajayan, *J. Am. Chem. Soc.*, 1994, **116**, 7935-7936.
23. A. J. Plomp, H. Vuori, A. O. I. Krause, K. P. de Jong and J. H. Bitter, *Appl. Catal., A*, 2008, **351**, 9-15.
24. J. Hajek, J. Warna and D. Y. Murzin, *Ind. Eng. Chem. Res.*, 2004, **43**, 2039-2048.
25. J. S. Qiu, H. Z. Zhang, X. N. Wang, H. M. Han, C. H. Liang and C. Li, *React. Kinet. Catal. Lett.*, 2006, **88**, 269-275.
26. G. Neri, L. Bonaccorsi, L. Mercadante and S. Galvagno, *Ind. Eng. Chem. Res.*, 1997, **36**, 3554-3562.
27. M. Lashdaf, A. O. I. Krause, M. Lindblad, A. Tiitta and T. Venalainen, *Appl. Catal., A*, 2003, **241**, 65-75.
28. Y. Wang, Z. M. Rong and J. P. Qu, *J. Catal.*, 2016, **333**, 8-16.
29. Y. Wang, Z. M. Rong, P. Zhang and J. P. Qu, *J. Catal.*, 2015, **329**, 95-106.

30. X. J. Ni, B. S. Zhang, C. Li, M. Pang, D. S. Su, C. T. Williams and C. H. Liang, *Catal. Commun.*, 2012, **24**, 65-69.
31. S. Galvagno, G. Capannelli, G. Neri, A. Donato and R. Pietropaolo, *J. Mol. Catal.*, 1991, **64**, 237-246.
32. S. Galvagno, A. Donato, G. Neri, R. Pietropaolo and G. Capannelli, *J. Mol. Catal.*, 1993, **78**, 227-236.
33. P. Gao, A. W. Wang, X. D. Wang and T. Zhang, *Catal. Lett.*, 2008, **125**, 289-295.
34. F. Q. Leng, L. C. Gerber, M. R. Axet and P. Serp, *C. R. Chim.*, 2018, **21**, 346-353.
35. M. K. Jha, J. C. Lee, M. S. Kim, J. Jeong, B. S. Kim and V. Kumar, *Hydrometallurgy*, 2013, **133**, 23-32.
36. M. A. Barakat and M. H. H. Mahmoud, *Hydrometallurgy*, 2004, **72**, 179-184.
37. M. Baghalha, H. K. Gh and H. R. Mortaheb, *Hydrometallurgy*, 2009, **95**, 247-253.
38. D. J. de Aberasturi, R. Pinedo, I. R. de Larramendi, R. de Larramendi and T. Rojo, *Miner. Eng.*, 2011, **24**, 505-513.
39. M. Benson, C. R. Bennett, J. E. Harry, M. K. Patel and M. Cross, *Resour., Conserv. Recycl.*, 2000, **31**, 1-7.
40. C. H. Kim, S. I. Woo and S. H. Jeon, *Ind. Eng. Chem. Res.*, 2000, **39**, 1185-1192.
41. N. Hodnik, C. Baldizzone, G. Polymeros, S. Geiger, J. P. Grote, S. Cherevko, A. Mingers, A. Zeradjanin and K. J. J. Mayrhofer, *Nat. Commun.*, 2016, **7**, 13164.
42. F. Gomollón-Bel, *Chem. Int.*, 2019, **41**(2), 12-17.
43. F. M. Akwi and P. Watts, *Chem. Commun.*, 2018, **54**, 13894-13928.
44. L. Vaccaro, D. Lanari, A. Marrocchi and G. Strappaveccia, *Green Chem.*, 2014, **16**, 3680-3704.
45. S. L. James, C. J. Adams, C. Bolm, D. Braga, P. Collier, T. Friscic, F. Grepioni, K. D. M. Harris, G. Hyett, W. Jones, A. Krebs, J. Mack, L. Maini, A. G. Orpen, I. P. Parkin, W. C. Shearouse, J. W. Steed and D. C. Waddell, *Chem. Soc. Rev.*, 2012, **41**, 413-447.
46. C. P. Xu, S. De, A. M. Balu, M. Ojeda and R. Luque, *Chem. Commun.*, 2015, **51**, 6698-6713.
47. M. J. Munoz-Batista, D. Rodriguez-Padron, A. R. Puente-Santiago and R. Luque, *ACS Sustainable Chem. Eng.*, 2018, **6**, 9530-9544.

## Results & Discussion

48. J. R. Chelikowsky, N. Troullier, J. L. Martins and H. E. King, *Phys. Rev. B: Condens. Matter Mater. Phys.*, 1991, **44**, 489-497.
49. J. Kaspar, P. Fornasiero and N. Hickey, *Catal. Today*, 2003, **77**, 419-449.
50. D. J. Morgan, *Surf. Interface Anal.*, 2015, **47**, 1072-1079.
51. W. Y. Ouyang, M. J. Munoz-Batista, A. Kubacka, R. Luque and M. Fernandez-Garcia, *Appl. Catal., B*, 2018, **238**, 434-443.
52. C. Bock, C. Paquet, M. Couillard, G. A. Botton and B. R. MacDougall, *J. Am. Chem. Soc.*, 2004, **126**, 8028-8037.
53. E. A. Paoli, F. Masini, R. Frydendal, D. Deiana, C. Schlaup, M. Malizia, T. W. Hansen, S. Horch, I. E. L. Stephens and I. Chorkendorff, *Chem. Sci.*, 2015, **6**, 190-196.
54. B. Ulgut and S. Suzer, *J. Phys. Chem. B*, 2003, **107**, 2939-2943.
55. M. Todea, E. Vanea, S. Bran, P. Berce and S. Simon, *Appl. Surf. Sci.*, 2013, **270**, 777-783.
56. W. Ouyang, A. Yopez, A. A. Romero and R. Luque, *Catal. Today*, 2018, **308**, 32-37.
57. D. Prat, J. Hayler and A. Wells, *Green Chem.*, 2014, **16**, 4546-4551.
58. A. Yopez, J. M. Hidalgo, A. Pineda, R. Cerny, P. Jisa, A. Garcia, A. A. Romero and R. Luque, *Green Chem.*, 2015, **17**, 565-572.
59. S. Ranaa and S. B. Jonnalagadda, *RSC Adv.*, 2017, **7**, 2869-2879.
60. S. Wei, Y. Zhao, G. Fan, L. Yang and F. Li, *Chem. Eng. J.*, 2017, **322**, 234-245.
61. R. A. Sheldon, *Chem. Ind.*, 1992, 903-906.

## Supporting Information

### Efficient Ru-based scrap waste automotive converter catalysts for the continuous-flow selective hydrogenation of cinnamaldehyde

Camilla Maria Cova, Alessio Zuliani, Mario J. Muñoz-Batista and Rafael Luque

Table S.1 ICP-MS analysis of CC0 (scrap catalytic converter, untreated)

Element	%wt
Mg	3.9
Al	36.4
Si	41.1
Fe	4.0
Ce	4.2
Ti	0.8
Zn	0.5
Zr	2.8
Pt	0.4

Fig.S.1 XRD patterns of 10%Ru/SiO<sub>2</sub>, 10%Ru/Al<sub>2</sub>O<sub>3</sub> activated and 10%Ru/Al<sub>2</sub>O<sub>3</sub> catalysts

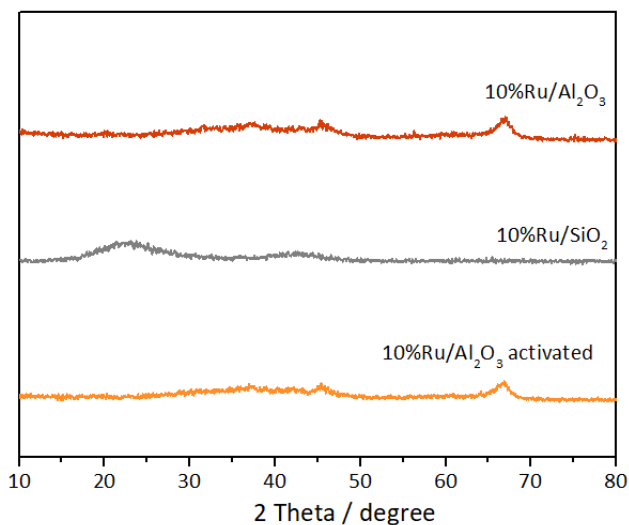
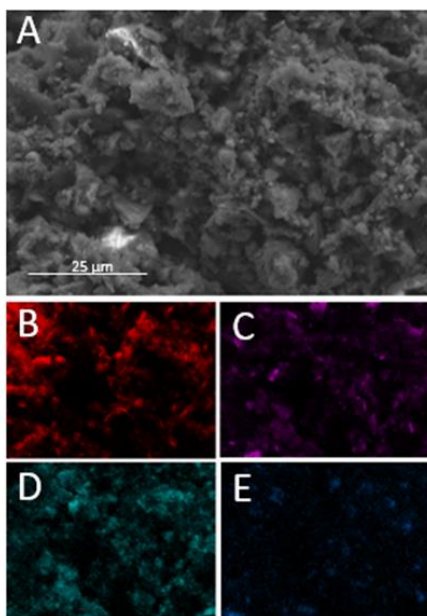
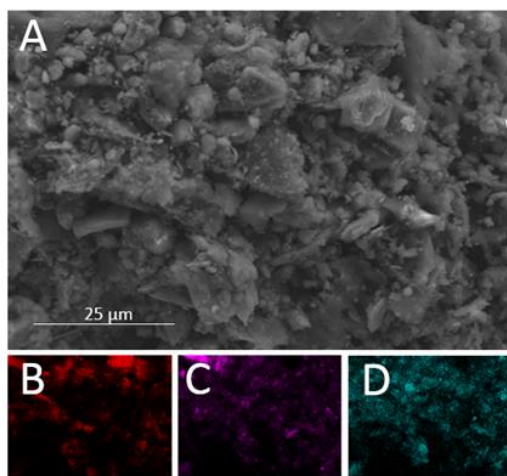


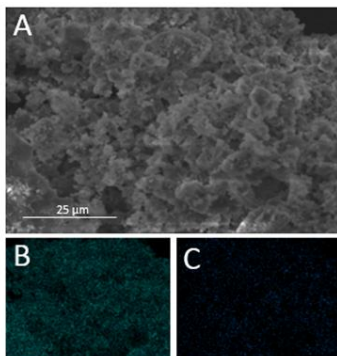
**Fig.S.2 SEM mapping of 5%Ru/CC, 0%Ru/CC, 10%Ru/SiO<sub>2</sub>, 10%Ru/Al<sub>2</sub>O<sub>3</sub> activated and 10%Ru/Al<sub>2</sub>O<sub>3</sub>**



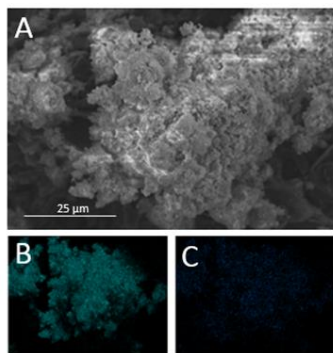
SEM images with mapping analysis of 5%Ru/CC catalyst (a) Distribution of Carbon (b), Silicon (c), Aluminum (d) and Ruthenium (e).



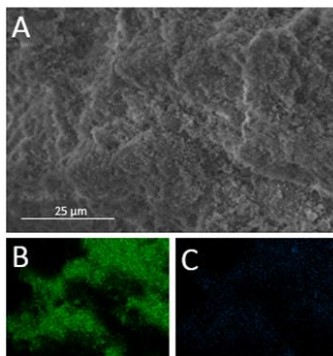
SEM images with mapping analysis of 0%Ru/CC (a) Distribution of Carbon (b), Silicon (c) and Aluminum (d).



SEM images with mapping analysis of 10%Ru/SiO<sub>2</sub> catalyst (a) Distribution Silicon (b) and Ruthenium (c).



SEM images with mapping analysis of 10%Ru/Al<sub>2</sub>O<sub>3</sub> activated catalyst (a) Distribution Aluminum (b) and Ruthenium (c).



SEM images with mapping analysis of 10%Ru/Al<sub>2</sub>O<sub>3</sub> catalyst (a) Distribution Aluminum (b) and Ruthenium (c).

**Fig.S.3 HRTEM images of 10%Ru/CC**

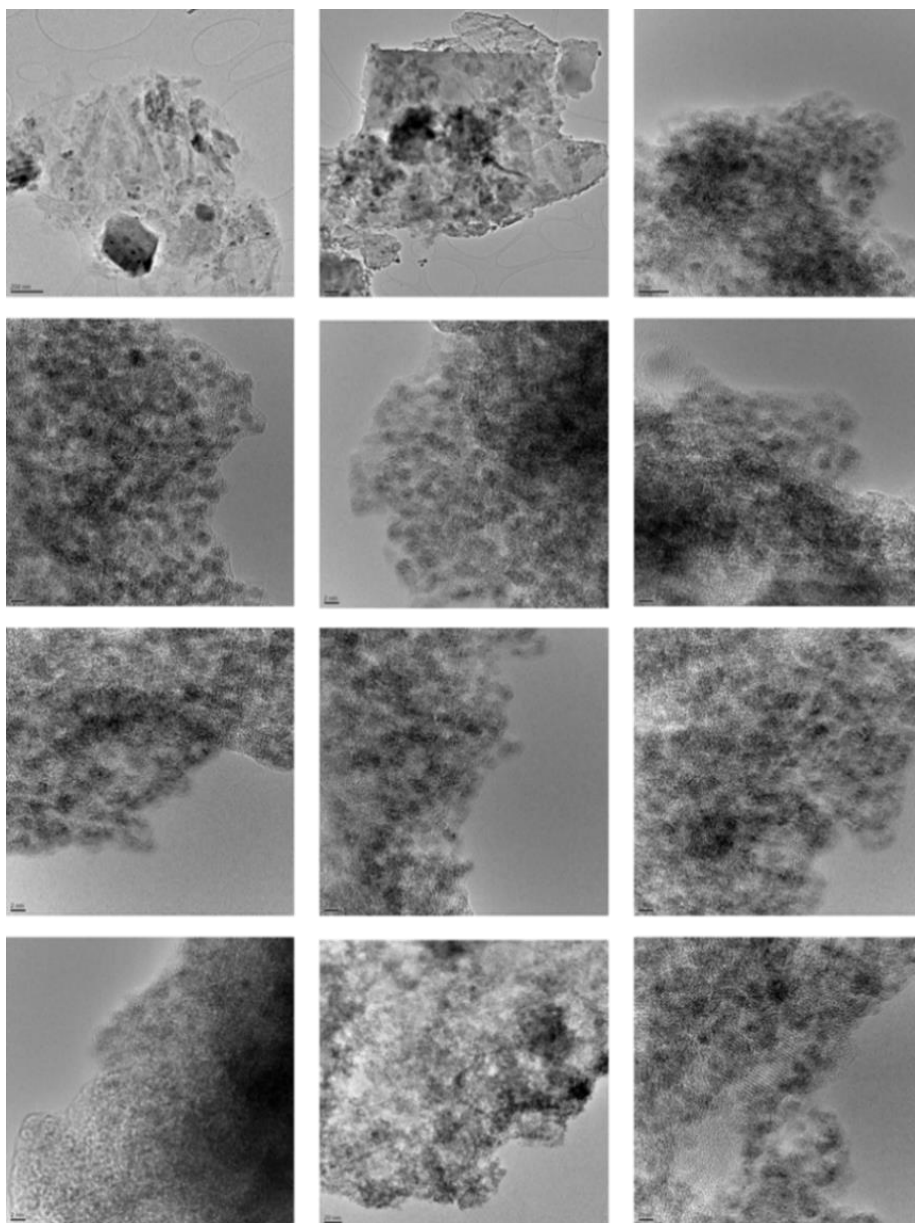


Fig.S.4 N<sub>2</sub> adsorption-desorption isotherm of CC0, 10%Ru/CC (before the chemical reduction) and 10%Ru/CC

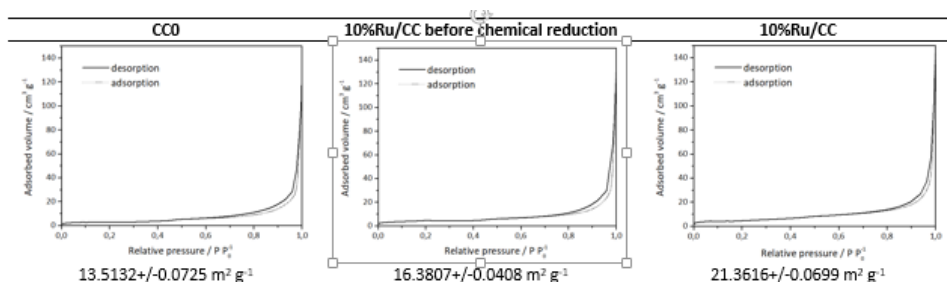
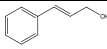
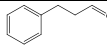
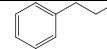


Table S.2 Selectivity and yield data for Ru/CC catalysts

Catalyst	Conversion /%	Selectivity/%				Yield to COL /%
		 COL	 HCAL	 HCOL	Others	
10%Ru/CC	94.4	79.7	-	9.2	11.1	75.2
5%Ru/CC	64.0	85.1	-	5.1	9.8	54.5
2.5%Ru/CC	29.1	82.4	-	7.0	10.6	24.0
1%Ru/CC	16.4	62.5	17.6	4.0	15.9	10.2
0%Ru/CC	4.9	57.3	22.1	5.8	14.8	2.8
CC0	<1%	-	-	-	-	-





# Conclusions



The research carried out in this Doctoral Thesis manuscript can be summarized into the following conclusions:

1. A sequence of Ag/Ag<sub>2</sub>S carbon hybrid composites has been synthesized *via* a microwave-assisted procedure, using different amounts of silver nitrate as metal precursor and by fixing the quantity of pig bristles as carbon and sulfur source. The synthesis has been proposed as a simple and sustainable methodology and allowed the valorization of a waste feedstock for the design of highly active electrocatalysts.
2. The structural and textural properties of the synthesized heterocomposites have been studied and the presence of metallic Ag and Ag<sub>2</sub>S has been confirmed by X-ray diffraction (XRD) technique. From X-ray photoelectron spectroscopy (XPS), Ag(0)/Ag(I) ratio has been found, which is dependent on pig bristles/silver precursor ratio.
3. The electrocatalytic activity of synthesized materials has been proved to be encouraging, especially in the hydrogen evolution reaction (HER), with the most performing catalyst allowed the production of a current density of 10 mA cm<sup>-2</sup> at -0.190 V potential. In addition, the catalytic performances were found linearly dependent on Ag(0)/Ag(I) ratio, which can be easily controlled in the preparation.
4. On the other hand, different zinc sulfides have been synthesized using zinc acetate dihydrate as metal precursor and pig bristles as sulfur source at different synthetic times. The preparation involved a facile refluxing procedure, allowing for a cheap, quick and easy methodology.
5. The presence of zinc sulfide has been proved recording XRD patterns and by XPS analysis. Moreover, other textural and structural properties have been

investigated performing scanning electron microscopy coupled with energy dispersive X-ray analysis (SEM-EDX) and N<sub>2</sub> physisorption.

6. The materials have been tested in the oxidation of toluene and benzyl alcohol to benzaldehyde. The most active sample achieved promising results including conversion of benzyl alcohol up to 63% with 86% selectivity and conversion of toluene up to 29% with 87% selectivity, without appreciable activity losses for up to 4 reuses.

7. The use of the mechanochemical methodology followed by a chemical reduction has allowed the direct preparation of ruthenium-based catalysts supported on ceramic-cores of scrap automotive catalytic converters. In addition, other Ru catalysts have been synthesized using other supports such as SiO<sub>2</sub> and Al<sub>2</sub>O<sub>3</sub> in order to investigate how the support and the interactions between that one and the metal influence the catalytic activity.

8. The physical and chemical properties of the synthesized materials have been studied using different techniques, including X-ray diffraction (XRD), N<sub>2</sub> physisorption, scanning electron microscopy coupled with energy dispersive X-ray analysis (SEM-EDX), X-ray photoelectron spectroscopy (XPS), inductively coupled plasma mass spectrometry (ICP-MS), transmission electron microscopy (TEM) and high-resolution transmission electron microscopy (HRTEM).

9. The catalysts have been tested in the selective hydrogenation of cinnamaldehyde under continuous-flow conditions. Moreover, various parameters have been studied and optimized including temperature, flow rate, pressure and ruthenium content. The catalytic activity of Ru/catalytic converter catalysts has been compared with commercially available hydrogenation catalysts.

10. Within optimized conditions, the best materials allowed 95% conversion with 80% selectivity to cinnamyl alcohol. Finally, the long-term stability of the materials was also investigated, showing no changes in conversion and selectivity performing the reaction for 10 hours TOS.

11. Finally, the *E*-factor of the entire protocol was calculated to be approximately 24.



# Summary





The scientific contributions described in this Doctoral Thesis were explored in the research group FQM-383, which main research topics include Nanochemistry, Heterogeneous Catalysis and Biomass/Waste Valorization (NANOVAL). More in detail, this Doctoral Thesis focused on the development of advanced materials for the catalytic transformation of biomass and waste into high value-added compounds through advanced methodologies. These methodologies were designed based on un-conventional and green procedures combined with technologies that offer environmentally friendly and low energy-impact characteristics. In particular, the potentiality of microwave, mechanochemistry and flow chemical processes were demonstrated in the production and in the application of novel waste/biomass derived materials.

Most important results obtained during the Doctoral Thesis have been published in three research articles, which have been included in Chapter “Results and Discussion” and are summarized below. Moreover, the first section of the Chapter “Introduction” is constituted of a review titled “Advances in mechanochemical processes for biomass valorization”. The manuscript describes the potential of mechanochemistry and its new attractive possibilities in the area of biomass and waste valorization.

In the first work, “Microwave-assisted preparation of Ag/Ag<sub>2</sub>S carbon hybrid structures from pig bristles as efficient HER catalysts”, a sequence of Ag/Ag<sub>2</sub>S heterostructures was successfully synthesized *via* a microwave-assisted procedure. The preparation was conducted employing silver nitrate in different amounts as silver precursor and a fixed quantity of pig bristles as carbon and sulphur source, resulting in a sequence on materials with different Ag(0)/Ag(I) ratios. The microwave method was proved to be simple, quick, and efficient, allowing the exploitation of wasted pig bristles as a toxic-free source of carbon and sulphur in contrast to hazardous and toxic substances (*e.g.*, thiols and H<sub>2</sub>S). The presence of metallic silver and silver sulphide was demonstrated

by recording and analyzing X-ray diffraction (XRD) patterns. From the X-ray photoelectronic spectroscopy (XPS) analysis, an Ag(0)/Ag(I) ratio was also recognized, linearly correlated on pig bristles/silver nitrate ratio. The use of material has been promising in electrocatalytic processes, especially in the hydrogen evolution reaction (HER). The current density values were found linearly correlated to the Ag(0)/Ag(I) ratio, which could be controlled during the synthetic procedure. The most active sample allowed the production of  $10 \text{ mA cm}^{-2}$  of current density at  $-0.190 \text{ V}$  applied potential.

The manuscript “A sustainable approach for the synthesis of catalytically active peroxidase-mimic ZnS catalysts” discloses a simple methodology for the preparation of zinc sulphides using pig bristles, an economic and largely-available waste rich in carbon and sulphur. The catalysts were synthesized employing zinc acetate dihydrate and pig bristles, with different preparation times, i.e. 1 hour, 3 hours, 5 hours. The methodology included an easy, facile and low-cost refluxing procedure (pig bristles and zinc precursor in an aqueous solution of KOH). The so-synthesized materials were characterized using different techniques including X-ray diffraction (XRD),  $\text{N}_2$  adsorption/desorption, scanning electron microscopy coupled with energy dispersive X-ray analysis (SEM-EDX) and X-ray photoelectronic spectroscopy (XPS). The presence of ZnS crystal structure was proved by XRD and by XPS analysis. The nanomaterials were demonstrated to possess high catalytic activity and high chemical stability in the selective microwave-assisted oxidations of toluene and benzyl alcohol to benzaldehyde (widely used compound in fragrances and perfumery industries). Finally, a reusability study was carried out in both reactions, demonstrating the stability of the novel nanosystem under the investigated reaction conditions, showing almost identical catalytic activities after 4 cycles.

The last paper “Efficient Ru-based scrap waste automotive converter catalysts for the continuous-flow selective hydrogenation of cinnamaldehyde” proved the potentiality of an industrial waste, *i.e* the ceramic-cores of scrap automotive catalytic converters (CATs) as low-cost and high stable supporting materials. More in details, CATs were used as supporting material for the preparation of nanoruthenium-based catalysts. The materials were synthesized using a simple mechanochemical approach followed by a chemical reduction. The physico-chemical properties of the materials were studied by X-ray diffraction (XRD), X-ray photoelectronic spectroscopy (XPS), N<sub>2</sub> physisorption, scanning electron microscopy coupled with energy dispersive X-ray analysis (SEM-EDX), inductively coupled plasma mass spectrometry (ICP-MS) and transmission electron microscopy (TEM/HRTEM). The catalysts were tested in the selective flow hydrogenation of cinnamaldehyde to cinnamyl alcohol. Different reaction and synthesis parameters were optimized including H<sub>2</sub> pressure, temperature, flow rate and ruthenium content. The catalytic activity of Ru/CATs was compared with Ru nanocatalysts supported on silica, alumina and activated alumina *via* the same mechanochemical procedure. The results indicated that Ru/CATs displayed outstanding catalytic performances and good stability with time-on-stream, proving also a synergism between ruthenium and the scrap catalytic converter. Finally, the *E*-factor of the entire protocol was calculated to validate the green credentials of the entire methodology.



Los trabajos de investigación que componen la presente Memoria de Tesis Doctoral fueron desarrollados en el Grupo de Investigación FQM-383, cuyos principales temas de investigación incluyen nanoquímica, catálisis heterogénea y valorización de biomasa/residuos (NANOVAL). Más detalladamente, ésta Tesis Doctoral se centró en el desarrollo de nuevos nanomateriales para la transformación catalítica de la biomasa y residuos a compuestos de alto valor añadido mediante técnicas avanzadas. Estas metodologías se diseñaron en base a procedimientos no convencionales y respetuosos con el medio ambiente combinados con tecnologías que ofrecen características ecológicas y de bajo impacto energético. En particular, el potencial que presentan los procesos asistidos mediante microondas, mecanoquímica y química de flujo quedó patente en el desarrollo y en la aplicación de nuevos materiales derivados de biomasa y residuos.

Los principales resultados derivados de los trabajos de investigación llevados a cabo durante la presente Tesis Doctoral han sido incluido en el Capítulo "Results & Discussion" y se resumen a continuación. Además, la primera sección del Capítulo "Introduction" está constituida por una revisión bibliográfica titulada "Advances in mechanochemical processes for biomass valorization". El manuscrito describe el potencial de la mecanoquímica y sus nuevas posibilidades aplicadas en el área de valorización de residuos y biomasa.

En el primer trabajo, "*Microwave-assisted preparation of Ag/Ag<sub>2</sub>S carbon hybrid structures from pig bristles as efficient HER catalysts*", se sintetizó con éxito una serie de heteroestructuras de carbón Ag/Ag<sub>2</sub>S mediante un procedimiento asistido por microondas. Su preparación se realizó empleando nitrato de plata como precursor de plata en distintas cantidades y una cantidad fija de pelos de cerdo como fuente de carbono y azufre, dando como resultado una serie de materiales con diferentes relaciones Ag (0)/Ag (I). De esta forma, la síntesis asistida por microondas se reveló como una metodología simple,

innovadora y eficiente, permitiendo la explotación de desechos de pelos de cerdo como fuente no tóxica de carbono y azufre en lugar de sustancias tóxicas y peligrosas. (por ejemplo, tioles y  $\text{H}_2\text{S}$ ). La presencia de plata metálica y sulfuro de plata se confirmó mediante la técnica de difracción de Rayos-X (DRX). Mediante el análisis de espectroscopía fotoelectrónica de rayos-X (XPS), ha sido posible establecer una relación  $\text{Ag}(0)/\text{Ag}(I)$ , la cuál muestra una dependencia lineal en función de la relación pelos de cerdo/nitrato de plata. La utilización de este material en procesos electrocatalíticos ha sido prometedora, en particular, para la reacción de producción de hidrogeno (HER). Los valores de densidad de corriente se encontraron linealmente correlacionados con la relación  $\text{Ag}(0)/\text{Ag}(I)$ , la cual podría controlarse con esta metodología. La muestra con mejor actividad catalítica ha permitido la producción de  $10 \text{ mA cm}^{-2}$  de densidad de corriente a un potencial aplicado de  $-0,190 \text{ V}$ .

En el trabajo “*A sustainable approach for the synthesis of catalytically active peroxidase-mimic ZnS catalysts*”, se ha presentado una metodología para la preparación de ZnS utilizando pelos de cerdo, un desecho económico y ampliamente disponible que contiene carbono y azufre. En concreto, los nanomateriales han sido sintetizados utilizando acetato de cinc dihidratado y cerdas de cerdo, llevando a cabo la síntesis a diferentes tiempos de reacción (1 hora, 3 horas, 5 horas). La metodología ha incluido un paso de ebullición, resultando en una preparación fácil, económica y rápida (pelos de cerdo y precursor de cinc en una solución acuosa de KOH). Los materiales sintetizados fueron caracterizados mediante diferentes técnicas que incluyeron la difracción de rayos-X (DRX), adsorción-desorción de  $\text{N}_2$ , microscopía electrónica de barrido con detector de energía dispersiva rayos-X para el análisis elemental (SEM-EDX) y espectroscopía fotoelectrónica de rayos-X (XPS). La estructura cristalina de ZnS se confirmó mediante las técnicas de DRX y XPS. Los nanocatalizadores sintetizados mostraron una actividad catalítica elevada, así

como estabilidad química en las reacciones de oxidación selectiva de tolueno y alcohol bencílico a benzaldehído (compuesto ampliamente utilizado en las industrias de fragancias y perfumería). Finalmente, se llevó a cabo el estudio de la reusabilidad de los nanocatalizadores en ambas reacciones demostrando la estabilidad de estos bajo las condiciones de reacción investigadas, así como una casi idéntica actividad catalítica tras cuatro ciclos de reacción.

El último trabajo “*Efficient Ru-based scrap waste automotive converter catalysts for the continuous-flow selective hydrogenation of cinnamaldehyde*” demostró el potencial de un residuo industrial, los núcleos cerámicos usados de los convertidores del coche (CATs) como materiales de soporte de bajo coste y alta estabilidad. Más en detalle, los CAT se usaron como material de soporte para la preparación directa de catalizadores basados en nano-rutenio. Los materiales fueron sintetizados mediante molienda mecanoquímica seguida de una reducción química. Las propiedades fisicoquímicas de los materiales fueron investigadas mediante las técnicas de DRX, fisisorción de N<sub>2</sub>, SEM-EDX, espectrometría de masas con plasma acoplado inductivamente (ICP-MS), microscopía electrónica de transmisión (TEM/HRTEM). Los catalizadores sintetizados fueron probados en la hidrogenación selectiva de cinemaldehído mediante flujo continuo. Se optimizaron distintos parámetros que incluyeron la presión de H<sub>2</sub>, temperatura, flujo y contenido en rutenio. La actividad catalítica de los materiales Ru/CATs fue comparada con otros catalizadores de rutenio soportados en distintos materiales, SiO<sub>2</sub>, Al<sub>2</sub>O<sub>3</sub> y Al<sub>2</sub>O<sub>3</sub> activado, sintetizados mediante la misma metodología mecanoquímica. Los resultados muestran que los catalizadores Ru/CATs poseen excelentes prestaciones catalíticas y buena estabilidad sin mostrar cambios en la conversión y selectividad con el tiempo en el flujo, demostrando una sinergia entre el rutenio y el convertidor catalítico usado de coche. Finalmente, las credenciales verdes de toda la metodología fueron evaluadas calculando el factor E del protocolo.





# Index of quality



Data taken from InCites Journal Citation Reports dataset, updated the 20<sup>th</sup> of June 2019. ©2019 Clarivate.

Journal	Journal of Material Chemistry A		
Publisher	Royal Society of Chemistry		
Title	Microwave-assisted preparation of Ag/Ag <sub>2</sub> S carbon hybrid structures from pig bristles as efficient HER catalysts		
Authors	C.M. Cova, A. Zuliani, A.R. Puente-Santiago, A. Caballero, M.J. Muñoz-Batista, R. Luque		
DOI	10.1039/C8TA06417B		
Citation	<i>J. Mater. Chem. A</i> , 2018, <b>6</b> , 21516-21523		
Journal Impact Factor 2018	10.733		
Thematic Area	Chemistry, Physical	Energy & Fuels	Materials science, Multidisciplinary
Position	14/148 (Q1)	6/103 (Q1)	21/293 (Q1)

Journal	ACS Sustainable Chemistry & Engineering		
Publisher	American Chemical Society		
Title	A sustainable approach for the synthesis of catalytically active peroxidase-mimic ZnS catalyst		
Authors	C.M. Cova, A. Zuliani, M.J. Muñoz-Batista, R. Luque		
DOI	10.1021/acssuschemeng.8b04968		
Citation	<i>ACS Sustain. Chem Eng.</i> , 2019, 7 (1), 1300-1307		
Journal Impact Factor 2018	6.970		
Thematic Area	Chemistry, Multidisciplinary	Engineering, Chemical	Green & Sustainable Science & Technology
Position	26/172 (Q1)	9/138 (Q1)	5/35 (Q1)

Journal	Green Chemistry	
Publisher	Royal Society of Chemistry	
Title	Efficient Ru-based scrap waste automotive converter catalysts for the continuous-flow selective hydrogenation of cinnamaldehyde	
Authors	C.M. Cova, A. Zuliani, M.J. Muñoz-Batista, R. Luque	
DOI	10.1039/C9GC01596E	
Citation	<i>Green Chem.</i> , 2019, <b>21</b> , 4712-4722	
Journal Impact Factor 2018	9.405	
Thematic Area	Chemistry, multidisciplinary	Green & Sustainable Science & Technology
Position	20/172 (Q1)	2/35 (Q1)



# Achievements





## Publications

1. Cova, C. M.; Zuliani, A.; Munoz-Batista, M. J.; Luque, R., A Sustainable Approach for the Synthesis of Catalytically Active Peroxidase-Mimic ZnS Catalysts. *Acs Sustainable Chemistry & Engineering*. **2019**, *7*(1), 1300-1307.
2. Cova, C. M.; Zuliani, A.; Puente-Santiago, A. R.; Caballero, A.; Munoz-Batista, M. J.; Luque, R., Microwave-assisted preparation of Ag/Ag<sub>2</sub>S carbon hybrid structures from pig bristles as efficient HER catalysts. *Journal of Materials Chemistry A*. **2018**, *6* (43), 21516-21523.
3. Cova, C. M.; Zuliani, A.; Muñoz-Batista, M. J.; Luque, R., Efficient scrap waste automotive converter Ru-based catalysts for the continuous-flow selective hydrogenation of cinnamaldehyde. *Green Chemistry*. **2019**, *21*, 4712-4722.
4. Cova, C. M.; Boffa, L., Pistocchi, M., Giorgini, S., Luque, R., Cravotto, G., Technology and Process Design for Phenols Recovery from Industrial Chicory (*Chicorium intybus*) Leftovers. *Molecules*. **2019**, *24*(15), 2681.
5. Cova, C. M.; Luque, R., Advances in mechanochemical processes for biomass valorization. *BMC Chemical Engineering*. **2019**, *1*, 16.

## Congress participation

1. Green Paths for the valorization of *Chicorium intybus* and *Ocimum basilicum*. Microwave/Ultrasound-assisted extraction of polyphenols. Poster: Cova, C. M., Boffa, Gunjević, V., Martina, K., Luque, R., Cravotto, G.; GENP 2018 Green Extraction of Natural Products. Bari (Italy), November 12-13, 2018.
2. A sustainable approach for the synthesis of catalytically active peroxidase-mimic ZnS catalysts. Poster: Cova, C. M., Zuliani, A., Muñoz-Batista, M. J., Balu, A. M., Luque, R.; VI Encuentro de nanociencia y nanotecnología de jóvenes investigadores (Nanouco VI). Córdoba (Spain), January 21-22, 2019.
3. Preparación asistida por microondas de estructuras híbridas de carbono Ag/Ag<sub>2</sub>S a partir de cerdas de cerdo como catalizadores eficientes en HER. Oral presentation: Cova, C. M., Zuliani, A., Muñoz-Batista, M. J., Balu, A. M., Luque, R.; VII congreso jóvenes investigadores. Córdoba (Spain), January 6-7, 2019.
4. Sustainable approaches for the synthesis of metal sulphides catalysts derived from wasted pig bristles. Poster: Zuliani, A., Cova, C. M., Muñoz-Batista, M. J., Balu, A. M., Luque, R.; 23<sup>rd</sup> Annual Green Chemistry & Engineering Conference and 9th International Conference on Green and Sustainable Chemistry, Washington (USA), June 11-13, 2019
5. Preparación asistida por microondas de estructuras híbridas de carbono Ag/Ag<sub>2</sub>S derivadas de cerdas de cerdo como catalizadores para producción de hidrogeno. Poster: Cova, C. M., Zuliani, A., Puente Santiago, A. R., Caballero, A., Muñoz-Batista, M. J., Luque, R.; SECAT Conference, Córdoba (Spain), June 24-26, 2019.
6. Approaches for the microwave-assisted synthesis of metal sulphides catalysts derived from wasted pig bristles. Poster: Zuliani, A., Cova, C. M., Muñoz-Batista, M. J., Balu, A. M., Luque, R.; Unconventional Catalysis, Reactors and Applications UCRA 2019, Zaragoza (Spain), October 16-18, 2019.

## **Collaboration & Secondments**

1. Technology-based company, PROVALUTA ESPAÑA RECICLAJE DE METALES SL, Córdoba (ES), 8<sup>th</sup> of January 2018 – 6<sup>th</sup> of July 2018: “Quantitative recovery of Pt, Pd and Rh presented in catalytic converter”.
2. University of Turin, Turin (IT), 1<sup>st</sup> of September 2018 – 3<sup>rd</sup> of December 2018: “Integration of microwaves with ultrasound for the synthesis of new nanomaterials”.  
Supervisor: G. Cravotto



# Acknowledgments



Time really flies, and I'm now at the end of my PhD thesis. First, I would like to thank my Supervisor Prof. Rafa. I would like to express my sincere gratitude for giving me the opportunity to join your research group. I wasn't expecting that! Thanks for helping and encouraging me throughout the research with great patience. Your motivation, great knowledge and dynamism have deeply inspired me. Thank you for the possibility to collaborate with a company and to accomplish a secondment in Turin. Thanks above all for the encouragement and for your support beside scientific investigation.

Thanks to my other supervisor Antonio Pineda for helping me in the laboratory research!

I am also happy to say thank you to all the people from Nanoval group, especially Prof. Antonio and Prof. Alina. Thank you for your patience, for helping me in the laboratory and for all the bureaucracy issues and documents. Thanks to the post-docs that I met during this Project: Alain, Alfonso, Maria and Pepijn. A special thanks to Mario: thank you a lot for your support, encouragements and collaboration during these years. Also, I would like to thank Araceli: for her empathy and especially for bringing my morale up a lot of times. Thanks to all the students from Nanoval that I met in the laboratory: Ana, Daily, Kenneth, Laura, Matilde, Noelia, Paloma, Paulette, Sole, Weiyi. Besides all these students I'd like to especially thank Loles and Layla: thank you for all the coffees, breakfasts and chatters. You are more than simple colleagues: thank you because you have kept me company during these years beside work. A very special thanks to Esther: I can say that I met a real friend. Thank you for your sincere friendship, for all the time spent together and for introducing me to your special family and friends. I'm sure that our friendship will last for all my life whatever road we will take. Thanks a lot also to the visiting students, post-docs and professors, Adriano, Ana Luisa, Bruna, Clemente, Gabriel, Nicola, Prabhat, Roberto, Sandra, Sareena, Valeria, Vidmantas. Above all, I'd



## Acknowledgments

like to thank Roberta, you are an amazing person. Thank you for the great time spent in Cordoba and in Zaragoza. Thanks a lot also to the laboratory technician, Pablo and Maria. I would like to thank also all the people from the SCAI, especially Isabel.

I'd like to deeply and especially thank my Supervisors during the Secondments in Turin. Thank you, Prof. Giancarlo and Prof. Katia. It was a great opportunity to work in your laboratory. I've learned a lot! You are great professors and persons. Thank you for welcoming me in a special moment of my life. And thanks a lot to all the people from the research group of Turin, especially to Andrea, Federica, Maria Jesus, Janet, Riccardo, Pietro, Veronica and Veronika. Among all, a special thanks to Luisa. Thank you for your support and all the help during the Secondments and after. It has been a pleasure to meet you.

I'd like also to thank Cordoba, wonderful city. Thanks to all the special friends that I met her. Thank you Victoria and "second mum" Rocío. You have welcomed and made to feel at home.

Thanks to my family and to my friends from Italy, you have been always with me despite the distance.

Lastly, thank you Alessio. Thanks for your infinite patience and care. Thank you to have shared such an adventure that is life! Thank you for being strong and certain through the challenges of life. Thank you for our angel and Gioele!





# Materials & Methods



The following Annex of the Doctoral Thesis aims to present and briefly explain the different techniques that have been used in the synthesis of the materials and in the determination of their physical-chemical properties. In the same way, the different experimental equipment and conditions used with their respective mathematical models are described.

The synthesized catalysts have been characterized using several instrumental techniques including adsorption/desorption of N<sub>2</sub>, powder X-ray diffraction (XRD), X-ray photoelectronic spectroscopy (XPS), scanning electron microscopy (SEM), transmission electron microscopy (TEM) and inductively coupled mass spectroscopy (ICP-MS).

Similarly, the catalytic activity of the materials was investigated for different chemical reactions using linear sweep voltammetries (LSV), microwave irradiation and continuous-flow processes. The reaction products have been analyzed by gas chromatography (GC) and/or gas chromatography coupled with mass spectrometry (GC-MS).

## Materials

### Pig bristles

Boiled and sterilized pig bristles were supplied by Pennellificio OMEGA S.p.A, Bologna (IT), and were used without any further processing and purification.

The industrial waste (cut in pieces of *ca.* 0.5 cm) was employed for the preparation of Ag/Ag<sub>2</sub>S and ZnS materials.

### Ceramic-core of scrap catalytic converter

The smashed ceramic-cores of scrap catalytic converters (CATs) were supplied by Provaluta España Reciclaje de Metales, S.L., Córdoba (ES).

The industrial wastes were used as supporting materials for the synthesis of ruthenium-based catalysts.

Prior to the utilization CATs were washed and dried. Specifically, 50 g of CATs were dispersed in 100 mL of distilled water and put in an ultrasonic bath for 2 h. Then, the powders were filtered and oven-dried at 100 °C.

## Methods

### Synthetic procedures

The different experimental techniques used to carry out the synthesis of the waste-based materials are: (i) microwave-assisted, (ii) conventional refluxing, and (iii) mechanochemical-assisted procedures.

#### Microwave synthesis

Microwave theory is described in the section ““Ride the wave!”: Microwave radiation” in the Chapter “Introduction”.

With regards to this Doctoral Thesis, the microwave-assisted synthesis of Ag/Ag<sub>2</sub>S hybrid composites was conducted into a multimode Milestone Ethos D microwave reactor (Milestone Srl, Italy). Specifically, silver nitrate was dissolved in 20 mL of ethylene glycol in a 50 mL Teflon microwave tube under vigorous stirring. Sequentially, pig bristles were added to the mixture. The mixture was kept at room temperature under magnetic stirring (700 rpm) for 10 min. Successively, the Teflon tube was closed and inserted into the microwave reactor. The tube was irradiated with microwaves at 500 W for 4 min.

#### Synthesis under conventional refluxing system

A simple conventional refluxing procedure was carried out for the synthesis of ZnS catalysts. Zinc acetate dihydrate was dissolved in a 1.0 M KOH solution in a 250 mL round flask equipped with a stirring bar and a reflux condenser. Sequentially, pig bristles were added. The mixture was kept at room temperature under vigorous magnetic stirring (800 rpm) for 10 min and was successively refluxing in an oil bath. After reaction completion, the solution was naturally cooled down to r.t. and the light-brown precipitate was filtrated



and washed with ethanol and acetone. Finally, the material was oven-dried at 100 °C for 24 h.

### **Mechanochemical-assisted synthesis**

Mechanochemical theory is described in the section ““Balling the jack!”: Mechanochemistry” in the Chapter “Introduction”.

A mechanochemical procedure followed by a chemical reduction was used for the synthesis of Ru-based catalysts supported on ceramic cores of scrap catalytic converters (CATs). CATs powders and the ruthenium salt were mixed in a 125 mL stainless steel milling jar equipped with eighteen 5 mm diameter stainless steel balls. The powders were ground in a Retsch PM-100 planetary ball mill at 350 rpm for 15 min, changing the direction of rotation every 2 min 30 s. Upon milling, the powders were reduced using NaBH<sub>4</sub> and ethanol and successively filtered and washed with ethanol and water. Finally, the resulting powders were oven-dried at 100 °C for 24 h. The same mechanochemical-assisted procedure was conducted for the synthesis of Ru-based catalysts supported on silica, alumina and activated alumina.

## Characterization techniques

### Determination of the surface area: BET

Surface area and porosity are important parameters for the study of porous materials. The most widely used techniques to calculate surface areas are based on physical adsorption of gas molecules on a solid surface. The BET (Brunauer-Emmet-Teller) technique is based on the adsorption of a gas (*e.g.*, nitrogen) at its condensation temperature, on the surface of the examined solid, in order to determine the specific surface area. Generally, gas adsorption on solid surfaces is a complex phenomenon involving mass and energy interaction.

Depending on the strength of the interaction, all adsorption processes can be subdivided into chemical or physical adsorption. The former one, also called chemisorption or irreversible, is characterized by large interaction potentials, which lead to chemical bonds with high enthalpy. Physical adsorption exhibits characteristics that make it most suitable for surface area determination. Indeed, physical adsorption is characterized by low enthalpy of adsorption with no disruptive structural changes occurring during measurements. Unlike chemisorption, physisorption may lead to surface coverage by more than one layer of adsorbate. Thus, pores can be filled by adsorbate for pore volume measurements. Physical adsorption equilibrium is rapidly reached since no activation energy is required as in chemisorption. Finally, physical adsorption is fully reversible, enabling both adsorption and desorption processes to be studied.

Brunauer, Emmett and Teller theorized a model that explains how that quantity of adsorbed gas depends on Van der Waals gas-solid interactions through the gas partial pressure. Using the BET technique, the molar quantity of a gas taken up, or released, at a constant temperature  $T$ , as a function of gas pressure  $p$ , is measured. Most frequently the measure is conducted at a

cryogenic temperature, usually that of liquid nitrogen at its boiling point (77.35 K at 1 atm pressure). The quantity of adsorbed gas is expressed as its volume at  $T$  and  $p$  standard conditions (0 °C and 760 torr and denoted by STP), while the pressure is expressed as a relative pressure, which is the actual pressure  $p$  divided by the vapor pressure  $p_o$  of the adsorbing gas.

The interpretation of  $N_2$  adsorption/desorption isotherms allows to characterize the porous properties of studied solids. According to the IUPAC classification based on the pore dimension, there are three different types of porous materials: microporous materials (pore diameter <2 nm), mesoporous materials (2 nm < pore diameter <50 nm) and macroporous materials (pore diameter >50 nm).

The first step in the interpretation of an adsorption isotherm is the identification of the type of the isotherm. The six types of isotherms (Fig. 1) are characteristics of adsorbents that are microporous (type I), non-porous or macroporous (type II, III and IV), or mesoporous (type IV and V). The adsorption hysteresis in type V and VI are classified and it is widely accepted that there is a correlation between the shape of the hysteresis loop and the texture of a mesoporous material [1,2].

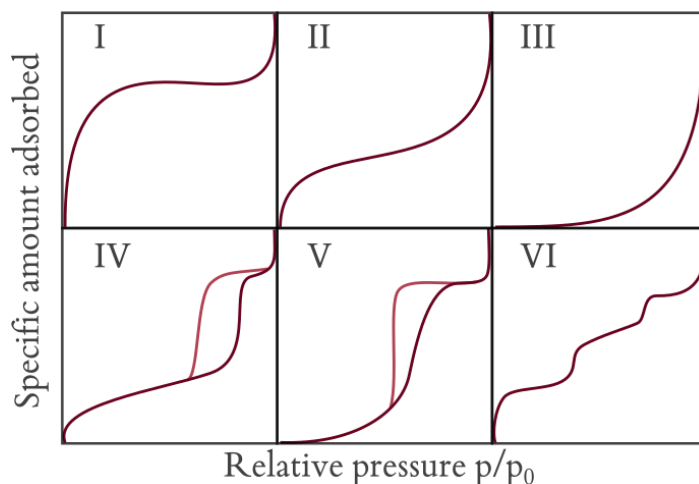


**Fig.1** Different types of isotherms according to IUPAC [1,2].

Concerning the hysteresis loop, usually associated to capillary condensation, it can exhibit a variety of possible shapes [1,2], as shown in the Figure 2:

- *H1 loop*, with the adsorption and desorption branches almost vertical and parallel one to each other, associated to porous agglomerates with narrow distribution of pore size.
- *H2 loop*. It is often attributed to differences in the adsorption and desorption mechanism happening in the presence of pores with a particular shape. They show narrow necks and wide bodies, and hence they are called “ink-bottle pores” or “bottle-neck pores”.
- *H3 loop*, without any limiting adsorption at high values of  $p/p^0$ . It is associated to aggregates of plate-like particles, forming slit-shaped pores.
- *H4 loop*, often attributed to slit-like pores, but the “type I” isotherm indicates the presence of microporosity.

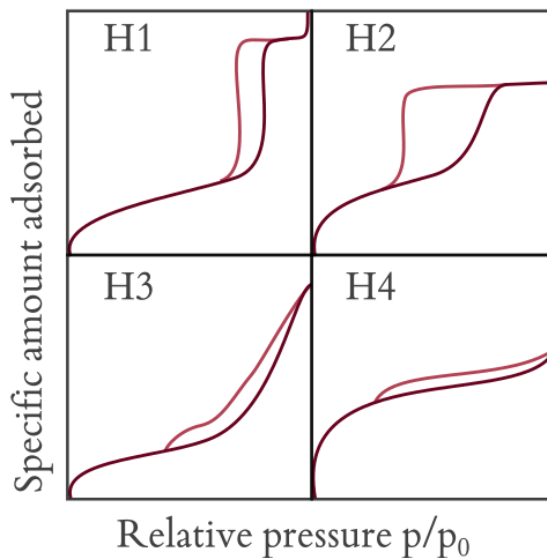


**Fig.2** Shapes of hysteresis loop [1,2].

For the application of Brunauer, Emmett and Teller model, some hypotheses are necessary:

- Adsorption is localized
- Surface sites are energetically equivalent
- There are no lateral interactions between successively adsorbed gas molecules
- There are no interactions between adsorbed layers
- There are no limits to the number of adsorbed layers
- The nature of adsorbed molecules from the second layers onward is liquid

Under those conditions Brunauer, Emmett, Teller established the relation between the quantity of gas adsorbed at the partial pressure  $p$  measured and  $p$ . This relation contains information about the volume occupied from a monolayer of the gas adsorbed, as it is reported in the following:

$$\frac{V}{V_m} = \frac{C \frac{p}{p^o}}{\left(1 - \frac{p}{p^o}\right) \cdot \left[1 + (C - 1) \frac{p}{p^o}\right]}$$

where  $V$  is the gas volume at pressure  $p$ ,  $V_m$  is the gas volume corresponding to the monolayer formation,  $p^o$  is the gas saturation pressure and  $C$  is a gas-surface interaction constant.

The value of parameter  $C$  is given by the following:

$$C \propto e^{\left(\frac{q_1 - q_L}{RT}\right)}$$

where  $q_1$  is equal to the heat of the first layer and  $q_L$  is the heat of liquefaction of the adsorptive.

Linearizing the previous equation, the following is obtained:

$$\frac{p}{V(p-p^{\circ})} = \frac{1}{V_m C} + \frac{(C-1)p}{V_m C p^{\circ}}$$

By plotting  $\frac{p}{V(p-p^{\circ})}$  vs  $\frac{p}{p^{\circ}}$ , a straight line is obtained, from which it is possible to obtain  $C$  and  $V_m$  respectively from the angular coefficient of the straight line is *ca.* 1.  $V_m$  is the parameter used to determine the specific surface area, it is significant only if the adsorbed gas forms a monolayer.

$C$  gives information about the gas behavior. There are two cases:

- if  $C \gg 1$ , the gas-solid affinity is greater than the gas-gas one and  $V_m$  has physical meaning.
- if  $C \ll 1$ ,  $V_m$  has no physical meaning.

BET equation represents well experimental results when  $p/(p^{\circ})$  is comprised between 0.05 and 0.35; for lower relative pressures, BET underestimates the adsorption. Knowing  $V_m$ , it is possible to estimate the value of the surface area of one sample, using the expression reported in the equation below:

$$S = \frac{V_m N_{Av} A}{22.414} \cdot 10^{-19}$$

$A = 16.2 \text{ \AA}^2$  (surface area occupied by a  $N_2$  molecule), dividing  $A$  for the mass of the substance (reported in grams), the specific surface area value is obtained.

This method has some drawbacks: the area of the adsorbed molecule is not experimentally controlled. Because the specific surface area is calculated on a dry powder, there can be morphological variations of the structure, that could modify the result.

In the current Doctoral Thesis, superficial areas (BET) and pore volumes have been obtained from  $N_2$  adsorption/desorption isotherms. The  $N_2$  physisorption were conducted at  $-196^{\circ}\text{C}$ , the  $T$  of liquid nitrogen, using an automotive analyzer, Micromeritics ASAP 2000. The sample weight used for the  $N_2$  physisorption analysis was around 0.20 g. In order to exclude the

presence of other chemical species in the examined sample, as water, a pre-treatment of the sample (100 °C, 24 h) under vacuum ( $p < 10^{-2}$  Pa) was done. The linear part of the BET equation (relative pressure between 0.05 and 0.30) were used to determine the specific surface area. The distribution of pore volume was calculated using the part relative to the adsorption of the N<sub>2</sub> adsorption/desorption isotherm, according to Barret, Joyner and Halenda' method (BJH) [3].

### **X-Ray diffraction (XRD)**

X-Ray powder diffraction allows the direct investigation on finely divided samples. The XRD method is based on the principle that XRD patterns are unique for each crystalline structure, being like a fingerprint of the analyzed material [4-6]. When an X-Ray beam interacts with the powder, it is diffused by the atoms constituting the material producing constructive or destructive interferences as function of the interatomic vectors.

X-Ray powder diffractometer consists of these basic instrumental components:

- A source, usually an X-Ray tube. The tube is evacuated and contains a copper block with a metal target anode (like copper, tungsten or chromium), and a tungsten filament cathode with a high voltage between them. The filament is heated by a separate circuit, and the large potential difference between the cathode and anode fires electrons at the metal target. The accelerated electrons knock core electrons out of the metal, and electrons in the outer orbitals drop down to fill the vacancies, emitting fluorescence X-rays. The X-rays exit the tube through a beryllium window.
- Filters or monochromators to select the specific wavelengths of the source.

- A sample holder, in which the sample is charged. It is mounted over a support which allows the rotation to increase the random orientation of the crystals.
- An X-ray detector that converts the radiant energy into an electric signal. There are three types of transducers: based on a gas, on a scintillation and on a semiconductor. As the elaboration of the signal is based on the count of the photons, the transducer must be characterized by short times of answer and of elaboration of the signal.

By finely grinding the sample, it is possible in many cases to obtain a random orientation of the crystals in each spatial direction; when the X-Ray beam passes through the material, a considerable number of particles is oriented to satisfy the Bragg's law, as represented in Figure 2:

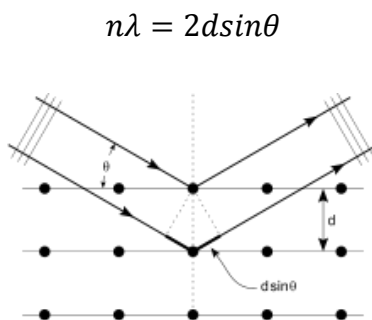


**Fig. 3** Representation of the Bragg's law.

$n$  is an inter natural number,  $\lambda$  is the wavelength of the incident radiation (nm),  $d$  is the distance between crystalline planes ( $\text{\AA}$ ) and  $\theta$  is the incident angle of the incident radiation. If the incident angles do not satisfy Bragg's equation the resultant interference will be destructive.

The X-Ray diffraction patterns report the relative intensity with respect to the diffraction angle,  $2\theta$  between the incident and the diffracted photon beam. Starting from  $2\theta$  position of the Bragg's peaks the Bragg's equation

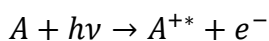


supplies the interplanar distance  $d$  and, therefore, the metric of the crystalline cell.

X-ray diffraction patterns were collected using a Bruker D8 DISCOVER A25 diffractometer (PanAnalytic/Philips, Lelweg, Almelo, The Netherlands) with  $\text{CuK}\alpha$  ( $\lambda = 1.518 \text{ \AA}$ ). Wide angle scanning patterns were recorded for all the samples over a range from  $10^\circ$  to  $80^\circ$  with a step size of  $0.018^\circ$  and counting time of 5 s per step.

### **X-ray photoelectron spectroscopy (XPS)**

The chemical composition of a solid surface is often very different from the bulk composition. Since the application of the synthesized materials is part of the heterogeneous catalysis, it is crucial to know the chemical nature of the species on the surface. X-Ray photoelectron spectroscopy (XPS) is a surface analysis technique that provides information not only about the atomic composition of a sample, but also about the oxidation state of elements detected near the surface, therefore within a thickness between a few angstroms and a few nanometers [7]. The analysis provides that the solid sample is irradiated with a primary monochromatic beam, constituted by photons  $X$  with known energy  $h\nu$ ; the impact of the beam on the surface of the material causes the expulsion of one electron from the orbital  $K$  with energy  $E_b$ , according to this relation:



$A$  can be an atom, a molecule or an ion; while  $A^{+*}$  represents the electronically excited ion that has a positive charge which is bigger than one unit with respect to the charge of  $A$ . The kinetic energy of the emitted electron,  $E_k$ , is studied with the electronic spectrometer. The binding energy of electron,  $E_b$ , can be studied using the following equation:

$$E_b = h\nu - E_k - w$$

$w$  is the work function of the spectrometer, a correction factor which is determinate with specific methods.

The electronic spectrometer consists of these structural components:

- A source that includes an X-Ray tube with a magnesium or aluminium target, and the filters.
- A sample holder, mounted in a fix position, the nearest with respect to the source of photons. In order to avoid the attenuation of the electronic beam, the sample holder must be evacuated at high pressure, almost at  $10^{-5}$  torr.
- An analyser that disperses the emitted electrons according to their kinetic energies.
- A transducer, based on solid-state electronic multiplier, consisting of lead or samarium doped glass tubes. By applying to these materials, a potential difference of some kilovolt, for each incident electron a waterfall of  $10^6$ - $10^8$  electrons is produced.

As the binding energies of the electrons belonging to the same orbitals enhance as the atomic number increased due to the increase of the positive charge of the nucleus, from the spectrum, that includes kinetic energies between 250 and 1500 eV, it is possible to obtain a quantitative analysis, assigning the recorded peaks to the elements of the periodic table. More than one peak can be found for every element as, according to the energy of the primary beam, it is allowed the multiply expulsion of electrons belonging to different orbitals. In most cases, peaks are well defined, and a certain identification is permitted provided that the element is present at a higher concentration of the detection limit. The position of the maximum of the peaks depends also from the surrounding chemical of the considered element since the variation of the number of valence electrons and of the types of binds influences

the binding energies. This implies that it is possible to obtain also information about the number of valence electrons, therefore about the oxidation state of the elements, from the XPS spectrum. If the solid sample is homogenous on the surface it is possible to obtain  $I$ , the number of detected photons (calculated from peak area or peak height), using the following equation:

$$I = n\Phi\sigma\varepsilon\eta ATl$$

$n$  is the numeric density of the atoms of the sample (atom  $\text{cm}^{-3}$ ),  $\Phi$  is the flux of incident X-Ray beam (photons  $\text{cm}^{-2} \text{s}^{-1}$ ),  $\varepsilon$  is the angular efficiency factor,  $\eta$  is the efficiency production of photons (photoelectrons photons $^{-1}$ ),  $A$  is the sample area in which the photons are detected ( $\text{cm}^2$ ),  $T$  is the detection efficiency of the photoelectrons and  $l$  is the free average path of the photoelectrons of the sample (cm). For a given transition, the last six terms of the equation can be assumed constant and their product is called atomic sensitivity factors  $S$ . As the atomic numeric density is directly proportional to the ratio  $I/S$ , calculating the peak area or the peak height, after an appropriate standardization method, it is also possible to obtain a quantitative analysis. However, this analysis provides reliable results only if the element is present at a concentration above 5% [2].

Measurements were performed at the Central Service of Research Support (SCAI) of the University of Cordoba, using an ultrahigh vacuum (UHV) multipurpose surface analysis system (Specs<sup>TM</sup>). The experiments were carried out at pressures  $<10^{-10}$  mbar, using a conventional X-Ray source (XR-50, Specs, Mg-K $\alpha$ ,  $h\nu = 1253.6$  eV,  $1 \text{ eV} = 1.603 \times 10^{-19}$  J) in a “stop and go” mode. The samples were evacuated overnight under vacuum ( $10^{-6}$  mbar). Spectra were collected at room temperature (pass energy: 25 and 10 eV, step size: 1 and 0.1 eV) with a Phoibos 150-MCD energy detector. The deconvolutions of the obtained curves and elemental quantification were carried out using the XPS CASA program.

### **Scanning electron microscopy with energy dispersive X-ray analysis (SEM-EDX)**

When an electronic beam impacts the surface of a solid, several phenomena take place: remission of part of the incident radiation, light emission, electrons Secondary, Auger electrons, X-rays, etc. All these signals can be used to obtain information about the nature of the sample (morphology, composition, etc.) and current equipment has detectors which allow the analysis of most of these signals [8].

In our investigations, we have used two of these phenomena that take place in the sample under the impact of electrons: A source that includes an X-Ray tube with a magnesium or aluminium target, and the filters.

- The most important phenomenon in SEM is the emission of secondary electrons with energies of a few tens of eV, followed by the emission of electrons backscattered with greater energy. There are suitable detectors that they discriminate electrons according to their energy, thus allowing form images with both types that represent the characteristics of the Sample surface.
- Another important issue that takes place when the electron beam interacts inelastically with the sample, both in SEM and TEM, is that of X-ray photons with energy and length of characteristic wave of the elements that form the sample, allowing Identify and establish the concentration of the elements present.

SEM images were recorded with a JEOL JSM-6300 scanning microscope (JEOL Ltd, Peabody, MA, USA) equipped with energy-dispersive X-Ray spectroscopy (EDX) at the Research Support Service Center (SCAI) from the University of Cordoba.

**Transmission electron microscopy and high-resolution transmission electron microscopy (TEM/HRTEM)**

Transmission electron microscopy is a microscopy technique in which a beam of electrons is transmitted through a specimen to form an image [7]. TEM gives information about the structure of the analyzed sample. The limit resolution of an optical system can be mathematically described by Abbe's equation:

$$d = \frac{A \cdot \lambda}{2n \cdot \sin\theta}$$

where  $d$  is the resolution,  $n$  the index of refraction,  $\theta$  the maximum half-angle of the cone of light that can enter the lens,  $\lambda$  the wavelength and  $A$  a constant. The electronic beam is produced by a heated tungsten filament, which is situated at the top of the vacuum column. This beam is accelerated towards the sample by a high potential. The thickness of the sample must be sufficiently high to allow that light can pass through it; during this crossing, many electrons are absorbed, and others are diverted. After that the beam has crossed the sample, it is focused on a lens and then enlarged and projected onto a fluorescent screen. The screen areas that appear dark are due to an unreasonable deviation of the electrons by the dislocations of the crystalline structure of the sample. Near to the sample there is a thin copper rod at low temperatures (thanks to a liquid nitrogen reserve), which attracts impurities and has a non-contaminating effect. The sample support, made up of a copper grid, is coated with a polymeric film, typically Formvar®.

Transmission Electronic microscopy (TEM) images were recorded in a Jeol 1200 equipped with energy-dispersive X-ray spectroscopy (EDX) at the Research Support Service Center (SCAI) of the University of Cordoba. Prior to the analysis, samples were prepared by suspension in ethanol, assisted by sonication and followed by a deposition on a copper grid.

High-resolution transmission electron microscopy (HRTEM) is a technique that allows to obtain the image of the crystalline structure of a sample on an atomic scale. Due to its high resolution, it is a very useful tool for the study of the nanoscale properties of crystalline materials.

HRTEM images were obtained in a FEI TITAN<sup>3</sup> (CEOS Company) equipped with a SuperTwin<sup>®</sup> objective lens and a CETCOR Cs-objective corrector (CEOS Company) at the Laboratorio de Microscopias Avanzadas of the Instituto de Aragon at the University of Zaragoza (Spain).

### **Inductively coupled plasma-mass spectrometry (ICP-MS)**

The mass spectrometry technique with inductive coupling plasma (ICP-MS), is a variant of mass spectrometry analysis techniques. This technique of inorganic elemental and isotopic analysis has established as one of the most important techniques in the last two decades for different applications in areas such as: chemistry, biology, materials physics, environment and geochemistry [8–10]. This is mainly due to its ability to discriminate isotopes and their low detection limits, which can be less than  $10^{-6}$  mg L<sup>-1</sup>. This technique can determine and quantify most of the elements of the periodic table (except for H, C, N, O, F and gases noble) in a linear dynamic range of 8 orders of magnitude (ppt or ppm). In addition, this analysis is characterized by a high degree of selectivity, good precision, and accuracy. Sample preparation operations depend on the nature of the sample, if it solid or liquid. For most solid samples a dissolution, is carried out, and this procedure is one of the most common operations in laboratories of analytic chemistry. Strongly combined strong mineral acids are used in order to obtain an appropriate digestion of the sample.

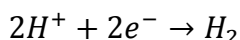
For the quantitative analysis of metals in the different synthesized catalysts an ICP-MS Elan DRC-e (PerkinElmer SCIEX) has been used.

## Catalytic activity

The catalytic activity of the synthesized catalysts was tested using: (i) linear sweep-voltammetry, (ii) microwave-assisted catalytic experiments, and (iii) continuous-flow processes.

### Linear sweep voltammetry

Ag/Ag<sub>2</sub>S catalysts were tested in the reaction of the evolution of the hydrogen performing linear sweep voltammetry (LSV). The hydrogen evolution reaction (HER) is the cathodic reaction in the electrochemical water splitting [11,12]:



The HER is a two electron-transfer reaction with one catalytic intermediate, and offers the possibility to generate H<sub>2</sub>, an interesting chemical reagent and fuel.

The development of new catalysts requires the study of their electrocatalytic activity in conditions comparable to a fuel cell. The most direct approach would be to assemble the membrane electrode and measure its activity in a single cell. However, it is very difficult to determine catalyst activity with this method, because of many uncertainties relative to the mass transport, to the incomplete use of the surface of the material and to the solvent effects.

Linear sweep voltammetry (LSV) is a voltammetric method in which the current at a working electrode is measured while the potential between the working electrode and a reference electrode is swept linearly in time [13,14]. LSV allows the study of the electrochemical behavior of the material deposited on the working electrode surface and it requires the presence of the following electrodes:

- Working electrode (WE): on its surface the material under study is deposited.

- Reference electrode (RE): this electrode must have a constant potential. The potential of WE is measured against the potential of this electrode.
- Counter electrode (CE): it closes the electric circuit on WE. The electrode is necessary to measure the current that circulates between WE and CE, at one specific potential.

All these electrodes are connected to a potentiostat that controls the potential value.

Prior to performing the electrocatalytic experiments, 10 x 10 mm indium tin oxide (ITO) glass was washed following a standard procedure. Firstly, the glass was washed with distilled water and soap. Sequentially, the electrodes were washed in an US bath with deionized water, ethanol and acetone. Ag/Ag<sub>2</sub>S/ITO electrodes were prepared by dispersing 1 mg of catalyst into 1 mL of ethanol and by drop casting the mixture over the ITO surfaces.

LSV measurements were performed in a three-electrode electrochemical cell Potentiostat/Galvanostat Autolab (Solartron1286). 50 mL of a 0.5 M H<sub>2</sub>SO<sub>4</sub> aqueous solution was used as the electrolyte. Ag/AgCl was used as the reference electrode; a Pt substrate was used as the counter electrode and the ag/Ag<sub>2</sub>S/ITO electrodes as the working electrodes, as showed in Figure 3.

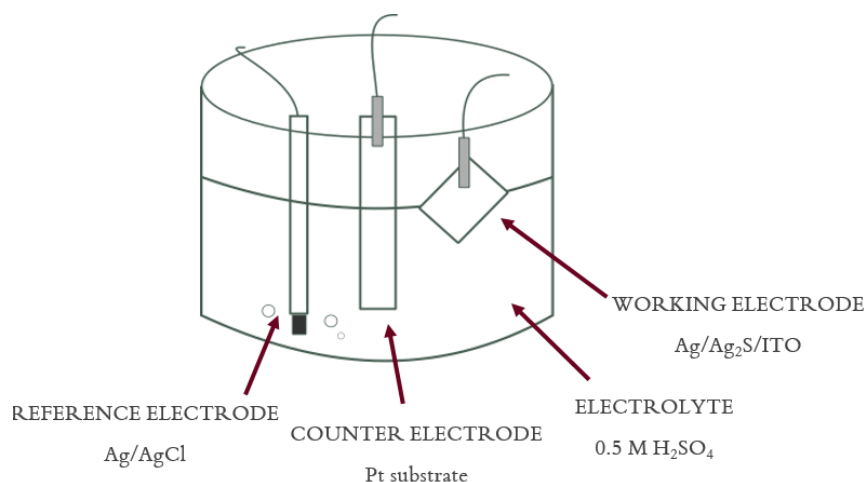


**Fig. 4** Schematic representation of the electrochemical cell.



All the electrochemical experiments were performed by applying a potential ranging from 0.2 V to -0.64 V *vs* Ag/AgCl at a scan rate of 2 mV s<sup>-1</sup>.

### **Microwave-assisted catalytic experiments**

Microwave theory is described in the section ““Ride the wave!”: Microwave radiation” in the Chapter “Introduction”.

The microwave-assisted catalytic tests have been carried out in a focused mono-mode microwave model CEM-Discover, equipped with a PC-controlled interface. The “discover” method was used under pressure, allowing the control of the irradiation power, the pressure and the temperature. The oxidation of toluene and benzyl alcohol to benzaldehyde were performed using a microwave-assisted procedure. The reaction solutions were irradiated for 45 min. The experiments were performed in closed vessels and the “discover” method was used under pressure, allowing the control of the irradiation power, of the pressure and of the temperature. The reactions were stirred and heated with microwave irradiations, fixing the temperature at 120 °C by an infrared probe.

The filtrates collected for both reactions were analyzed by GC, using an Agilent 19091J-413 GC model equipped with a Supelco 2-8047-U (30 m x 0.32 mm x 0.25 µm) capillary column and a FID detector. The temperature of the column was ramped at 25 °C min<sup>-1</sup> to 25 °C (1 min hold time) then at 25 °C min<sup>-1</sup> to 250 °C (5 min hold time), and finally to 300 °C at 20 °C min<sup>-1</sup> (10 min hold time). The nitrogen gas flow set at 1.3 mL min<sup>-1</sup>.

### **Continuous-flow process**

Flow chemistry technique is described in the section ““Roll with the flow!”: Continuous-flow chemistry” in the Chapter “Introduction”.

The selective hydrogenation of cinnamaldehyde was tested using a continuous-flow process. Catalytic tests were performed under liquid-phase

continuous-flow conditions in an H-Cube Mini Plus<sup>TM</sup> flow hydrogenation reactor. The materials were packed in 30 mm-long ThalesNano CatCarts. The reactor was washed with methanol and acetonitrile. A solution of cinnamaldehyde in acetonitrile was pumped in the reactor and the reaction conditions were set. The required hydrogen was generated in situ during the reaction through the water electrolysis in the H-Cube reactor.

The reaction was analyzed by gas chromatograph (GC) in an Agilent 6890N gas chromatograph (60 mL min<sup>-1</sup> N<sub>2</sub> carrier flow, 20 psi column top head pressure) using a flame ionization detector (FID). A capillary column, HP-5 (30 m x 0.32 mm x 0.25 μm) was used. In addition, the liquid fractions were analyzed by GC-MS using an Agilent 7820A GC/5977B high efficiency source (HES) MSD.

## References

1. Sing, K. S. W.; Everet, D. H.; Haul, R. A. W.; Moscou, L.; Pierotti, R. A.; Rouquerol, J.; Siemienwska, T. Reporting physisorption data for gas/solid systems with special reference to the determination of surface area and porosity. *Pure Appl. Chem.* **1985**, *57*, 603–619.
2. Rouquerol, J.; Rouquerol, F.; Llewellyn, P.; Maurin, G.; Sing, K. Adsorption by powders and porous solids: principles, methodology and applications. *Academic Press*. **2013**.
3. Barrett, E. P.; Joyner, L. G.; Halenda, P. P. The Determination of pore volume and area distributions in porous substances. I. Computations from Nitrogen Isotherms. *J. Am. Chem. Soc.* **1951**, *73*, 373–380.
4. Thibault, P.; Dierolf, M.; Menzel, A.; Bunk, O.; David, C.; Pfeiffer, F. High-resolution scanning X-ray diffraction microscopy. *Science*. **2008**, *321*, 379–382.
5. Cullity, B. D.; Stock, S. R. Elements of X-ray Diffraction. *Pearson Education*. **2014**.
6. Goldstein, J. I.; Newbury, D. E.; Michael, J. R.; Ritchie, N. W. M.; Scott, J. H. J.; Joy, D. C. Scanning electron microscopy and X-ray microanalysis. *Springer*. **2017**.
7. Faraldos, M.; Goberna, C. Técnicas de análisis y caracterización de materiales. *CSIC*. **2002**.
8. Skoog, D. A.; Holler, F. J.; Crouch, S. L. Principles of Instrumental Analysis. *Thomson Learning*. **2007**.
9. Mermet, J. M. Ionic to atomic line intensity ratio and residence time in inductively coupled plasma-atomic emission spectrometry. *Spectrochim. Acta Part B At. Spectrosc.* **1989**, *44*, 1109-1116.
10. Thomas, R. Practical guide to ICP-MS: a tutorial for beginners. *CRC press*. **2013**.
11. Walter, M. G.; Warren, E. L.; McKone, J. R.; Boettcher, S. W.; Mi, Q. X.; Santori, E. A.; Lewis, N. S. Solar Water Splitting Cells. *Chem. Rev.* **2010**, *110*(11), 6446-6473.
12. Zou, X. X.; Zhang, Y. Noble metal-free hydrogen evolution catalysts for water splitting. *Chem. Soc. Rev.* **2015**, *44*(15), 5148-5180.
13. Laviron, E. Adsorption, autoinhibition and autocatalysis in polarography and in linear potential sweep voltammetry. *J. Electroanal. Chem.* **1974**, *52*(3), 355-393.
14. Laviron, E. Use of linear potential sweep voltammetry and of ac voltammetry for the study of the surface electrochemical reaction of strongly adsorbed systems and of redox modified electrodes. *J. Electroanal. Chem.* **1979**, *100*(1-2), 263-270.





# Articles permissions



Gmail - Permission Request Form: Camilla Maria Cova

<https://mail.google.com/mail/u/0?ik=021f64a8ae&view=pt&search=all&...>

camilla cova &lt;camillacova@gmail.com&gt;

**Permission Request Form: Camilla Maria Cova**

2 messaggi

**noreply@rsc.org** <noreply@rsc.org>  
 A: contracts-copyright@rsc.org  
 Cc: camillacova@gmail.com

10 ottobre 2019 21:09

Name : Camilla Maria Cova  
 Address :

Calle Sevilla 2A  
 14003  
 Cordoba  
 Spain

Tel : +393484655182  
 Fax :  
 Email : [camillacova@gmail.com](mailto:camillacova@gmail.com)

I am preparing the following work for publication:

Article/Chapter Title :  
 Journal/Book Title : PhD Thesis: ENVIRONMENTALLY FRIENDLY PATHS FOR WASTES AND BIOMASS  
 VALORIZATION  
 Editor/Author(s) : Camilla Maria Cova  
 Publisher : Universidad de Cordoba

I would very much appreciate your permission to use the following material:

Journal/Book Title : Journal of Materials Chemistry A  
 Editor/Author(s) : C.M. Cova, A. Zuliani, A.R. Puente-Santiago, A. Caballero, M.J. Muñoz-Batista, R. Luque  
 Volume Number : 6  
 Year of Publication : 2018  
 Description of Material : Microwave-assisted preparation of Ag/Ag<sub>2</sub>S carbon hybrid structures from pig bristles as efficient HER catalysts  
 Page(s) : 21516-21523  
 Journal/Book Title : Green Chemistry  
 Editor/Author(s) : C.M. Cova, A. Zuliani, M.J. Muñoz-Batista, R. Luque  
 Volume Number : 21  
 Year of Publication : 2019  
 Description of Material : Efficient Ru-based scrap waste automotive converter catalysts for the continuous-flow selective hydrogenation of cinnamaldehyde  
 Page(s) : 4712-4722

Any Additional Comments :

I would like to use, if possible, the two entire articles for my PhD thesis. Thank you.

**CONTRACTS-COPYRIGHT (shared)** <Contracts-Copyright@rsc.org>  
 A: "camillacova@gmail.com" <camillacova@gmail.com>

11 ottobre 2019 15:45



## Article permissions

Gmail - Permission Request Form: Camilla Maria Cova

<https://mail.google.com/mail/u/0?ik=021f64a8ae&view=pt&search=all&...>

Many thanks for sending the permissions request below. The Royal Society of Chemistry (RSC) hereby grants permission for the use of your paper(s) specified below in the printed and microfilm version of your thesis. You may also make available the PDF version of your paper(s) that the RSC sent to the corresponding author(s) of your paper(s) upon publication of the paper(s) in the following ways: in your thesis via any website that your university may have for the deposition of theses, via your university's Intranet or via your own personal website. We are however unable to grant you permission to include the PDF version of the paper(s) on its own in your institutional repository. The Royal Society of Chemistry is a signatory to the STM Guidelines on Permissions (available on request).

Please note that if the material specified below or any part of it appears with credit or acknowledgement to a third party then you must also secure permission from that third party before reproducing that material.

Please ensure that the thesis states the following:

Reproduced by permission of The Royal Society of Chemistry

and include a link to the paper on the Royal Society of Chemistry's website.

Please ensure that your co-authors are aware that you are including the paper in your thesis.

Best wishes,

**Chloe Szebrat**  
Contracts and Copyright Executive  
Royal Society of Chemistry  
Thomas Graham House  
Science Park, Milton Road  
Cambridge, CB4 0WF, UK  
Tel: +44 (0) 1223 438329

[www.rsc.org](http://www.rsc.org)

[Testo tra virgolette nascosto]

[Testo tra virgolette nascosto]

This communication is from The Royal Society of Chemistry, a company incorporated in England by Royal Charter (registered number RC000524) and a charity registered in England and Wales (charity number 207890). Registered office: Burlington House, Piccadilly, London W1J 0BA. Telephone: +44 (0) 20 7437 8656.

The content of this communication (including any attachments) is confidential, and may be privileged or contain copyright material. It may not be relied upon or disclosed to any person other than the intended recipient(s) without the consent of The Royal Society of Chemistry. If you are not the intended recipient(s), please (1) notify us immediately by replying to this email, (2) delete all copies from your system, and (3) note that disclosure, distribution, copying or use of this communication is strictly prohibited.

Any advice given by The Royal Society of Chemistry has been carefully formulated but is based on the information available to it. The Royal Society of Chemistry cannot be held responsible for accuracy or completeness of this

Gmail - Permission Request Form: Camilla Maria Cova

<https://mail.google.com/mail/u/0?ik=021f64a8ac&view=pt&scarch=all&...>

communication or any attachment. Any views or opinions presented in this email are solely those of the author and do not represent those of The Royal Society of Chemistry. The views expressed in this communication are personal to the sender and unless specifically stated, this e-mail does not constitute any part of an offer or contract. The Royal Society of Chemistry shall not be liable for any resulting damage or loss as a result of the use of this email and/or attachments, or for the consequences of any actions taken on the basis of the information provided. The Royal Society of Chemistry does not warrant that its emails or attachments are Virus-free; The Royal Society of Chemistry has taken reasonable precautions to ensure that no viruses are contained in this email, but does not accept any responsibility once this email has been transmitted. Please rely on your own screening of electronic communication.

More information on The Royal Society of Chemistry can be found on our website: [www.rsc.org](http://www.rsc.org)

This communication is from The Royal Society of Chemistry, a company incorporated in England by Royal Charter (registered number RC000524) and a charity registered in England and Wales (charity number 207890). Registered office: Burlington House, Piccadilly, London W1J 0BA. Telephone: +44 (0) 20 7437 8656.

The content of this communication (including any attachments) is confidential, and may be privileged or contain copyright material. It may not be relied upon or disclosed to any person other than the intended recipient(s) without the consent of The Royal Society of Chemistry. If you are not the intended recipient(s), please (1) notify us immediately by replying to this email, (2) delete all copies from your system, and (3) note that disclosure, distribution, copying or use of this communication is strictly prohibited.

Any advice given by The Royal Society of Chemistry has been carefully formulated but is based on the information available to it. The Royal Society of Chemistry cannot be held responsible for accuracy or completeness of this communication or any attachment. Any views or opinions presented in this email are solely those of the author and do not represent those of The Royal Society of Chemistry. The views expressed in this communication are personal to the sender and unless specifically stated, this e-mail does not constitute any part of an offer or contract. The Royal Society of Chemistry shall not be liable for any resulting damage or loss as a result of the use of this email and/or attachments, or for the consequences of any actions taken on the basis of the information provided. The Royal Society of Chemistry does not warrant that its emails or attachments are Virus-free; The Royal Society of Chemistry has taken reasonable precautions to ensure that no viruses are contained in this email, but does not accept any responsibility once this email has been transmitted. Please rely on your own screening of electronic communication.

More information on The Royal Society of Chemistry can be found on our website: [www.rsc.org](http://www.rsc.org)



Cite this: *J. Mater. Chem. A*, 2018, 6, 21516

## Microwave-assisted preparation of Ag/Ag<sub>2</sub>S carbon hybrid structures from pig bristles as efficient HER catalysts†

Camilla Maria Cova,<sup>a</sup> Alessio Zuliani,<sup>a</sup> Alain R. Puente Santiago,<sup>b</sup> Alvaro Caballero,<sup>b</sup> Mario J. Muñoz-Batista<sup>b</sup> and Rafael Luque<sup>b</sup>\*ac

Ag/Ag<sub>2</sub>S hybrid structures have recently attracted significant interest due to their high chemical and thermal stability, in addition to their unique optical and electrical properties. However, their standard synthetic protocols have important drawbacks including long term and harsh reaction conditions and the utilization of highly toxic sulfur precursors. Herein, an innovative, simple one-pot green approach for the synthesis of the Ag/Ag<sub>2</sub>S carbon hybrid structures is reported. The procedure involves a one-step microwave-assisted method using ethylene glycol as a solvent and reducing agent, pig bristles as a sulphur and carbon source and silver nitrate as a metal precursor. Different amounts of silver nitrate were employed in order to investigate the synthetic mechanism for the formation of zerovalent silver over silver sulphide nanoparticles, producing three different samples. The materials were characterized by XRD, SEM, EDX, N<sub>2</sub> physisorption and XPS spectroscopy. Aiming to prove the efficiency of the as-synthesized compounds, their electrocatalytic activities were explored in the hydrogen evolution reaction (HER) using linear sweep voltammetry.

Received 4th July 2018  
Accepted 8th October 2018

DOI: 10.1039/c8ta06417b

rs.c.li/materials-a

### Introduction

Environmental and economic metrics are becoming increasingly and equally important in the design of new materials. Currently, most industrially available compounds are derived from non-renewable resources, following the so-defined linear economy. However, the rising costs of gas and crude oil and more importantly the drive towards a more sustainable future utilisation of low toxicity reagents is pushing research towards the valorisation of renewable resources through sustainable synthetic processes.<sup>1</sup> In this context, meeting the principles of green chemistry can be considered as the key to the sustainable design of innovative materials.<sup>2–4</sup>

In the last few decades, different metal chalcogenides have attracted interest because of their unique physical and chemical properties that make them suitable in diverse areas ranging from electronics to biomedicine. These materials include copper sulphide (Cu<sub>2</sub>S), silver sulphide (Ag<sub>2</sub>S), nickel sulphide

(NiS), lead sulphide (PbS), cadmium sulphide (CdS) and mercury sulphide (HgS).<sup>5–7</sup> Silver sulphide emerged as an excellent material for the preparation of metal-semiconductor heterostructures.<sup>8,9</sup> These heterostructures may exhibit a behaviour not limited to the combination of the properties of the separated components, but also the synergistic effects of the two constituents.<sup>10</sup> For example, Ag/Ag<sub>2</sub>S heterostructures have attracted special attention as antibacterial agents, biosensing probes and photocatalysts.<sup>11,12</sup> The Ag/Ag<sub>2</sub>S heterostructures have also been proposed as efficient catalysts for the hydrogen evolution reaction (HER).<sup>13,14</sup> Hydrogen is in fact a promising candidate as an alternative green energy source that can be produced *via* water splitting. Consequently, the development of suitable, low cost, high performance catalysts for hydrogen evolution reactions (HER) is of great importance and practical needs. However, despite the reported scope for the production of green hydrogen as an alternative energy source, the synthesis of the Ag/Ag<sub>2</sub>S materials entails some sustainability restrictions. All reported synthetic protocols for these materials are normally time and energy consuming.<sup>15</sup> Most importantly, these syntheses involve the utilization of expensive and toxic sulphur sources including highly hazardous compounds such as H<sub>2</sub>S, thiols or Na<sub>2</sub>S and less aggressive (but still toxic) silver thiol salts.<sup>8,15,16</sup>

Based on recent endeavours from our group in microwave chemistry and biomass valorisation, herein we report a sustainable and innovative one-step synthesis of pig bristles-derived Ag/Ag<sub>2</sub>S carbon hybrid structures *via* a microwave-

<sup>a</sup>Departamento de Química Orgánica, Universidad de Córdoba, Edificio Marie-Curie (C-3), Ctra Nnal IV-A, Km 396, Córdoba, Spain. E-mail: rafael.luque@uco.es

<sup>b</sup>Departamento de Química Inorgánica e Ingeniería Química, Campus de Rabanales, Edificio Marie Curie (C-3), Ctra Nnal IV-A, Km 396, E1A014, Córdoba, Spain

<sup>c</sup>Peoples Friendship University of Russia (RUDN University), 6 Miklukho-Maklaya Str. Moscow, 117198, Russia

† Electronic supplementary information (ESI) available: SEM mapping of the samples; complete list of XRD peaks; N<sub>2</sub> absorption-desorption isotherm of the sample 1.4Ag/Ag<sub>2</sub>S; LSV curves of the samples and Pe/C normalized by the electrochemical surface area. See DOI: 10.1039/c8ta06417b



Cite this: *Green Chem.*, 2019, **21**, 4712

## Efficient Ru-based scrap waste automotive converter catalysts for the continuous-flow selective hydrogenation of cinnamaldehyde†

Camilla Maria Cova,<sup>a</sup> Alessio Zuliani,<sup>b</sup> Mario J. Muñoz-Batista<sup>\*,a</sup> and Rafael Luque<sup>†,a,b</sup>

The selective, efficient and sustainable continuous flow hydrogenation of a  $\alpha,\beta$ -unsaturated aldehyde, *i.e.* cinnamaldehyde, to the corresponding unsaturated alcohol, *i.e.* cinnamyl alcohol, using a novel catalyst based on Ru-containing scrap waste automotive converters is reported. The catalyst was prepared by recycling and upgrading waste ceramic-cores of scrap automotive catalytic converters as supporting materials. Ruthenium was incorporated into the ceramic structures using a simple, fast and solventless mechano-chemically assisted procedure followed by a chemical reduction step. Different catalysts were prepared with varying Ru contents. The materials were characterized by XRD,  $N_2$  physisorption, XPS, TEM, HRTEM and SEM/mapping analyses. Compared to Ru supported over most studied silica and alumina supports, the new system displayed an outstanding catalytic performance under continuous-flow conditions in terms of conversion and selectivity and a remarkable stability with time-on-stream, demonstrating a synergistic action between Ru and the waste catalytic converter support. A Ru loading of 10 wt% provided the optimum results, including a cinnamaldehyde conversion of up to 95% with a selectivity to cinnamyl alcohol of 80%.

Received 13th May 2019.  
Accepted 21st July 2019  
DOI: 10.1039/c9gc01596e  
rsc.li/greenchem

### 1. Introduction

Chemoselectivity is the bedrock of catalytic processes since it involves the activation of specific functional groups within more complex starting reactants. The chemoselective hydrogenation of  $\alpha,\beta$ -unsaturated aldehydes represents a critical step in the synthetic preparation of chemicals for the pharmaceutical and flavour/fragrance industries. For example, citral, an  $\alpha,\beta$ -unsaturated aldehyde extracted from plants, can be selectively hydrogenated to geraniol, a commonly used fragrance tasting peach, raspberry, grapefruit and red apple.<sup>1–5</sup> In general, the chemoselective hydrogenation of  $\alpha,\beta$ -unsaturated aldehydes has been widely investigated from a mechanistic point using different catalytic systems.<sup>6–8</sup> The results demonstrated that the activation of the double carbon bond is kinetically and thermodynamically favoured, leading to the formation of saturated aldehydes.<sup>1,9–11</sup> However, the less-favoured unsaturated alcohols ( $\Delta E \sim 35 \text{ kJ mol}^{-1}$  less favoured)<sup>12</sup> are of high value and broadly employed in industry.<sup>10,13–15</sup> As a consequence, designing of catalytically

active materials that preferentially hydrogenate the carbonyl bond within yields is a captivating yet significant challenge still nowadays.

A largely investigated reaction for the selective hydrogenation of  $\alpha,\beta$ -unsaturated aldehydes is the hydrogenation of cinnamaldehyde (CAL) to cinnamyl alcohol (COL). COL is a fragrance smelling as hyacinth with balsamic and spicy notes widely used in perfumes, drugs and food formulations.<sup>16–18</sup>

As illustrated in Scheme 1, besides COL, the other principal products of the hydrogenation of cinnamaldehyde include hydrocinnamaldehyde (HCAL) and hydrocinnamyl alcohol (HCOL).<sup>19–21</sup>

Most studied chemoselective heterogeneous catalysts for the hydrogenation of CAL to COL are based on supported ruthenium compounds.<sup>22–25</sup> In particular, significant conversion and selectivity values have been reported using ruthenium supported on porous alumina<sup>26</sup> or silica.<sup>27</sup> More recently, also different carbon materials such as graphene,<sup>28</sup> carbon nanotubes,<sup>22,29,30</sup> activated carbons<sup>31,32</sup> or mesoporous carbons<sup>33</sup> have been reported as efficient supporting materials. The choice of an appropriate supporting material is of primary importance since its intrinsic properties and, more importantly, the interaction between the metals and the support can deeply modify the reaction selectivity, as reported by Leng *et al.*<sup>34</sup> Firstly, a lower metal dispersion generally boosts the selectivity to COL. Furthermore, an enhanced charge transfer between the metal and the support material can also lead to

<sup>a</sup>Departamento de Química Orgánica, Universidad de Córdoba, Edificio Marie-Curie (C-3), Ctra Nnal IV-A, Km 396, Córdoba, Spain. E-mail: rafael.luque@uco.es

<sup>b</sup>Peoples Friendship University of Russia (RUDN University), 6 Mikulsho Maklaya str., 117198 Moscow, Russia

† Electronic supplementary information (ESI) available. See DOI: 10.1039/c9gc01596e



RightsLink®

Home

Account Info

Help



ACS Publications  
Most Trusted. Most Cited. Most Read.

**Title:** A Sustainable Approach for the Synthesis of Catalytically Active Peroxidase-Mimic ZnS Catalysts

**Author:** Camilla M. Cova, Alessio Zuliani, Mario J. Muñoz-Batista, et al

**Publication:** ACS Sustainable Chemistry & Engineering

**Publisher:** American Chemical Society

**Date:** Jan 1, 2019

Copyright © 2019, American Chemical Society

Logged in as:  
Camilla Maria Cova  
Universidad de cordoba  
Account #:  
3001413367

LOGOUT

**PERMISSION/LICENSE IS GRANTED FOR YOUR ORDER AT NO CHARGE**

This type of permission/license, instead of the standard Terms & Conditions, is sent to you because no fee is being charged for your order. Please note the following:

- Permission is granted for your request in both print and electronic formats, and translations.
- If figures and/or tables were requested, they may be adapted or used in part.
- Please print this page for your records and send a copy of it to your publisher/graduate school.
- Appropriate credit for the requested material should be given as follows: "Reprinted (adapted) with permission from (COMPLETE REFERENCE CITATION). Copyright (YEAR) American Chemical Society." Insert appropriate information in place of the capitalized words.
- One-time permission is granted only for the use specified in your request. No additional uses are granted (such as derivative works or other editions). For any other uses, please submit a new request.

BACK

CLOSE WINDOW

Copyright © 2019 Copyright Clearance Center, Inc. All Rights Reserved. [Privacy statement](#), [Terms and Conditions](#).  
Comments? We would like to hear from you. E-mail us at [customercare@copyright.com](mailto:customercare@copyright.com)

# 1 A Sustainable Approach for the Synthesis of Catalytically Active 2 Peroxidase-Mimic ZnS Catalysts

3 Camilla M. Cova,<sup>†</sup> Alessio Zuliani,<sup>‡</sup> Mario J. Muñoz-Batista,<sup>†</sup> and Rafael Luque<sup>\*,†,‡,§</sup>

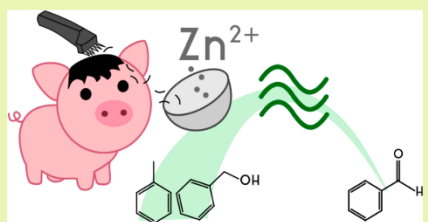
4 <sup>†</sup>Departamento de Química Orgánica, Universidad de Córdoba, Edificio Marie-Curie (C-3), Ctra Nnal IV-A, Km 396, E-14014  
5 Córdoba, Spain

6 <sup>‡</sup>Peoples Friendship University of Russia (RUDN University), 6 Miklukho-Maklaya str., 117198, Moscow, Russia

7 <sup>§</sup> Supporting Information

8 **ABSTRACT:** Zinc sulfides are emerging as promising  
9 catalysts in different fields such as photochemistry or organic  
10 synthesis. Nevertheless, the synthesis of ZnS compounds  
11 normally requires the utilization of toxic sulfur precursors, e.g.,  
12 thiourea which is a contaminant and carcinogenic agent. As a  
13 result, new green and sustainable synthetic methodologies are  
14 needed. Herein, an innovative, simple, and cheap approach for  
15 the synthesis of ZnS carbon composites is reported. Zinc  
16 acetate dihydrate was employed as metal precursor while  
17 wasted pig bristles were employed as carbon and sulfur source.  
18 The phase and the morphology of the compounds were  
19 analyzed by XRD, XPS, SEM, and EDX and the surface area  
20 was determined by nitrogen physisorption. ZnS carbon  
21 materials showed remarkable peroxidase-like catalytic activity  
22 for two different model reactions: the liquid-phase selective  
23 oxidation of benzyl alcohol and toluene to benzaldehyde (conversions up to 63% and 29% and selectivities up to 86% and 87%,  
24 respectively) using hydrogen peroxide as oxidant under microwave irradiation.

**KEYWORDS:** Zinc sulfide, Pig bristles, Microwave chemistry, Selective oxidations



## 25 ■ INTRODUCTION

26 Zinc sulfide has been studied as an important compound due  
27 to its unique physical and photochemical properties.<sup>1–3</sup> It has  
28 demonstrated an extraordinary versatility and potentiality for  
29 different applications including light-emitting diodes (LEDs),  
30 electroluminescence, infrared windows, sensors, lasers, and  
31 biodevices.<sup>4–6</sup> Additionally, ZnS possesses many interesting  
32 characteristics such as excellent transport properties, an  
33 intrinsically *n*-type semiconductivity, good thermal stability,  
34 high electronic mobility, nontoxicity, water insolubility, and  
35 low-production costs.<sup>1–7</sup>

36 All reported synthetic protocols for ZnS preparation involve  
37 the utilization of highly toxic sulfur sources including extremely  
38 hazardous compounds such as H<sub>2</sub>S, or Na<sub>2</sub>S as well as  
39 thioureas, highly contaminant and carcinogenic agents.<sup>8–10</sup>  
40 New green and low-toxicity sulfur sources are therefore  
41 required for sustainable development. In this context, pig  
42 bristles represent a cheap and largely available source of sulfur  
43 (and carbon). Pig bristles are considered as a waste toxic-free  
44 feedstock, easily collectable and accessible at industrial scale. In  
45 fact, ca. ~225k tons of wasted pig bristles are yearly produced  
46 only in European slaughterhouses.<sup>11</sup> However, only a few  
47 works to date are available on the reutilization/use of pig  
48 bristles as food fodder supplements, while their valorization as  
49 chemical source is extremely limited.<sup>11–13</sup>

Herein, a simple and innovative synthesis of ZnS carbon  
50 composites derived from wasted pig bristles is reported. The  
51 synthetic procedure involved a facile heating step in a diluted  
52 aqueous solution of potassium hydroxide. Wasted pig bristles  
53 were employed as sulfur and carbon source while zinc acetate  
54 dihydrate was used as metal source. The material was  
55 characterized by XPS, XRD, N<sub>2</sub> physisorption, SEM, and  
56 EDX, demonstrating the successful formation of zinc sulfides  
57 carbon compounds.<sup>58</sup>

58 In order to validate the practical application of the new  
59 material, ZnS carbon composites were tested as catalysts in two  
60 different model reactions: the selective oxidation of benzyl  
61 alcohol and toluene to benzaldehyde. Among all known  
62 oxidative transformations, the selective oxidations of alcohols  
63 to the corresponding carbonyl compounds have gained  
64 attention due to their broad range of industrial applica-  
65 tions.<sup>14,15</sup> Specifically, the conversion of benzyl alcohol to  
66 benzaldehyde has attracted significant interest since benzalde-  
67 hyde is a widely used chemical in food, pharmaceutical, and  
68 perfumery industries as well as building block in other  
69 chemical industries.<sup>16–22</sup> For example, benzaldehyde is  
70 commonly used as a flavor and fragrance agent tasting of 71

Received: September 27, 2018

Revised: November 5, 2018

Published: December 7, 2018

Gmail - Case #00903657 - Permission request [ ref:\_00D30oeGz\_5000... https://mail.google.com/mail/u/0/?ik=021f64a8ac&view=pt&search=all&...



camilla cova <camillacova@gmail.com>

**Case #00903657 - Permission request [ ref:\_00D30oeGz\_5000c1uSU3l:ref ]**

customer care@copyright.com <customer care@copyright.com>  
A: "camillacova@gmail.com" <camillacova@gmail.com>

14 ottobre 2019 08:37

Dear Camila Maria Cova,

Thank you for contacting Copyright Clearance Center (CCC). We act on behalf of copyright owners in providing permissions to our customers. Permission availability can vary depending on a rights holder and also on the permission type.

My name is Marko, and it would be my pleasure to assist you. After checking "Advances in mechanochemical processes for biomass valorization", I can see that this is an open access article under the terms of [Creative Commons Attribution 4.0 International License \(CC BY 4.0\)](#). Therefore, the permission to reuse it in your PhD Thesis is not required under the following terms:

- **Attribution** — You must give appropriate credit, provide a link to the license, and indicate if changes were made. You may do so in any reasonable manner, but not in any way that suggests the licensor endorses you or your use
- **No additional restrictions** — You may not apply legal terms or technological measures that legally restrict others from doing anything the license permits

I hope this has been helpful, and if you need any further guidance, do not hesitate to contact us again.

Best regards,  
Marko

Marko Randjelovic  
Customer Account Specialist  
Copyright Clearance Center  
[222 Rosewood Drive](#)  
Danvers, MA 01923  
[www.copyright.com](#)  
Toll Free US +1.855.239.3415  
International +1.978.646.2600  
[Facebook](#) - [Twitter](#) - [LinkedIn](#)

ref:\_00D30oeGz\_5000c1uSU3l:ref

----- Original Message -----

**From:** camilla cova [[camillacova@gmail.com](mailto:camillacova@gmail.com)]  
**Sent:** 10/10/2019 3:18 PM  
**To:** [customer care@copyright.com](mailto:customer care@copyright.com)  
**Subject:** Permission request

Dear Customer Service team,

I'm writing you to formally request the permission for reuse the following article in my PhD Thesis titled "Environmentally friendly paths for wastes and biomass valorization" at the Universidad de Cordoba (Spain):

Gmail - Case #00903657 - Permission request [ ref:\_00D30oeGz.\_5000... <https://mail.google.com/mail/u/0?ik=021f64a8ae&view=pt&search=all&...>

**"Advances in mechanochemical processes for biomass valorization"**

**Camilla Maria Cova, Rafael Luque**  
**BMC Chemical Engineering (Springer Nature) 1, 16, 2019**

Thank you for your kind attention.

Camila Maria Cova



Mail priva di virus. [www.avast.com](http://www.avast.com)

This message (including attachments) is confidential, unless marked otherwise. It is intended for the addressee(s) only. If you are not an intended recipient, please delete it without further distribution and reply to the sender that you have received the message in error.

ref:\_00D30oeGz.\_5000c1uSU3l:ref



## REVIEW

## Open Access

# Advances in mechanochemical processes for biomass valorization

Camilla Maria Cova<sup>1</sup> and Rafael Luque<sup>1,2\*</sup>

## Abstract

Compared to standard time and solvent consuming procedures, mechanically-assisted processes offer numerous environmentally-friendly advantages for nano-catalytically active materials design. Mechanochemistry displays high reproducibility, simplicity, cleanliness and versatility, avoiding, in most cases, the use of any solvent. Moreover, mechanically-assisted procedures are normally faster and cheaper as compared to conventional processes. Due to these outstanding characteristics, mechanochemistry has evolved as an exceptional technique for the synthesis of novel and advanced catalysts designed for a large range of applications. The literature reports numerous works showing that mechanochemical procedures offer more promising paths than traditional solvent-based techniques. This review aims to disclose the latest advances in the mechanochemical assisted synthesis of catalytically active materials, focusing on nanocatalysts designed for biomass conversion and on bio-based catalysts.

**Keywords:** Mechanochemistry, Catalysis, Bio-based catalysts, Biomass conversion

## Introduction

### Mechanochemistry timeline

As formalized by IUPAC, a mechanical-assisted reaction is “a reaction caused by the mechanical energy” [1]. In fact, mechanical actions, such as compression, stress, or friction, usually provides the energy to activate a process. According to Takacs, the most ancient document concerning a mechanical-assisted process is described in a book in 315 B.C.. The document, titled “On Stones”, was written by Theophrastus, one of Aristotle’s students. The philosopher-scientist described the reduction of cinnabar (HgS) to mercury (Hg<sup>0</sup>) using a copper vessel and a copper pestle filled with some vinegar (containing acetic acid) [2, 3]. After that first experiment reported by Theophrastus, no mechanical-based protocols were reported for the following 2000 years. Only in 1820 mechanochemistry appeared again, when Faraday carried out mechanical-assisted trials, reducing AgCl to elemental Ag using zinc, copper, tin or iron in a pestle. Faraday noticed that mechanical-assisted reaction could give different products compared to the ones obtained by normal thermal heating.

Specifically, he proved that the mechanical-assisted processes favoured the decomposition of Ag and Hg halides to their elements by chemical reaction, rather than by melting or sublimation [4]. A few years later, Wilhelm Ostwald (1853–1932) defined “mechanochemistry” as one of four chemistry disciplines (together with photo-, electro- and thermo-chemistry). In 1894, Gerard Heinicke formalized mechanochemistry as “the discipline relative to physical-chemical modifications of the solid produced by the action of mechanical factors” [5]. Figure 1 gives a summary of the milestones of mechanochemistry evolution.

### Mechanochemistry theory

The principal feature of mechanical-assisted process is the achievement of chemical changes by the only action of grinding (or milling), without needing to dissolve reagents (therefore without using any solvent). Grinding is a broad term that describes the effect of mechanical forces on a compound that allow a solid breaking into small parts. By grinding, the improved potential energy together with friction and shear contributions, generate surface and shape defects in the reactants. These defects can considerably change the reactivity of chemicals, giving the final product, as described in Fig. 2.

\* Correspondence: [g62alsor@uco.es](mailto:g62alsor@uco.es)

<sup>1</sup>Departamento de Química Orgánica, Universidad de Córdoba, Edificio Marie-Curie (C-3), Ctra Nnal IV-A, Km 396, Córdoba, Spain

<sup>2</sup>Peoples Friendship University of Russia (RUDN University), 6 Miklukho Maklaya str, 117198 Moscow, Russia



© The Author(s). 2019 **Open Access** This article is distributed under the terms of the Creative Commons Attribution 4.0 International License (<http://creativecommons.org/licenses/by/4.0/>), which permits unrestricted use, distribution, and reproduction in any medium, provided you give appropriate credit to the original author(s) and the source, provide a link to the Creative Commons license, and indicate if changes were made. The Creative Commons Public Domain Dedication waiver (<http://creativecommons.org/publicdomain/zero/1.0/>) applies to the data made available in this article, unless otherwise stated.

